2022

Carbon and nitrogen cycling in vegetated coastal ecosystems

BOSTON UNIVERSITY

GRADUATE SCHOOL OF ARTS AND SCIENCES

Dissertation

CARBON AND NITROGEN CYCLING IN VEGETATED COASTAL ECOSYSTEMS

by

ALIA NINA AL-HAJ

B.S., University of Virginia, 2010
M.S., University of Virginia, 2014

Submitted in partial fulfillment of the

requirements for the degree of

Doctor of Philosophy

2022

Approved by

First Reader

Robinson W. Fulweiler, Ph.D.
Professor of Earth and Environment
Professor of Biology

Second Reader

Jennifer Bhatnagar, Ph.D.
Assistant Professor of Biology

Third Reader

Alyssa Novak, Ph.D.
Research Assistant Professor of Earth and Environment

Fourth Reader

Nathan Phillips, Ph.D.
Professor of Earth and Environment

ACKNOWLEDGEMENTS

This dissertation would not have been possible without the help of the people I have had the pleasure to work with during my time at Boston University. First and foremost, I would like to thank my advisor, Dr. Robinson "Wally" Fulweiler. During my time at BU, Wally pushed me to become a better scientist and mentor. I look forward to continuing to make "dream science" a reality with her in the future. I would like to thank my committee, Dr. Jennifer Bhatnagar, Dr. Alyssa Novak, and Dr. Nathan Phillips who have supported me throughout this this process and have pushed me to view my science from a different perspective.

I owe a huge thanks to past and present graduate students in the Fulweiler lab: Emily Chua, Hollie Emery, Sarah Foster, Tim Maguire, and especially to Nick Ray, Nia Bartolucci, and Claudia Mazur who spent long days with me in the field. I look forward to continuing to work with all of these amazing scientists in the future. Claudia, my lab twin, has been a source of personal and professional support since day one as a Ph.D. student.

I am also fortunate to have worked with truly impressive undergraduate students. I would particularly like to thank Jenn Soukup, Victoria Momyer, Tony Pham, and Tyler Chidsey who allowed me to mentor them through their own research projects. They have all helped me grow as a mentor and it has been an honor to watch them grow as scientists.

Numerous other members of BU Earth and Environment, Biology, and the Fulweiler Lab helped me in the field and in the lab including: Gretchen McCarthy, Ena

Miculinic, Anniina Haka, John Rezza, Kwetz Mexika, John Angell, and Corinne Vietorisz. I am particularly grateful for the help of Brendan Kelly who spent many long days in the field with me testing my *in situ* chambers and to Melissa Hagy who helped me in the field and ran my nutrient samples on the Seal. I would also like to thank Joel Sparks for all of the time he spent helping me put together my *in situ* chambers, Cedric Fichot for letting me use the elemental analyzer in his laboratory, and to Nilotpal Ghosh for training me to run the elemental analyzer.

I was also fortunate to have the opportunity to work with several external scientists during my time at BU. Phil Colarusso at the US EPA invited to me to share my work at Zosterapalooza, Julie Simpson at MIT Sea Grant showed me their process for collecting sediment cores for dating, and Damien Maher supported me through the process of applying to the Limnology and Oceanography Research Exchange as well as planning for field research in Australia that was unfortunately derailed by COVID. I would also like to thank Judith Rosentreter and Phillip Williams who pushed me to think more critically about my work. I would also like to thank my OCEAN mentors Bob Chen, Jennifer Bowen, and Ashley Bulseco for the valuable career advice they have given me.

Finally, I would like to thank my family and friends. My parents and siblings have always supported me though every endeavor. Thanks for always answering when I call and being there on the good and bad days. Thank you to my friends near and far. I would particularly like to thank Matt Long and Jennie Rheuban for not only being there as science buddies, but for always supporting me. I would also like to thank our COVID

crew Drew Trlica and Ana Roboredo Segovia for keeping us sane during lockdown. Thank you to the rest of my Boston crew for pushing me out of my shell. Last, but not least, I would like to thank my partner, Cristian Triana, for making sure I take breaks, supporting me through the dissertation process, and bringing laughter to my life every day.

CARBON AND NITROGEN CYCLING IN VEGETATED COASTAL ECOSYSTEMS

Alia N. Al-Haj

Boston University Graduate School of Arts and Sciences, 2022

Major Professor: Robinson W. Fulweiler, Professor of Earth and Environment, Professor of Biology

ABSTRACT

Coastal ecosystems comprise a relatively small area of the ocean, yet they play a disproportionate role in greenhouse gas (carbon dioxide (CO_2), methane (CH_4), and nitrous oxide (N_2O)) and nutrient cycling. Vegetated coastal ecosystems (e.g., mangroves, salt marshes, and seagrasses) are key drivers of coastal greenhouse gas and nutrient cycling because of their environmental characteristics (e.g., shallow depths, organic matter rich sediments, etc.). My dissertation addresses the role of vegetated coastal ecosystems in greenhouse gas budgets and biogeochemical cycling. In Chapter 1, I conducted a meta-analysis to quantify the global emissions of CH_4 from mangrove, salt marsh, and seagrass ecosystems. Here I show that mangrove ecosystems contribute the most CH_4 out of these vegetated areas to the global marine CH_4 budget. Further, while a well-known negative relationship between salinity and CH_4 fluxes exists for salt marshes globally, this relationship does not hold for mangrove or seagrass meadows, suggesting that other environmental drivers are more important for predicting CH_4 fluxes in these ecosystems. In Chapter 2, I present *in situ* fluxes of CH_4 and N_2O across the sediment-water interface as well as air-sea fluxes in seagrass meadows and adjacent non-vegetated

sediments in two temperate coastal lagoons. Here I demonstrate that seagrass meadows can be sources or sinks of CH_4 and that N_2O uptake can enhance carbon sequestration in seagrass meadows by ~10%. In Chapter 3, I quantify fluxes of dissolved inorganic carbon, nitrogen, and phosphorous across the sediment-water interface in seagrass meadows and adjacent non-vegetated sediments in the same two coastal lagoons. I found that both seagrass and non-vegetated sediments exhibited dissolved inorganic carbon emission and denitrification, and that dissolved inorganic phosphorous fluxes varied by site and not with vegetation presence. This dissertation highlights the dynamic role coastal ecosystems play in biogeochemical cycling and the importance of vegetated coastal ecosystems in coastal greenhouse gas budgets.

PREFACE

Chapter 1 Citation:

Al-Haj, A. N., and R. W. Fulweiler. 2020. A synthesis of methane emissions from shallow vegetated coastal ecosystems. Glob. Chang. Biol. **26**: 2988–3005. doi:10.1111/gcb.15046

Chapter 2:

Al-Haj, A. N., T. J. Chidsey, and R.W. Fulweiler. Temperate seagrass meadow carbon sequestration can be enhanced by methane and nitrous oxide uptake.

Chapter 3:

Al-Haj, A.N. and R.W. Fulweiler. Fluxes of dissolved inorganic carbon, nitrogen, and phosphorus, are highly variable in *Z. marina* meadows.

TABLE OF CONTENTS

LIST OF TABLES

LIST OF FIGURES

LIST OF ABBREVIATIONS

Abs……..absolute value

Anammox.....anaeobic ammonium oxidation

C……..carbon

ºC.....degrees Celsius

cc.....cubic centimeter

CH_4……...methane

cm.....centimeter

C:N.....carbon to nitrogen ratio

CO_2…….carbon dioxide

CO_{2eq}.....carbon dioxide equivalent

CRDS……cavity ring-down spectroscopy

d……day

DIC.....dissolved inorganic carbon

DIN.....dissolved inorganic nitrogen

DIP.....dissolved inorganic phosphorous

dist…….distance

DNRA.....dissimalatory nitrate reduction to ammonium

DO.....dissolved oxygen

EH.....East Harbor

EST.....Eastern standard time

g…….gram

GFF.....glass fiber grade F

GFR…….mean global CH_4 flux rate

GHG.....greenhouse gas

GWP……..global warming potential

h.....hour

H_2……hydrogen

HCO_3.....bicarbonate

hr……....hour

km^2.....kilometers squared

L.....liter

LAI.....leaf area index

Lat……..latitude

m……...meter

MA.....Massachusetts

mg.....milligram

Mha……..million hectares

min.....minutes

mL.....milliliter

mmol……...millimole

mol…….mole

n.....number of samples

N……...nitrogen

N_2.....di-nitrogen gas

N_2-N.....di-nitrogen gas

N_2O.....nitrous oxide

ºN…….degress North

NDIR……..nondispersive infrared

NEP…….net ecosystem productivity

NH_4^+.....ammonium

NOAA.....National Oceanic and Atmospheric Administration

NO_2^-.....nitrite

NO_3^-.....nitrate

NO_x.....nitrate + nitrite

NPI.....nutrient pollution index

O_2……oxygen

OM……..organic matter

P.....phosphorus

p……..probability value

PB.....Pleasant Bay

ppb……parts per billion

ppt…….parts per thousand

p-value……probability value

ºS…….degrees South

SAV.....submerged aquatic vegetation

SGCP.....sustained flux global cooling potential

SGWP…….sustained flux global warming potential

Tg……Teragram

Tmol……Teramole

USA.....United States of America

U.S.....United States

VCE……..vegetated coastal ecosystem

µmol……..micromole

WWII……World War II

Z. marina.....*Zostera marina*

ZnCl.....Zinc Chloride

µL.....microliter

µM.....micromolar

%.....percent

±……plus or minus

>……..greater than

≥……greater than or equal to

<……...less than

≤…….less than or equal to

CHAPTER ONE: A SYNTHESIS OF METHANE EMISSIONS FROM SHALLOW VEGETATED COASTAL ECOSYSTEMS

Alia N. Al-Haj[1*], Robinson W. Fulweiler[1,2]

[1]Boston University, Department of Earth and Environment, 675 Commonwealth Avenue, Room 130, Boston, MA 02215

[2]Boston University, Department of Biology, 5 Cummington Mall, Room 101, Boston, MA 02215

Corresponding author: Alia N. Al-Haj (email: aalhaj@bu.edu, telephone: (571) 242 - 3971)

Keywords: methanogenesis, methanotrophy, salt marsh, mangrove, seagrass, global carbon budget

Abstract

Vegetated coastal ecosystems (VCEs; i.e., mangroves, salt marshes, and seagrasses) play a critical role in global carbon (C) cycling, storing 10x more C than temperate forests. Methane (CH_4), a potent greenhouse gas, can form in the sediments of these ecosystems. Currently, CH_4 emissions are a missing component of VCE C budgets. This review summarizes 97 studies describing CH_4 fluxes from mangrove, salt marsh, and seagrass ecosystems and discusses factors controlling CH_4 flux in these systems. CH_4 fluxes from these ecosystems were highly variable yet they all act as net methane sources (median, range; mangrove: 279.17, −67.33 to 72,867.83; salt marsh: 224.44, −92.60 to 94,129.68; seagrass: 64.80, 1.25–401.50 μmol CH_4 m^{-2} day^{-1}). Together CH_4 emissions from mangrove, salt marsh, and seagrass ecosystems are about 0.33–0.39 Tmol CH_4-C/year—an addition that increases the current global marine CH_4 budget by more than 60%. The majority (~45%) of this increase is driven by mangrove CH_4 fluxes. While organic matter content and quality were commonly reported in individual studies as the most important environmental factors driving CH_4 flux, they were not significant predictors of CH_4 flux when data were combined across studies. Salinity was negatively correlated with CH_4 emissions from salt marshes, but not seagrasses and mangroves. Thus, the available data suggest that other environmental drivers are important for predicting CH_4 emissions in vegetated coastal systems. Finally, we examine stressor effects on CH_4 emissions from VCEs and we hypothesize that future changes in temperature and other anthropogenic activities (e.g., nitrogen loading) will likely increase

CH_4 emissions from these ecosystems. Overall, this review highlights the current and growing importance of VCEs in the global marine CH_4 budget.

1. Introduction

Methane (CH_4) is a potent greenhouse gas with a global warming potential (GWP) 32x that of carbon dioxide (CO_2) and a sustained flux GWP 45x that of CO_2 at a 100 year timescale (Neubauer & Megonigal, 2015). Atmospheric CH_4 concentrations have been increasing since the industrial revolution (Etheridge, Steele, Francey, & Langenfelds, 1998; Turner, Frankenberg, & Kort, 2019). Recently rates of CH_4 increase in the atmosphere have accelerated from a stagnant period of 0.5 ± 3.1 ppb/year in 2000–2006 to ~10 ppb/year in 2014–2017 (Dlugokencky, Nisbet, Fisher, & Lowry, 2011; Nisbet et al., 2019; Saunois, Jackson, Bousquet, Boulter, & Canadell, 2016). About two-thirds of the total global CH_4 emissions can be attributed to human activity (e.g., agriculture, sewage and landfill waste, fossil fuel consumption; Saunois et al., 2016).

Vegetated coastal ecosystems (VCEs; i.e., mangroves, salt marshes, and seagrasses) play a critical role in global carbon (C) cycling (McLeod et al., 2011). They are highly productive ecosystems, taking up CO_2 from the atmosphere, and they are effective at capturing organic matter (OM) from terrestrial and marine environments (Gacia & Duarte, 2001; Gacia, Granata, & Duarte, 1999; Hendriks, Sintes, Bouma, & Duarte, 2008). However, the same qualities that make these systems effective at sequestering C may also make them “ideal” environments for methanogenesis to occur—for example, their sediments are rich in OM, often anoxic, and occasionally low in sulfate

due to variable freshwater–saltwater inputs (Martens & Berner, 1974). CH_4 emissions are an understudied component of C budgets for VCEs and have the potential to turn these systems into net C sources instead of sinks (Eong, 1993; Pendleton et al., 2012). Although CH_4 emissions from forested and wetland (including mangrove and salt marsh) ecosystems have been reviewed previously (Bartlett & Harriss, 1993; Bridgham, Cadillo-Quiroz, Keller, & Zhuang, 2013), they did not specifically address coastal ecosystems or include seagrass-dominated systems in their analysis. This review fills this knowledge gap.

Here we review CH_4 emissions from VCEs. We first examine variability in sampling techniques and temporal scales used in the studies through a literature review. We then determine the median global CH_4 flux from each VCE and we assess the environmental characteristics driving these emissions through meta-analysis and a literature review. We then estimate the amount of C lost via CH_4 emissions from each VCE. We also discuss the impact of CH_4 emissions on net C burial estimates and the global marine methane budget. Finally, we consider the impact of environmental and anthropogenic stressors on CH_4 emissions.

Throughout this synthesis we argue that VCEs should be included in the marine, and not the terrestrial, CH_4 budget. This review is timely because there is a growing emphasis on understanding C cycling and quantifying C sequestration potential in marine ecosystems (e.g., Benway et al., 2016; Fennel et al., 2019). Blue carbon (i.e., carbon buried in marine systems) has been identified as a way to sequester large amounts of C while simultaneously restoring lost and degraded ecosystems (Duarte, Middelburg, &

Caraco, 2005; McLeod et al., 2011; Nellemann et al., 2009). Without quantifying the C lost from VCEs via CH_4 emissions, however, we are potentially missing an important component of the marine CH_4 budget and we are unable to constrain the impact of these systems on the global climate.

2. Studies reviewed

Before beginning our literature search, we defined "marine" as stated in Cowardin, Carter, Golet, and LaRoe (1979), which includes the open ocean, continental shelf, and coastline to the inland limit of tidal inundation where the salinity is ≥0.5 ppt. We binned the data according to the salinity categories presented in Cowardin et al. (1979): oligohaline (0.5–5 ppt), mesohaline (5–18 ppt), polyhaline (18–30 ppt), and euhaline (≥30 ppt).

To find the literature used in this analysis, we used the "Advanced Search" feature on Google Scholar and we included other literature cited within these papers that were not returned in the Google Scholar search results for a total of 97 studies (54 mangrove, 40 salt marsh, and 8 seagrass; Al-Haj & Fulweiler, 2020) reviewed here. Down-selection methods are described in detail in Supporting Text 1.1 in Data S1.1 (Figure S1.1). We collected the mean air–sea/air–sediment methane flux, maximum and minimum methane flux, and average site salinity, as well as vegetation genus and species from each site within each study. Mean CH_4 flux was collected because the majority of studies did not report median and/or only reported the mean flux for each site (Supporting Text 1.2 in Data S1.1). When available, we collected the average sediment %C, %N, C:N, %OM, the

average water column and sediment chemical composition (nitrate, nitrite, ammonia, ortho-phosphate, sulfate, and sulfide), net ecosystem productivity (NEP), and biomass from each site within each study. As needed, we converted all methane flux data to μmol CH_4 m^{-2} day^{-1} scaling by 24 hr.

Within each study, individual flux observations were identified as the mean flux for each site over the time period presented in the study for a total of 110 mangrove fluxes, 85 salt marsh fluxes, and 28 seagrass fluxes. All studies estimate CH_4 flux on a per area basis. Time periods were highly variable across studies, with studies spanning hours to years, but to simplify the analysis, time periods presented in each study were combined. These published studies are limited in their temporal and global extent (Figure 1.1a–c). For example, greater than 75% of the mangrove CH_4 flux data points were located in the eastern hemisphere mostly clustered in southeast Asia and China. Although the largest percentage of mangroves are found between 5°N and 5°S latitude (Giri et al., 2011), ~90% of the fluxes came from areas of higher latitude (Figure 1.1a). All but one salt marsh CH_4 flux was from the northern hemisphere despite the existence of extensive salt marshes in South America, Australia, and Africa (Saintilan, Wilson, Rogers, Rajkaran, & Krauss, 2014). Seagrass data were mostly concentrated in Africa and Europe (Figure 1.1a) even though seagrasses are found in shallow waters of all oceans (Short, Carruthers, Dennison, & Waycott, 2007). There is also a temporal bias with a majority of the temperate data points collected during the summer. Because we gave equal weight to studies with multiseasonal flux measurements and those with singular flux

measurements, the lack of winter data may cause overestimates of CH_4 fluxes from temperate ecosystems.

2.1 Sampling techniques

CH_4 emissions were measured in several different ways across the studies: static chambers in the field and laboratory, continuous measurements from flow-through incubations, eddy flux, floating chambers, and discrete water and air samples. The static chamber method was most commonly used making up 65% of all measurements. This involves placing a clear or opaque airtight chamber in the sediment and taking discrete gas or water samples from the headspace of the chamber over a known time period to calculate the flux (e.g., Emery & Fulweiler, 2014; Foster & Fulweiler, 2016; Livingston & Hutchinson, 1995). CH_4 concentration in these samples is then typically measured via gas chromatography (Weiss, 1981). About 10% of the studies also used flow-through chambers, where air or water is continuously pumped through the chamber, paired with a cavity ring down spectrometer (CRDS) for CH_4 concentration measurements (Bahlmann et al., 2015; Garcias-Bonet & Duarte, 2017). To determine the water–air flux, floating chambers were used in a similar fashion as the static chambers (Chuang et al., 2017) or water–air fluxes were calculated using empirical relationships that determine the flux from CH_4 concentrations in discrete water and air samples (Dutta, Bianchi, & Mukhopadhyay, 2017; Raymond & Cole, 2001). Finally, eddy flux towers integrate gas fluxes over large areas (Aubinet, Vesala, & Papale, 2012). Eddy flux towers are commonly used for CO_2 fluxes in salt marshes (e.g., Forbrich, Giblin, & Hopkinson,

2018; Holm et al., 2016; Krauss et al., 2016). We found one study using eddy flux towers to measure salt marsh CH_4 emissions (Negandhi et al., 2019), two studies for mangroves (Ganguly, Dey, Mandal, De, & Jana, 2008; Jha, Rodda, Thumaty, Raha, & Dadhwal, 2014), and none for seagrasses. In salt marsh and seagrass systems, median CH_4 flux did not differ among sampling techniques. However, in mangrove ecosystems, median methane flux was significantly lower when CRDS was used as opposed to the static chamber or discrete water and air sampling techniques (Kruskall–Wallis, $p = .013$; Table S1.3).

All sampling techniques introduce some bias into measurements and thus our understanding is also biased. The methods used for quantifying CH_4 fluxes are no different. Well known, and discussed in detail elsewhere, are the impacts of gas transfer equations and wind data type used for the discrete water sampling method (Murray, Erler, & Eyre, 2015; Raymond & Cole, 2001; Rosentreter et al., 2017; Zhang, Zhang, Liu, Ren, & Zhao, 2010). Static chamber incubations generally do not account for pulsed events such as ebullitive fluxes. Furthermore, in static chamber incubations gas concentrations should increase or decrease linearly over time, if they do not, high points may be discounted or may skew the flux higher and nonlinear fluxes are often designated as a net zero flux (Banta, Giblin, Hobbie, & Tucker, 1995; Heiss, Fields, & Fulweiler, 2012). During flow-through chamber incubations the continuous measurements allow these events to be captured and included in flux calculations (Bahlmann et al., 2015). If ebullition is common in VCEs, the static chamber method could under- or overestimate CH_4 fluxes depending on the method used for flux detection. For example, the highest

CH_4 flux from mangrove ecosystems was measured using continuous NDIR measurements from a floating chamber (Yang, Yuan, Huang, Tong, & Yang, 2018). This flux was 2x higher than the highest flux using the static chamber method (Welti, Hayes, & Lockington, 2017). However, median mangrove flux measured via CRDS was significantly lower than the static chamber and discreet water sampling methods (Table S1.3). Given the lack of ancillary data, it is hard to interpret these results. Perhaps the static chamber and discreet water sampling methods overestimate CH_4 emissions or perhaps there are other factors that correlate with the chosen method.

2.2 Temporal scales

Both long (e.g., annual, interannual) and short (e.g., hourly, daily) temporal scales of the available flux data are important to consider. Logistical and financial constraints as well as ecological theory (e.g., metabolism scales with temperature, Gillooly, Brown, West, Savage, & Charnov, 2001; Yvon-Durocher et al., 2014) often encourage sampling during warm seasons at low tide. Most of the studies from temperate ecosystems did not include winter sampling (e.g., Chmura, Kellman, & Guntenspergen, 2011; Emery & Fulweiler, 2017; Hirota, Senga, Seike, Nohara, & Kunii, 2007). Of the few that did include winter sampling, most found that CH_4 flux varied seasonally, with lower CH_4 fluxes during winter when plant productivity was at its lowest (Atkinson & Hall, 1976; Bartlett, Harriss, & Sebacher, 1985; Emery & Fulweiler, 2014; King & Wiebe, 1978). One study found no difference in CH_4 fluxes across seasons (Ford, Garbutt, Jones, & Jones, 2012). Because of the difficulties of winter sampling, most studies that did

measure CH_4 flux during the winter did so infrequently. Diefenderfer, Cullinan, Borde, Gunn, and Thom (2018) measured CH_4 flux continuously in the winter and demonstrated that CH_4 emissions remain low over extended periods of time in winter, but continuous measurements are needed to capture diurnal variability which can switch a system from a CH_4 sink to a source.

In temperate ecosystems, winter temperatures are highly variable with warm temperature anomalies becoming more frequent (Guirguis, Gershunov, Schwartz, & Bennett, 2011). In temperate Australia, such winter events can increase air temperature by up to 10°C (Cowan et al., 2014) while in the northern hemisphere, they can increase air temperature by >20°C (Dole et al., 2014; Guirguis et al., 2011). There is currently no information documenting the impact of winter/spring heat waves on CH_4 fluxes in temperate VCEs. Yet evidence from a temperate freshwater marsh suggests that CH_4 emissions increase during these events (Chu et al., 2014). If CH_4 flux in VCEs also increases with temperature during winter/spring heat waves, then the yearly contribution of CH_4 from temperate VCEs could be underestimated.

Seasonal differences in aboveground biomass are also important to consider when scaling CH_4 fluxes by temperature (Emery & Fulweiler, 2014). For example, spring and fall often have the same temperature range, but studies that measured CH_4 flux during both seasons in salt marsh and mangrove systems found that fluxes were higher, although not always significantly, during spring than fall likely due to higher availability of labile OM when the growing season begins (Emery & Fulweiler, 2014; Ford et al., 2012; Livesley & Andrusiak, 2012). Because of this, simply scaling CH_4 fluxes using a

temperature relationship derived during summer months may not be an accurate annual CH_4 emission estimate (Bartlett & Harriss, 1993).

In VCEs, CH_4 emissions change over the tidal cycle with patterns differing in intertidal and subtidal areas (Bahlmann et al., 2015; Deborde et al., 2010; Emery, Angell, & Fulweiler, 2019; Kristensen et al., 2008; Mukhopadhyay et al., 2002). In intertidal systems, CH_4 emissions peaked as water was arriving at the site (Bahlmann et al., 2015; Middelburg et al., 1996) and tidal phase has been identified as a driver of CH_4 flux (Emery et al., 2019). In subtidal systems, the opposite pattern was true—sediment–water column CH_4 flux increased when the tide was falling (Deborde et al., 2010). Over a longer time scale, Emery et al. (2019) found that in a sandy salt marsh, CH_4 fluxes were higher under spring tides compared to neap tides likely due to higher soil water content during spring tide. Physical forcing is also a driving force in CH_4 emissions over the tidal cycle. In intertidal systems, CH_4 is pushed out of the sediment during peak tidal influx (Bahlmann et al., 2015). In subtidal systems, as water levels fall, pressure gradients within the sediments change, increasing CH_4 flux into the water column and atmosphere (Deborde et al., 2010; Santos et al., 2009).

Tidal pumping of groundwater can increase water column CH_4 concentrations (e.g., Cable, Bugna, Burnett, & Chanton, 1996; Kim & Hwang, 2002; Santos et al., 2009). CH_4 concentrations are usually higher in groundwater than in receiving waters (Cable et al., 1996). Groundwater CH_4 concentrations are high when groundwater is anoxic and is fed by a carbon and nitrogen source, such as wastewater (Slomp & Van Cappellen, 2004).

CH_4 is transported from the sediment into the water column, and ultimately the atmosphere, by three different processes: diffusion, advection, and ebullition (Reeburgh, 2007). As described above, traditional methods for measuring CH_4 flux (e.g., static flux chambers, eddy covariance) do not allow us to differentiate between transport mechanisms and may miss the nonlinear changes in CH_4 flux that are often signs of ebullition. Ebullitive flux may be a significant, yet largely unconstrained, portion of the air–sea CH_4 flux (Leifer & Patro, 2002).

Although several of the reviewed studies include measurements of CH_4 fluxes over several seasons and/or tidal cycles (Adams, Andrews, & Jickells, 2012; Bahlmann et al., 2015; Diefenderfer et al., 2018; Emery & Fulweiler, 2014; Li, Wang, et al., 2018), none of these studies continuously measure CH_4 flux over multiple annual cycles to capture changes driven by climate that may otherwise be missed. Continuous measurements of CH_4 flux over several years, daily and/or several times a season with greater spatial coverage, would help increase the accuracy of CH_4 flux estimates from VCEs as is shown in terrestrial systems (Ueyama et al., 2015). Recent sensor developments are making ebullition measurements possible (Maher, Drexl, Tait, Johnston, & Jeffrey, 2019).

3. Median methane fluxes

On average, VCEs are net CH_4 emitters (net uptake of −92.6 to a net efflux of 164,588.5 μmol CH_4 m^{-2} day^{-1}, Table 1.1; Figure 1.2). However, we do not include the highest observation in any further analysis because this was the only observation that

used NDIR (Yang et al., 2018) and other measurements from the same site using static chamber methods report lower fluxes (0–672.48; Gao et al., 2018; Zheng et al., 2018). Overall median CH_4 fluxes from the VCEs are low (mangrove: 279.17 μmol CH_4 m^{-2} day^{-1}, salt marsh: 224.44 μmol CH_4 m^{-2} day^{-1}, seagrass: 64.80 μmol CH_4 m^{-2} day^{-1}). In systems adversely impacted by humans, however, CH_4 emissions increased by 1–2 orders of magnitude (1.1×10^4 to 1.64×10^5 μmol CH_4 m^{-2} day^{-1}; Konnerup, Betancourt-Portela, Villamil, & Parra, 2014; Purvaja & Ramesh, 2000, 2001; Welti et al., 2017; Yang et al., 2018). Median reported CH_4 fluxes varied significantly by ecosystem (Kruskall–Wallis, $p < .001$; Table 1.1) with seagrass median flux >70% lower than salt marsh and mangrove median fluxes.

4. Drivers

The net flux of methane to the atmosphere is the net flux of methane produced (methanogenesis) minus the amount of methane that is either consumed (methanotrophy) or chemically oxidized before reaching the atmosphere. There are many pathways for CH_4 consumption and production (e.g., acetoclastic methanogenesis, methylotrophic methanogenesis, anaerobic oxidation of methane, sulfate reduction, aerobic oxidation; Costa & Leigh, 2014; Reeburgh, 2007). The studies reviewed here most often discuss competition between sulfate reducers and methanogens for OM and methane oxidation by sulfate reducers as the main factors determining biological CH_4 emission (Biswas, Mukhopadhyay, Sen, & Jana, 2007; Garcias-Bonet & Duarte, 2017; Magenheimer, Moore, Chmura, & Daoust, 1996; Sun et al., 2013). Although geological sources of CH_4

(e.g., cold-seeps, mud volcanoes) are common in marine environments (Kvenvolden & Rogers, 2005), they are not considered important in VCEs and are not discussed here.

We used Pearson correlations to examine environmental drivers of CH_4 fluxes across the reviewed studies. We were unable to conduct other statistical analyses (e.g., multiple linear regression) because studies did not report similar site characteristics or ancillary data.

4.1 Organic Matter

A common theme in the studies reviewed here is the role of OM availability as the main environmental factor controlling methanogenesis. Abundant OM in the sediments can reduce competition between sulfate reducers and methanogens by providing more competitive substrate and/or providing more noncompetitive substrate for methanogenesis (King, 1984; Reeburgh, 2007; Zhuang et al., 2018). Vegetated habitats typically have higher sediment OM concentrations compared to sediments without vegetation (e.g., Banerjee et al., 2018; Marinho, Campos, Guimarães, & Esteves, 2012; Yuan et al., 2015). Generally, there is a reported increase in CH_4 emissions in vegetated compared to nonvegetated areas (e.g., Bahlmann et al., 2015; Wang et al., 2016). When plants are photosynthesizing, they deposit labile OM into the sediment around their roots or rhizosphere (Blaabjerg & Finster, 1998; Holmer, Andersen, Nielsen, & Boschker, 2001), thereby providing a substrate to stimulate CH_4 production (Bridgham et al., 2013). The abundance of labile OM in VCEs is thought to be the driver for CH_4 emissions from these systems. For example, there is a positive linear relationship between CH_4

production rates and concentration of labile OM in salt marsh and mangrove sediments (e.g., Giani, Bashan, Holguin, & Strangmann, 1996; Gonsalves, Fernandes, Fernandes, Kirchman, & Bharathi, 2011; Xiang, Liu, Ding, Yuan, & Lin, 2015). Additionally, in these same ecosystems, experimental manipulations show increasing CH_4 production when labile OM is added to sediments (e.g., Oremland, Marsh, & Polcin, 1982; Zhuang et al., 2018). The positive impact of OM on CH_4 emissions was not universal. Several studies reported no relationship (e.g., Chauhan, Datta, Ramanathan, & Adhya, 2015; Emery & Fulweiler, 2014). When combined across studies and within and across ecosystems, we found no statistically significant relationship between %OM and CH_4 flux and no relationship between C:N and CH_4 flux (Table 1.2; Figure 1.3a,b). These statistical results may be a product of low sample number and simple correlations can obstruct the complex ecological relationships driving CH_4 emissions in vegetated systems.

4.2 Plant-mediated transport

Many types of vegetation emit CH_4 by transporting it from the sediment into the atmosphere through aerenchyma (Laanbroek, 2010). For example, CH_4 flux in mangroves is positively correlated with the number of tree pneumatophores (Krithika, Purvaja, & Ramesh, 2008; Livesley & Andrusiak, 2012; Purvaja, Ramesh, & Frenzel, 2004). A recent study reported 26% of the CH_4 emissions from a mangrove ecosystem came via the trees themselves (Jeffrey et al., 2019). In salt marshes, there is evidence that some plants (e.g., *Juncus* spp.) transport more CH_4 than other plants (Ford

et al., 2012; Magenheimer et al., 1996; Roslev & King, 1996). Furthermore, there is evidence that freshwater submerged macrophytes transport CH_4 through their aerenchyma (Sorrell & Downes, 2004). To date, there is no direct evidence that seagrasses transport CH_4 through their aerenchyma but this might be a yet unconstrained transport mechanism in these plants as well.

Given the above, plant biomass should, at least in theory, be positively correlated with CH_4 flux. This hypothesis is supported by several individual studies from salt marsh (e.g., Cheng et al., 2007; Hirota et al., 2007; Li, Wang, et al., 2018; Wang et al., 2019) and mangrove ecosystems (Alongi et al., 2008). There is currently no evidence of a similar relationship in seagrass ecosystems. When we combined the limited data on biomass and CH_4 fluxes from the studies reviewed here we found no relationship between biomass and CH_4 flux across or within vegetation types (Table 1.2). We also examined the relationship between CH_4 flux and NEP (the difference between gross primary production and net ecosystem respiration). NEP is considered a better predictor of productivity as it captures biomass production and consumption over a longer time period (i.e., is a reflection of the metabolism of an ecosystem) through CO_2 or O_2 flux while biomass is a static measurement. Of the studies that reported net ecosystem exchange or NEP, most did not test the relationship between CH_4 flux and NEP and the four studies that did reported mixed results (Bahlmann et al., 2015; Banerjee et al., 2018; Wilson, Mortazavi, & Kiene, 2015; Yuan et al., 2015). Not surprisingly then, when combining data across systems we found no relationship between NEP and CH_4 flux (Table 1.2).

Of course, there might not be a simple positive linear relationship between plants and CH_4 flux because more plant biomass will not only increase OM, but will also increase oxygen availability in the system via root bioturbation and oxygen pumping (Caffrey & Kemp, 1991; Holmer, Gribsholt, & Kristensen, 2002; Howes & Teal, 1994; Pedersen, Borum, Duarte, & Fortes, 1998; Pi, Tam, Wu, & Wong, 2009; Scholander, van Dam, & Scholander, 1955). This oxygen may then stimulate methane consumption via aerobic oxidation (Reeburgh, 2007; Timmers et al., 2017). For example, although vegetated areas in seagrass ecosystems have higher CH_4 emissions than areas without vegetation (Bahlmann et al., 2015), when photosynthesis is abruptly stopped by trimming seagrasses, CH_4 emission increases indicating reduced CH_4 oxidation (Lyimo et al., 2018). The same pattern has been found in mangrove forests that experienced recent deforestation (Giani et al., 1996). Night photosynthesis cessation provides another opportunity to examine the role of O_2 availability in driving CH_4 emissions. Reviewed studies reporting continuous measurements over several days have found varying results. The one seagrass study that measured methane flux continuously for a few days reported maximum CH_4 emissions at night indicating that CH_4 oxidation was reduced (Bahlmann et al., 2015). In contrast, maximum mangrove and salt marsh CH_4 emissions can occur during the day (Yang et al., 2018), at night (Diefenderfer et al., 2018), or exhibit no diurnal cycle (Jha et al., 2014; Li, Dai, et al., 2018). Length of measurement period may play a role in these results as studies that measured CH_4 fluxes over an entire year did not find clear diurnal patterns (Jha et al., 2014; Li, Dai, et al., 2018), while studies performed

over a few days noted diurnal differences in CH_4 flux (Bahlmann et al., 2015; Diefenderfer et al., 2018; Yang et al., 2018).

4.3 Salinity

Salinity has long been offered as a key controller of CH_4 emissions in salt marshes and mangroves (Bartlett, Bartlett, Harriss, & Sebacher, 1987; Lu, Wong, Tam, Ye, & Lin, 1999; Magenheimer et al., 1996; Poffenbarger, Needelman, & Megonigal, 2011; Purvaja & Ramesh, 2001). Salinity is a good proxy for sulfate availability which affects the rate of hydrogenotrophic and acetoclastic methanogenesis and methanotrophy. The competition between sulfate reducers and hydrogenotrophic and acetoclastic methanogens for organic substrates has been documented extensively, with sulfate reducers outcompeting methanogens in ecosystems with limited OM supply (Oremland & Taylor, 1978; Winfrey & Ward, 1983). This effect can be seen in vertical profiles of sediment CH_4 and sulfate concentrations (Martens & Berner, 1974). Salinity is negatively correlated with the log of CH_4 emissions across all ecosystems combined, and in salt marsh and mangrove ecosystems alone; but there is no correlation in seagrass ecosystems (Table 1.2). However, the predictive power of this relationship is generally low and especially so for mangroves (Figure 1.4a,b). Median reported CH_4 fluxes varied significantly by salinity category (Kruskall–Wallis, $p < .001$) with euhaline median fluxes 98%, 73%, and 85% lower than oligohaline, mesohaline, and polyhaline median CH_4 fluxes, respectively (Table S1.1; Figure S1.2). Poffenbarger et al. (2011) reported declining methane flux as salinity increases. They also noted that polyhaline marshes had

significantly lower CH_4 emissions than mesohaline and oligohaline marshes. Here we found no difference between polyhaline and oligohaline or mesohaline median CH_4 flux (Wilcoxon Rank Sum, $p > .05$). When separated by vegetation type, saltmarsh CH_4 fluxes seem to be driving the differences among salinity categories (Kruskall–Wallis, $p = .017$; Figure S1.3). These results indicate a fundamental difference between methanogenesis in salt marsh sediments and methanogenesis in seagrass and mangrove sediments. Recent studies have proposed that methanogenesis in unvegetated subtidal sediments is dominated by methylotrophic methanogens whose substrate is methyl-OM, as opposed to the sulfate-reducer competitive substrates, H_2, CO_2, and acetate, in salt marsh sediments (Lyimo, Pol, & Camp, 2002; Zhuang et al., 2016, 2018). Perhaps seagrass and mangrove sediments are also dominated by methylotrophic methanogenesis.

4.4 Temperature

CH_4 emissions are generally higher during warmer seasons (e.g., Allen, Dalal, Rennenberg, & Schmidt, 2011; Emery & Fulweiler, 2014), due to increased microbial activity at higher temperatures (Yvon-Durocher et al., 2014). While we did find evidence that CH_4 emission increases with temperature in salt marsh systems, we found no statistically significant correlation between CH_4 emission and mean annual temperature, expressed as the absolute value of latitude, across or within mangrove and seagrass ecosystems from the reviewed literature (Table 1.2). While CH_4 production increases during warmer seasons, there is evidence that CH_4 consumption does not (Bartlett & Harriss, 1993; Dubey, 2005; Le Mer & Roger, 2001; Parashar, Gupta, Rai, Sharma, &

Singh, 1993). We propose that CH_4 fluxes are likely driven by site-specific environmental parameters that increase or decrease methane production and consumption differently, leaving temperature alone as a poor predictor of CH_4 fluxes.

5. Global Estimates

Previous estimates of total CH_4 emissions from VCEs have involved upscaling direct CH_4 flux measurements from a few field sites within these environments (e.g., Chauhan, Ramanathan, & Adhya, 2008; Garcias-Bonet & Duarte, 2017). These estimates multiply mean flux from a few studies by estimates of the global extent of each ecosystem. Few have yet done a comprehensive review to calculate global CH_4 fluxes for each ecosystem using all available studies, like we attempt in this review (Bartlett & Harriss, 1993). Although our estimates are the most comprehensive and globally distributed to date, our dataset, and thus our understanding, is still limited in geographic and temporal extent with data largely lacking in the southern hemisphere and sampling in temperate regions mostly restricted to summer months. We hope this review acts as a clear call to action to measure CH_4 fluxes in more locations and throughout the year.

Here we scale local CH_4 emissions from all available studies by the estimated global surface area of each ecosystem type. As mean flux was most often reported in the literature, we use the mean values of observed CH_4 flux ranges, when available. If mean CH_4 flux was not reported, we calculated mean CH_4 flux based on the reported data. The mean of these data was multiplied by the most recent maximum and minimum estimated

areal extent of the respective ecosystem type (Supporting Text 1.3 in Data S1; Duarte, 2017; Hamilton & Casey, 2016; Mcowen et al., 2017).

Using the mean CH_4 flux and the reported range of areal extent (13.7 and 15.2 Mha worldwide; Giri et al., 2011; McLeod et al., 2011; Pendleton et al., 2012; Spalding, 2010), we calculated a global range of mean CH_4 flux of 0.23–0.25 Tmol CH_4–C/year from mangrove forests (Table 1). McLeod et al. (2011) estimate that mangroves bury 2.59–2.86 Tmol C/year. Here we find that CH_4 emissions would offset mangrove C burial by ~9%. Including mangrove ecosystems in the global marine CH_4 budget, currently estimated at 0.57 Tmol/year (EPA, 2010), would increase marine CH_4 emissions by ~45% (Supporting Text 1.4 in Data S1.1).

Salt marsh global area is estimated at about 5.5 Mha (Davidson & Finlayson, 2019; Mcowen et al., 2017). This is a conservative estimate only considering areas mapped and does not include unmapped saltmarsh in the Arctic (Mcowen et al., 2017). Using this areal estimate, we estimate a salt marsh mean CH_4 flux of 7.10×10^{-2} Tmol CH_4-C/year (Table 1). McLeod et al. (2011) report that salt marshes bury 18.15 ± 2.00 mol C m^{-2} $year^{-1}$. Scaling up to the most recent global estimate of salt marsh areal extent, salt marshes bury 1.00 ± 0.11 Tmol C/year. Including salt marsh CH_4 emissions in this estimate would offset C burial by ~7%. Overall mean salt marsh CH_4 emissions make up a small amount of the global marine CH_4 budget and including them would increase the budget by ~13%.

Seagrasses cover from 78.8 to 164.7 Mha of area worldwide (Davidson & Finlayson, 2019; Jayathilake & Costello, 2018). Across seagrass studies mean CH_4 flux

ranged from 3.11×10^{-2} to 6.51×10^{-2} Tmol CH_4-C/year (Table 1.1)—the lowest estimates from the reviewed VCEs. Seagrasses bury between 9.05 and 18.92 Tmol C/year (McLeod et al., 2011). CH_4 emissions could offset C burial in seagrass ecosystems by <0.5%.

Overall, we estimate that seagrass CH_4 fluxes would increase the global marine CH_4 budget by ~5%–11%. If we use the same global seagrass areal extent as Garcias-Bonet and Duarte (2017), 15–432 Mha, then, like them, we find that seagrass CH_4 emission could increase the global marine CH_4 budget between ~1% and ~30%. These large ranges in global CH_4 emissions are due to high uncertainty in areal estimates for each ecosystem and the large variability in local flux estimates, ultimately driven by a lack of data. Currently, global ground-truthed estimates of areal coverage only exist for mangroves and salt marshes which account for the smaller reported range in areal coverage (Duarte, 2017; Mcowen et al., 2017). Local flux estimates are made using many different methods and over varying spatial and temporal scales. Because of this, they may not capture the full range of CH_4 emission. In order to better estimate global CH_4 emission from VCEs, standard methods for detecting fluxes over long time periods need to be employed and areal coverage estimates should be updated regularly.

The increases in the global marine methane budget reported above for each of the VCEs are based on the the EPA (2010) global marine methane budget of 0.57 Tmol/year. In total, including VCEs would increase the global marine methane budget by 60%–70%. This may be a conservative increase as recently, Weber, Wiseman, and Kock (2019) estimated the global marine methane budget to be 0.37–0.75 Tmol/year. The inclusion of

VCEs in this recent estimate, increases the global marine methane budget by ~50%–90%. Regardless, these calculations highlight that VCEs are an important contributor to the global marine methane budget and should be included in future methane budgets.

6. Global Warming Potential

Here we compare GWP (one-time event gas flux) to sustained flux global warming potential (SGWP; persistent gas emissions; Neubauer & Megonigal, 2015). When only considering C lost and buried, VCEs remain C sinks with CH_4 emissions accounting for a large offset of buried C in salt marsh and mangrove ecosystems and a small offset in seagrass ecosystems (Table 1.1). However, when comparing C burial and CH_4 emissions in terms of GWP and SGWP the story is less favorable for mangrove and salt marsh systems. For every molecule of CO_2 buried by mangroves about four molecules of CO_2 equivalent CH_4 are released. For salt marshes, about three molecules of CO_2 equivalent CH_4 are released for every one molecule of CO_2 buried (Table 1.1). For seagrasses, only one molecule of CO_2 equivalent CH_4 is released for every six to nine molecules of CO_2 that are buried.

7. Stressor effects on CH_4 emissions from VCEs

The current literature indicates that the most important factors controlling CH_4 fluxes are OM content and quality and oxygen availability which can be affected by plant density and productivity, tidal cycles, and nutrient availability among other variables. However, these patterns were not statistically clear in this review, suggesting we may be

missing key drivers and/or are limited by sampling numbers. We anticipate, like other greenhouse gas emissions (e.g., Murray et al., 2015), anthropogenic disturbances, including nutrient loading and climate change, modify the factors controlling CH_4 fluxes in VCEs (Figure 1.5a,b).

7.1 Excess nitrogen loading

Excess N loading is one of the greatest threats to coastal ecosystems worldwide (Nixon, 1995). However, N loading is not increasing uniformly across the globe and the impact N loading has on CH_4 emissions from VCEs is unclear. Currently, N loading into coastal ecosystems is increasing in tropical and subtropical developing countries and declining in developed nations such as Europe and the United States (Breitburg et al., 2018). In tropical and subtropical areas, it is likely that mangrove and seagrass ecosystems will be most highly impacted by nutrient pollution leading to increased CH_4 emissions. For example, Purvaja and Ramesh (2001) found that CH_4 emission was enhanced when sullage, domestic sewage, and industrial effluents were dumped into coastal wetlands in Tamil Nadu, India. Others have found similar patterns in mangrove ecosystems in Brazil, Mexico, and China (Chen, Tam, Wong, & Ye, 2011; Chuang et al., 2017; Cotovicz et al., 2016; Giani et al., 1996; Nóbrega et al., 2016; Yang et al., 2018). In areas where nutrient loading has declined, such as in Europe and the United States, CH_4 fluxes are variable from salt marsh ecosystems (Emery & Fulweiler, 2014, 2017; Martin & Moseman-Valtierra, 2017). N addition experiments in salt marshes suggest that CH_4 emission is both inhibited (Martin & Moseman-Valtierra, 2017; Zhang, Ding, Cai,

Valerie, & Han, 2010) and stimulated (Irvine, Vivanco, Bentley, & Martiny, 2012; Zhang, Ding, et al., 2010) under excess N loading conditions. Zhang, Ding, et al. (2010) proposed that there are differing responses in salt marsh ecosystems due to differences in gas transport among salt marsh species with plants that are known to transport gas (e.g., *Spartina alterniflora*) having higher CH_4 emissions under excess N loading conditions than plants that do not transport gas (e.g., *Sueda salsa*). Although there are no direct studies on the impact of N loading on CH_4 emissions in seagrass ecosystems, Lyimo et al. (2018) found that high shading increased CH_4 emissions. In coastal ecosystems, N is often limited for primary production (Nixon, 1995). When N is added to these systems, phytoplankton and macroalgae bloom and block light from reaching seagrasses (McGlathery, 2001). Because of this, we hypothesize that excess N loading will increase CH_4 emissions in seagrass ecosystems as has been demonstrated in salt marsh and mangrove ecosystems (Chen et al., 2011; Irvine et al., 2012; Zhang, Ding, et al., 2010). Phytoplankton blooms also increase the amount of labile OM in sediments, potentially stimulating methanogenesis and in turn increasing CH_4 emissions from VCEs (Giani et al., 1996; Gonsalves et al., 2011; Xiang et al., 2015).

Although we could not find a direct link between N-loading and CH_4 emissions with the available data, most mangrove and salt marsh studies did qualitatively report if their site was impacted by human or industrial waste. However, median CH_4 fluxes did not differ between the reported impacted and nonimpacted mangrove and salt marsh ecosystems (Kruskall–Wallis, $p = .109$ and .576, respectively).

7.2 Hypoxia

Oxygen concentrations in coastal areas are declining globally (Breitburg et al., 2018). Many of the issues causing the decline of oxygen concentrations in the water column are related to human disturbance in coastal ecosystems. For example, increasing nutrient loading to coastal ecosystems can increase the frequency and extent of hypoxia and anoxia in coastal waters (Caballero-Alfonso, Carstensen, & Conley, 2015), loss of vegetation and benthic infauna can reduce the depth of O_2 penetration into the sediments (Burkholder, Tomasko, & Touchette, 2007; Gammal, Norkko, Pilditch, & Norkko, 2017), and rising water temperatures decrease the solubility of O_2 in water while increasing respiration (Breitburg et al., 2018). Because methanogenesis is an anaerobic process (Martens & Berner, 1974; Reeburgh, 2007), increased anoxia or hypoxia in coastal sediments may favor methanogenesis and cause a decline in aerobic methane oxidation ultimately increasing CH_4 emissions (Gelesh, Marshall, Boicourt, & Lapham, 2016; Zhang, Gilbert, et al., 2010).

In VCEs, estimating the impact of hypoxic and anoxic events on CH_4 emissions from these systems as a whole is difficult as mangroves, salt marshes, and seagrasses thrive at different levels of inundation. We hypothesize that overall low oxygen will cause an increase in CH_4 emissions. Several studies from mangrove ecosystems have found that areas experiencing hypoxia and anoxia in the water column have higher CH_4 emissions than those with oxygenated water columns (Chauhan et al., 2008; Cotovicz et al., 2016; Purvaja & Ramesh, 2000). Currently, there is no literature relating dissolved oxygen concentrations to CH_4 fluxes in salt marsh and seagrass systems. Because salt

marsh systems are only inundated for part of the day, it is likely that water column hypoxic and anoxic conditions will have a limited impact on their CH_4 emissions. For subtidal seagrass ecosystems, we can use estuarine systems to help predict the impacts of hypoxia on CH_4 emissions. Estuarine responses to hypoxia are variable with some studies finding increases in CH_4 emissions under hypoxic conditions (Gelesh et al., 2016; Ye et al., 2016) and others finding decreases in CH_4 emissions under hypoxia (Bange et al., 2010; Foster & Fulweiler, 2019). The response of a system to hypoxic events will likely depend on the availability of labile OM in the system with systems containing high concentrations of labile OM experiencing increased CH_4 emission under hypoxic conditions.

7.3 Macrophyte loss

VCEs have declined by between 25% and 50% since WWII due to anthropogenic impacts (Alongi, 2002; Mcowen et al., 2017; Waycott et al., 2009). Even though these ecosystems are net sources of CH_4, the benefits supplied by the ecosystem services VCEs provide far outweigh the cost in greenhouse gas emissions (Barbier et al., 2011; Lee et al., 2014; Nordlund, Koch, Barbier, & Creed, 2016; Shepard, Crain, & Beck, 2011). For example, VCEs provide habitat for many commercially important organisms (Cattrijsse & Hampel, 2006; Nagelkerken et al., 2008; Thayer & Stuart, 1974), stabilize coastal sediments (Carlton, 1974; Christianen et al., 2013; Friedrichs & Perry, 2001), buffer the coastline against storm surges and winds (Möller et al., 2014; Ondiviela et al., 2014; Othman, 1994), and store large amounts of C in their sediments (Alongi, 2008; Lavery,

Mateo, Serrano, & Rozaimi, 2013; Macreadie et al., 2017; McLeod et al., 2011). Currently, VCEs are sequestering more C than they emit as CH_4 (Table 1.1).

Across systems, different anthropogenic impacts that lead to loss or altering of vegetation cause increases in CH_4 emissions. For example, vegetation loss in mangrove and seagrass ecosystems increase CH_4 fluxes compared to undisturbed areas (Chen et al., 2014; Lyimo et al., 2018; Purvaja & Ramesh, 2000). Decreasing deforestation in mangrove ecosystems and propeller scarring and dredging in seagrass ecosystems may help mitigate their CH_4 emissions. In salt marsh ecosystems, predicting the impact of preventing salt marsh loss on CH_4 emissions is more difficult as results are more variable. In general salt marshes are transformed into three types of systems when they are lost or destroyed: mudflat, agricultural land, or impervious surface. When salt marshes are transformed into mudflats, we would expect CH_4 emissions to increase (Adams et al., 2012). Currently, data on CH_4 fluxes after salt marsh loss to agricultural land and impervious surfaces are too scarce to make predictions for these changes. Invasions of plant species from different areas can also impact CH_4 emissions. For example, preventing the spread of invasive *S. alterniflora* in China may lower global CH_4 emissions from salt marshes as invasive *S. alterniflora* marshes emitted ~4 and ~1.5 times more CH_4 than native *Phragmites australis* and *S. salsa* (Yuan et al., 2015; Zhang, Ding, et al., 2010).

7.4 Climate

Global climate change will continue to increase temperature, sea level, and oceanic CO_2 concentrations, change evaporation– precipitation balance, and alter wind speed (Cloern et al., 2016). Because salt marsh methane emission is positively correlated with mean annual temperature, we can estimate end of century salt marsh methane emissions with predicted 3.7°C warming (IPCC, 2014). As temperatures rise, we propose that there will be an increase in methane emission from salt marsh ecosystems of ~0.01 Tmol CH_4-C/year. As temperatures have risen over the past three decades, mangrove forests have started to migrate into salt marsh territory (Cavanaugh et al., 2019; Kelleway et al., 2016). While mangrove encroachment into salt marshes is expected to double C storage (Doughty et al., 2016), increasing area for mangrove growth may also increase CH_4 emissions. In seagrass and salt marsh systems, there will likely be range expansions of warmer climate species (Hyndes et al., 2016), but how range expansions of warm climate salt marsh and seagrass species will change CH_4 emissions remains unknown.

Sea-level rise is already having negative impacts on VCEs. Currently, there is not enough information on VCE biogeochemical responses to predict the response of CH_4 emissions to sea level rise. For example, salt marsh and mangrove ecosystems must have an appropriate sediment supply to keep up with sea level rise (Raposa, Weber, Ekberg, & Ferguson, 2017; Woodroffe et al., 2016). If all drowned salt marsh is converted into mudflats, CH_4 emissions will likely increase (Adams et al., 2012). However, there is not enough information on mangrove conversion to mudflats to determine the impact of sea level rise on mangrove CH_4 emissions. For seagrass systems, sea level rise will likely

cause seagrass loss in deeper areas and permit increased colonization in shallow areas (Davis, Harasti, Smith, & Kelaher, 2016) making it difficult to predict the impact of sea-level rise on CH_4 emissions from these systems.

Changes in precipitation regimes as well as episodic inundation and flooding in coastal ecosystems have varying effects on CH_4 emission. For example, areas that see increases in precipitation and freshwater flooding may have declines in salinity. If salinity declines in salt marsh ecosystems, we would expect to see a sharp increase in CH_4 emissions (Poffenbarger et al., 2011). Episodic inundation and flooding caused by coastal storms can severely damage VCEs causing mass mortality in some cases (Cahoon et al., 2003). In mangrove systems, mass mortality events have been shown to increase methane emissions (Jeffrey et al., 2019). In wetland and forested ecosystems, methane production and methane emissions are lower under drought conditions (Davidson, Ishida, & Nepstad, 2004; Dowrick, Freeman, Lock, & Reynolds, 2006; Freeman et al., 2002). If sediments become drier due to increased frequency of drought, we may expect to see more methane oxidation in mangrove and salt marsh ecosystems and, therefore, lower CH_4 emissions. In our dataset, mangrove forests in areas with low annual rainfall, such as the eastern coast of the Red Sea in Saudi Arabia (Almazroui, Nazrul Islam, Athar, Jones, & Rahman, 2012), have some of the lowest methane fluxes (0–13 μmol CH_4 m^{-2} day^{-1}). However, experimental evidence from temperate salt marsh ecosystems shows that 1 year of drought does not change CH_4 emissions (Emery et al., 2019).

As the climate is changing, wind speeds are changing worldwide with decreases in North America and Eastern Russia and increases in parts of Eastern Australia, Brazil,

and South Africa (Cloern et al., 2016; Jung & Schindler, 2019; Nixon et al., 2009). In general, gas transfer velocity is positively correlated with wind speed (Wanninkhof, 1992). However, the ultimate impact changing wind patterns have on CH_4 emissions from VCEs will vary with stratification. For example, historically stratified coastal systems in areas with increasing wind speeds, may experience increased mixing. If high wind speeds are more episodic, such as during storms, large pulses of CH_4 may escape during those periods as in lakes (Engle & Melack, 2000). Drops in barometric pressure, such as those accompanied by storms, have been shown to increase methane emissions from landfills (Xu, Lin, Amen, Welding, & McDermitt, 2014). If high wind speeds occur regularly, mixing of the water column could increase oxygen concentrations in the water column and sediments, thereby ultimately increasing CH_4 oxidation. Alternatively, declining wind speeds may increase stratification in coastal ecosystems (Nixon et al., 2009) making storms and other episodic mixing events periods of high methane emissions (Engle & Melack, 2000). These episodic events, such as storms, may prove to be important in driving the global marine methane budget (Shakhova et al., 2014). Currently, there is not enough information on the impact of changes in wind speed on VCEs to make reliable predictions about future CH_4 fluxes.

Increased CO_2 availability may increase the productivity of VCEs (McKee & Rooth, 2008; Rozema et al., 1991; Takahashi, Noonan, Fabricius, & Collier, 2016). As productivity increases, the availability of labile OM in the sediments should also increase. This should, in turn, increase CH_4 emissions or as observed in some studies could decrease CH_4 emissions as oxygen is pumped into roots increasing aerobic methane

consumption (Laanbroek, 2010; Lyimo et al., 2018). However, there are no current studies available which could test this hypothesis.

Although each climate change factor was discussed independently, these factors have interacting impacts on coastal ecosystems.

8. Conclusions

VCEs are a source of CH_4—emitting 0.33–0.39 Tmol CH_4-C/year. Compared to the current estimate of global natural and anthropogenic CH_4 emissions (35 Tmol CH_4/year), the flux from VCEs is small accounting for just 1.1% if we use the maximum values estimated here (Saunois et al., 2016). However, their CH_4 emissions drastically alter marine methane budgets: accounting for ~60% to ~70% of the marine emissions when using the often cited EPA (2010) marine methane budget or ~50% to ~90% of marine methane emissions when considering a more recent estimate (Weber et al., 2019).

CH_4 flux rates are highly variable across vegetation types, sites, seasons, and days, and several factors, including labile OM availability and quality, vegetation type, O_2 concentration, salinity, and groundwater, appear to drive CH_4 emissions. However, limited ancillary data from these ecosystems when CH_4 fluxes are measured have made determining global drivers exceedingly difficult.

Anthropogenic stressors such as global climate change, increased N-loading, and hypoxia are expected to increase CH_4 emissions from VCEs. Changes in coastal salinity and macrophyte cover may slightly inhibit CH_4 emission, while decreased O_2 availability

and increases in productivity due to CO2 fertilization are expected to increase rates of methanogenesis. More research is needed to untangle these relationships and better predict the impacts anthropogenic- driven changes in coastal ecosystems will have on CH_4 cycling and C cycling in general. Thus this meta-analysis is a call to action to measure methane fluxes and key environmental parameters (e.g., salinity, temperature, OM) in VCEs. Additionally, we need to conduct experiments designed to constrain drivers of these methane emissions as well as the role of anthropogenic activities on VCE methane cycling.

Table 1.1 Global CH_4 emission estimates from VCEs and their impact on global carbon cycling. Median CH_4 fluxes, global CH_4 flux estimates (Supporting Text 1.3), increase in global marine methane budget (Supporting Text 1.4), global warming potential (Supporting Text 1.5), and sustained flux global warming potential (Supporting Text 1.6) from VCEs. Values with the same lower-case letter are not significantly different.

		Mangrove	Salt marsh	Seagrass
CH_4 flux rate ($\mu mol\ CH_4\ m^{-2}\ d^{-1}$)	median	279.17[a]	224.44[a]	64.80[b]
	range	-67.33 - 72867.83	-92.60 - 94129.68	1.25 - 401.50
Areal Extent (km^2)		137760 - 152361	55000	788000 - 1646788
Global CH_4 flux rate ($Tmol\ CH_4\text{-}C\ yr^{-1}$)	mean ± SE	0.23 ± 0.01 0.25 ± 0.06	0.071 ± 0.027	0.031 ± 0.006 0.065 ± 0.012
Increase in global marine CH_4 budget (%)		40.2 - 44.5	12.5	5.4 - 11.4
Global C burial ($Tmol\ C\ yr^{-1}$)	mean ± SE	2.59 ± 0.45 2.86 ± 0.49	1.00 ± 0.11	9.05 ± 2.49 18.92 ± 5.21
Global Warming Potential ($Tmol\ CO_{2\ eq}\ y^{-1}$)		7.33 - 8.11	2.27	1.00 - 2.08
Sustained Flux Global Warming Potential ($Tmol\ CO_{2eq}\ y^{-1}$)		10.31 - 11.40	3.19	1.40 - 2.93
Global Area Source		McLeod et al. 2011	Mcowen et al. 2017	Jayathilake & Costello, 2018; Davidson & Finlayson, 2019

*Global C burial rates from McLeod et al., 2011.

Table 1.2 Relationship between VCE CH_4 fluxes and potential drivers. Significant (p-value ≤ 0.05) Pearson correlations are highlighted in bold. Italicized results indicate log transformed CH_4 flux was used for test.

Test Parameter	Vegetation Type			
	All	Mangrove	Salt marsh	Seagrass
Latitude (º)	-0.022	0.073	-0.113	0.092
Abs Lat (º) (dist from equator)	*-0.111*	*-0.055*	***-0.357***	*-0.094*
Salinity (‰)	***-0.361***	***-0.293***	***-0.493***	*-0.317*
Biomass (g m^{-2})	-0.019	-	0.283	0.166
NEP (mmol C m^{-2} d^{-1})	-0.075	-	0.008	-
OM (%)	0.258	-0.173	0.247	-
C:N	-0.057	-0.092	-0.096	-

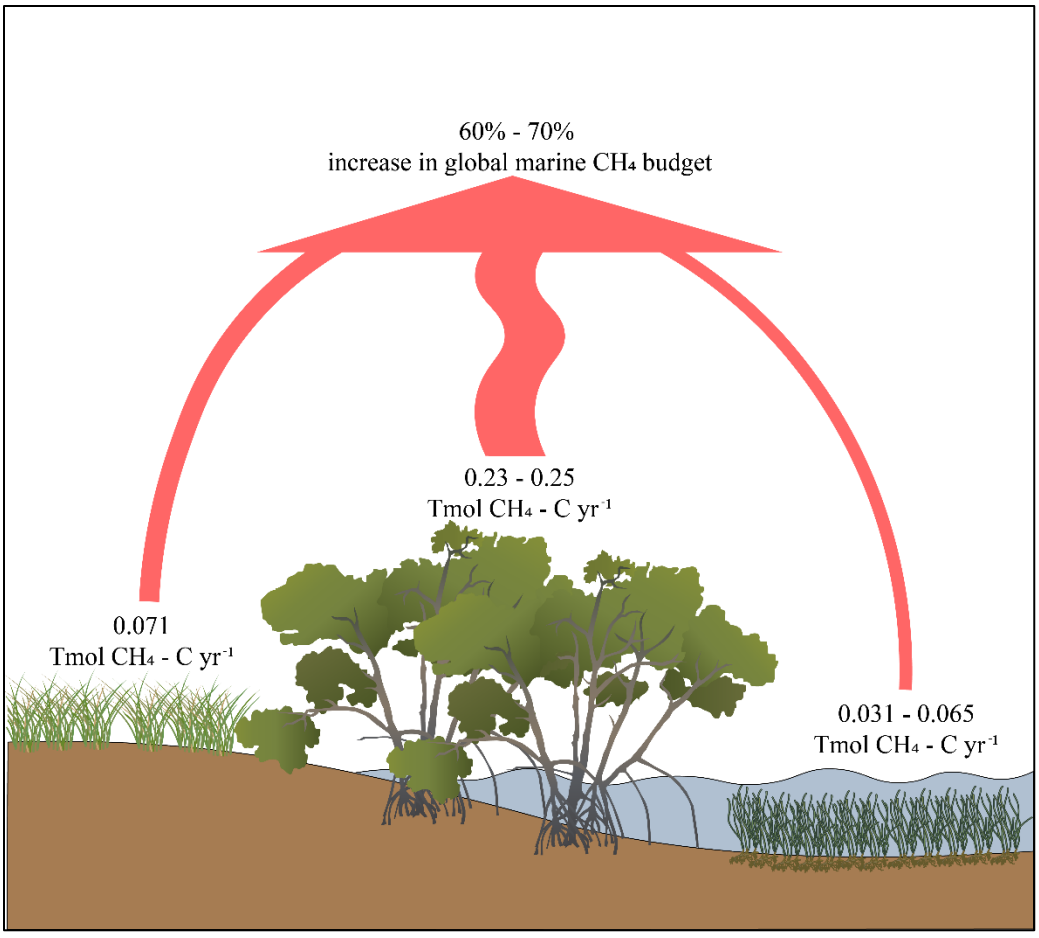

Figure 1.GA Vegetated coastal ecosystems (VCEs: mangroves, salt marshes, and seagrasses) are well-known for their carbon storage capacity. However, most studies on the carbon cycle in VCEs overlook a potentially important mechanism of carbon loss - methane emissions. Remarkably, methane emissions from VCEs are not currently included in global marine methane budget estimates. Here we show that VCEs are net methane emitters and that carbon loss through methane emissions is relatively small when compared to carbon stored. Further, we demonstrate that accounting for their methane emissions leads to a 60-70% increase in the global marine methane budget.

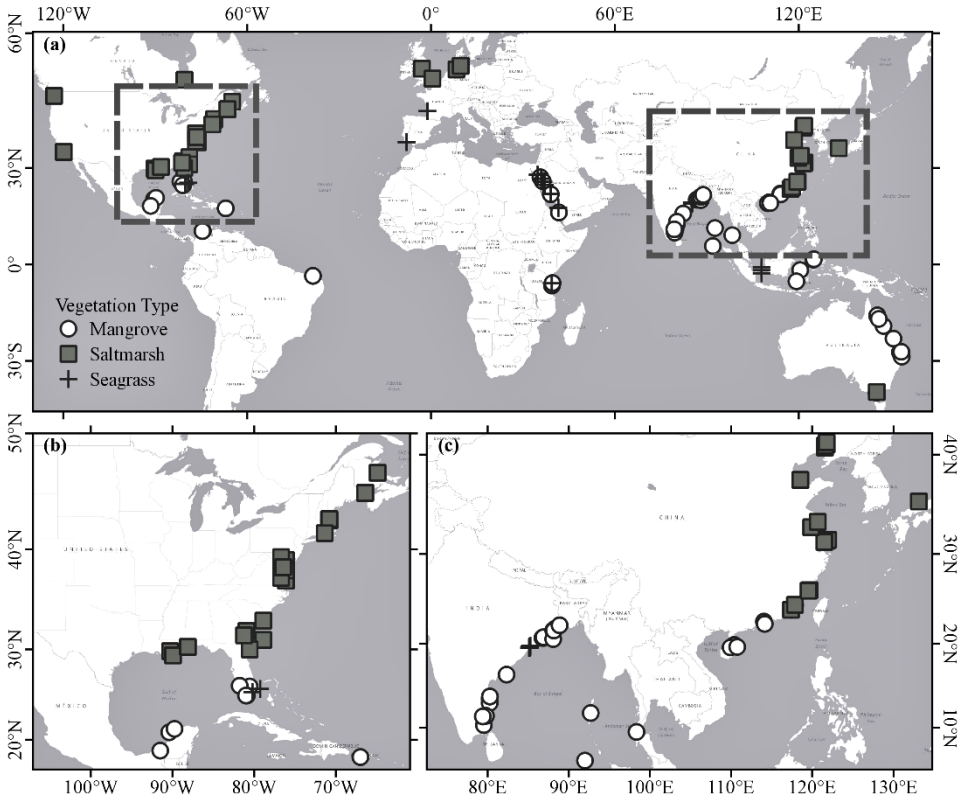

Figure 1.1 Locations of CH_4 flux measurements reviewed: (a) worldwide, (b) in the eastern United States, and (c) in Southeast Asia and Eastern Asia.

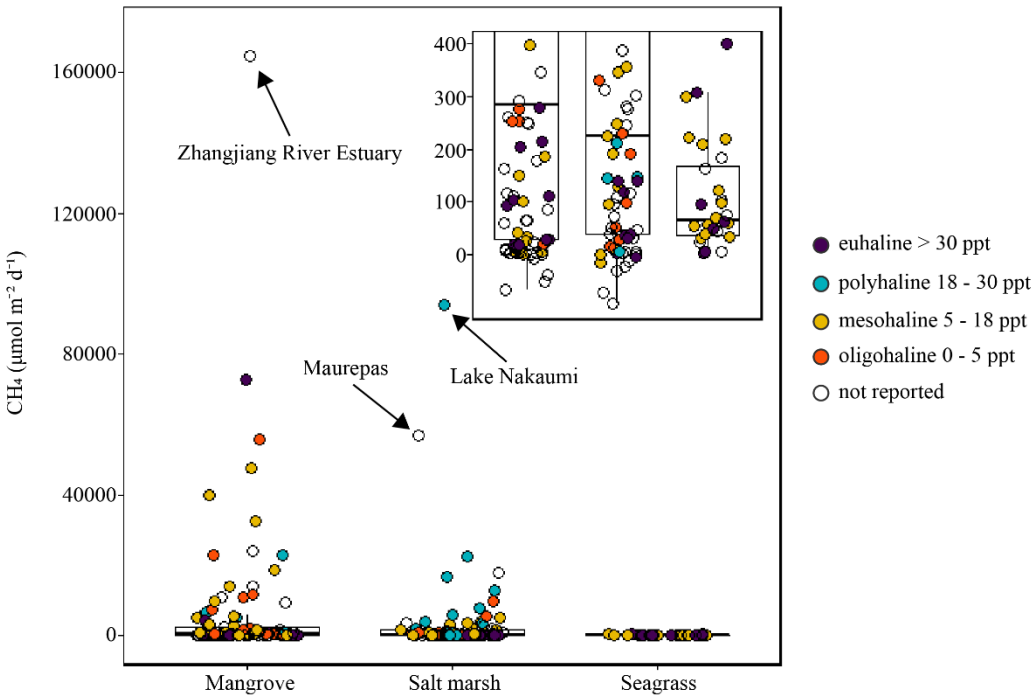

Figure 1.2 Mean CH_4 fluxes for each vegetated ecosystem type binned by salinity. Several studies did not report salinity. We name the several sites exhibiting high CH_4 fluxes. The Yang et al. (2018) Zhangjiang River Estuary observation was not included in further analysis.

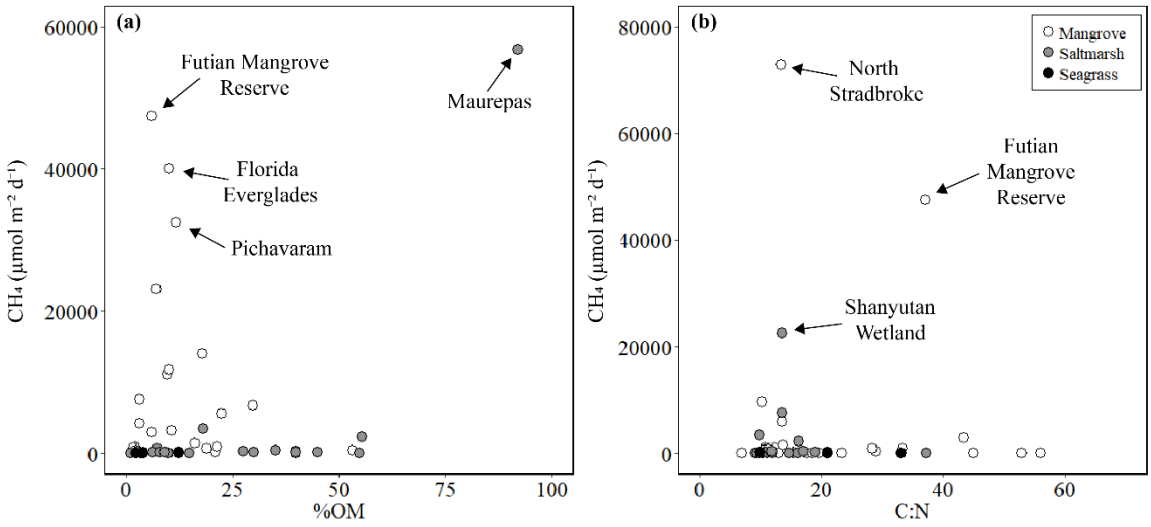

Figure 1.3 Relationships between organic matter characteristics and CH_4 fluxes: (a) CH_4 fluxes as a function of sediment organic matter content (%organic matter [OM]) and (b) sediment C:N for all vegetation types. Note that several mangrove and salt marsh sites exhibit high CH_4 fluxes given sediment OM and/or C:N values.

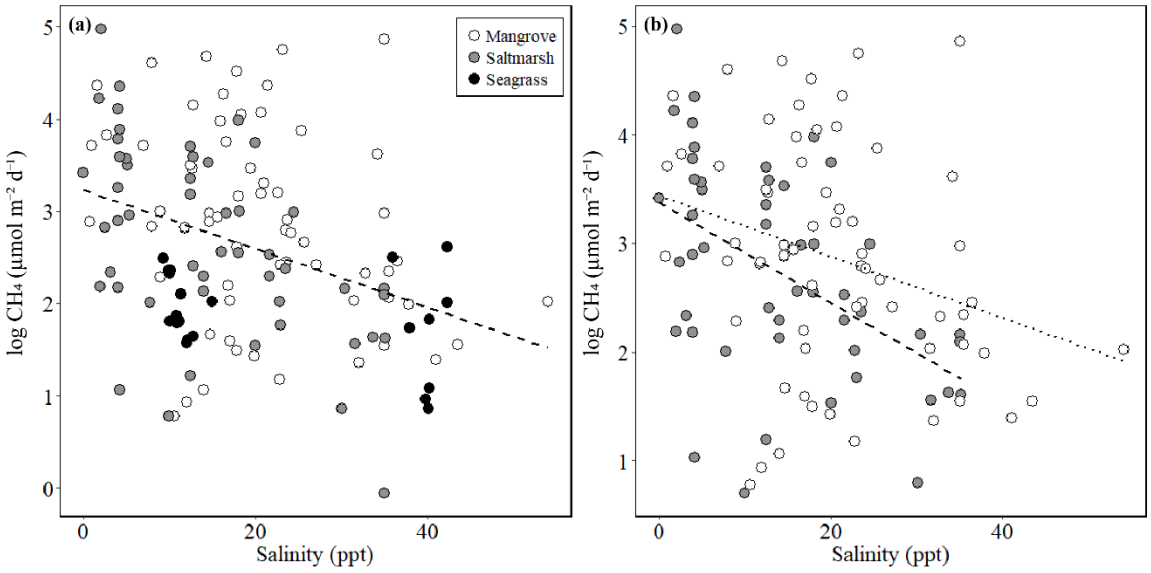

Figure 1.4 Relationship between salinity and CH_4 fluxes: (a) Salinity concentrations versus log CH_4 fluxes for all vegetation types (R^2 = .12; y = -0.03x + 3.22; p < .001) and (b) salinity concentrations versus salt marsh fluxes (R^2 = 0.23; y = -0.05x + 3.38; p < .001) and mangrove fluxes (R^2 = .07; y = -0.03x + 3.44; p = .018).

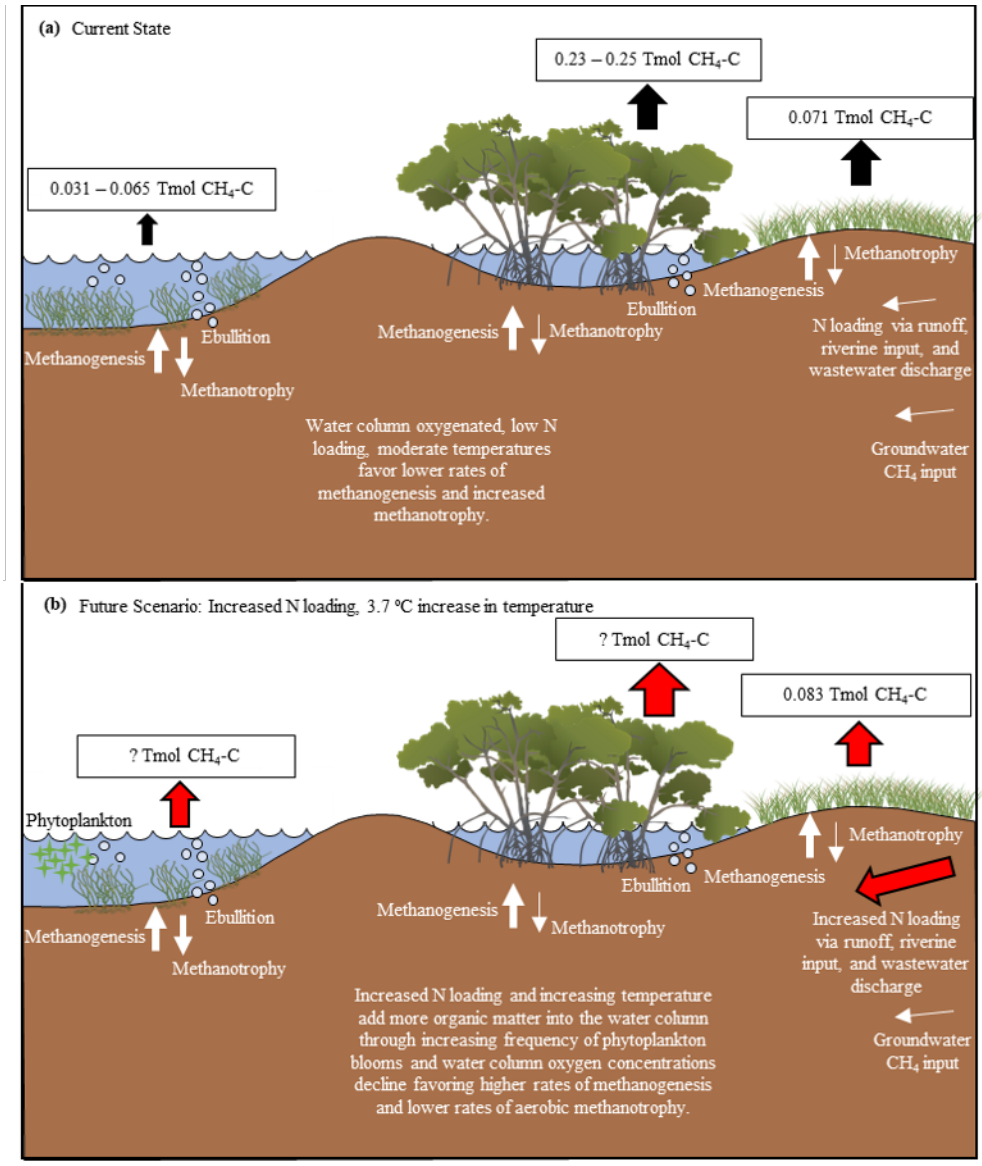

Figure 1.5 Fluxes of CH_4 (Tmol CH_4-C/year) under (a) current conditions and (b) under current trajectory for end of the century climate conditions. The future scenario considers increase in CH_4 flux due to likely increases in N loading to coastal systems and predicted 3.7 ºC warming by the end of the century (IPCC, 2014). Figure modified from Murray et al. (2015).

Acknowledgements

A.N.A. was supported through funding from Boston University through the Martin Luther King, Jr. Fellowship, the Cape Cod National Seashore Advisory Commission, Atlantic Research & Learning Center, and friends of the Cape Cod National Seashore through the Joshua A. Nickerson Conservation Fellowship. Funding from Woods Hole Sea Grant and Rhode Island Sea Grant helped support R.W.F. We would like to thank Dr. Hollie Emery for providing helpful comments on this manuscript and Dr. Alyssa Novak, Nick Ray, Claudia Mazur, Dr. Sarah Foster, and Emily Chua for their feedback.

Data availability statement

The data that support the findings of this study are openly available in “figshare” at https://doi.org/10.6084/m9.figsh are.92020 97.v1.

References

Adams, C. A., Andrews, J. E., & Jickells, T. (2012). Nitrous oxide and methane fluxes vs. carbon, nitrogen and phosphorous burial in new intertidal and saltmarsh sediments. *Science of the Total Environment*, *434*, 240–251. https://doi.org/10.1016/j.scitotenv.2011.11.058

Allen, D., Dalal, R. C., Rennenberg, H., & Schmidt, S. (2011). Seasonal variation in nitrous oxide and methane emissions from subtropical estuary and coastal mangrove sediments, Australia. *Plant Biology*, *13*(1), 126–133. https://doi.org/10.1111/j.1438-8677.2010.00331.x

Almazroui, M., Nazrul Islam, M., Athar, H., Jones, P. D., & Rahman, M. A. (2012). Recent climate change in the Arabian Peninsula: annual rainfall and temperature analysis of Saudi Arabia for 1978-2009. *International Journal of Climatology*, *32*(6), 953–966. https://doi.org/10.1002/joc.3446

Alongi, D. M. (2002). Present state and future of the world's mangrove forests. *Environmental Conservation*, *29*(3), 331–349. https://doi.org/10.1017/S0376892902000231

Alongi, D. M. (2008). *Carbon Cycling and Storage in Mangrove Forests*. https://doi.org/10.1146/annurev-marine-010213-135020

Alongi, D. M., Trott, L. A., Rachmansyah, Tirendi, F., McKinnon, A. D., & Undu, M. C. (2008). Growth and development of mangrove forests overlying smothered coral reefs, Sulawesi and Sumatra, Indonesia. *Marine Ecology Progress Series*, *370*, 97–109. https://doi.org/10.3354/meps07661

Atkinson, L. P., & Hall, J. R. (1976). Methane Distribution and Production in Georgia Salt-Marsh. *Estuarine and Coastal Marine Science*, *4*(6), 677–686. https://doi.org/10.1016/0302-3524(76)90074-8

Aubinet, M., Vesala, T., & Papale, D. (2012). *Eddy Covariance: A Practical Guide to Measurement and Data Analysis*. Springer.

Bahlmann, E., Weinberg, I., Lavrič, J. V., Eckhardt, T., Michaelis, W., Santos, R., & Seifert, R. (2015). Tidal controls on trace gas dynamics in a seagrass meadow of the Ria Formosa lagoon (southern Portugal). *Biogeosciences*, *12*(6), 1683–1696. https://doi.org/10.5194/bg-12-1683-2015

Banerjee, K., Paneerselvam, A., Ramachandran, P., Ganguly, D., Singh, G., & Ramesh, R. (2018). Seagrass and macrophyte mediated CO2 and CH4 dynamics in shallow coastal waters. *PLoS ONE*, *13*(10), 1–22.

https://doi.org/10.1371/journal.pone.0203922

Bange, H. W., Bergmann, K., Hansen, H. P., Kock, A., Koppe, R., Malien, F., & Ostrau, C. (2010). Dissolved methane during hypoxic events at the Boknis Eck time series station (Eckernförde Bay, SW Baltic Sea). *Biogeosciences*, *7*(4), 1279–1284. https://doi.org/10.5194/bg-7-1279-2010

Banta, G. T., Giblin, A. E., Hobbie, J. E., & Tucker, J. (1995). Benthic respiration and nitrogen release in Buzzards Bay, Massachusetts. *Journal of Marine Research*, *53*, 107–135. https://doi.org/10.1357/0022240953213287

Barbier, E. B., Hacker, S. D., Kennedy, C., Koch, E. W., Stier, A. C., & Silliman, B. R. (2011). The value of estuarine and coastal ecosystem services. *Ecological Monographs*, *81*(2), 169–193. https://doi.org/10.1890/10-1510.1

Bartlett, K. B., Bartlett, D. S., Harriss, R. C., & Sebacher, D. I. (1987). Methane Emissions along a Salt Marsh Salinity Gradient. *Biogeochemistry*, Vol. 4, pp. 183–202. https://doi.org/10.2307/1468663

Bartlett, K. B., & Harriss, R. C. (1993). Review and assessment of methane emissions from wetlands. *Chemosphere*, *26*(1–4), 261–320. https://doi.org/10.1016/0045-6535(93)90427-7

Bartlett, K. B., Harriss, R. C., & Sebacher, D. I. (1985). Methane flux form coastal salt marshes. *Journal of Geophysical Research*, *90*(D3), 5710–5720. https://doi.org/10.1029/JD090iD03p05710

Benway, H. M., Alin, S. R., Boyer, E., Cai, W.-J., Coble, P. G., Cross, J. N., … Smith, R. A. (2016). *A science plan for carbon cycle research in North American coastal waters. Report of the Coastal CARbon Synthesis (CCARS) community workshop, August 19-21, 2014*. https://doi.org/10.1575/1912/7777

Biswas, H., Mukhopadhyay, S. K., Sen, S., & Jana, T. K. (2007). Spatial and temporal patterns of methane dynamics in the tropical mangrove dominated estuary, NE coast of Bay of Bengal, India. *Journal of Marine Systems*, *68*(1–2), 55–64. https://doi.org/10.1016/j.jmarsys.2006.11.001

Blaabjerg, V., & Finster, K. (1998). Sulphate reduction associated with roots and rhizomes of the marine macrophyte Zostera marina. *Aquatic Microbial Ecology*, *15*(3), 311–314. https://doi.org/10.3354/ame015311

Breitburg, D., Levin, L. A., Oschlies, A., Grégoire, M., Chavez, F. P., Conley, D. J., … Zhang, J. (2018). Declining oxygen in the global ocean and coastal waters. *Science (New York, N.Y.)*, *359*(6371), eaam7240. https://doi.org/10.1126/science.aam7240

Bridgham, S. D., Cadillo-Quiroz, H., Keller, J. K., & Zhuang, Q. (2013). Methane emissions from wetlands: biogeochemical, microbial, and modeling perspectives from local to global scales. *Global Change Biology*, *19*(5), 1325–1346. https://doi.org/10.1111/gcb.12131

Burkholder, J. M., Tomasko, D. A., & Touchette, B. W. (2007). Seagrasses and eutrophication. *Journal of Experimental Marine Biology and Ecology*, *350*(1–2), 46–72. https://doi.org/10.1016/J.JEMBE.2007.06.024

Caballero-Alfonso, A. M., Carstensen, J., & Conley, D. J. (2015). Biogeochemical and environmental drivers of coastal hypoxia. *Journal of Marine Systems*, *141*, 190–199. https://doi.org/10.1016/J.JMARSYS.2014.04.008

Cable, J. E., Bugna, G. C., Burnett, W. C., & Chanton, J. P. (1996). Application of ^{222}Rn and CH_4 for assessment of groundwater discharge to the coastal ocean. *Limnology and Oceanography*, *41*(6), 1347–1353. https://doi.org/10.4319/lo.1996.41.6.1347

Caffrey, J. M., & Kemp, W. M. (1991). Seasonal and spatial patterns of oxygen production, respiration and root-rhizome release in Potamogeton perfoliatus L. and Zostera marina L. *Aquatic Botany*, *40*(2), 109–128. https://doi.org/10.1016/0304-3770(91)90090-R

Cahoon, D. R., Hensel, P., Rybczyk, J., McKee, K. L., Proffitt, C. E., & Perez, B. C. (2003). Mass tree mortality leads to mangrove peat collapse at Bay Islands, Honduras after Hurricane Mitch. *Journal of Ecology*, *91*(6), 1093–1105. https://doi.org/10.1046/j.1365-2745.2003.00841.x

Carlton, J. M. (1974). Land-building and Stabilization by Mangroves. *Environmental Conservation*, *1*(4), 285–294. https://doi.org/10.1017/S0376892900004926

Cattrijsse, A., & Hampel, H. (2006). European intertidal marshes: a review of their habitat functioning and value for aquatic organisms. *Marine Ecology Progress Series*, *324*, 293–307. https://doi.org/10.3354/meps324293

Cavanaugh, K. C., Dangremond, E. M., Doughty, C. L., Park Williams, A., Parker, J. D., Hayes, M. A., … Feller, I. C. (2019). Climate-driven regime shifts in a mangrove–salt marsh ecotone over the past 250 years. *Proceedings of the National Academy of Sciences of the United States of America*, *116*(43), 21602–21608. https://doi.org/10.1073/pnas.1902181116

Chauhan, R., Ramanathan, A. L., & Adhya, T. K. (2008). Assessment of methane and nitrous oxide flux from mangroves along Eastern coast of India. *Geofluids*, *8*(4), 321–332. https://doi.org/10.1111/j.1468-8123.2008.00227.x

Chauhan, Rita, Datta, A., Ramanathan, A. L., & Adhya, T. K. (2015). Factors influencing spatio-temporal variation of methane and nitrous oxide emission from a tropical mangrove of eastern coast of India. *Atmospheric Environment*, *107*, 95–106. https://doi.org/10.1016/j.atmosenv.2015.02.006

Chen, G. C., Tam, N. F. Y., Wong, Y. S., & Ye, Y. (2011). Effect of wastewater discharge on greenhouse gas fluxes from mangrove soils. *Atmospheric Environment*, *45*(5), 1110–1115. https://doi.org/10.1016/j.atmosenv.2010.11.034

Chen, Guang C., Ulumuddin, Y. I., Pramudji, S., Chen, S. Y., Chen, B., Ye, Y., … Wang, J. K. (2014). Rich soil carbon and nitrogen but low atmospheric greenhouse gas fluxes from North Sulawesi mangrove swamps in Indonesia. *Science of the Total Environment*, *487*(1), 91–96. https://doi.org/10.1016/j.scitotenv.2014.03.140

Cheng, X., Peng, R., Chen, J., Luo, Y., Zhang, Q., An, S., … Li, B. (2007). CH4 and N2O emissions from Spartina alterniflora and Phragmites australis in experimental mesocosms. *Chemosphere*, *68*(3), 420–427. https://doi.org/10.1016/J.CHEMOSPHERE.2007.01.004

Chmura, G. L., Kellman, L., & Guntenspergen, G. R. (2011). The greenhouse gas flux and potential global warming feedbacks of a northern macrotidal and microtidal salt marsh. *Environmental Research Letters*, *6*(4). https://doi.org/10.1088/1748-9326/6/4/044016

Christianen, M. J. A., van Belzen, J., Herman, P. M. J., van Katwijk, M. M., Lamers, L. P. M., van Leent, P. J. M., & Bouma, T. J. (2013). Low-Canopy Seagrass Beds Still Provide Important Coastal Protection Services. *PLoS ONE*, *8*(5), e62413. https://doi.org/10.1371/journal.pone.0062413

Chu, H., Chen, J., Gottgens, J. F., Ouyang, Z., John, R., Czajkowski, K., & Becker, R. (2014). Net ecosystem methane and carbon dioxide exchanges in a Lake Erie coastal marsh and a nearby cropland. *Journal of Geophysical Research: Biogeosciences*, *119*, 722–740. https://doi.org/10.1002/2013JG002520

Chuang, P. C., Young, M. B., Dale, A. W., Miller, L. G., Herrera-Silveira, J. A., & Paytan, A. (2017). Methane fluxes from tropical coastal lagoons surrounded by mangroves, Yucatán, Mexico. *Journal of Geophysical Research: Biogeosciences*, *122*(5), 1156–1174. https://doi.org/10.1002/2017JG003761

Cloern, J. E., Abreu, P. C., Carstensen, J., Chauvaud, L., Elmgren, R., Grall, J., … Yin, K. (2016). Human activities and climate variability drive fast-paced change across the world's estuarine-coastal ecosystems. *Global Change Biology*, *22*(2), 513–529. https://doi.org/10.1111/gcb.13059

Costa, K. C., & Leigh, J. A. (2014). Metabolic versatility in methanogens. *Current Opinion in Biotechnology*, *29*, 70–75. https://doi.org/10.1016/J.COPBIO.2014.02.012

Cotovicz, L. C., Knoppers, B. A., Brandini, N., Poirier, D., Costa Santos, S. J., & Abril, G. (2016). Spatio-temporal variability of methane (CH4) concentrations and diffusive fluxes from a tropical coastal embayment surrounded by a large urban area (Guanabara Bay, Rio de Janeiro, Brazil). *Limnology and Oceanography*, *61*, S238–S252. https://doi.org/10.1002/lno.10298

Cowan, T., Purich, A., Perkins, S., Pezza, A., Boschat, G., Sadler, K., … Sadler, K. (2014). More Frequent, Longer, and Hotter Heat Waves for Australia in the Twenty-First Century. *Journal of Climate*, *27*(15), 5851–5871. https://doi.org/10.1175/JCLI-D-14-00092.1

Cowardin, L. M., Carter, V., Golet, F. C., & LaRoe, E. T. (1979). *Classification of Wetlands and Deepwater Habitats of the United States*. Washington, DC.

Davidson, E. A., Ishida, F. Y., & Nepstad, D. C. (2004). Effects of an experimental drought on soil emissions of carbon dioxide, methane, nitrous oxide, and nitric oxide in a moist tropical forest. *Global Change Biology*, *10*(5), 718–730. https://doi.org/10.1111/j.1365-2486.2004.00762.x

Davidson, N. C., & Finlayson, C. M. (2019). Updating global coastal wetland areas presented in Davidson and Finlayson (2018). *Marine and Freshwater Research*. https://doi.org/10.1071/MF19010

Davis, T. R., Harasti, D., Smith, S. D. A., & Kelaher, B. P. (2016). Using modelling to predict impacts of sea level rise and increased turbidity on seagrass distributions in estuarine embayments. *Estuarine, Coastal and Shelf Science*, *181*, 294–301. https://doi.org/10.1016/J.ECSS.2016.09.005

Deborde, J., Anschutz, P., Guérin, F., Poirier, D., Marty, D., Boucher, G., … Abril, G. (2010). Methane sources, sinks and fluxes in a temperate tidal Lagoon: The Arcachon lagoon (SW France). *Estuarine, Coastal and Shelf Science*, *89*(4), 256–266. https://doi.org/10.1016/j.ecss.2010.07.013

Diefenderfer, H. L., Cullinan, V. I., Borde, A. B., Gunn, C. M., & Thom, R. M. (2018). High-frequency greenhouse gas flux measurement system detects winter storm surge effects on salt marsh. *Global Change Biology*, *24*(12), 5961–5971. https://doi.org/10.1111/gcb.14430

Dlugokencky, E. J., Nisbet, E. G., Fisher, R., & Lowry, D. (2011). Global atmospheric

methane: budget, changes and dangers. *Philosophical Transactions of the Royal Society A: Mathematical, Physical and Engineering Sciences*, *369*(1943), 2058–2072. https://doi.org/10.1098/rsta.2010.0341

Dole, R., Hoerling, M., Kumar, A., Eischeid, J., Perlwitz, J., Quan, X.-W., … Zhang, T. (2014). The Making of an Extreme Event: Putting the Pieces Together. *Bulletin of the American Meteorological Society*, *95*(3), 427–440. https://doi.org/10.1175/BAMS-D-12-00069.1

Doughty, C. L., Langley, J. A., Walker, W. S., Feller, I. C., Schaub, R., & Chapman, S. K. (2016). Mangrove Range Expansion Rapidly Increases Coastal Wetland Carbon Storage. *Estuaries and Coasts*, *39*(2), 385–396. https://doi.org/10.1007/s12237-015-9993-8

Dowrick, D. J., Freeman, C., Lock, M. A., & Reynolds, B. (2006). Sulphate reduction and the suppression of peatland methane emissions following summer drought. *Geoderma*. https://doi.org/10.1016/j.geoderma.2005.06.003

Duarte, C M, Middelburg, J. J., & Caraco, N. (2005). Major role of marine vegetation on the oceanic carbon cycle. In *Biogeosciences* (Vol. 2).

Duarte, Carlos M. (2017). Reviews and syntheses: Hidden forests, the role of vegetated coastal habitats in the ocean carbon budget. *Biogeosciences*, *14*(2), 301–310. https://doi.org/10.5194/bg-14-301-2017

Dubey, S. K. (2005). Microbial ecology of methane emission in rice agroecosystem: a review. *Applied Ecology and Environmental Research*, *3*(2), 1–27.

Dutta, M. K., Bianchi, T. S., & Mukhopadhyay, S. K. (2017). Mangrove Methane Biogeochemistry in the Indian Sundarbans: A Proposed Budget. *Frontiers in Marine Science*, *4*(June), 1–15. https://doi.org/10.3389/fmars.2017.00187

Emery, H. E., Angell, J. H., & Fulweiler, R. W. (2019). Salt Marsh Greenhouse Gas Fluxes and Microbial Communities Are Not Sensitive to the First Year of Precipitation Change. *Journal of Geophysical Research: Biogeosciences*, 2018JG004788. https://doi.org/10.1029/2018JG004788

Emery, H. E., & Fulweiler, R. W. (2014). Spartina alterniflora and invasive Phragmites australis stands have similar greenhouse gas emissions in a New England marsh. *Aquatic Botany*, *116*, 83–92. https://doi.org/10.1016/j.aquabot.2014.01.010

Emery, H. E., & Fulweiler, R. W. (2017). Incomplete tidal restoration may lead to persistent high CH4 emission. *Ecosphere*, *8*(12), e01968. https://doi.org/10.1002/ecs2.1968

Engle, D., & Melack, J. M. (2000). Methane emissions from an Amazon floodplain lake: Enhanced release during episodic mixing and during falling water. *Biogeochemistry*, *51*(1), 71–90. https://doi.org/10.1023/A:1006389124823

Eong, O. J. (1993). Mangroves - a carbon source and sink. *Chemosphere*, *27*(6), 1097–1107. https://doi.org/10.1016/0045-6535(93)90070-L

Etheridge, D. M., Steele, L. P., Francey, R. J., & Langenfelds, R. L. (1998). Atmospheric methane between 1000 A.D. and present: Evidence of anthropogenic emissions and climatic variability. *Journal of Geophysical Research: Atmospheres*, *103*(D13), 15979–15993. https://doi.org/10.1029/98JD00923

Fennel, K., Alin, S., Barbero, L., Evans, W., Bourgeois, T., Cooley, S., … Wang, Z. A. (2019). Carbon cycling in the North American coastal ocean: a synthesis. *Biogeosciences*, *16*(6), 1281–1304. https://doi.org/10.5194/bg-16-1281-2019

Forbrich, I., Giblin, A. E., & Hopkinson, C. S. (2018). Constraining Marsh Carbon Budgets Using Long-Term C Burial and Contemporary Atmospheric CO_2 Fluxes. *Journal of Geophysical Research: Biogeosciences*, *123*(3), 867–878. https://doi.org/10.1002/2017JG004336

Ford, H., Garbutt, A., Jones, L., & Jones, D. L. (2012). Methane, carbon dioxide and nitrous oxide fluxes from a temperate salt marsh: Grazing management does not alter Global Warming Potential. *Estuarine, Coastal and Shelf Science*, *113*, 182–191. https://doi.org/10.1016/j.ecss.2012.08.002

Foster, S. Q., & Fulweiler, R. W. (2019). Estuarine Sediments Exhibit Dynamic and Variable Biogeochemical Responses to Hypoxia. *Journal of Geophysical Research: Biogeosciences*, *124*(4), 737–758. https://doi.org/10.1029/2018JG004663

Foster, Sarah Q., & Fulweiler, R. W. (2016). Sediment Nitrous Oxide Fluxes Are Dominated by Uptake in a Temperate Estuary. *Frontiers in Marine Science*, *3*(March), 1–13. https://doi.org/10.3389/fmars.2016.00040

Freeman, C., Nevison, G. B., Kang, H., Hughes, S., Reynolds, B., & Hudson, J. A. (2002). Contrasted effects of simulated drought on the production and oxidation of methane in a mid-Wales wetland. *Soil Biology and Biochemistry*. https://doi.org/10.1016/S0038-0717(01)00154-7

Friedrichs, C. T., & Perry, J. E. (2001). Tidal Salt Marsh Morphodynamics: A Synthesis. In *Journal of Coastal Research*.

Gacia, E., & Duarte, C. M. (2001). Sediment Retention by a Mediterranean Posidonia

oceanica Meadow: The Balance between Deposition and Resuspension. *Estuarine, Coastal and Shelf Science*, *52*, 505–514. https://doi.org/10.1006

Gacia, E., Granata, T. C., & Duarte, C. M. (1999). An approach to measurement of particle flux and sediment retention within seagrass (Posidonia oceanica) meadows. *Aquatic Botany*, *65*, 255–268.

Gammal, J., Norkko, J., Pilditch, C. A., & Norkko, A. (2017). Coastal Hypoxia and the Importance of Benthic Macrofauna Communities for Ecosystem Functioning. *Estuaries and Coasts*, *40*(2), 457–468. https://doi.org/10.1007/s12237-016-0152-7

Ganguly, D., Dey, M., Mandal, S. K., De, T. K., & Jana, T. K. (2008). Energy dynamics and its implication to biosphere-atmosphere exchange of CO2, H2O and CH4in a tropical mangrove forest canopy. *Atmospheric Environment*, *42*(18), 4172–4184. https://doi.org/10.1016/j.atmosenv.2008.01.022

Gao, G. F., Li, P. F., Shen, Z. J., Qin, Y. Y., Zhang, X. M., Ghoto, K., … Zheng, H. L. (2018). Exotic Spartina alterniflora invasion increases CH4 while reduces CO2 emissions from mangrove wetland soils in southeastern China. *Scientific Reports*, *8*(1), 9243. https://doi.org/10.1038/s41598-018-27625-5

Garcias-Bonet, N., & Duarte, C. M. (2017). Methane Production by Seagrass Ecosystems in the Red Sea. *Frontiers in Marine Science*, *4*(November). https://doi.org/10.3389/fmars.2017.00340

Gelesh, L., Marshall, K., Boicourt, W., & Lapham, L. (2016). Methane concentrations increase in bottom waters during summertime anoxia in the highly eutrophic estuary, Chesapeake Bay, U.S.A. *Limnology and Oceanography*, *61*, S253–S266. https://doi.org/10.1002/lno.10272

Giani, L., Bashan, Y., Holguin, G., & Strangmann, A. (1996). Characteristics and methanogenesis of the Balandra lagoon mangrove soils, Baja California sur, Mexico. *Geoderma*, *72*(1–2), 149–160. https://doi.org/10.1016/0016-7061(96)00023-7

Gillooly, J. F., Brown, J. H., West, G. B., Savage, V. M., & Charnov, E. L. (2001). Effects of Size and Temperature on Metabolic Rate. *Science*, *293*(5538), 2248–2248.

Giri, C., Ochieng, E., Tieszen, L. L., Zhu, Z., Singh, A., Loveland, T., … Duke, N. (2011). Status and distribution of mangrove forests of the world using earth observation satellite data. *Global Ecology and Biogeography*, *20*(1), 154–159. https://doi.org/10.1111/j.1466-8238.2010.00584.x

Gonsalves, M.-J., Fernandes, C. E. G., Fernandes, S. O., Kirchman, D. L., & Bharathi, P. A. L. (2011). Effects of composition of labile organic matter on biogenic production of methane in the coastal sediments of the Arabian Sea. *Environmental Monitoring and Assessment*, *182*(1–4), 385–395. https://doi.org/10.1007/s10661-011-1883-3

Guirguis, K., Gershunov, A., Schwartz, R., & Bennett, S. (2011). Recent warm and cold daily winter temperature extremes in the Northern Hemisphere. *Geophysical Research Letters*, *38*(17), n/a-n/a. https://doi.org/10.1029/2011GL048762

Hamilton, S. E., & Casey, D. (2016). Creation of a high spatio-temporal resolution global database of continuous mangrove forest cover for the 21st century (CGMFC-21). *Global Ecology and Biogeography*, *25*(6), 729–738. https://doi.org/10.1111/geb.12449

Heiss, E. M., Fields, L., & Fulweiler, R. W. (2012). Directly measured net denitrification rates in offshore New England sediments. *Continental Shelf Research*, *45*, 78–86. https://doi.org/10.1016/j.csr.2012.06.002

Hendriks, I. E., Sintes, T., Bouma, T. J., & Duarte, C. M. (2008). Experimental assessment and modeling evaluation of the effects of the seagrass Posidonia oceanica on flow and particle trapping. *Marine Ecology Progress Series*, *356*, 163–173. https://doi.org/10.3354/meps07316

Hirota, M., Senga, Y., Seike, Y., Nohara, S., & Kunii, H. (2007). Fluxes of carbon dioxide, methane and nitrous oxide in two contrastive fringing zones of coastal lagoon, Lake Nakaumi, Japan. *Chemosphere*, *68*(3), 597–603. https://doi.org/10.1016/j.chemosphere.2007.01.002

Holm, G. O., Perez, B. C., McWhorter, D. E., Krauss, K. W., Johnson, D. J., Raynie, R. C., & Killebrew, C. J. (2016). Ecosystem Level Methane Fluxes from Tidal Freshwater and Brackish Marshes of the Mississippi River Delta: Implications for Coastal Wetland Carbon Projects. *Wetlands*, *36*(3), 401–413. https://doi.org/10.1007/s13157-016-0746-7

Holmer, M., Andersen, F. Ø., Nielsen, S. L., & Boschker, H. T. S. (2001). The importance of mineralization based on sulfate reduction for nutrient regeneration in tropical seagrass sediments. *Aquatic Botany*, *71*(1), 1–17. https://doi.org/10.1016/S0304-3770(01)00170-X

Holmer, M., Gribsholt, B., & Kistensen, E. (2002). Effects of sea level rise on growth of Spartina anglica and oxygen dynamics in rhizosphere and salt marsh sediments. *MARINE ECOLOGY PROGRESS SERIES Mar Ecol Prog Ser*, *225*, 197–204.

Howes, B. L., & Teal, J. M. (1994). Oxygen loss from Spartina alterniflora and its

relationship to salt marsh oxygen balance. *Oecologia*, *97*(4), 431–438. https://doi.org/10.1007/BF00325879

Hyndes, G. A., Heck, K. L., Vergés, A., Harvey, E. S., Kendrick, G. A., Lavery, P. S., … Wilson, S. (2016). Accelerating Tropicalization and the Transformation of Temperate Seagrass Meadows. *BioScience*, *66*(11), 938–948. https://doi.org/10.1093/biosci/biw111

IPCC, Pachauri, R. K., & Meyer, L. A. (2014). Climate Change 2014: Synthesis Report. Contribution of Working Groups I, II, and III to the Fifth Assessment Report of the Intergovernmental Panel on Climate Change. In *IPCC AR5 Synthesis Report Website*. Geneva, Switzerland.

Irvine, I. C., Vivanco, L., Bentley, P. N., & Martiny, J. B. H. (2012). The effect of nitrogen enrichment on C1-cycling microorganisms and methane flux in salt marsh sediments. *Frontiers in Microbiology*, *3*(MAR), 1–10. https://doi.org/10.3389/fmicb.2012.00090

Jayathilake, D. R. M., & Costello, M. J. (2018). A modelled global distribution of the seagrass biome. *Biological Conservation*, *226*, 120–126. https://doi.org/10.1016/J.BIOCON.2018.07.009

Jeffrey, L. C., Reithmaier, G., Sippo, J. Z., Johnston, S. G., Tait, D. R., Harada, Y., & Maher, D. T. (2019). Are methane emissions from mangrove stems a cryptic carbon loss pathway? Insights from a catastrophic forest mortality. *New Phytologist*. https://doi.org/10.1111/nph.15995

Jha, C. S., Rodda, S. R., Thumaty, K. C., Raha, A. K., & Dadhwal, V. K. (2014). Eddy covariance based methane flux in Sundarbans mangroves, India. *Journal of Earth System Science*, *123*(5), 1089–1096. https://doi.org/10.1007/s12040-014-0451-y

Jung, C., & Schindler, D. (2019). Changing wind speed distributions under future global climate. *Energy Conversion and Management*, *198*. https://doi.org/10.1016/j.enconman.2019.111841

Kelleway, J. J., Saintilan, N., Macreadie, P. I., Skilbeck, C. G., Zawadzki, A., & Ralph, P. J. (2016). Seventy years of continuous encroachment substantially increases “blue carbon” capacity as mangroves replace intertidal salt marshes. *Global Change Biology*, *22*(3), 1097–1109. https://doi.org/10.1111/gcb.13158

Kim, G., & Hwang, D.-W. (2002). Tidal pumping of groundwater into the coastal ocean revealed from submarine ^{222} Rn and CH $_4$ monitoring. *Geophysical Research Letters*, *29*(14), 23-1-23–24. https://doi.org/10.1029/2002GL015093

King, G M, & Wiebe, W. J. (1978). Methane release from soils of a South Carolina salt marsh. *Geochimica et Cosmochimica Acta*, *42*, 343–348.

King, Gary M. (1984). Utilization of hydrogen, acetate, and "noncompetitive"; substrates by methanogenic bacteria in marine sediments. *Geomicrobiology Journal*, *3*(4), 275–306. https://doi.org/10.1080/01490458409377807

Konnerup, D., Betancourt-Portela, J. M., Villamil, C., & Parra, J. P. (2014). Nitrous oxide and methane emissions from the restored mangrove ecosystem of the Ciénaga Grande de Santa Marta, Colombia. *Estuarine, Coastal and Shelf Science*, *140*, 43–51. https://doi.org/10.1016/j.ecss.2014.01.006

Krauss, K. W., Holm, G. O., Perez, B. C., McWhorter, D. E., Cormier, N., Moss, R. F., … Raynie, R. C. (2016). Component greenhouse gas fluxes and radiative balance from two deltaic marshes in Louisiana: Pairing chamber techniques and eddy covariance. *Journal of Geophysical Research: Biogeosciences*, *121*(6), 1503–1521. https://doi.org/10.1002/2015JG003224

Kristensen, E., Flindt, M. R., Ulomi, S., Borges, A. V., Abril, G., & Bouillon, S. (2008). Emission of CO2 and CH4 to the atmosphere by sediments and open waters in two Tanzanian mangrove forests. *Marine Ecology Progress Series*, *370*, 53–67. https://doi.org/10.3354/meps07642

Krithika, K., Purvaja, R., & Ramesh, R. (2008). Fluxes of methane and nitrous oxide from an Indian mangrove. *Current Science*, *94*(2), 218–224.

Kvenvolden, K. A., & Rogers, B. W. (2005). Gaia's breath—global methane exhalations. *Marine and Petroleum Geology*, *22*(4), 579–590. https://doi.org/10.1016/J.MARPETGEO.2004.08.004

Laanbroek, H. J. (2010). Methane emission from natural wetlands: interplay between emergent macrophytes and soil microbial processes. A mini-review. *Annals of Botany*, *105*(1), 141–153. https://doi.org/10.1093/aob/mcp201

Lavery, P. S., Mateo, M. Á., Serrano, O., & Rozaimi, M. (2013). Variability in the Carbon Storage of Seagrass Habitats and Its Implications for Global Estimates of Blue Carbon Ecosystem Service. *PLoS ONE*, *8*(9). https://doi.org/10.1371/journal.pone.0073748

Le Mer, J., & Roger, P. (2001). Production, oxidation, emission and consumption of methane by soils: A review. *European Journal of Soil Biology*, *37*(1), 25–50. https://doi.org/10.1016/S1164-5563(01)01067-6

Lee, S. Y., Primavera, J. H., Dahdouh-Guebas, F., McKee, K., Bosire, J. O., Cannicci, S.,

… Record, S. (2014). Ecological role and services of tropical mangrove ecosystems: a reassessment. *Global Ecology and Biogeography*, *23*(7), 726–743. https://doi.org/10.1111/geb.12155

Leifer, I., & Patro, R. K. (2002). The bubble mechanism for methane transport from the shallow sea bed to the surface: A review and sensitivity study. *Continental Shelf Research*, *22*(16), 2409–2428. https://doi.org/10.1016/S0278-4343(02)00065-1

Li, H., Dai, S., Ouyang, Z., Xie, X., Guo, H., Gu, C., … Zhao, B. (2018). Multi-scale temporal variation of methane flux and its controls in a subtropical tidal salt marsh in eastern China. *Biogeochemistry*, *137*(1–2), 163–179. https://doi.org/10.1007/s10533-017-0413-y

Li, Y., Wang, D., Chen, Z., Jin, H., Hu, H., Chen, J., … Yang, Z. (2018). Role of Scirpus mariqueter on Methane Emission from an Intertidal Saltmarsh of Yangtze Estuary. *Sustainability*, *10*(4), 1139. https://doi.org/10.3390/su10041139

Livesley, S. J., & Andrusiak, S. M. (2012). Temperate mangrove and salt marsh sediments are a small methane and nitrous oxide source but important carbon store. *Estuarine, Coastal and Shelf Science*, *97*, 19–27. https://doi.org/10.1016/j.ecss.2011.11.002

Livingston, G. P., & Hutchinson, G. L. (1995). Enclosure-based measurement of trace gas exchange; applications and sources of error. In P. A. Matson, R. C. Harriss, & P. A. Matson (Eds.), *Biogenic Trace Gases : Measuring Emissions From Soil And Water.* (pp. 14–51). John Wiley & Sons.

Lu, C. Y., Wong, Y. S., Tam, N. F. Y., Ye, Y., & Lin, P. (1999). Methane flux and production from sediments of a mangrove wetland on Hainan Island, China. *Mangroves and Salt Marshes*, *3*(1), 41–49. https://doi.org/10.1023/A:1009989026801

Lyimo, L. D., Gullström, M., Lyimo, T. J., Deyanova, D., Dahl, M., Hamisi, M. I., & Björk, M. (2018). Shading and simulated grazing increase the sulphide pool and methane emission in a tropical seagrass meadow. *Marine Pollution Bulletin*, *134*, 89–93. https://doi.org/10.1016/J.MARPOLBUL.2017.09.005

Lyimo, T. J., Pol, A., & Camp, H. J. M. O. (2002). Methane emission, sulphide concentration and redox potential profiles in Mtoni mangrove sediment, Tanzania. *Western Indian Ocean Journal of Marine Science*, *1*, 71–80.

Macreadie, P. I., Ollivier, Q. R., Kelleway, J. J., Serrano, O., Carnell, P. E., Ewers Lewis, C. J., … Lovelock, C. E. (2017). Carbon sequestration by Australian tidal marshes. *Scientific Reports*, *7*(1), 44071. https://doi.org/10.1038/srep44071

Magenheimer, J. F., Moore, T. R., Chmura, G. L., & Daoust, R. J. (1996). Methane and Carbon Dioxide Flux from a Macrotidal Salt Marsh, Bay of Fundy, New Brunswick. *Estuaries*, *19*(1), 139. https://doi.org/10.2307/1352658

Maher, D. T., Drexl, M., Tait, D. R., Johnston, S. G., & Jeffrey, L. C. (2019). iAMES: An i nexpensive, A utomated M ethane E bullition S ensor. *Environmental Science & Technology*, *53*(11), 6420–6426. https://doi.org/10.1021/acs.est.9b01881

Marinho, C., Campos, E., Guimarães, J., & Esteves, F. (2012). Effect of sediment composition on methane concentration and production in the transition zone of a mangrove (Sepetiba Bay, Rio de Janeiro, Brazil). *Brazilian Journal of Biology*, *72*(3), 429–436. https://doi.org/10.1590/S1519-69842012000300003

Martens, C. S., & Berner, R. A. (1974). Methane production in the interstitial waters of sulfate-depleted marine sediments. *Science*, *185*(4157), 1167–1169. https://doi.org/10.1126/science.185.4157.1167

Martin, R. M., & Moseman-Valtierra, S. (2017). Different short-term responses of greenhouse gas fluxes from salt marsh mesocosms to simulated global change drivers. *Hydrobiologia*, *802*(1), 71–83. https://doi.org/10.1007/s10750-017-3240-1

McGlathery, K. J. (2001). MACROALGAL BLOOMS CONTRIBUTE TO THE DECLINE OF SEAGRASS IN NUTRIENT-ENRICHED COASTAL WATERS. *Journal of Phycology*, *37*(4), 453–456. https://doi.org/10.1046/j.1529-8817.2001.037004453.x

McKEE, K. L., & ROOTH, J. E. (2008). Where temperate meets tropical: multi-factorial effects of elevated CO $_2$, nitrogen enrichment, and competition on a mangrove-salt marsh community. *Global Change Biology*, *14*(5), 971–984. https://doi.org/10.1111/j.1365-2486.2008.01547.x

McLeod, E., Chmura, G. L., Bouillon, S., Salm, R., Björk, M., Duarte, C. M., … Silliman, B. R. (2011). A blueprint for blue carbon: Toward an improved understanding of the role of vegetated coastal habitats in sequestering CO2. *Frontiers in Ecology and the Environment*, *9*(10), 552–560. https://doi.org/10.1890/110004

Mcowen, C. J., Weatherdon, L. V, Bochove, J.-W. Van, Sullivan, E., Blyth, S., Zockler, C., … Fletcher, S. (2017). A global map of saltmarshes. *Biodiversity Data Journal*, (5), e11764. https://doi.org/10.3897/BDJ.5.e11764

Middelburg, J. J., Klaver, G., Nieuwenhuize, J., Wielemaker, A., De Haas, W., Vlug, T., & Van Der Nat, J. F. W. A. (1996). Organic matter mineralization in intertidal

sediments along an estuarine gradient. *Marine Ecology Progress Series*, *132*, 157–168.

Möller, I., Kudella, M., Rupprecht, F., Spencer, T., Paul, M., van Wesenbeeck, B. K., … Schimmels, S. (2014). Wave attenuation over coastal salt marshes under storm surge conditions. *Nature Geoscience*, *7*(10), 727–731. https://doi.org/10.1038/ngeo2251

Mukhopadhyay, S. K., Biswas, H., De, T. K., Sen, B. K., Sen, S., & Jana, T. K. (2002). Impact of Sundarban mangrove biosphere on the carbon dioxide and methane mixing ratios at the NE Coast of Bay of Bengal, India. *Atmospheric Environment*, *36*(4), 629–638. https://doi.org/10.1016/S1352-2310(01)00521-0

Murray, R. H., Erler, D. V., & Eyre, B. D. (2015). Nitrous oxide fluxes in estuarine environments: response to global change. *Global Change Biology*, *21*(9), 3219–3245. https://doi.org/10.1111/gcb.12923

Nagelkerken, I., Blaber, S. J. M., Bouillon, S., Green, P., Haywood, M., Kirton, L. G., … Somerfield, P. J. (2008). The habitat function of mangroves for terrestrial and marine fauna: A review. *Aquatic Botany*, *89*(2), 155–185. https://doi.org/10.1016/J.AQUABOT.2007.12.007

Negandhi, K., Edwards, G., Kelleway, J. J., Howard, D., Safari, D., & Saintilan, N. (2019). Blue carbon potential of coastal wetland restoration varies with inundation and rainfall. *Scientific Reports*, *9*(1), 4368. https://doi.org/10.1038/s41598-019-40763-8

Nellemann, C., & Corcoran, E. (2009). *Blue Carbon: The Role of Healthy Oceans in Binding Carbon : a Rapid Response Assessment*. UNEP/Earthprint.

Neubauer, S. C., & Megonigal, J. P. (2015). Moving Beyond Global Warming Potentials to Quantify the Climatic Role of Ecosystems. *Ecosystems*, *18*(6), 1000–1013. https://doi.org/10.1007/s10021-015-9879-4

Nisbet, E. G., Manning, M. R., Dlugokencky, E. J., Fisher, R. E., Lowry, D., Michel, S. E., … White, J. W. C. (2019). Very Strong Atmospheric Methane Growth in the 4 Years 2014–2017: Implications for the Paris Agreement. *Global Biogeochemical Cycles*, *33*(3), 318–342. https://doi.org/10.1029/2018GB006009

Nixon, S. W. (1995). Coastal marine eutrophication: A definition, social causes, and future concerns. *Ophelia*, Vol. 41, pp. 199–219. https://doi.org/10.1080/00785236.1995.10422044

Nixon, S. W., Fulweiler, R. W., Buckley, B. A., Granger, S. L., Nowicki, B. L., & Henry, K. M. (2009). The impact of changing climate on phenology, productivity, and

benthic–pelagic coupling in Narragansett Bay. *Estuarine, Coastal and Shelf Science*, *82*(1), 1–18. https://doi.org/10.1016/J.ECSS.2008.12.016

Nóbrega, G. N., Ferreira, T. O., Siqueira Neto, M., Queiroz, H. M., Artur, A. G., Mendonça, E. D. S., … Otero, X. L. (2016). Edaphic factors controlling summer (rainy season) greenhouse gas emissions (CO2and CH4) from semiarid mangrove soils (NE-Brazil). *Science of the Total Environment*, *542*, 685–693. https://doi.org/10.1016/j.scitotenv.2015.10.108

Nordlund, L. M., Koch, E. W., Barbier, E. B., & Creed, J. C. (2016). Seagrass Ecosystem Services and Their Variability across Genera and Geographical Regions. *PLOS ONE*, *11*(10), e0163091. https://doi.org/10.1371/journal.pone.0163091

Ondiviela, B., Losada, I. J., Lara, J. L., Maza, M., Galván, C., Bouma, T. J., & van Belzen, J. (2014). The role of seagrasses in coastal protection in a changing climate. *Coastal Engineering*, *87*, 158–168. https://doi.org/10.1016/J.COASTALENG.2013.11.005

Oremland, R. S., Marsh, L. M., & Polcin, S. (1982). Methane production and simultaneous sulphate reduction in anoxic, salt marsh sediments. *Nature*, *296*(5853), 143–145. https://doi.org/10.1038/296143a0

Oremland, R. S., & Taylor, B. F. (1978). Sulfate reduction and methanogenesis in marine sediments. *Geochimica et Cosmochimica Acta*, *42*(2), 209–214. https://doi.org/10.1016/0016-7037(78)90133-3

Othman, M. A. (1994). Value of mangroves in coastal protection. *Hydrobiologia*, *285*(1–3), 277–282. https://doi.org/10.1007/BF00005674

Parashar, D. C., Gupta, P. K., Rai, J., Sharma, R. C., & Singh, N. (1993). Effect of soil temperature on methane emission from paddy fields. *Chemosphere*, *26*(1–4), 247–250. https://doi.org/10.1016/0045-6535(93)90425-5

Pedersen, O., Borum, J., Duarte, C., & Fortes, M. (1998). Oxygen dynamics in the rhizosphere of Cymodocea rotundata. *Marine Ecology Progress Series*, *169*, 283–288. https://doi.org/10.3354/meps169283

Pendleton, L., Donato, D. C., Murray, B. C., Crooks, S., Jenkins, W. A., Sifleet, S., … Baldera, A. (2012). Estimating Global "Blue Carbon" Emissions from Conversion and Degradation of Vegetated Coastal Ecosystems. *PLoS ONE*, *7*(9), e43542. https://doi.org/10.1371/journal.pone.0043542

Pi, N., Tam, N. F. Y., Wu, Y., & Wong, M. H. (2009). Root anatomy and spatial pattern of radial oxygen loss of eight true mangrove species. *Aquatic Botany*, *90*(3), 222–

230. https://doi.org/10.1016/J.AQUABOT.2008.10.002

Poffenbarger, H. J., Needelman, B. A., & Megonigal, J. P. (2011). Salinity influence on methane emissions from tidal marshes. *Wetlands*, *31*(5), 831–842. https://doi.org/10.1007/s13157-011-0197-0

Purvaja, R., & Ramesh, R. (2000). Human impacts on methane emission from mangrove ecosystems in India. *Regional Environmental Change*, *1*(2), 86–97. https://doi.org/10.1007/PL00011537

Purvaja, R., & Ramesh, R. (2001). Natural and and anthropogenic methane emission from coastal wetlands of South India. *Environmental Management*, *27*(4), 547–557. https://doi.org/10.1007/s002670010169

Purvaja, Ramachandran, Ramesh, R., & Frenzel, P. (2004). Plant-mediated methane emission from an Indian mangrove. *Global Change Biology*, *10*(11), 1825–1834. https://doi.org/10.1111/j.1365-2486.2004.00834.x

Raposa, K. B., Weber, R. L. J., Ekberg, M. C., & Ferguson, W. (2017). Vegetation Dynamics in Rhode Island Salt Marshes During a Period of Accelerating Sea Level Rise and Extreme Sea Level Events. *Estuaries and Coasts*, *40*(3), 640–650. https://doi.org/10.1007/s12237-015-0018-4

Raymond, P. A., & Cole, J. J. (2001). Gas Exchange in Rivers and Estuaries: Choosing a Gas Transfer Velocity. *Estuaries*, *24*(2), 312. https://doi.org/10.2307/1352954

Reeburgh, W. S. (2007). *Oceanic Methane Biogeochemistry*. https://doi.org/10.1021/CR050362V

Rosentreter, J. A., Maher, D. T., Ho, D. T., Call, M., Barr, J. G., & Eyre, B. D. (2017). Spatial and temporal variability of CO_2 and CH_4 gas transfer velocities and quantification of the CH_4 microbubble flux in mangrove dominated estuaries. *Limnology and Oceanography*, *62*(2), 561–578. https://doi.org/10.1002/lno.10444

Roslev, P., & King, G. M. (1996). Regulation of methane oxidation in a freshwater wetland by water table changes and anoxia. *FEMS Microbiology Ecology*, *19*(2), 105–115. https://doi.org/10.1111/j.1574-6941.1996.tb00203.x

Rozema, J., Dorel, F., Janissen, R., Lenssen, G., Broekman, R., Arp, W., & Drake, B. G. (1991). Effect of elevated atmospheric CO2 on growth, photosynthesis and water relations of salt marsh grass species. *Aquatic Botany*, *39*(1–2), 45–55. https://doi.org/10.1016/0304-3770(91)90021-V

Saintilan, N., Wilson, N. C., Rogers, K., Rajkaran, A., & Krauss, K. W. (2014).

Mangrove expansion and salt marsh decline at mangrove poleward limits. *Global Change Biology*, *20*(1), 147–157. https://doi.org/10.1111/gcb.12341

Santos, I. R., Dimova, N., Peterson, R. N., Mwashote, B., Chanton, J., & Burnett, W. C. (2009). Extended time series measurements of submarine groundwater discharge tracers (222Rn and CH4) at a coastal site in Florida. *Marine Chemistry*, *113*(1–2), 137–147. https://doi.org/10.1016/J.MARCHEM.2009.01.009

Saunois, M., Jackson, R. B., Bousquet, P., Boulter, B., & Canadell, J. G. (2016). The growing role of methane in anthropogenic climate change. *Environmental Research Letters*, *11*. https://doi.org/10.1088/1748-9326/11/12/120207

Scholander, P. F., van Dam, L., & Scholander, S. I. (1955). Gas Exchange in the Roots of Mangroves. *American Journal of Botany*, *42*(1), 92. https://doi.org/10.2307/2438597

Shakhova, N., Semiletov, I., Leifer, I., Sergienko, V., Salyuk, A., Kosmach, D., … Gustafsson, Ö. (2014). Ebullition and storm-induced methane release from the East Siberian Arctic Shelf. *Nature Geoscience*, *7*(1), 64–70. https://doi.org/10.1038/ngeo2007

Shepard, C. C., Crain, C. M., & Beck, M. W. (2011). The Protective Role of Coastal Marshes: A Systematic Review and Meta-analysis. *PLoS ONE*, *6*(11), e27374. https://doi.org/10.1371/journal.pone.0027374

Short, F., Carruthers, T., Dennison, W., & Waycott, M. (2007). Global seagrass distribution and diversity: A bioregional model. *Journal of Experimental Marine Biology and Ecology*, *350*(1–2), 3–20. https://doi.org/10.1016/J.JEMBE.2007.06.012

Slomp, C. P., & Van Cappellen, P. (2004). Nutrient inputs to the coastal ocean through submarine groundwater discharge: controls and potential impact. *Journal of Hydrology*, *295*(1–4), 64–86. https://doi.org/10.1016/J.JHYDROL.2004.02.018

Sorrell, B. K., & Downes, M. T. (2004). Water velocity and irradiance effects on internal transport and metabolism of methane in submerged Isoetes alpinus and Potamogeton crispus. *Aquatic Botany*, *79*(2), 189–202. https://doi.org/10.1016/J.AQUABOT.2004.02.004

Spalding, M. (2010). *World Atlas of Mangroves*. https://doi.org/10.4324/9781849776608

Sun, Z., Wang, L., Tian, H., Jiang, H., Mou, X., & Sun, W. (2013). Fluxes of nitrous oxide and methane in different coastal Suaeda salsa marshes of the Yellow River estuary, China. *Chemosphere*, *90*(2), 856–865. https://doi.org/10.1016/J.CHEMOSPHERE.2012.10.004

Takahashi, M., Noonan, S. H. C., Fabricius, K. E., & Collier, C. J. (2016). The effects of long-term *in situ* CO 2 enrichment on tropical seagrass communities at volcanic vents. *ICES Journal of Marine Science: Journal Du Conseil*, *73*(3), 876–886. https://doi.org/10.1093/icesjms/fsv157

Thayer, G. W., & Stuart, H. H. (1974). The Bay Scallop Makes Its Bed of Seagrass. *Marine Fisheries Review*, *36*(7), 27–30.

Timmers, P. H. A., Welte, C. U., Koehorst, J. J., Plugge, C. M., Jetten, M. S. M., & Stams, A. J. M. (2017). Reverse Methanogenesis and Respiration in Methanotrophic Archaea. *Archaea*, *2017*, 1–22. https://doi.org/10.1155/2017/1654237

Turner, A. J., Frankenberg, C., & Kort, E. A. (2019). Interpreting contemporary trends in atmospheric methane. *Proceedings of the National Academy of Sciences of the United States of America*, *116*(8), 2805–2813. https://doi.org/10.1073/pnas.1814297116

Ueyama, M., Takeuchi, R., Takahashi, Y., Ide, R., Ataka, M., Kosugi, Y., … Saigusa, N. (2015). Methane uptake in a temperate forest soil using continuous closed-chamber measurements. *Agricultural and Forest Meteorology*, *213*, 1–9. https://doi.org/10.1016/J.AGRFORMET.2015.05.004

Wang, F., Chen, N., Yan, J., Lin, J., Guo, W., Cheng, P., … Tian, Y. (2019). Major Processes Shaping Mangroves as Inorganic Nitrogen Sources or Sinks: Insights From a Multidisciplinary Study. *Journal of Geophysical Research: Biogeosciences*, 2018JG004875. https://doi.org/10.1029/2018JG004875

Wang, H., Liao, G., D'Souza, M., Yu, X., Yang, J., Yang, X., & Zheng, T. (2016). Temporal and spatial variations of greenhouse gas fluxes from a tidal mangrove wetland in Southeast China. *Environmental Science and Pollution Research*, *23*(2), 1873–1885. https://doi.org/10.1007/s11356-015-5440-4

Wanninkhof, R. (1992). Relationship between wind speed and gas exchange over the ocean. *Journal of Geophysical Research*, *97*(C5), 7373. https://doi.org/10.1029/92JC00188

Waycott, M., Duarte, C. M., Carruthers, T. J. B., Orth, R. J., Dennison, W. C., Olyarnik, S., … Williams, S. L. (2009). Accelerating loss of seagrasses across the globe threatens coastal ecosystems. *Proceedings of the National Academy of Sciences*, *106*(30), 12377–12381. https://doi.org/10.1073/pnas.0905620106

Weber, T., Wiseman, N. A., & Kock, A. (2019). Global ocean methane emissions dominated by shallow coastal waters. *Nature Communications*, *10*(1), 4584.

https://doi.org/10.1038/s41467-019-12541-7

Weiss, R. F. (1981). Determinations of Carbon Dioxide and Methane by Dual Catalyst Flame Ionization Chromatography and Nitrous Oxide by Electron Capture Chromatography. *Journal of Chromatographic Science*, *19*(12), 611–616. https://doi.org/10.1093/chromsci/19.12.611

Welti, N., Hayes, M., & Lockington, D. (2017). Seasonal nitrous oxide and methane emissions across a subtropical estuarine salinity gradient. *Biogeochemistry*, *132*(1–2), 55–69. https://doi.org/10.1007/s10533-016-0287-4

Wilson, B. J., Mortazavi, B., & Kiene, R. P. (2015). Spatial and temporal variability in carbon dioxide and methane exchange at three coastal marshes along a salinity gradient in a northern Gulf of Mexico estuary. *Biogeochemistry*, *123*(3), 329–347. https://doi.org/10.1007/s10533-015-0085-4

Winfrey, M. R., & Ward, D. M. (1983). Substrates for sulfate reduction and methane production in intertidal sediments. *Applied and Environmental Microbiology*, *45*(1), 193–199.

Woodroffe, C. D., Rogers, K., McKee, K. L., Lovelock, C. E., Mendelssohn, I. A., & Saintilan, N. (2016). Mangrove Sedimentation and Response to Relative Sea-Level Rise. *Annual Review of Marine Science*, *8*(1), 243–266. https://doi.org/10.1146/annurev-marine-122414-034025

Xiang, J., Liu, D., Ding, W., Yuan, J., & Lin, Y. (2015). Invasion chronosequence of Spartina Alterniflora on methane emission and organic carbon sequestration in a coastal marsh. *Atmospheric Environment*, *112*, 72–80. https://doi.org/10.1016/j.atmosenv.2015.04.035

Xu, L., Lin, X., Amen, J., Welding, K., & McDermitt, D. (2014). Impact of changes in barometric pressure on landfill methane emission. *Global Biogeochemical Cycles*, *28*(7), 679–695. https://doi.org/10.1002/2013GB004571

Yang, W.-B., Yuan, C.-S., Huang, B.-Q., Tong, C., & Yang, L. (2018). Emission Characteristics of Greenhouse Gases and Their Correlation with Water Quality at an Estuarine Mangrove Ecosystem – the Application of an In-situ On-site NDIR Monitoring Technique. *Wetlands*, *38*, 723–738. https://doi.org/10.1007/s13157-018-1015-8

Ye, W., Zhang, G., Zhu, Z., Han, Y., Wang, L., & Sun, M. (2016). Methane distribution and sea-to-air flux in the East China Sea during the summer of 2013: Impact of hypoxia. *Deep Sea Research Part II: Topical Studies in Oceanography*, *124*, 74–83. https://doi.org/10.1016/J.DSR2.2015.01.008

Yuan, J., Ding, W., Liu, D., Kang, H., Freeman, C., Xiang, J., & Lin, Y. (2015). Exotic Spartina alterniflora invasion alters ecosystem-atmosphere exchange of CH4and N2O and carbon sequestration in a coastal salt marsh in China. *Global Change Biology*, *21*(4), 1567–1580. https://doi.org/10.1111/gcb.12797

Yvon-Durocher, G., Allen, A. P., Bastviken, D., Conrad, R., Gudasz, C., St-Pierre, A., … del Giorgio, P. A. (2014). Methane fluxes show consistent temperature dependence across microbial to ecosystem scales. *Nature*, *507*(7493), 488–491. https://doi.org/10.1038/nature13164

Zhang, G.-L., Zhang, J., Liu, S.-M., Ren, J.-L., & Zhao, Y.-C. (2010). Nitrous oxide in the Changjiang (Yangtze River) Estuary and its adjacent marine area: Riverine input, sediment release and atmospheric fluxes. *Biogeosciences*, *7*, 3505–3516. https://doi.org/10.5194/bg-7-3505-2010

Zhang, J., Gilbert, D., Gooday, A. J., Levin, L., Naqvi, S. W. A., Middelburg, J. J., … Van der Plas, A. K. (2010). Natural and human-induced hypoxia and consequences for coastal areas: synthesis and future development. *Biogeosciences*, *7*(5), 1443–1467. https://doi.org/10.5194/bg-7-1443-2010

Zhang, Y., Ding, W., Cai, Z., Valerie, P., & Han, F. (2010). Response of methane emission to invasion of Spartina alterniflora and exogenous N deposition in the coastal salt marsh. *Atmospheric Environment*, *44*(36), 4588–4594. https://doi.org/10.1016/j.atmosenv.2010.08.012

Zheng, X., Guo, J., Song, W., Feng, J., Lin, G., Zheng, X., … Lin, G. (2018). Methane Emission from Mangrove Wetland Soils Is Marginal but Can Be Stimulated Significantly by Anthropogenic Activities. *Forests*, *9*(12), 738. https://doi.org/10.3390/f9120738

Zhuang, G.-C., Elling, F. J., Nigro, L. M., Samarkin, V., Joye, S. B., Teske, A., & Hinrichs, K.-U. (2016). Multiple evidence for methylotrophic methanogenesis as the dominant methanogenic pathway in hypersaline sediments from the Orca Basin, Gulf of Mexico. *Geochimica et Cosmochimica Acta*, *187*, 1–20. https://doi.org/10.1016/J.GCA.2016.05.005

Zhuang, G.-C., Heuer, V. B., Lazar, C. S., Goldhammer, T., Wendt, J., Samarkin, V. A., … Hinrichs, K.-U. (2018). Relative importance of methylotrophic methanogenesis in sediments of the Western Mediterranean Sea. *Geochimica et Cosmochimica Acta*, *224*, 171–186. https://doi.org/10.1016/J.GCA.2017.12.024

Corrigendum to: A synthesis of methane emissions from shallow vegetated coastal ecosystems (Global Change Biology, (2020), 26, 5, (2988-3005), 10.111/gcb.15046)

Al-Haj, A. N., and R. W. Fulweiler. 2020. Glob. Chang. Biol. **26**: 5342. doi:10.1111/gcb.15192

In the paper by Al-Haj and Fulweiler (2020), global warming potential (GWP) and sustained flux global warming potential (SGWP) were calculated incorrectly. GWP should be calculated using gas emissions in gas mass units (Neubauer & Megonigal, 2015). We thank Judith Rosentreter for bringing the calculation error to our attention and Damien Maher and Patrick Megonigal for consultation on the correction.

The updated version of Table 1.1 includes global flux rate, GWP or SGWP calculated via the following equations for the mean CH_4 flux rate of each ecosystem:

$$Global\ flux\ rate\ (Tmol\ CH_4\ yr^{-1}) = r * \left(\frac{365\ days\ yr^{-1}}{1\ x\ 10^{18}\ \mu mol\ Tmol^{-1}}\right) * A\ * \frac{10^6\ m^2}{km^2}$$

where r is the mean CH_4 flux rate in μmol m^{-2} day^{-1} for each ecosystem and A is the area of the ecosystem in km^2.

$$GWP\ (Tg\ CO_2eq\ yr^{-1}) = GFR * (16.04\ Tg\ CH_4\ Tmol^{-1}) *\ 32$$

$$SGWP\ (Tg\ CO_2eq\ yr^{-1}) = GFR * (16.04\ Tg\ CH_4\ Tmol^{-1}) *\ 45$$

where GFR is the mean global CH_4 flux rate for each ecosystem, and we use the 100 year global warming potential multiplier (32 or 45, respectively) from Neubauer and Megonigal (2015).

Subsequently, section 6: Global warming potential is also incorrect. Using the correct calculations for GWP and SGWP, mangroves and salt marshes release ~1–1.5 g of CO_2 equivalent CH_4 for every gram of CO_2-eq C stored when considering the mean CH_4 flux rate and seagrasses remain CO_2 sinks releasing 1 g of CO_2 equivalent CH_4 for every 17 g of CO_2-eq C stored (Table 1.C1). These results indicate that mangroves and salt marsh ecosystems may be net C storers in some systems and may have net C loss in others.

Code detailing step-by-step calculations can be found at https://github.com/aliaalhaj/Al-HajFulweiler2020_MethanefromVCEs_Code.

Table 1.C1 Global CH_4 emission estimates from vegetated coastal ecosystems (VCEs) and their impact on global carbon cycling. Median CH_4 fluxes, global CH_4 flux estimates (Supporting Text 1.3 in Data S1.1), increase in global marine methane budget (Supporting Text 1.4 in Data S1.1), global warming potential (above), and sustained flux global warming potential (above) from VCEs. Values with the same lower case letter are not significantly different.

		Mangrove	Salt marsh	Seagrass
CH_4 flux rate (μmol CH_4 m^{-2} d^{-1})	mean ± SE	4556.96 ± 1102.06	3534.90 ± 1331.21	108.24 ± 19.72
	median	279.17[a]	224.44[a]	64.80[b]
	range	-67.33 - 72867.83	-92.60 - 94129.68	1.25 - 401.50
Areal Extent (km^2)		137760 - 152361	55000	788000 - 1646788
Global CH_4 flux rate (Tmol CH_4 yr^{-1})	mean ± SE	0.23 ± 0.06 0.25 ± 0.06	0.071 ± 0.027	0.031 ± 0.006 0.065 ± 0.012
Increase in global marine CH_4 budget (%)		40.2 - 44.5	12.5	5.4 - 11.4
Global C burial (Tg C yr^{-1})	mean ± SE	31.1 ± 5.4 34.4 ± 5.9	11.99 ± 1.32	108.74 ± 29.90 227.26 ± 62.57
Global Warming Potential (Tg $CO_{2\ eq}$ y^{-1})	mean	117.61 - 130.08	36.42	15.98 - 33.39
Sustained Flux Global Warming Potential (Tg CO_{2eq} y^{-1})	mean	165.39 - 182.92	51.22	22.47 - 46.96

Global Area Source	McLeod et al. 2011	Mcowen et al. 2017	Jayathilake & Costello, 2018; Davidson & Finlayson, 2019

*Global C burial rates from McLeod et al. (2011)

REFERENCE

Al-Haj AN, Fulweiler RW. A synthesis of methane emissions from shallow vegetated coastal ecosystems. *Glob Change Biol*. 2020;26:2988–3005. https://doi.org/10.1111/gcb.15046

CHAPTER TWO: TEMPERATE SEAGRASS MEADOW CARBON SEQUESTRATION CAN BE ENHANCED BY NITROUS OXIDE UPTAKE

Alia N. Al-Haj[1] (https://ocid.org/0000-0003-1899-5117), Tyler Chidsey[2], & Robinson W. Fulweiler[1,2] (https://orcid.org/0000-0003-0871-4246)

[1]Department of Earth & Environment, Boston University, Boston, MA, U.S.A

[2]Deparment of Biology, Boston University, Boston, MA, U.S.A

Correspondence to: Alia N. Al-Haj (aalhaj@bu.edu)

Running Head: Seagrass methane & nitrous oxide fluxes

Key words**:** methane, nitrous oxide, seagrass, Blue Carbon, carbon sequestration, greenhouse gas

Abstract

Seagrasses are globally important ecosystems that can help mitigate climate change by sequestering carbon. The net impact seagrass meadows have on the climate, however, also depends on methane (CH_4) and nitrous oxide (N_2O) fluxes. By not accounting for CH_4 and N_2O fluxes, we may be over- or underestimating the true C sequestration capacity of seagrasses. Yet, few observations of seagrass CH_4 and N_2O fluxes are available. Here we quantified summer, dark/light CH_4 and N_2O fluxes across the sediment-water interface from seagrass meadows (*Zostera marina*) and adjacent non-vegetated sediments in two temperate bays with different environmental characteristics. We also determined system wide air-sea CH_4 and N_2O fluxes. We found the CH_4 fluxes across the sediment-water interface varied between the two sites with peak mean emissions from one of the seagrass meadows in the dark (3.90 ± 0.92 μmol CH_4 m^{-2} h^{-1}). In contrast, N_2O fluxes across the sediment-water interface were low (-0.005 ± 0.010 μmol m^{-2} h^{-1}) and did not differ between vegetated and non-vegetated sediments or between light and dark treatments. Importantly, one system was a net CH_4 sink from the atmosphere while both systems were net sinks of N_2O from the atmosphere. While the N_2O uptake rates were low, they enhanced the overall cooling potential of both seagrass meadows by ~10%.

Introduction

Vegetated marine ecosystems help mitigate climate change by storing carbon (C) for thousands of years (McLeod et al. 2011; Lovelock and Duarte 2019). Chief among

these “blue carbon” systems are seagrass meadows which store > 10 times more C per unit area than temperate forests (McLeod et al. 2011). To date, most research on C sequestration in seagrass ecosystems has focused on carbon dioxide (CO_2) uptake often ignoring two other greenhouse gases – methane (CH_4) and nitrous oxide (N_2O) (McLeod et al. 2011; Fourqurean et al. 2012; Tokoro et al. 2014). CH_4 and N_2O are important because they have a sustained flux global warming potential (SGWP) 96 and 250 times that of CO_2, respectively, on a 20-year time scale (Neubauer and Megonigal 2015). Thus, by neglecting CH_4 and N_2O, we are potentially miscalculating C budgets for seagrass ecosystems.

Seagrass meadows are likely “hot spots” for both the production and consumption of CH_4 and N_2O. On the one hand, the high sediment organic matter content and low/no sediment oxygen concentrations are ideal conditions for CH_4 and N_2O formation (Murray et al. 2015; Al-Haj and Fulweiler 2020; Rosentreter et al. 2021a). Being coastal systems, seagrasses are also often exposed to high inorganic nitrogen loading which can stimulate N_2O production (Orth et al. 2006; Murray et al. 2015). Additionally, the shallow water column in seagrass meadows can allow CH_4 and N_2O to quickly escape to the atmosphere before being oxidized or reduced (Gao et al. 2013; Egger et al. 2016). Finally, the seagrass plants themselves may act as a pipe for CH_4 and N_2O transport from the sediment to the atmosphere (Kim et al. 1999; Jørgensen et al. 2012; Jeffrey et al. 2019). On the other hand, an oxic water column and the oxygenated seagrass rhizosphere provide an opportunity for CH_4 and N_2O uptake from the atmosphere (Deborde et al. 2010; Reading et al. 2017). For example, CH_4 oxidizing bacteria in the water column and

seagrass rhizosphere can take up more CH_4 than is being produced in some ecosystems (Gerard and Chanton 1993), and N_2O consumption can occur via denitrification when other sources of dissolved inorganic nitrogen are low (Murray et al. 2015). Despite the potential for these ecosystems to be important sources or sinks of greenhouse gases, there is a paucity of data on CH_4 and N_2O fluxes from seagrass meadows.

Filling this knowledge gap is important because increasingly, seagrass ecosystems are valued in terms of their capacity to mitigate climate change through "blue carbon" sequestration (Needelman et al. 2018; Macreadie et al. 2019). Yet, depending on the sum of CO_2, CH_4, and N_2O fluxes, a seagrass ecosystem may have a positive (warming) or negative (cooling) radiative balance. Some studies report enhanced CH_4 and N_2O emissions from seagrass ecosystems reduce, or partially offset, their "blue carbon" benefit (Garcias-Bonet and Duarte 2017; Rosentreter et al. 2018). Here, we use "offset" to mean a reduction of CO_{2eq} (CO_2 equivalent) C sequestration. For example, if CO_2 equivalent (CO_{2eq}) emissions of CH_4 and N_2O are greater than the CO_{2eq} C sequestered, the system will have net CO_{2eq} emission, or a positive radiative balance (Rosentreter et al. 2021a). However, there are only two studies that measure both CH_4 and N_2O fluxes in seagrass ecosystems simultaneously (Camillini 2020; Oreska et al. 2020). Currently, other vegetated coastal ecosystems (i.e., mangrove ecosystems) are included in several countries' Nationally Determined Contributions and C trading markets are being established around their restoration and maintenance (Zeng et al. 2021). However, there is not enough information on CH_4 and N_2O emissions from seagrass ecosystems to include seagrasses in these frameworks.

It is within this context that we wanted to determine the contribution of CH_4 and N_2O fluxes to the radiative balance of seagrass ecosystems. To do so, we quantified CH_4 and N_2O fluxes in the dark and in the light across the sediment-water interface in *Zostera marina* (eelgrass) meadows in two coastal lagoons with different environmental characteristics. We also estimated system-wide air-sea fluxes of CH_4 and N_2O from each lagoon. Additionally, we measured a suite of environmental parameters that could help explain CH_4 and N_2O fluxes from each system. Finally, we estimated CH_4 and N_2O offsets (reduction) of C sequestration for each lagoon. We anticipated the lagoons would be sources of CH_4 and N_2O to the atmosphere. More specifically we hypothesized that fluxes of CH_4 and N_2O across the sediment-water interface would be higher from vegetated sediments when compared to bare sediments, that CH_4 and N_2O fluxes would be higher from vegetated sediments in the light than in the dark, that the lagoon with higher organic matter content would have higher sediment methane emissions, and that the lagoon with higher water column dissolved inorganic nitrogen concentration would have higher sediment N_2O fluxes. Additionally, we hypothesized that the lagoons would maintain a negative radiative balance when CO_{2eq} CH_4 and N_2O fluxes are included in their greenhouse gas budgets.

Methods

Site descriptions

This study was conducted in the U.S. National Park Service Cape Cod National Seashore in East Harbor (42°3'24.42"N, 70°7'10.84"W) in Truro, MA and Pleasant Bay (41°42'33.98"N, 69°57'43.96"W) in Chatham, MA (Permit # CACO-2018-SCI-0001)

(Figure 2.1) between July and September 2018 (n=1) and 2019 (n=2). All sampling occurred in *Zostera marina* (eelgrass) dominated sediments and nearby (>2 m) non-vegetated sediments.

East Harbor is a 2.9 km^2 back-barrier lagoon that was cut-off from tidal flow from 1869 until 2002. In 2002, tidal flow was partially restored to East Harbor through a 200 m long, 2.2 m diameter culvert (Portnoy et al. 2006). The lagoon has an average depth of 1 m with a tidal range of < 0.5 m. Salinity in the lagoon ranges from 12 ppt to 32 ppt and temperature ranges from ~10 ºC to ~30 ºC during the summer months (Portnoy et al. 2006). Water residence time in the lagoon is 133 days (Watts et al. 2011). Although East Harbor is dominated by *Ruppia maritima*, *Z. marina* is present near the opening of the culvert (Portnoy et al. 2006) at about 1.0 m depth. There are currently no published estimates of *Z. marina* areal coverage in East Harbor.

Pleasant Bay is a 31.7 km^2 coastal lagoon connected to the Atlantic Ocean by two tidal inlets. It has a tidal range of 1.4 – 1.6 m and an average depth of 2.0 m (Howes et al. 2006; Borrelli 2009). Salinity ranges from 29 ppt to 31 ppt while summer water temperatures range from 12 ºC to 25 ºC (Legare et al. 2020). Pleasant Bay contains approximately 7.3 km^2 of *Z. marina* (Howes et al. 2006). While there are natural gas deposits in Pleasant Bay, they are limited to the deeper portions of the Bay away from the shallow < 2.0 m depth seagrass ecosystems where we sampled (Borrelli et al. 2020).

Greenhouse gas fluxes across the sediment-water interface

To compare fluxes of CH_4 and N_2O across the sediment-water interface between sites, we measured fluxes in representative stands of vegetation (n=3) and in non-

vegetated (n=3) sediments using static chambers (Emery and Fulweiler 2014). Chambers were covered with jackets of opaque fabric for dark incubations and the jackets were removed for light incubations. For a more in-depth description of the *in situ* benthic chambers, see Supplementary Information S2.1. Sampling locations were chosen haphazardly but were separated by a minimum of ~2 m. Due to logistical constraints, non-vegetated and vegetated sediments were not sampled on the same day but were sampled on consecutive days.

We sampled the chambers immediately after sealing and at four additional time points over 80 – 160 min for a dark incubation with the jacket on the chamber. We then began the light incubation by removing the jacket and sampling immediately and again at four additional time points over an additional 80 – 160 min. We collected duplicate water samples for CH_4 and N_2O concentration in 12 mL exetainer vials (Labco Exetainers®). Vials were filled from the bottom up and were allowed to overflow three times before being preserved with 25 µL of saturated zinc chloride (ZnCl) solution (Ray et al. 2019). Vials were capped and stored underwater at 20 ºC until analysis.

We measured dissolved oxygen (DO) concentration, salinity, and temperature of the chamber water at each time point using a Hach LDO101 DO sensor and a Hach CDC401 conductivity sensor. HOBO pendant light and temperature loggers recorded at one-minute intervals in each chamber for the duration of the incubation. We also collected initial and final dissolved nutrient (dissolved inorganic phosphorous (DIP), ammonium (NH_4^+), nitrite (NO_2^-), and nitrate (NO_3^-)) samples. Water samples were filtered in the field using a GFF filter (0.7 micron pore size) and polypropylene syringe

and were stored in an acid washed, deionized water leached polypropylene bottle at the beginning of the dark incubation, between the dark and light incubations, and at the end of the light incubation. Nutrient samples were stored on ice in the field and then at -20 ºC until analysis.

After each incubation was completed, we counted and collected *Z. marina* aboveground biomass from within each collar. Before removing the collar from vegetated and non-vegetated sediments, cut-off 60 cc syringes were used to collect surface (0-4 cm) sediment. Sediment sub-cores were sectioned into 1 cm increments for %C, %N, and C:N. Sections were stored on ice in the field and at -20 ºC until analysis.

Greenhouse gas fluxes across the air-sea interface

We estimated air-sea CH_4 and N_2O fluxes from East Harbor and Pleasant Bay on two occasions each during July – September 2019 using the discreet sampling method (Rhee et al. 2009). Briefly, we collected duplicate water samples (in 12 mL Labco Exetainers) from the water surface and duplicate air samples from ~ 1 m above the water surface every hour for 6 to 9 hours between the hours of 9:00 EST and 17:00 EST. Water samples were stored and preserved in the same manner as sediment-water interface flux water samples and gas samples were stored at 4 ºC until analysis. Although we collected these samples within the *Z. marina* meadows, we consider them to be representative of the entire system (i.e., influenced by seagrass and bare sediment) as these are open system measurements in sediments with tidal water transport.

Sample analysis and flux determination

Greenhouse gas sample analysis

We quantified CH_4 and N_2O concentrations in each water sample using a headspace equilibration technique with the headspace then analyzed on a GC-2014 gas chromatograph (Shimadzu, Japan) (Emery and Fulweiler 2014; Ray et al. 2019). See a full description of this technique in Supplementary Information S2.2.

We determined concentrations of CH_4 and N_2O by comparing sample peak area to a standard curve calculated from the peak area of 6 different concentrations of an externally mixed standard (Airgas, Billerica MA; Supplementary Information S2.3). The amount of gas in the headspace was calculated using the ideal gas law and the amount of dissolved gas was determined using Henry's law and the solubility coefficients determined by the equations and constants for CH_4 (Wiesenburg and Guinasso 1979) and N_2O (Weiss and Price 1980).

Flux calculations

Fluxes across the sediment-water interface were determined as the linear change in concentration of CH_4 or N_2O over time accounting for chamber volume and area (Ray et al. 2019). For a flux to be considered significant, $R^2 \geq 0.65$ and $p \leq 0.10$. If $R^2 < 0.65$, no flux was exhibited and a value of 0 was assigned (Ray et al. 2019).

Air – sea fluxes were determined as the change in CH_4 or N_2O concentration between surface water and atmospheric gas samples:

$$F = k(C_w - C_a)$$

where F is the flux (μmol m^{-2} h^{-1}), k is the gas transfer velocity (cm h^{-1}), C_w is the concentration of the gas in water (μmol L^{-1}), and C_a is the concentration of the gas in air (μmol L^{-1}) (Wanninkhof 2014). Because we do not have system specific gas transfer velocity equations, we used the average gas transfer velocity calculated from five equations commonly used in coastal ecosystems (Table 2.1). Gas transfer velocity (*k)* is most commonly calculated as a function of wind speed (Clark et al. 1995; Carini et al. 1996; Jiang et al. 2008; Wanninkhof 2014) with others adding terms for current velocity and depth in shallow coastal systems (Borges et al. 2004; Rosentreter et al. 2017). We did not measure water velocity in our basins, so we only used gas transfer velocity calculations that are a function of wind speed. Average daily wind speed during the sampling period was obtained from the nearest NOAA meteorological station to each site (Pleasant Bay: Chatham Airport USW00094624, 3.5 km from site; East Harbor: Station 44018, 17 km from site). Wind speeds were recalculated to a height of 10 m (U_{10}) using the equation provided in Amorocho and DeVries (1980)

$$U_z = U_{10}\left[1 - \frac{(C_{10})^{1/2}}{\kappa}\ln\left(\frac{10}{z}\right)\right] \quad (1)$$

where C_{10} is the surface drag coefficient for wind at 10 m, κ is the Van Karman constant (0.41) and *z* is the height the wind speed was measured at above the water surface (m) (Rosentreter et al. 2017). We normalized *k* to a Schmidt number (*Sc*) of 600 as a function of temperature and salinity for each gas using the equations provided in Wanninkhof (2014).

$$k_{600} = k(\frac{600}{Sc})^{-0.5} \quad (2)$$

where Sc is the Schmidt number and -0.5 is the Schmidt exponent.

Nutrient analysis

Dissolved inorganic nutrient (dissolved inorganic phosphorous (DIP), ammonium (NH_4^+), nitrite (NO_2^-), and nitrate (NO_3^-)) concentrations were determined via digital colorimetry on a SEAL Auto-Analyzer 3 using standard techniques (Strickland and Parsons 1968) with method detection limits of 0.010 µM, 0.080 µM, 0.006 µM, and 0.013 µM, respectively.

Sediment characteristics

Sediment subsections were homogenized and dried at 60 ºC for at least 48 hours before being ground. % C and % N of dried sediments were determined on an Elemental Combustion System 4010 (Costech Analytical Technologies; Valencia, CA) elemental analyzer.

Plant morphometrics and biogeochemistry

To characterize each seagrass meadow, we determined seagrass density, aboveground biomass, leaf area index (LAI), and nutrient pollution indicator (NPI). Seagrass density at each sampling location was determined by counting the number of ramets within each chamber base area. Above-ground biomass was collected by trimming the seagrass at the sediment surface at the end of the incubation. Shoots were stored at 3 ºC until leaves were separated from sheaths and leaf length and width were measured.

Aboveground biomass was determined by drying the leaves and collected sheaths at 60 ºC for a minimum of 48 hours, weighing, and normalizing over chamber base area.

LAI was calculated using the following equation:

$$LAI = l\ x\ w \quad (3)$$

where l is the length of the seagrass blade and w is the width of the seagrass blade. NPI was calculated as the ratio of leaf % N to area normalized leaf mass where leaf % N was determined via elemental analysis (Lee et al. 2004).

Greenhouse gas reduction of C sequestration

We calculated CO_2-equivalent CH_4 and N_2O emissions and uptake in East Harbor and Pleasant Bay by multiplying air-sea fluxes by the sustained flux global warming potential (SGWP) for emission and the sustained flux global cooling potential (SGCP) for uptake (Neubauer and Megonigal 2015). Because we did not measure C sequestration rates in this study, we compared our system wide air-sea fluxes to previously published C sequestration rates for *Z. marina* vegetated sediments in Pleasant Bay (Novak et al. 2020). C sequestration has not been measured for *Z. marina* vegetated sediments in East Harbor, so for this site we used the median C sequestration rate for *Z. marina* vegetated sediments from Novak et al. (2020). We also compared our system wide air-sea fluxes to minimum and median C sequestration rates from non-vegetated sediments in the Pacific Northwest, USA (Prentice et al. 2020), due to a lack of data from non-vegetated sediments in the Northeast U.S. To make the comparison between system-wide air-sea CH_4 and N_2O fluxes and C sequestration rates, we calculated a system-wide C

sequestration rate by multiplying the non-vegetated or vegetated area by the non-vegetated or vegetated C sequestration rate and dividing by the total basin area. We then added vegetated and non-vegetated C sequestration rates together (Supplementary Information S2.4, Table S2.1).

To calculate how much CH_4 and N_2O fluxes could offset (or reduce) the C sequestered in the seagrass meadows, we multiplied $CO_{2\text{-}eq}$ air-sea CH_4 and N_2O emissions and uptake by 12.01/44.01 (mass of C/mass of CO_2) and divided emissions or uptake by the C storage rate for each system. To calculate the amount of C taken up by Pleasant Bay and East Harbor each year, we multiplied the sum of CH_4 and N_2O fluxes and uptake in g C_{eq} m^{-2} y^{-1} by the area of *Z. marina* in each system. Because there are no published estimates of *Z. marina* area in East Harbor, we estimate that *Z. marina* makes up 5% of the area of the basin based on our field observations. We then calculated the net CO_{2eq}-C uptake rate by subtracting the CO_{2eq}-CH_4 and N_2O fluxes from the CO_{2eq}-C sequestration rate (Supplementary Information S2.5).

Statistical analysis

All statistical analysis was performed using R version 4.0.3. Results of statistical tests were considered significant when $p < 0.05$. We tested whether sediment and water column characteristics and CH_4 and N_2O fluxes across the sediment-water interface differed between sites and with eelgrass presence or absence using a least square means test.

We determined the environmental drivers for CH_4 and N_2O fluxes across the sediment-water interface using a mixed model approach. Because the gas flux data are zero-inflated, we modelled our zeros using a zero-adjusted gamma modification to the classic hurdle model (Zuur & Ieno, 2016). Briefly, we performed a Gamma log-link generalized linear model (GLM) on the non-zero data using location, vegetation presence, light treatment, month, and year as fixed effects. We then performed a Bernoulli GLM to identify the chance that a data point is not zero. We subsequently combined the models, calculated Pearson residuals, and combined modelled zeros with the non-zero flux data into one data frame. We then determined the distribution of these data using the *fitdistrplus* package (Delignette-Muller and Dutang 2015). We found that CH_4 and N_2O data best fit a normal distribution.

Before determining the best model for our data, we determined if predictor variables were correlated (Table S2.2) and chose non-correlated predictor variables to use in the model. We then generated multiple generalized linear models using the *lme4* package (Bates et al. 2015; Ray et al. 2019). The presence or absence of seagrass, location, and light treatment were treated as fixed effects in the models along with other non-correlated predictor variables (e.g. O_2 flux, salinity, LAI, %C of the top 0-1 cm sediment) (Table S2.2). This resulted in the construction of 125 models for fluxes of each gas and we used Akaike information criterion (AIC) to select the best models (Bozdogan 1987). We then compared the top two models using likelihood ratio tests through the *lrtest* function in the *lmtest* package (Hothorn et al. 2020) (Table S2.3). When the top two models were not significantly different, we chose to use the simpler model (Table S2.4).

Results.

Site characterization

Water column salinity, NH_4^+, NOx, DIN, and DIP concentrations differed significantly between sites with higher salinity and nutrient concentrations in Pleasant Bay (Table 2.2). However, there was no statistical difference between seagrass density, LAI, or NPI between sites (Table 2.2). Sediment characteristics differed between sites and with vegetation presence. In Pleasant Bay, there was significantly higher %N in the top 0-1 cm of sediment in eelgrass vegetated sediments than in non-vegetated sediments. Eelgrass vegetated sediments in Pleasant Bay also had higher %N than both vegetated and non-vegetated sediments in East Harbor. Similarly, vegetated sediments in Pleasant Bay had higher %C in the top 0-1 cm of sediment than in other vegetated and non-vegetated sediments, however this difference was not statistically significant. Non-vegetated sediments of East Harbor had a significantly higher C:N in the top 0-1 cm of sediment than vegetated sediments of East Harbor and both vegetated and non-vegetated sediments of Pleasant Bay (Table 2.2).

Greenhouse gas fluxes

Fluxes of CH_4 and N_2O across the sediment-water interface were highly variable and zero-inflated with >50% of sediment-water interface measurements exhibiting a net zero flux. CH_4 fluxes ranged from -2.52 μmol m^{-2} h^{-1} to 7.38 μmol m^{-2} h^{-1} with 51% of

the CH_4 flux measurements exhibiting a net zero flux. N_2O fluxes ranged from -0.42 μmol m^{-2} h^{-1} to 0.41 μmol m^{-2} h^{-1} with 84% of the N_2O flux measurements exhibiting a net zero flux.

On average, CH_4 was released by sediments into the water column and N_2O was taken up by sediments from the water column (Table 2.3). There was greater CH_4 flux across the sediment-water interface from vegetated sediments in Pleasant Bay than from non-vegetated sediments in Pleasant Bay (t_{33} = -5.22, $p < 0.0001$). There was no difference in CH_4 flux across the sediment-water interface from vegetated and non-vegetated sediments in East Harbor (t_{31} = -0.05, p = 0.96) (Table S2.5). Vegetated sediments in Pleasant Bay released ~13 times more CH_4 into the water column than non-vegetated sediments in Pleasant Bay take-up (mean ± se: 3.10 ± 0.63 μmol CH_4 m^{-2} h^{-1}, -0.23 ± 0.18 μmol CH_4 m^{-2} h^{-1}, respectively). The vegetated sediments in Pleasant Bay also release ~5 times more CH_4 into the water column than both vegetated and non-vegetated sediments in East Harbor (t_{64} = -4.43, p = 0.0002; t_{64} = -4.68, p = 0.0001) (Figure 2.2a). There was no difference in CH_4 flux across the sediment-water interface for light and dark treatments within Pleasant Bay and East Harbor (t_{33} = 1.02, p = 0.32; t_{31} = -1.03, p = 0.31, respectively) (Table S2.6) nor between Pleasant Bay and East Harbor (t_{66} = -1.62, p = 0.11) (Table 2.3; Table S2.7). There was no difference in flux of N_2O across the sediment-water interface between eelgrass vegetated and non-vegetated sediments, between East Harbor and Pleasant Bay, or between light treatments (Table 2.3; Tables S2.5-S2.8; Figure 2.2b).

Air-sea fluxes of CH_4 and N_2O were relatively low in both systems. Air-sea flux of CH_4 differed between locations with East Harbor acting as a net sink of atmospheric CH_4 and Pleasant Bay acting as a source of CH_4 to the atmosphere (t_{42} = -4.53, p < 0.0001) (Table 2.3). Air-sea flux of N_2O did not differ between sites with both systems acting as a small net sink of atmospheric N_2O (t_{42} = -0.80, p = 0.43) (Table 2.3).

Drivers of greenhouse gas fluxes across the sediment-water interface

CH_4 fluxes across the sediment-water interface were best explained by presence or absence of seagrass and %C in the top 0-1 cm of sediment (Figure 2.3). Specifically, in vegetated sediments there was a positive relationship between CH_4 flux across the sediment-water interface and %C in the top 0-1 cm of sediment. There was no relationship between CH_4 flux across the sediment-water interface and %C in the top 0-1 cm of sediment for non-vegetated sediments. The environmental variables we measured did not explain N_2O fluxes (Table S2.3).

Greenhouse gas reduction of C sequestration

Z. marina meadows in both East Harbor and Pleasant Bay had combined CH_4 and N_2O offsets (i.e., reduction) of C sequestration of less than 100% meaning that, overall, these systems are a net sink of C (Table 2.5). The air-sea CH_4 and N_2O fluxes increased the amount of CO_2 equivalent greenhouse gas uptake by East Harbor by ~84%. CH_4 emissions in Pleasant Bay reduced C storage by 27%. However, the N_2O uptake

counteracts these CH_4 emissions so that when combined the net CH_4 + N_2O reduction of C storage is 19.3% (Table 2.5).

Discussion

CH_4 and N_2O fluxes across the sediment-water interface

Here we show that CH_4 fluxes from *Z. marina* meadows in two temperate ecosystems were highly variable and that N_2O fluxes, at least when we sampled, were negligible. As we hypothesized, CH_4 fluxes across the sediment-water interface were higher from *Z. marina* sediments in Pleasant Bay compared to non-vegetated sediments, emitting more than ten times the CH_4 from non-vegetated sediments (Figure 2.2A). In contrast, there were no significant difference in CH_4 fluxes from East Harbor between seagrass and non-vegetated sediments. In addition, dark and light CH_4 fluxes were not significantly different. N_2O fluxes, however, did not vary between sites, between vegetated and non-vegetated sediments, nor between dark and light incubations (Table 2.3). While seagrass presence and C content (i.e. % C) drove CH_4 fluxes, there were no clear drivers of N_2O fluxes (Figure 2.3, Supplementary Table S2.4). Overall, fluxes of CH_4 and N_2O across the sediment-water interface in East Harbor and Pleasant Bay were low compared to median fluxes from other vegetated coastal ecosystems (Mangrove: 279.17 μmol CH_4 m^{-2} d^{-1}, Salt marsh: 224.44 μmol CH_4 m^{-2} d^{-1}, Al-Haj and Fulweiler 2020; Mangrove: 22.80 μmol N_2O m^{-2} d^{-1}, Salt marsh: 8.16 μmol N_2O m^{-2} d^{-1}, Murray et al. 2015) and were within the range of literature values for other seagrass ecosystems

(Table 2.4). These results indicate that seagrass sediments are small sources of CH_4 and can be very small sources or sinks of N_2O to the water column.

The results from East Harbor were different from previous studies on *Z. marina* as well as from other seagrass species where it has been consistently shown that vegetated sediments have higher CH_4 fluxes than non-vegetated sediments (Table 2.4). One reason for this could be due to the age of the meadow in East Harbor. Eelgrass was planted in East Harbor in 2011 (Bayley 2012) and at the time of sampling, this meadow was only 7 – 8 years old. Previous studies have shown that it takes greater than 10 years following restoration for restored seagrass meadows to provide the same C and N cycling benefits as mature meadows (Greiner et al. 2013; Macreadie et al. 2015). As the seagrass meadow in East Harbor matures and sediment characteristics beneath the seagrass change, CH_4 fluxes from vegetated sediments may exceed those from non-vegetated sediments. These results highlight the importance of taking continuous measurements over several years to determine the CH_4 emission capacity of these systems.

Another reason for the differences in CH_4 emissions between the two *Z. marina* systems studied here could be due to organic matter quantity and quality. Previous studies in wetland ecosystems have found positive correlations between organic matter content and quality and methane emissions (mangrove: Harttung et al., 2021; Konnerup et al., 2014, freshwater: Grasset et al. 2021). For example, soil organic matter content was a strong predictor of CH_4 emissions across three saltmarsh to mangrove transition zones in Florida, USA (Harttung et al. 2021). Methane emission and organic matter content were also highly positively correlated ($r = 0.75$) in the restored mangrove forests of Ciénaga

Grande de Santa Marta, Colombia (Konnerup et al. 2014) and for inland waters, CH_4 production can be predicted by organic matter content and quality (Grasset et al. 2021). In our study, the results are more complicated. %C was a significant predictor of CH_4 flux across the sediment-water interface in vegetated sediments alone (Figure 2.3). C:N was ~2x higher in non-vegetated sediments of East Harbor compared to eelgrass vegetated sediments of Pleasant Bay where we found the lowest C:N and the highest CH_4 emissions (Table 2.2, Table 2.3). However, this is not a simple relationship – as there was a positive relationship between sediment C:N and CH_4 flux for vegetated sediments within East Harbor and Pleasant Bay, separately, and no relationship between C:N and CH_4 flux in non-vegetated sediments (Figure S2.1). This relationship suggests that less labile organic matter is driving CH_4 emissions in vegetated areas. However, the relationship may be driven by labile organic matter from seagrasses being used up quickly, leaving less labile organic material in the sediments (Trevathan-Tackett et al. 2018). Regardless, data from this study and those previously published suggest that sediment C:N and/or %C may be an important predictor variable for CH_4 fluxes.

Substrate availability and competition for substrates for methanogenesis drive CH_4 source and sink dynamics in coastal ecosystems. For example, CH_4 fluxes in tidal marshes are driven by the competition between sulfate reducers and methanogens (Poffenbarger et al. 2011). Similar to other studies in seagrass ecosystems (Garcias-Bonet and Duarte 2017; Al-Haj and Fulweiler 2020), we did not observe a negative relationship between CH_4 emissions and salinity, further demonstrating that the negative correlation between CH_4 emission and salinity observed for tidal marshes (Poffenbarger et al. 2011)

does not hold in seagrass ecosystems. While CH_4 fluxes in saline tidal marshes are driven by competition between sulfate reducing bacteria and hydrogenotrophic and acetoclastic methanogens (DeLaune et al. 1983; Bartlett et al. 1987), different mechanisms may control CH_4 production in seagrass ecosystems. For seagrass ecosystems, methane emission may occur because there is either enough organic matter in the system to meet the demands of sulfate reducing bacteria allowing hydrogenotrophic and acetoclastic methanogens access to organic material to produce CH_4 or a non-competitive form of methanogenesis (methylotrophic or aerobic) is occurring in these systems (Reeburgh 2007). A recent study comparing methanogenic communities in trimethylamine amended *Z. marina* vegetated and non-vegetated sediments, found that methane emissions increased with amendment and that there were higher concentrations of methylotrophic methanogens in vegetated sediments (Zheng et al. 2020). Recent studies from unvegetated coastal sediments also suggest methylotrophic methanogenesis dominates (Zhuang et al. 2018; Yuan et al. 2019). Because of this, we hypothesize that methylotrophic methanogenesis is driving methane emissions in East Harbor and Pleasant Bay.

We hypothesized that N_2O emissions would be higher in vegetated sediments compared to non-vegetated sediments. However, we found no difference in N_2O emissions between eelgrass vegetated and non-vegetated sediments at either site. The results differ from another study on *Z. marina*, which found that vegetation increased N_2O emission (Oreska et al. 2020), but the results were similar to a study on three other seagrass species, which found N_2O uptake in vegetated sediments within the same range

as our results (Camillini 2020) (Table 2.4). One reason for the difference between Oreska et al. (2020) and our study could be due to differences in methods. While we and Camillini (2020) measured diffusive N_2O flux across the sediment-water interface, Oreska et al. (2020) measured ebullitive flux. In other systems (e.g. streams, reservoirs, peatlands), ebullitive fluxes of N_2O are lower than diffusive fluxes (Sturm et al. 2014; Descloux et al. 2017). Oreska et al. (2020), however, report ebullitive fluxes more than 10 times higher than the diffusive fluxes we observed and those reported in Camillini (2020). Part of the ebullitive flux Oreska et al. (2020) detected may have been due to flux through the eelgrass itself. Plant mediated fluxes of N_2O have been shown to be important in other vegetated systems. For example, in rice paddy ecosystems, up to 80% of N_2O emissions are plant-mediated (Yu et al. 1997). Because *Z. marina* is predominantly submerged, plant mediated flux of gases would take the form of bubbles and become part of the ebullitive flux (Long et al. 2020) during light incubations, suggesting that plant mediated flux may be an important pathway for N_2O emission in seagrass ecosystems and may have the potential to change systems from a sink to a source of N_2O. Because we performed dark incubations before light incubations to keep O_2 concentrations below 100% saturation and to prevent bubble formation, we did not see bubble release from the seagrass during light incubations. This indicates that if plant-mediated flux was occurring during the light incubations in East Harbor and Pleasant Bay, that the gases dissolved in the water column and were included in the diffusive flux. If this were the case, there would be an increase in N_2O emission during the light incubations, which is not seen in the data for vegetated sediments in East Harbor and

Pleasant Bay indicating that plant-mediated flux is not an important pathway for N_2O emission in these systems when O_2 concentrations are below 100% saturation.

Because the N_2O fluxes across the sediment-water interface were so low in our system, we were unable to determine what drives the fluxes we did measure. Although our best model contained vegetation presence, there was no significant relationship between N_2O flux across the sediment-water interface and vegetation presence (Table S2.2). Other studies found that vegetation presence and vegetation type significantly impacted N_2O emissions (Murray et al. 2015; Gao et al. 2019; Yang et al. 2020). For other common drivers of N_2O emission, such as DIN or O_2 concentrations, there is no evidence from seagrass ecosystems that there is a pattern between DIN or O_2 concentrations and N_2O flux, unlike in mangrove, salt marsh, and non-vegetated estuarine systems (Murray et al. 2015). However, Camillini (2020) suggests that the N_2O uptake in seagrass systems is due to denitrifiers scavenging N_2O under stable oxic conditions and emission is due to variable oxic conditions stimulating incomplete nitrification. The low fluxes of N_2O that we measured could be the result of both N_2O production and consumption occurring at similar rates. Alternatively, environmental conditions could simply not favor N_2O production or consumption. For example, in coastal systems N_2O emission is primarily observed when nitrate concentrations are high (Murray et al. 2015). In contrast, N_2O uptake is typically observed when nitrate concentrations are low (Ray et al. 2020; Foster and Fulweiler 2016).

Air-sea fluxes of CH_4 and N_2O

Diffusive air-sea fluxes of CH_4 were variable between systems while on average N_2O was taken up by both systems (Figure 2.4). Air-sea CH_4 fluxes from Pleasant Bay were within the range found for other seagrass dominated systems (Table 2.4). However, no other currently published studies from seagrass ecosystems exhibit air-sea CH_4 uptake like we measured in East Harbor. CH_4 uptake from the atmosphere is normally characteristic of upland soils (Grosso et al. 2000), while CH_4 emission to the atmosphere is common across marine and freshwater ecosystems (Rosentreter et al. 2021b). There are, however, some examples of mangrove and tidal marsh ecosystems with net CH_4 uptake from the atmosphere (Bartlett et al. 1985; Sun et al. 2013; Cabezas et al. 2018) and a few examples of submerged coastal and marine ecosystems with CH_4 uptake (Weber et al. 2019). For example, Cabezas et al. (2018) found CH_4 emission from a hydrologically disturbed mangrove creek and CH_4 uptake in an undisturbed mangrove creek, but they could not link any ancillary data (e.g. electrical conductivity, hydroperiod, plant community structure) to these results. Sun et al. (2013), on the other hand, attributed consistent CH_4 uptake in a *Suaeda salsa* marsh to thermal conditions, soil moisture, and salinity. While East Harbor emits 0.6 μmol CH_4 m^{-2} h^{-1} across the sediment-water interface, that CH_4 appears to be oxidized through the water column and ~5 times more CH_4 (mean ± se: -3.03 ± 0.95 μmol m^{-2} h^{-1}; range: -16.52 – 4.36 μmol m^{-2} h^{-1}) is taken from the atmosphere and oxidized in East Harbor. The atmospheric concentration of CH_4 in East Harbor ranged from 1350.6 ppb (55.4 nmol L^{-1}) to 4344.2 ppb (178.1 nmol L^{-1}), and water concentrations ranged from 21.8 nmol L^{-1} to 175.8 nmol

L^{-1}. Low concentrations of CH_4 in the water column may be explained by aerobic methane oxidation by methane-consuming bacteria. Methane oxidizing bacteria have been shown to oxidize CH_4 in coastal ecosystems at rates ranging from 0.5 – 3.4 μmol CH_4 m^{-2} h^{-1} (Steinle et al. 2017), within the range needed for uptake from the atmosphere in East Harbor.

High atmospheric concentrations of CH_4 above East Harbor may be explained by natural (e.g. ebullition) or anthropogenic (e.g. natural gas leaks, septic tank) emissions (Bastviken et al. 2004; McKain et al. 2015). East Harbor was an oligohaline to mesohaline system (4 – 10 ppt) from when it was diked in 1869 to more than a century later when some tidal flow was resumed in 2002 (Portnoy et al. 2006; Watts et al. 2011). Currently, East Harbor has a salinity of 20 – 25 ppt, but is still tidally restricted with 0.5 m tides compared to the 2.5 – 3.5 m tidal range in nearby systems (Portnoy et al. 2006). Thus, East Harbor may function hydrologically more like a shallow lake or pond. Ebullition from lakes and ponds can contribute up to 40% - 60% of system CH_4 emissions and are more important in shallow ecosystems, like East Harbor (Bastviken et al. 2004; Deemer and Holgerson 2021). As of 2015, there was no natural gas service to the area surrounding East Harbor, making pipeline leaks in the area an unlikely source of high atmospheric CH_4 concentrations (www.mass.gov). However, the residential areas on the dunes surrounding East Harbor and on the southern border have septic systems (Portnoy et al. 2006). Septic systems have been shown to emit 2.9 x 10^4 μmol CH_4 $capita^{-1}$ h^{-1} or 3.7 μmol CH_4 m^{-2} h^{-1} using the average lot size for Cape Cod, MA (Nowicki 1994; Diaz-Valbuena et al. 2011), making the combination of ebullition and septic

sources of CH_4 likely causes of elevated atmospheric CH_4 concentrations above East Harbor.

In Pleasant Bay, there is an 84% increase in CH_4 emission between the sediment-water interface and air-sea interface. This indicates that CH_4 oxidation in Pleasant Bay is low and/or that there is likely another source of CH_4 in the basin. This source could be the natural gas deposit located in another area of the system (Borrelli et al. 2020) or it could be due to microbial CH_4 production in the water column (Bižić-Ionescu et al. 2018). Unlike in East Harbor, 95% of atmospheric concentrations of CH_4 measured in Pleasant Bay were within ± 250 ppb of atmospheric concentrations during August, 2019, 1863.0 ppb (https://gml.noaa.gov).

We hypothesized that N_2O would be emitted to the atmosphere in both East Harbor and Pleasant Bay. However, we found uptake of N_2O in both systems. Air-sea N_2O uptake in East Harbor and Pleasant Bay were lower than uptake measured in Wallagoot, Australia (Table 2.4; Camillini, 2020). Although N_2O uptake was measured in these three seagrass ecosystems, N_2O uptake from the atmosphere is not common in non-vegetated coastal areas (Tian et al. 2020). However, other coastal vegetated systems such as mangrove and tidal marshes can be sources or sinks of N_2O seasonally (Murray et al. 2018; Yang et al. 2020) and across spatial gradients (Emery and Fulweiler 2017; Reading et al. 2017). For example, Murray et al. (2018) found that mangrove ecosystems are net sources of N_2O during the dry season and net sinks during the wet season. Emery and Fulweiler (2017) found that unimpacted salt marshes are net sinks of N_2O, that restricted and restored salt marshes can be greater sinks if they have high freshwater input, and that

drier restricted and restored salt marshes are not as strong sinks of N_2O. Diffusive air-sea uptake of N_2O was 124 times greater than sediment-water column uptake in Pleasant Bay and 6 times greater in East Harbor suggesting that these systems have N_2O consumption in the water-column. This N_2O consumption could either occur via denitrification in anaerobic microsites within the water column or occur via aerobic denitrification (Coates and Wyman 2017; Rees et al. 2021).

GHG budget

Overall, we found that both *Z. marina* sediments and non-vegetated sediments in East Harbor and Pleasant Bay were net C sinks. Air-sea CH_4 and N_2O fluxes increased the CO_{2eq}-C uptake in East Harbor from 56.9 g CO_{2eq}-C m^{-2} y^{-1} to 104.6 g CO_{2eq}-C m^{-2} y^{-1} over a 20-year time-scale (Table 2.5). In Pleasant Bay, the air-sea CH_4 and N_2O fluxes reduced C sequestration rates by 9.6 g CO_{2eq}-C m^{-2} y^{-1} on a 20-year time scale (Table 2.5). Although N_2O fluxes seemed negligible in both bays, putting these emissions in the context of CO_2 equivalents and offsets shows that N_2O increased the cooling potential (CO_{2eq} uptake) by ~10% in each bay. CH_4 emissions offset 27% of the carbon sequestration rates in Pleasant Bay and CH_4 uptake increased the cooling potential of East Harbor by ~72% (Figure 2.5, Table 2.5). Our combined CH_4 + N_2O offset of 19.3% for Pleasant Bay is slightly lower than the offset calculated for subtropical seagrass meadows, 31.7 ± 16.6%, and is ~3x higher than the offset calculated for a temperate seagrass meadow, 5.9% (Camillini 2020). CH_4 and N_2O fluxes do not offset C storage in East Harbor.

Overall, seagrass ecosystems emit less CH_4 and N_2O than mangrove and salt marsh ecosystems (CH_4 median: mangrove 279.17; salt marsh 224.44; seagrass 51.9 μmol CH_4 m^{-2} d^{-1}) (N_2O median: mangrove 22.8; salt marsh 8.16; seagrass -0.9 μmol N_2O m^{-2} d^{-1}) (Murray et al. 2015; Al-Haj and Fulweiler 2020; Rosentreter et al. 2021b). Although seagrass meadows, on average, store less C than mangrove and salt marsh ecosystems, (mean ± se: 138 ± 38, 226 ± 39, 218 ± 24 g C m^{-2} y^{-1}, respectively) (McLeod et al. 2011), they have much lower GHG emissions. Thus, restoration and maintenance of seagrass ecosystems may prove to be a better investment in terms of C credits per unit area than for mangrove and salt marsh ecosystems. As CH_4 and N_2O emissions as well as C storage rates are known to be highly variable across coastal ecosystems (Rosentreter et al. 2021a), it is increasingly important to measure GHG fluxes in these systems to determine their true C sequestration value.

Conclusions

The *Z. marina* ecosystems in this study are overall net C sinks. While one system acts as a CH_4 source to the atmosphere and the other acts as a sink, both exhibit consistent diffusive N_2O uptake across the air-sea interface. Even though N_2O fluxes appear negligible in these systems, the net impact N_2O uptake had increased the net cooling benefit of these systems by ~10% and uptake of both CH_4 and N_2O enhance the net CO_{2eq}-C uptake of these seagrass meadows significantly. Consumption of CH_4 and N_2O through the water column can alter the amount of these gases that make it from the sediment to the atmosphere switching even very shallow, <5 m depth, systems from net

sources to net sinks of CH_4 and N_2O. The two *Z. marina* meadows in this study had varying CH_4 source/sink dynamics across the sediment-water interface. While one meadow had higher sediment-water interface CH_4 emissions from vegetated sediments than non-vegetated sediments, as has been demonstrated in other systems, there was no difference in vegetated and non-vegetated CH_4 flux across the sediment-water interface in the other meadow. These results highlight the importance of measuring both CH_4 and N_2O emissions from seagrass ecosystems when determining C budgets.

References

Al-Haj, A. N., and R. W. Fulweiler. 2020. A synthesis of methane emissions from shallow vegetated coastal ecosystems. Glob. Chang. Biol. **26**: 2988–3005. doi:10.1111/gcb.15046

Amorocho, J., and J. J. DeVries. 1980. A new evaluation of the wind stress coefficient over water surfaces. J. Geophys. Res. Ocean. **85**: 433–442. doi:10.1029/JC085IC01P00433

Bartlett, K. B., D. S. Bartlett, R. C. Harriss, and D. I. Sebacher. 1987. Methane Emissions along a Salt Marsh Salinity Gradient. Biogeochemistry **4**: 183–202. doi:10.2307/1468663

Bartlett, K. B., R. C. Harriss, and D. I. Sebacher. 1985. Methane flux form coastal salt marshes. J. Geophys. Res. **90**: 5710–5720. doi:10.1029/JD090iD03p05710

Bastviken, D., J. Cole, M. Pace, and L. Tranvik. 2004. Methane emissions from lakes: Dependence of lake characteristics, two regional assessments, and a global estimate.

Global Biogeochem. Cycles **18**: 1–12. doi:10.1029/2004GB002238

Bates, D. ;, M. ; Mächler, B. ; Bolker, and S. Walker. 2015. Fitting Linear Mixed-Effects Models Using lme4.doi:10.3929/ethz-b-000105397

Bayley, H. K. 2012. The role of eelgrass (Zostera marina L.) source population characteristics in resilience to stress and restoration success. Masters Abstr. Int. Vol. 51, no. 05, 120 p. 2012. 1–120.

Bižić-Ionescu, M., D. Ionescu, M. Günthel, K. W. Tang, and H.-P. Grossart. 2018. Oxic Methane Cycling: New Evidence for Methane Formation in Oxic Lake Water.doi:10.1007/978-3-319-53114-4_10-1

Borges, A. V., J. P. Vanderborght, L. S. Schiettecatte, F. Gazeau, S. Ferrón-Smith, B. Delille, and M. Frankignoulle. 2004. Variability of the gas transfer velocity of CO2 in a macrotidal estuary (the Scheldt). Estuaries **27**: 593–603. doi:10.1007/BF02907647

Borrelli, M. 2009. 37 YEARS OF SHORELINE CHANGE IN PLEASANT BAY: 1868 TO 2005 A Report Prepared for the Pleasant Bay Resource Management Alliance.

Borrelli, M., B. A. Oakley, J. B. Hubeny, H. Love, T. L. Smith, B. J. Legare, and T. Lucas. 2020. The Use of Multimodal Data to Augment Shallow-Water Benthic Habitat Maps for Pleasant Bay, Cape Cod, Massachusetts: Stratigraphic Data and Seafloor Maps. Northeast. Nat. **27**: 48–75. doi:10.1656/045.027.S1003

Bozdogan, H. 1987. Model selection and Akaike's Information Criterion (AIC): The general theory and its analytical extensions. Psychometrika **52**: 345–370. doi:10.1007/BF02294361

Cabezas, A., W. J. Mitsch, C. MacDonnell, L. Zhang, F. Bydałek, and A. Lasso. 2018. Methane emissions from mangrove soils in hydrologically disturbed and reference mangrove tidal creeks in southwest Florida. Ecol. Eng. **114**: 57–65. doi:10.1016/j.ecoleng.2017.08.041

Camillini, N. 2020. Carbon and Nitrogen Cycling in Soil. Ph.D. Thesis, Southern Cross Univ.

Carini, S., N. Weston, C. Hopkinson, J. Tucker, A. Giblin, and J. Vallino. 1996. Gas exchange rates in the Parker River estuary, Massachusetts. Biol. Bull. **191**: 333–335.

Clark, J. F., P. Schlosser, H. J. Simpson, M. Stute, R. Wanninkhof, and D. T. Ho. 1995. Relationship between Gas Transfer Velocities and Wind Speeds in The Tidal Hudson River Determined by the Dual Tracer Technique. *Air-Water Gas Transfer: Selected papers from the third international symposium on air-water gas transfer*. 785–800.

Coates, C. J., and M. Wyman. 2017. A denitrifying community associated with a major, marine nitrogen fixer. Environ. Microbiol. **19**: 4978–4992. doi:10.1111/1462-2920.14007

Deborde, J., P. Anschutz, F. Guérin, and others. 2010. Methane sources, sinks and fluxes in a temperate tidal Lagoon: The Arcachon lagoon (SW France). Estuar. Coast. Shelf Sci. **89**: 256–266. doi:10.1016/j.ecss.2010.07.013

Deemer, B. R., and M. A. Holgerson. 2021. Drivers of Methane Flux Differ Between Lakes and Reservoirs, Complicating Global Upscaling Efforts. J. Geophys. Res. Biogeosciences **126**: e2019JG005600. doi:10.1029/2019JG005600

DeLaune, R. D., C. J. Smith, and W. H. Patrick. 1983. Methane release from Gulf coast wetlands. Tellus B **35 B**: 8–15. doi:10.1111/j.1600-0889.1983.tb00002.x

Delignette-Muller, M. L., and C. Dutang. 2015. fitdistrplus: An R package for fitting distributions. J. Stat. Softw. **64**: 1–34. doi:10.18637/jss.v064.i04

Descloux, S., V. Chanudet, D. Serça, and F. Guérin. 2017. Methane and nitrous oxide annual emissions from an old eutrophic temperate reservoir. Sci. Total Environ. **598**: 959–972. doi:10.1016/J.SCITOTENV.2017.04.066

Diaz-Valbuena, L. R., H. L. Leverenz, C. D. Cappa, G. Tchobanoglous, W. R. Horwath, and J. L. Darby. 2011. Methane, Carbon Dioxide, and Nitrous Oxide Emissions from Septic Tank Systems. Environ. Sci. Technol. **45**: 2741–2747. doi:10.1021/ES1036095

Egger, M., W. Lenstra, D. Jong, and others. 2016. Rapid sediment accumulation results in high methane effluxes from coastal sediments. PLoS One **11**: e0161609. doi:10.1371/journal.pone.0161609

Emery, H. E., and R. W. Fulweiler. 2014. Spartina alterniflora and invasive Phragmites australis stands have similar greenhouse gas emissions in a New England marsh. Aquat. Bot. **116**: 83–92. doi:10.1016/j.aquabot.2014.01.010

Emery, H. E., and R. W. Fulweiler. 2017. Incomplete tidal restoration may lead to persistent high CH4 emission. Ecosphere **8**: e01968. doi:10.1002/ecs2.1968

Fourqurean, J. W., C. M. Duarte, H. Kennedy, and others. 2012. Seagrass ecosystems as a globally significant carbon stock. Nat. Geosci. **5**: 505–509. doi:10.1038/ngeo1477

Gao, G. F., P. F. Li, J. X. Zhong, and others. 2019. Spartina alterniflora invasion alters

soil bacterial communities and enhances soil N2O emissions by stimulating soil denitrification in mangrove wetland. Sci. Total Environ. **653**: 231–240. doi:10.1016/J.SCITOTENV.2018.10.277

Gao, Y., X. Liu, N. Yi, Y. Wang, J. Guo, Z. Zhang, and S. Yan. 2013. Estimation of N2 and N2O ebullition from eutrophic water using an improved bubble trap device. Ecol. Eng. **57**: 403–412. doi:10.1016/j.ecoleng.2013.04.020

Garcias-Bonet, N., and C. M. Duarte. 2017. Methane Production by Seagrass Ecosystems in the Red Sea. Front. Mar. Sci. **4**. doi:10.3389/fmars.2017.00340

Gerard, G., and J. Chanton. 1993. Quantification of methane oxidation in the rhizosphere of emergent aquatic macrophytes: defining upper limits. Biogeochem. 1993 232 **23**: 79–97. doi:10.1007/BF00000444

Grasset, C., S. Moras, A. Isidorova, R.-M. Couture, A. Linkhorst, and S. Sobek. 2021. An empirical model to predict methane production in inland water sediment from particular organic matter supply and reactivity. Limnol. Oceanogr. **9999**: lno.11905. doi:10.1002/LNO.11905

Greiner, J. T., K. J. McGlathery, J. Gunnell, and B. A. McKee. 2013. Seagrass Restoration Enhances “Blue Carbon” Sequestration in Coastal Waters. PLoS One **8**: 1–8. doi:10.1371/journal.pone.0072469

Grosso, S. J. Del, W. J. Parton, A. R. Mosier, and others. 2000. General CH4 oxidation model and comparisons of CH4 Oxidation in natural and managed systems. Global Biogeochem. Cycles **14**: 999–1019. doi:10.1029/1999GB001226

Harttung, S. A., K. R. Radabaugh, R. P. Moyer, J. M. Smoak, and L. G. Chambers. 2021.

Coastal riverine wetland biogeochemistry follows soil organic matter distribution along a marsh-to-mangrove gradient (Florida, USA). Sci. Total Environ. **797**: 149056. doi:10.1016/J.SCITOTENV.2021.149056

Hemminga, M. A. 1998. The root/rhizome system of seagrasses: An asset and a burden. J. Sea Res. **39**: 183–196. doi:10.1016/S1385-1101(98)00004-5

Hothorn, T., A. Zeileis, R. W. Farebrother, C. Cummins, G. Millo, and D. Mitchell. 2020. Testing Linear Regression Models.

Howes, B., S. Kelley, J. Ramsey, R. Samimy, D. Schlesinger, and E. Eichner. 2006. Massachusetts Estuaries Project Linked Watershed-Embayment Model to Determine Critical Nitrogen Loading Thresholds for the Pleasant Bay System, Towns of Orleans.

Jeffrey, L. C., G. Reithmaier, J. Z. Sippo, S. G. Johnston, D. R. Tait, Y. Harada, and D. T. Maher. 2019. Are methane emissions from mangrove stems a cryptic carbon loss pathway? Insights from a catastrophic forest mortality. New Phytol. doi:10.1111/nph.15995

Jiang, L.-Q., W.-J. Cai, and Y. Wang. 2008. A comparative study of carbon dioxide degassing in river- and marine-dominated estuaries. Limnol. Oceanogr. **53**: 2603–2615. doi:10.4319/LO.2008.53.6.2603

Jørgensen, C. J., S. Struwe, and B. Elberling. 2012. Temporal trends in N2O flux dynamics in a Danish wetland – effects of plant-mediated gas transport of N2O and O2 following changes in water level and soil mineral-N availability. Glob. Chang. Biol. **18**: 210–222. doi:10.1111/J.1365-2486.2011.02485.X

Kim, J., S. B. Verma, and D. P. Billesbach. 1999. Seasonal variation in methane emission from a temperate Phragmites-dominated marsh: effect of growth stage and plant-mediated transport. Glob. Chang. Biol. **5**: 433–440. doi:10.1046/j.1365-2486.1999.00237.x

Konnerup, D., J. M. Betancourt-Portela, C. Villamil, and J. P. Parra. 2014. Nitrous oxide and methane emissions from the restored mangrove ecosystem of the Ciénaga Grande de Santa Marta, Colombia. Estuar. Coast. Shelf Sci. **140**: 43–51. doi:10.1016/j.ecss.2014.01.006

Lee, K. S., F. T. Short, and D. M. Burdick. 2004. Development of a nutrient pollution indicator using the seagrass, Zostera marina, along nutrient gradients in three New England estuaries. Aquat. Bot. **78**: 197–216. doi:10.1016/j.aquabot.2003.09.010

Legare, B. J., O. C. Nichols, A. Mittermayr, and M. Borrelli. 2020. Relationships between Species Communities as Determined by Analysis of Data from Multiple Surveys of Pleasant Bay, Cape Cod, MA. Northeast. Nat. **27**: 114–131. doi:10.1656/045.027.s1005

Long, M. H., K. Sutherland, S. D. Wankel, D. J. Burdige, and R. C. Zimmerman. 2020. Ebullition of oxygen from seagrasses under supersaturated conditions. Limnol. Oceanogr. **65**: 314–324. doi:10.1002/lno.11299

Lovelock, C. E., and C. M. Duarte. 2019. Dimensions of Blue Carbon and emerging perspectives. Biol. Lett. **15**: 23955–6900. doi:10.1098/RSBL.2018.0781

Macreadie, P. I., A. Anton, J. A. Raven, and others. 2019. The future of Blue Carbon science. Nat. Commun. **10**. doi:10.1038/s41467-019-11693-w

Macreadie, P. I., S. M. Trevathan-Tackett, C. G. Skilbeck, J. Sanderman, N. Curlevski, G. Jacobsen, and J. R. Seymour. 2015. Losses and recovery of organic carbon from a seagrass ecosystem following disturbance. Proc. R. Soc. B Biol. Sci. **282**: 20151537. doi:10.1098/rspb.2015.1537

McKain, K., A. Down, S. M. Raciti, and others. 2015. Methane emissions from natural gas infrastructure and use in the urban region of Boston, Massachusetts. Proc. Natl. Acad. Sci. **112**: 1941–1946. doi:10.1073/PNAS.1416261112

McLeod, E., G. L. Chmura, S. Bouillon, and others. 2011. A blueprint for blue carbon: Toward an improved understanding of the role of vegetated coastal habitats in sequestering CO2. Front. Ecol. Environ. **9**: 552–560. doi:10.1890/110004

Murray, R., D. Erler, J. Rosentreter, D. Maher, and B. Eyre. 2018. A seasonal source and sink of nitrous oxide in mangroves: Insights from concentration, isotope, and isotopomer measurements. Geochim. Cosmochim. Acta **238**: 169–192. doi:10.1016/j.gca.2018.07.003

Murray, R. H., D. V. Erler, and B. D. Eyre. 2015. Nitrous oxide fluxes in estuarine environments: response to global change. Glob. Chang. Biol. **21**: 3219–3245. doi:10.1111/gcb.12923

Needelman, B. A., I. M. Emmer, S. Emmett-Mattox, S. Crooks, J. P. Megonigal, D. Myers, M. P. J. Oreska, and K. McGlathery. 2018. The Science and Policy of the Verified Carbon Standard Methodology for Tidal Wetland and Seagrass Restoration. Estuaries and Coasts **41**: 2159–2171. doi:10.1007/s12237-018-0429-0

Neubauer, S. C., and J. P. Megonigal. 2015. Moving Beyond Global Warming Potentials

to Quantify the Climatic Role of Ecosystems. Ecosystems **18**: 1000–1013. doi:10.1007/s10021-015-9879-4

Novak, A. B., M. C. Pelletier, P. Colarusso, and others. 2020. Factors Influencing Carbon Stocks and Accumulation Rates in Eelgrass Meadows Across New England, USA. Estuaries and Coasts **43**: 2076–2091. doi:10.1007/s12237-020-00754-9

Nowicki, T. P. 1994. The Prospects for Coastal Residential Development Under the Cape Cod Commission Stewardship. Massachusetts Institute of Technology.

Oreska, M. P. J., K. J. McGlathery, L. R. Aoki, A. C. Berger, P. Berg, and L. Mullins. 2020. The greenhouse gas offset potential from seagrass restoration. Sci. Rep. **10**: 1–15. doi:10.1038/s41598-020-64094-1

Orth, R. J., T. J. B. Carruthers, W. C. Dennison, and others. 2006. A Global Crisis for Seagrass Ecosystems. Bioscience **56**: 987–996. doi:10.1641/0006-3568(2006)56[987:agcfse]2.0.co;2

Poffenbarger, H. J., B. A. Needelman, and J. P. Megonigal. 2011. Salinity influence on methane emissions from tidal marshes. Wetlands **31**: 831–842. doi:10.1007/s13157-011-0197-0

Portnoy, J., S. Smith, E. Gwilliam, and K. Chapman. 2006. Annual Report on Estuarine Restoration at East Harbor (Truro, MA), Cape Cod National Seashore, September 2006.

Prentice, C., K. L. Poppe, M. Lutz, and others. 2020. A Synthesis of Blue Carbon Stocks, Sources, and Accumulation Rates in Eelgrass (Zostera marina) Meadows in the Northeast Pacific . Global Biogeochem. Cycles **34**. doi:10.1029/2019gb006345

Ray, N. E., T. J. Maguire, A. N. Al-Haj, M. C. Henning, and R. W. Fulweiler. 2019. Low Greenhouse Gas Emissions from Oyster Aquaculture. Environ. Sci. Technol. **53**: 9118–9127. doi:10.1021/acs.est.9b02965

Reading, M. J., I. R. Santos, D. T. Maher, L. C. Jeffrey, and D. R. Tait. 2017. Shifting nitrous oxide source/sink behaviour in a subtropical estuary revealed by automated time series observations. Estuar. Coast. Shelf Sci. **194**: 66–76. doi:10.1016/j.ecss.2017.05.017

Reeburgh, W. S. 2007. Oceanic Methane Biogeochemistry.doi:10.1021/CR050362V

Rees, A. P., I. J. Brown, A. Jayakumar, G. Lessin, P. J. Somerfield, and B. B. Ward. 2021. Biological nitrous oxide consumption in oxygenated waters of the high latitude Atlantic Ocean. Commun. Earth Environ. 2021 21 **2**: 1–8. doi:10.1038/s43247-021-00104-y

Rhee, T. S., A. J. Kettle, and M. O. Andreae. 2009. Methane and nitrous oxide emissions from the ocean: A reassessment using basin-wide observations in the Atlantic. J. Geophys. Res. Atmos. **114**. doi:10.1029/2008JD011662

Rosentreter, J. A., A. N. Al-Haj, R. W. Fulweiler, and P. Williamson. 2021a. Methane and Nitrous Oxide Emissions Complicate Coastal Blue Carbon Assessments. Global Biogeochem. Cycles **35**: e2020GB006858. doi:10.1029/2020GB006858

Rosentreter, J. A., A. V. Borges, B. R. Deemer, and others. 2021b. Half of global methane emissions come from highly variable aquatic ecosystem sources. Nat. Geosci. **14**: 225–230. doi:10.1038/s41561-021-00715-2

Rosentreter, J. A., D. T. Maher, D. V Erler, R. H. Murray, and B. D. Eyre. 2018. Methane

emissions partially offset “blue carbon” burial in mangroves. Sci. Adv. **4**: eaao4985. doi:10.1126/sciadv.aao4985

Rosentreter, J. A., D. T. Maher, D. T. Ho, M. Call, J. G. Barr, and B. D. Eyre. 2017. Spatial and temporal variability of CO_2 and CH_4 gas transfer velocities and quantification of the CH_4 microbubble flux in mangrove dominated estuaries. Limnol. Oceanogr. **62**: 561–578. doi:10.1002/lno.10444

Steinle, L., J. Maltby, T. Treude, and others. 2017. Effects of low oxygen concentrations on aerobic methane oxidation in seasonally hypoxic coastal waters. Biogeosciences **14**: 1631–1645. doi:10.5194/bg-14-1631-2017

Strickland, J., and T. Parsons. 1968. A practical handbook of seawater analysis, 2nd ed. Fisheries Research Board of Canada.

Sturm, K., Z. Yuan, B. Gibbes, U. Werner, and A. Grinham. 2014. Methane and nitrous oxide sources and emissions in a subtropical freshwater reservoir, South East Queensland, Australia. Biogeosciences **11**: 5245–5258. doi:10.5194/BG-11-5245-2014

Sun, Z., L. Wang, H. Tian, H. Jiang, X. Mou, and W. Sun. 2013. Fluxes of nitrous oxide and methane in different coastal Suaeda salsa marshes of the Yellow River estuary, China. Chemosphere **90**: 856–865. doi:10.1016/J.CHEMOSPHERE.2012.10.004

Tian, H., R. Xu, J. G. Canadell, and others. 2020. A comprehensive quantification of global nitrous oxide sources and sinks. Nature **586**: 248–256. doi:10.1038/s41586-020-2780-0

Tokoro, T., S. Hosokawa, E. Miyoshi, K. Tada, K. Watanabe, S. Montani, H. Kayanne,

and T. Kuwae. 2014. Net uptake of atmospheric CO_2 by coastal submerged aquatic vegetation. Glob. Chang. Biol. **20**: 1873–1884. doi:10.1111/gcb.12543

Trevathan-Tackett, S. M., A. C. G. Thomson, P. J. Ralph, and P. I. Macreadie. 2018. Fresh carbon inputs to seagrass sediments induce variable microbial priming responses. Sci. Total Environ. **621**: 663–669. doi:10.1016/j.scitotenv.2017.11.193

Wanninkhof, R. 2014. Relationship between wind speed and gas exchange over the ocean revisited. Limnol. Oceanogr. Methods **12**: 351–362. doi:10.4319/lom.2014.12.351

Watts, I. M., J. Dean Rosati, and M. Borrelli. 2011. Re-Establishing a Historical Inlet At East Harbor, Cape Cod, Masssachusetts. Proc. Coast. Sediments 419–429. doi:10.1142/9789814355537_0032

Weber, T., N. A. Wiseman, and A. Kock. 2019. Global ocean methane emissions dominated by shallow coastal waters. Nat. Commun. **10**: 4584. doi:10.1038/s41467-019-12541-7

Weiss, R. F., and B. A. Price. 1980. Nitrous oxide solubility in water and seawater. Mar. Chem. **8**: 347–359. doi:10.1016/0304-4203(80)90024-9

Wiesenburg, D. A., and N. L. J. Guinasso. 1979. Equilibrium solubilities of methane, carbon monoxide, and hydrogen in water and sea water. J. Chem. Eng. Data **24**: 356–360. doi:10.1021/JE60083A006

Yang, B., X. Li, S. Lin, Z. Xie, Y. Yuan, M. Espenberg, J. Pärn, and Ü. Mander. 2020. Invasive Spartina alterniflora can mitigate N2O emission in coastal salt marshes. Ecol. Eng. **147**: 105758. doi:10.1016/J.ECOLENG.2020.105758

Yu, K. W., Z. P. Wang, and G. X. Chen. 1997. Nitrous oxide and methane transport

through rice plants. Biol. Fertil. Soils 1997 243 **24**: 341–343. doi:10.1007/S003740050254

Yuan, J., D. Liu, Y. Ji, J. Xiang, Y. Lin, M. Wu, and W. Ding. 2019. Spartina alterniflora invasion drastically increases methane production potential by shifting methanogenesis from hydrogenotrophic to methylotrophic pathway in a coastal marsh. J. Ecol. **107**: 2436–2450. doi:10.1111/1365-2745.13164

Zeng, Y., D. A. Friess, T. V. Sarira, K. Siman, and L. P. Koh. 2021. Global potential and limits of mangrove blue carbon for climate change mitigation. Curr. Biol. doi:10.1016/j.cub.2021.01.070

Zheng, S., B. Wang, G. Xu, and F. Liu. 2020. Effects of Organic Phosphorus on Methylotrophic Methanogenesis in Coastal Lagoon Sediments With Seagrass (Zostera marina) Colonization. Front. Microbiol. **0**: 1770. doi:10.3389/FMICB.2020.01770

Zhuang, G.-C., V. B. Heuer, C. S. Lazar, and others. 2018. Relative importance of methylotrophic methanogenesis in sediments of the Western Mediterranean Sea. Geochim. Cosmochim. Acta **224**: 171–186. doi:10.1016/J.GCA.2017.12.024

Acknowledgements

Funding for this research was provided to ANA by the Cape Cod National Seashore Nickerson Fellowship, Sigma Xi, Boston University Biogeoscience, the Limnology & Oceanography Research Exchange (LOREX), and the Boston University Martin Luther King, Jr. Fellowship, and the Boston University Department of Earth & Environment.

RWF was supported by funding from Rhode Island Sea Grant and Woods Hole Sea Grant. We wish to acknowledge Dr. Alyssa Novak for help identifying research sites and Mr. Norval Reece and Mrs. Anne Reece for parking and beach access to one of the sites. Thank you to Brendan Kelly, Nick Ray, Claudia Mazur, Nia Bartolucci, Melissa Hagy, Cristian Triana, Gretchen McCarthy, Anniina Haka, and Ena Miculinic for field help and to John Rezza, Kwetz Mexika, Joel Sparks, and Nilotpal Ghosh for help in the lab. Thank you to Cedric Fichot for the use of their elemental analyser. The authors declare no conflicts of interest. Data presented in this study can be accessed upon publication via Figshare (doi: 10.6084/m9.figshare.16725166).

Tables

Table 2.1. Mean (± standard error) gas transfer velocities of CO_2, CH_4, and N_2O for each site (East Harbor: EH, Pleasant Bay: PB) calculated from equations derived in previously published studies. The average gas transfer velocity (final row) represents an average of the five methods from the previously published studies and is the gas transfer velocity used here.

Citation	Equation	k_{600}-CH_4 (cm h^{-1})		k_{600}-N_2O (cm h^{-1})	
		EH	***PB***	***EH***	***PB***
Wanninkhof (2014)	$k = 0.251u^2(Sc/660)^{-0.5}$	4.80 (± 1.15)	1.69 (± 0.28)	4.81 (± 1.15)	1.69 (± 0.28)
Jiang et al. (2008)	$k_{600} = 0.314U_{10}^2 - 0.436U_{10} + 3.99$	8.17 (± 1.15)	4.75 (± 0.24)	7.63 (± 1.06)	5.09 (± 0.24)
Borges et al. (2004)	$k_{600} = 5.141u_{10}^{0.758}$	14.90 (± 1.31)	10.57 (± 0.70)	14.96 (± 1.32)	10.64 (± 0.70)
Carini et al. (1996)	$k_{600} = 0.045 + 2.0277U_{10}$	8.29 (± 0.97)	5.29 (± 0.45)	8.33 (± 0.97)	5.33 (± 0.45)
Clark et al. (1995)	$k_{600} = 2.0 + 0.24U_{10}^2$	8.44 (± 0.97)	6.10 (± 0.26)	6.12 (± 0.97)	3.69 (± 0.26)
Average	-	8.45 (± 1.11)	5.19 (± 0.38)	8.37 (± 1.10)	5.29 (± 0.39)

Table 2.2. Overview of site characteristics for vegetated and non-vegetated sediments of East Harbor and Pleasant Bay. Mean (± standard error) seagrass density, leaf area index (LAI), and nutrient pollution indicator (NPI: % leaf N/ area normalized leaf mass), surface (top ~ 10 cm) water column salinity and nutrient concentrations (ammonium: NH_4^+, nitrite: NO_2^-, nitrate + nitrite: NO_x, dissolved inorganic nitrogen: DIN and dissolved inorganic phosphorous: DIP), and sediment surface (top 0-1 cm depth) % nitrogen (N), % carbon (C), and carbon to nitrogen molar ratio (C:N) from one sampling date for each site during summer 2018 and two sampling dates for each site during summer 2019. Superscripts of differing letters indicate statistically different (least square means, $p < 0.05$) values between sites and vegetated and non-vegetated sediments.

		East Harbor		Pleasant Bay	
		eelgrass	non-vegetated	eelgrass	non-vegetated
Seagrass	Density (shoots m^{-2})	305.9 (± 34.9)^{a}	0.0 (± 0.0)^{b}	410.3 (± 48.2)^{a}	0.0 (± 0.0)^{b}
	LAI (m^2m^{-2})	0.0084 (± 0.0013)^{a}	0.0 (± 0.0)^{b}	0.0072 (± 0.0014)^{a}	0.0 (± 0.0)^{b}
	NPI (%N/leaf mass)	0.65 (± 0.23)^{a}	--	1.15 (± 0.27)^{a}	--
Water column	Salinity (ppt)	25.6 (± 0.5)^{a}	25.9 (± 0.4)^{a}	32.4 (± 0.1)^{b}	32.6 (± 0.1)^{b}
	NH_4^+ (µM)	0.74 (± 0.18)^{a}	0.99 (± 0.14)^{a}	3.52 (± 0.73)^{b}	2.02 (± 0.19)^{ab}
	NO_2^- (µM)	0.04 (± 0.005)^{a}	0.04 (± 0.005)^{a}	0.04 (± 0.007)^{a}	0.05 (± 0.005)^{a}
	NO_x (µM)	0.13 (± 0.031)^{ac}	0.11 (± 0.011)^{a}	0.21 (± 0.033)^{bc}	0.24 (± 0.013)^{b}
	DIN (µM)	0.90 (± 0.211)^{a}	1.01 (± 0.158)^{a}	3.77 (± 0.754)^{b}	2.05 (± 0.250)^{a}
	DIP (µM)	0.38 (± 0.036)^{a}	0.45 (± 0.023)^{a}	1.07 (± 0.137)^{b}	0.76 (± 0.029)^{c}
Sediment	N (%)	0.039 (± 0.005)^{a}	0.043 (± 0.003)^{a}	0.092 (± 0.009)^{b}	0.036 (± 0.005)^{a}
	C (%)	0.448 (± 0.071)^{ac}	0.728 (± 0.081)^{ab}	0.902 (± 0.118)^{b}	0.373 (± 0.031)^{c}
	C:N	13.28 (± 0.59)^{a}	20.18 (± 2.30)^{b}	11.14 (± 0.60)^{a}	13.37 (± 1.27)^{a}

Table 2.3. Fluxes (mean ± standard error) of methane (CH_4) and nitrous oxide (N_2O) from eelgrass vegetated and non-vegetated sediments in East Harbor and Pleasant Bay. Fluxes across the sediment-water interface are the mean of measurements from summer 2018 and 2019. Air-Sea fluxes are from summer 2019. Letters indicate statistically significant (least square means, $p < 0.05$) differences between sites, vegetated and non-vegetated sediments, and light treatment.

		East Harbor				Pleasant Bay			
		eelgrass		non-vegetated		eelgrass		non-vegetated	
		light	dark	light	dark	light	dark	light	dark
Sediment-Water Interface Flux	CH_4 (μmol m^{-2} h^{-1})	0.746 (± 0.443)^{ab}	0.553 (± 0.495)^{ab}	0.905 (± 0.444)^{ab}	0.312 (± 0.164)^{ab}	2.210 (± 0.917)^{bc}	3.897 (± 0.824)^{c}	-0.174 (± 0.311)^{a}	-0.276 (± 0.184)^{a}
	N_2O (μmol m^{-2} h^{-1})	-0.017 (± 0.017)^{a}	-0.019 (± 0.013)^{a}	-0.006 (± 0.006)^{a}	-0.003 (± 0.003)^{a}	-0.018 (± 0.067)^{a}	0.039 (± 0.047)^{a}	0.000 (± 0.000)^{a}	-0.025 (± 0.020)^{a}
Whole System Air-Sea Flux	CH_4 (μmol m^{-2} h^{-1})	-3.03 (± 0.95)^{a}				1.00 (± 0.19)^{b}			
	N_2O (μmol m^{-2} h^{-1})	-0.07 (± 0.03)^{a}				-0.04 (± 0.02)^{a}			

Table 2.4. Fluxes of methane (CH_4) and nitrous oxide (N_2O) across the air-sea or sediment-water column (sed-wc) interface in seagrass vegetated sediments from previously published studies. Diffusive fluxes are dissolved gas fluxes while ebullitive fluxes are bubble fluxes. The bottom two rows are the mean (± standard error (se)) sediment-water column interface and air-sea fluxes. The mean sediment-water column interface and air-sea fluxes (final two rows) represent an average of the sediment-water column interface and air-sea fluxes from the previously published studies and this study

Site	Species	Flux Type	CH_4 Flux ($\mu mol\ m^{-2}\ d^{-1}$)	N_2O Flux ($\mu mol\ m^{-2}\ d^{-1}$)	Citation
Ria Formosa Lagoon, Portugal	*Zostera noltii*	air-sea diffusive	307.4		Bahlmann et al., 2015
Chilika Lagoon, India	*Halodule-Halophila* spp.	air-sea diffusive	120.0		Banerjee et al., 2018
Arcachon Lagoon, France	*Zostera marina*	air-sea diffusive	294.0		Deborde et al., 2010
Chwaka Bay, Tanzania	*Thalassia hemprichii*	air-sea diffusive	74.8		Lyimo et al., 2017
Red Sea, Saudi Arabia	*Halophila stipulacea*	air-sea diffusive	43.7		Burkholz et al., 2020
Wallagoot, Australia	*Ruppia megacarpa*	air-sea diffusive	33.8	-0.9	Camillini 2020
East Harbor, MA	*Zostera marina*	air-sea diffusive	-72.7	-1.7	This study
Pleasant Bay, MA	*Zostera marina*	air-sea diffusive	24.0	-1.0	This study
Awerange Bay, Indonesia	*Enhalus acoroides*	sed-wc diffusive	95.7		Alongi et al., 2008
Florida, USA	*Thalassia testudinum*	sed-wc diffusive	183.3		Barber and Carlson, 1993
Arcachon Lagoon, France	*Zostera marina*	sed-wc diffusive	48.8		Deborde et al., 2010
Red Sea, Saudi Arabia	*Halodule uninervis*	sed-wc diffusive	48.0		Garcias-Bonet and Duarte, 2017
Red Sea, Saudi Arabia	*Cymodocea and Halodule* spp.	sed-wc diffusive	401.5		Garcias-Bonet and Duarte, 2017
Red Sea, Saudi Arabia	*Enhalus acoroides*	sed-wc diffusive	96.0		Garcias-Bonet and Duarte, 2017
Red Sea, Saudi Arabia	*Thalassodendron ciliatum*	sed-wc diffusive	3.1		Garcias-Bonet and Duarte, 2017
Red Sea, Saudi Arabia	*Halophila decipiens*	sed-wc diffusive	1.2		Garcias-Bonet and Duarte, 2017
Red Sea, Saudi Arabia	*Thalassia hemprichii*	sed-wc diffusive	6.2		Garcias-Bonet and Duarte, 2017
Red Sea, Saudi Arabia	*Halophila and Halodule spp.*	sed-wc diffusive	61.1		Garcias-Bonet and Duarte, 2017
Florida, USA	*Thalassia testudinum*	sed-wc diffusive	44.3		Oremland, 1975
Bimini, Bahamas	*Syringodium filiforme*	sed-wc diffusive	5.6		Oremland, 1975
South Bay, VA, USA	*Zostera marina*	sed-wc ebullitive	136.7	3.7	Oreska et al., 2020
Tomales Bay, CA, USA	*Zostera marina*	sed-wc diffusive	35.7		Sansone et al., 1998
Wallis Lake (Australia)	*Halophila ovalis*	sed-wc diffusive	45.4	0.3	Camillini 2020
Wallis Lake (Australia)	*Posidonia australia*	sed-wc diffusive	279.3	-0.6	Camillini 2020
Wallis Lake (Australia)	*Zostera muelleri*	sed-wc diffusive	46.0	-1.2	Camillini 2020
Moreton Bay, Australia	*Zostera muelleri*	sed-wc diffusive	10.9		Moriarty, 1985
East Harbor, MA	*Zostera marina*	sed-wc diffusive	15.1	-0.4	This study
Pleasant Bay, MA	*Zostera marina*	sed-wc diffusive	74.4	0.3	This study
Mean (± standard error)		air-sea	103.1 (± 44.2)	-1.2 (± 0.2)	
		sed-wc	81.9 (± 22.2)	0.3 (± 0.6)	

Table 2.5. Offsets (reduction) of organic C (C_{org}) accumulation calculated from sustained global warming potential (positive) or sustained global cooling potential (negative) over a 20 (SGW/CP_{20}) year time scale for CH_4 and N_2O fluxes from East Harbor and Pleasant Bay. C_{org} is adjusted for the area of vegetated and non-vegetated sediments in each basin (Supplementary Information S4, Table S1). CO_{2eq}-C uptake rates are the difference between C_{org} accumulation rates and air-sea CH_4 and N_2O fluxes (Supplementary Information S2.5).

		East Harbor	Pleasant Bay
	Area adjusted C_{org} accumulation rate (g CO_{2eq}-C m^{-2} y^{-1})	56.9	49.9
CH_4	**Air-Sea Flux (mg m^{-2} y^{-1})**	-425.7 ± 133.5	140.5 ± 26.7
	SGW/CP_{20} (g CO_{2eq} m^{-2} y^{-1})	-40.9	13.5
N_2O	**Air -Sea Flux (mg m^{-2} y^{-1})**	-27.0 ± 11.6	-15.4 ± 7.7
	SGW/CP_{20} (g CO_{2eq} m^{-2} y^{-1})	-6.7	-3.9
Offsets	**CH_4 SGW/CP_{20} (%)**	-71.8	27.0
	N_2O SGW/CP_{20} (%)	-11.8	-7.7
	CH_4 + N_2O SGW/CP_{20} (%)	-83.6	19.3
CO_{2eq}-C Uptake Rate	**SGW/CP_{20} (g CO_{2eq} m^{-2} y^{-1})**	104.6	40.3

Figures

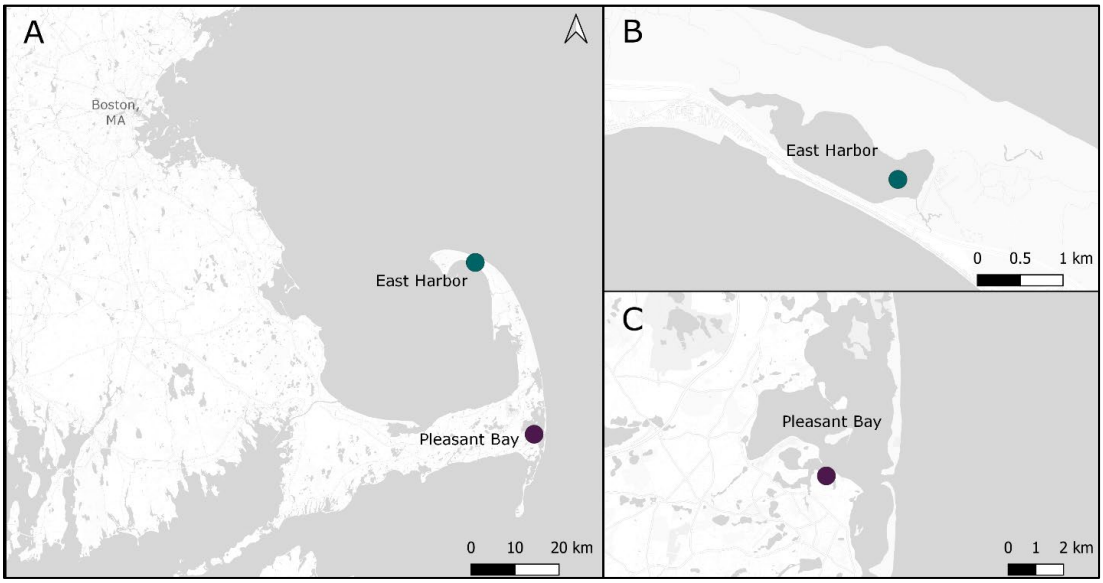

Figure 2.1. Map of sampling locations on Cape Cod, Massachusetts, USA. (A) Map of Southeastern Massachusetts, USA with East Harbor (green) and Pleasant Bay (purple) highlighted by colored circles. (B) Map of East Harbor with sampling location depicted by green circle. (C) Map of Pleasant Bay with sampling location depicted by purple circle.

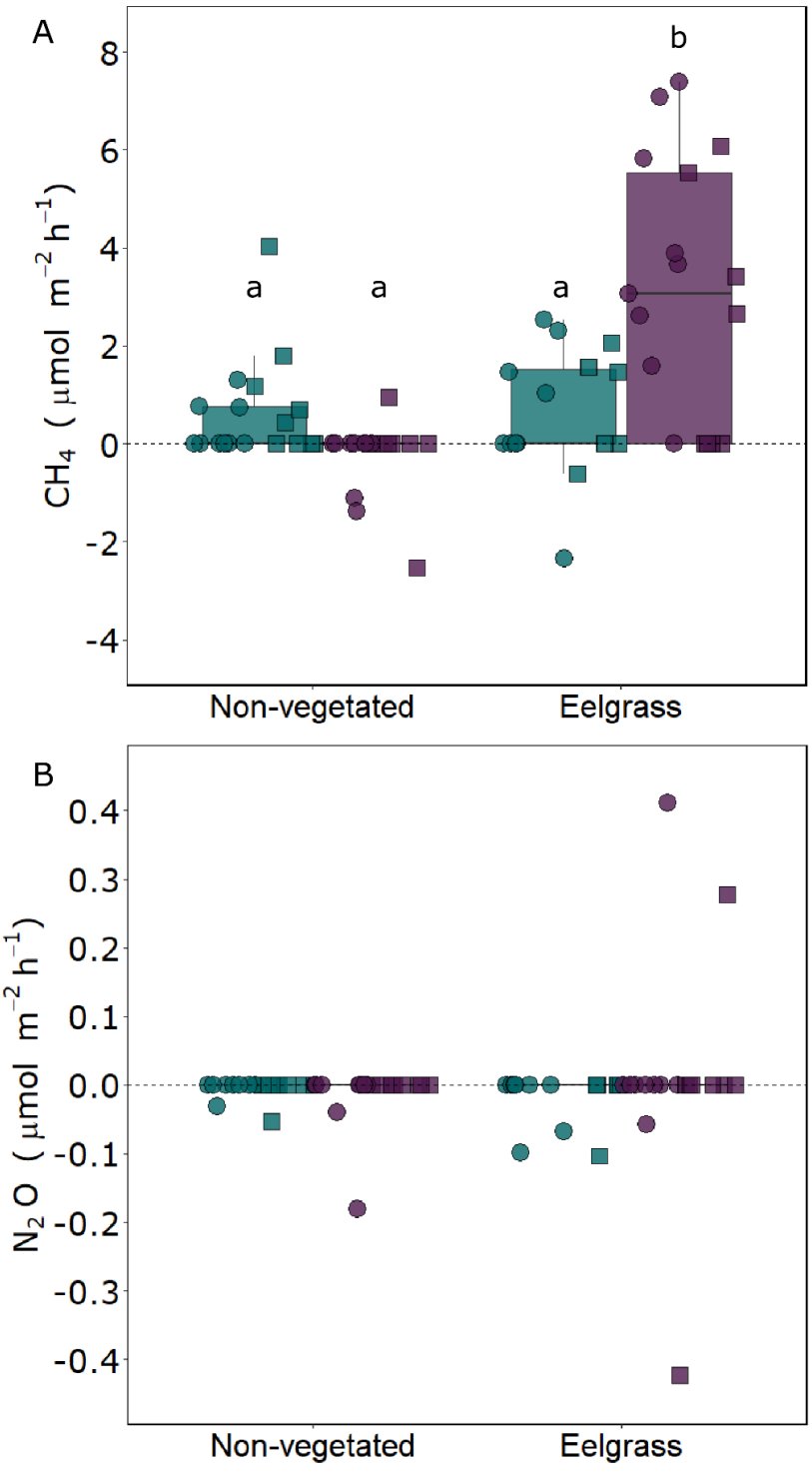
A
8
6
4
2
0
-2
-4
CH_4 (µmol m^{-2} h^{-1})
a
a
a
b
Non-vegetated
Eelgrass
B
0.4
0.3
0.2
0.1
0.0
-0.1
-0.2
-0.3
-0.4
N_2O (µmol m^{-2} h^{-1})
Non-vegetated
Eelgrass

Figure 2.2. Fluxes of methane (CH_4) (A) and nitrous oxide (N_2O) across the sediment-water interface (B) from eelgrass vegetated and non-vegetated sediments in East Harbor (green) and Pleasant Bay (purple) over light (square) and dark (circle) incubations. Positive fluxes indicate emission into the water column while negative fluxes indicate uptake by the sediment. Lower-case letters indicate significant differences ($p \leq 0.05$) across both vegetation treatment and site following least-square means test. There were no significant differences across site and vegetation treatment for N_2O fluxes. Individual points represent flux measurements.

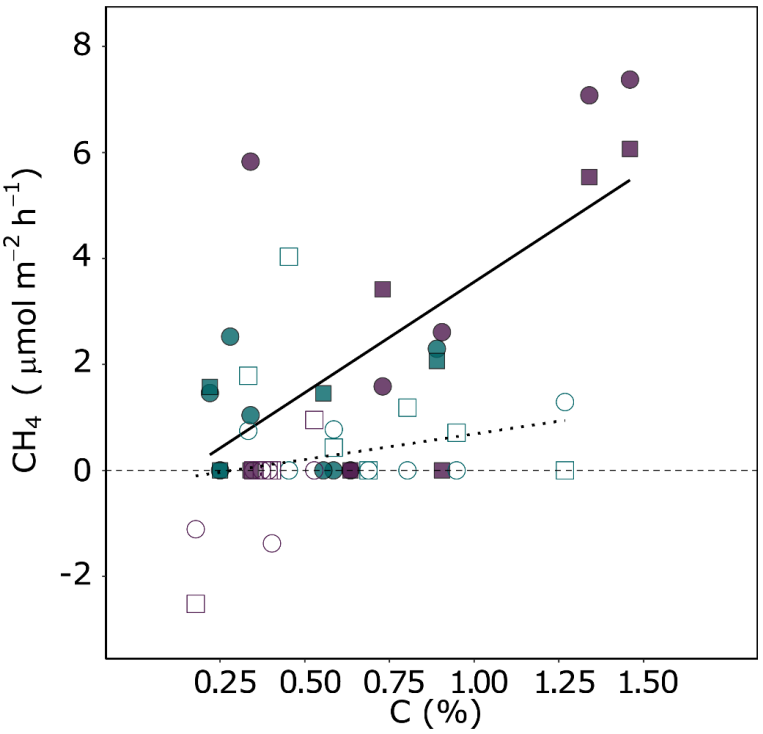

Figure 2.3. Fluxes of methane (CH_4) across the sediment-water interface as a function of %C in the surface (top 0-1 cm) of sediment from eelgrass vegetated (filled points) and non-vegetated (open points) sediments in East Harbor (green) and Pleasant Bay (purple) over light (square) and dark (circle) incubations. Positive fluxes indicate emission into the water column while negative fluxes indicate uptake by the sediment. The solid line indicates the relationship between CH_4 flux and %C in vegetated sediments ($y = 4.18x - 0.63$, $R^2 = 0.45$, $p < 0.0005$). There is no relationship between CH_4 flux and %C in non-vegetated sediments (dotted line, $R^2 = 0.02$, $p = 0.23$).

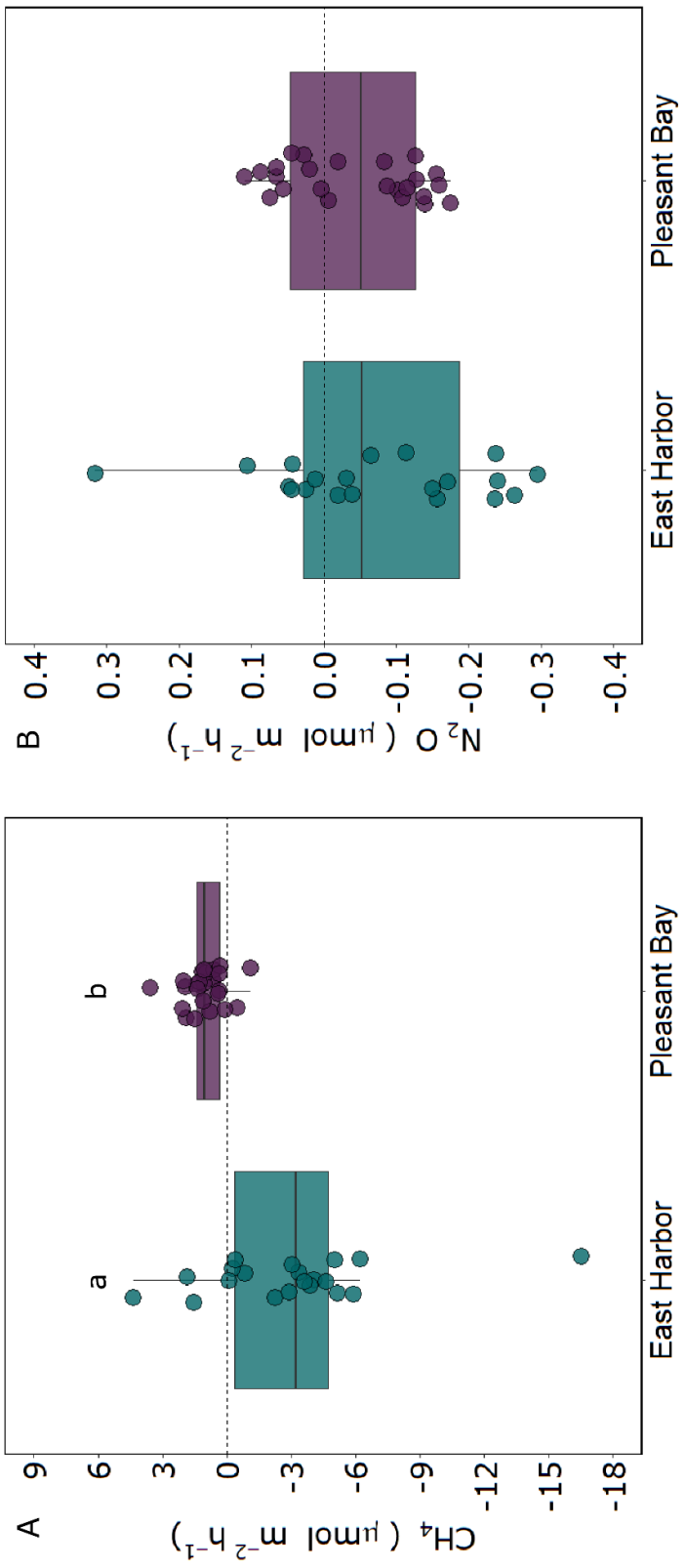
A
B
CH_4 (μmol m^{-2} h^{-1})
N_2O (μmol m^{-2} h^{-1})
9
6
3
0
-3
-6
-9
-12
-15
-18
0.4
0.3
0.2
0.1
0.0
-0.1
-0.2
-0.3
-0.4
a
b
East Harbor
Pleasant Bay

Figure 2.4. Methane (CH_4) (A) and nitrous oxide (N_2O) (B) fluxes across the air-sea interface from East Harbor (green) and Pleasant Bay (purple). Positive fluxes indicate emission into the atmosphere while negative fluxes indicate flux into the water. Lower-case letters indicate significant differences ($p \leq 0.05$) across sites following least-square means test. There were no significant differences across site and vegetation treatment for N_2O fluxes. Individual points represent flux measurements.

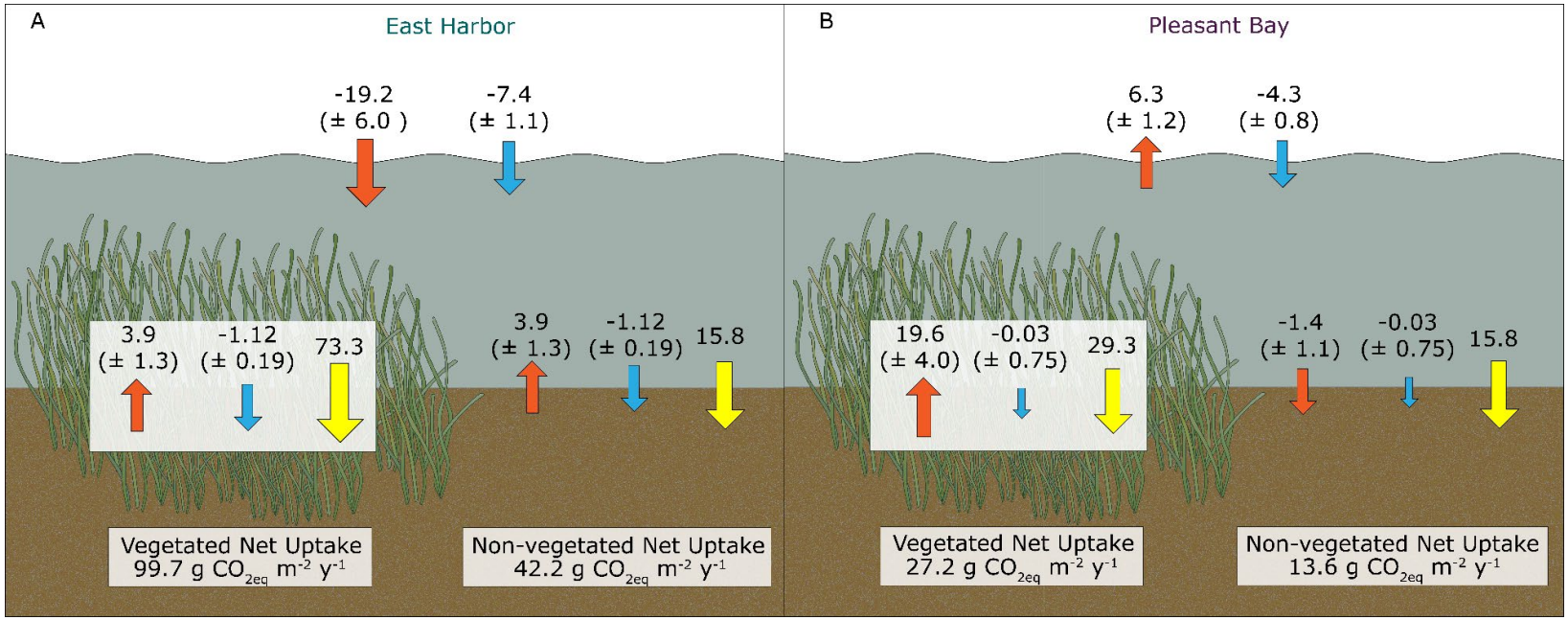
A
East Harbor
-19.2
(± 6.0)
-7.4
(± 1.1)
3.9
(± 1.3)
-1.12
(± 0.19)
73.3
3.9
(± 1.3)
-1.12
(± 0.19)
15.8
Vegetated Net Uptake
99.7 g CO2eq m-2 y-1
Non-vegetated Net Uptake
42.2 g CO2eq m-2 y-1
B
Pleasant Bay
6.3
(± 1.2)
-4.3
(± 0.8)
19.6
(± 4.0)
-0.03
(± 0.75)
29.3
-1.4
(± 1.1)
-0.03
(± 0.75)
15.8
Vegetated Net Uptake
27.2 g CO2eq m-2 y-1
Non-vegetated Net Uptake
13.6 g CO2eq m-2 y-1

Figure 2.5. Greenhouse gas budgets for the two seagrass-vegetated coastal bays studied here. Carbon (C) (yellow) storage and fluxes of methane (CH_4) (orange) and nitrous oxide (N_2O) (blue) across the air-sea and sediment-water interface in vegetated and non-vegetated sediments of East Harbor (A) and Pleasant Bay (B). All fluxes are presented in g CO_{2eq} m^{-2} y^{-1} (± standard error) over a 100-year time scale. Net uptake is the sum of C storage, CH_4 flux, and N_2O flux.

.

CHAPTER THREE: FLUXES OF DISSOLVED INORGANIC CARBON, NITROGEN, PHOSPHORUS ARE HIGHLY VARIABLE IN *Z. marina* MEADOWS

Alia N. Al-Haj[1] (https://ocid.org/0000-0003-1899-5117) & Robinson W. Fulweiler[1,2] (https://orcid.org/0000-0003-0871-4246)

[1]Department of Earth & Environment, Boston University, Boston, MA, U.S.A

[2]Deparment of Biology, Boston University, Boston, MA, U.S.A

Correspondence to: Alia N. Al-Haj (aalhaj@bu.edu)

Abstract

Seagrass meadows are hot spots of biogeochemical cycling. Previous studies have found that some seagrass meadows increase fluxes of oxygen (O_2) and dissolved inorganic carbon (DIC) as well as increase nitrogen removal and enhance phosphorus fluxes compared to bare (non-vegetated) areas. Here we used *in situ* benthic chambers to quantify dark/light net O_2, DIC, N_2 (i.e., net denitrification or net nitrogen fixation), dissolved inorganic nitrogen (NO_2^-, NO_2^- + NO_3^-, NH_4^+), and dissolved inorganic phosphorus (DIP) fluxes in *Zostera marina* meadows and adjacent non-vegetated sediments of two coastal bays in the northeastern, U.S (Cape Cod, MA) over two summers. O_2 and DIC fluxes were similar at both sites. We observed no statistical differences in N_2 fluxes between *Z. marina* sediments and non-vegetated sediments (0.73 ± 0.48 mmol N_2-N m^{-2} h^{-1} and 1.16 ± 0.47 mmol N_2-N m^{-2} h^{-1}, respectively; $p = 0.52$) or

between dark and light incubations (1.48 ± 0.47 mmol N_2-N m^{-2} h^{-1} and 0.39 ± 0.47 mmol N_2-N m^{-2} h^{-1}, respectively; $p = 0.11$). However, the mean denitrification rate of non-vegetated sediments and dark incubations were roughly 3X greater than rates from vegetated and light incubations. While NO_2^- fluxes did not vary with presence of vegetation, site, or light, NO_2^- + NO_3^-, NH_4^+, and DIP fluxes varied by location and light with significantly higher fluxes from dark incubations at one site. This study highlights the variability in inorganic carbon, nitrogen, and phosphorus fluxes across seagrass ecosystems.

Introduction

Seagrass meadows provide many ecosystem services to coastal areas and act as hotspots for biogeochemical cycling (Marbà et al. 2006; Barbier et al. 2011). Seagrasses impact oxygen (O_2) gradients in the water column and sediments (Pedersen et al. 1998; Borum et al. 2007) and store more carbon (C) than adjacent non-vegetated areas (Oreska et al. 2020). In turn, seagrass meadows, compared to non-vegetated sediments, have unique microbial community composition, as well as different rates of organic matter decomposition and nutrient cycling (Sun et al. 2020; Garcias-Bonet et al. 2021). However, the magnitude and direction of O_2, inorganic C, inorganic nitrogen (N), and inorganic phosphorus (P) fluxes vary across studies, indicating that these processes are highly site specific.

Oxygen concentrations in coastal ecosystems are primarily driven by production and consumption in the water column and sediment (Long et al. 2019). Photosynthesis is

the primary process controlling production of O_2, while consumption processes include respiration and secondary oxidation of reduced metabolites (Canfield et al. 2005). Seagrasses impact both O_2 production and consumption in coastal ecosystems. During the day, when seagrasses are photosynthesizing, O_2 production can exceed consumption and more O_2 is released into the water column than in non-vegetated systems (Eyre et al. 2011b; Long et al. 2019). At night, or in the dark, O_2 consumption dominates and more O_2 is consumed in seagrass ecosystems than in non-vegetated ecosystems (Eyre et al. 2011b). For example, Eyre et al. (2011b) found that the O_2 emission from *Zostera capricorni* dominated sediments was ~10x higher than O_2 emission from non-vegetated sediments during the day and O_2 uptake by *Z. capricorni* dominated sediments in the dark was ~5x higher than O_2 uptake by non-vegetated sediments. Although seagrass photosynthesis and respiration play a role in this increase in magnitude of the oxygen flux, it is the environment that they create that drives the increased oxygen uptake. Specifically, seagrasses provide habitat for heterotrophic organisms and stimulate microbial respiration by exuding O_2 and labile organic matter from their roots into the sediments (Smith et al. 1984; Moriarty et al. 1986; Mukai et al. 1989; Duarte 2017). Previous studies have highlighted that O_2 fluxes vary across seagrass ecosystems with time of year, species, age of meadows, and stressors (Apostolaki et al. 2010; Eyre et al. 2011a; Berg et al. 2019). This variability in O_2 fluxes is linked to seagrass and microbial community metabolism which is also a strong control on inorganic carbon fluxes.

Seagrasses also have a large impact on the cycling of dissolved inorganic carbon (i.e. CO_2, bicarbonate, and carbonate) in coastal ecosystems. During the day, seagrasses

take up CO_2 and bicarbonate from the water column to use as a carbon source for photosynthesis (Invers et al. 2001; Larkum et al. 2007). During both day and night, seagrass and the microbial community respire, releasing CO_2 into the water column (Rasmusson et al. 2020). Seagrasses increase microbial respiration in coastal areas by exuding labile organic matter into the sediments and trapping organic material from the water column by slowing down currents (Moriarty et al. 1986; Watanabe and Kuwae 2015). Respiration in seagrass meadows is largely driven by temperature with some seagrass meadows switching from net autotrophic during cooler months to net heterotrophic in the summer (Berg et al. 2019; Van Dam et al. 2021). Seagrass meadows can also switch from net autotrophic to net heterotrophic due to environmental stressors such as low O_2 conditions, excess nutrient loading, low light conditions, or high sediment sulfide concentrations. Many of these stressors occur concurrently and can both reduce seagrass photosynthesis and respiration while increasing microbial respiration (Burkholder et al. 2007). There is high variability in fluxes of CO_2 and DIC across seagrass ecosystems. For example, respiration is higher in tropical seagrass meadows than in temperate seagrass meadows (Duarte et al. 2010) and DIC fluxes in tropical seagrass meadows can become uncoupled from O_2 fluxes due to carbonate dissolution increasing the DIC flux (Van Dam et al. 2019). Therefore, net CO_2 and DIC fluxes can give insights into the impact varying environmental conditions have on seagrass communities with communities in higher stress environments acting as inorganic C sources to the water column, while communities in lower stress environments act as inorganic C sinks.

Seagrasses are also heavily impacted by N loading and can enhance N cycling in coastal areas. Seagrasses prefer to grow in low N environments where light is more abundant (Eyre et al. 2011a). In areas with excess N loading, seagrass meadows die-off because their light requirements increase due to low O_2 availability, and high sediment sulfide concentrations, yet the amount of light reaching them declines because of enhanced phytoplankton, macroalgae, or epiphytic growth (Orth et al. 2006; McGlathery et al. 2007; Burkholder et al. 2007). One way seagrasses solve the issue of not having enough N for growth is by providing habitat for nitrogen fixers and potentially, nitrifiers (Nakagawa et al. 2019; Mohr et al. 2021). For example, it was recently discovered that N_2 fixing microbes live in *Posidonia oceanica* root tissue providing ammonia and dissolved organic nitrogen to the seagrass in exchange for sugars (Mohr et al. 2021). Seagrass meadows can also enhance N burial (Aoki et al. 2020) and can help permanently remove N from coastal areas by stimulating coupled nitrification-denitrification (Aoki and McGlathery 2018). However, recent studies have found mixed results when comparing denitrification in seagrass vegetated sediments to non-vegetated sediments with some studies finding elevated rates of denitrification with the presence of vegetation and others reporting equivalent rates regardless of absence or presence of seagrass (Seymour et al. 2018). Therefore, the role of seagrass meadows in N cycling is unclear.

Like other nutrient fluxes, dissolved inorganic phosphorus (DIP) fluxes are variable across seagrass ecosystems (Yarbro and Carlson 2008; Eyre et al. 2011a; Lohrer et al. 2016). In general, studies have found low DIP fluxes in seagrass ecosystems with

some systems displaying net uptake (Lohrer et al. 2016) and others displaying net emissions (Eyre et al. 2011a). Reactive P adsorbs to iron oxyhydroxides in temperate coastal ecosystems and adsorbs to calcium carbonate in tropical ecosystems (Jensen et al. 1995, 1998). In temperate ecosystems, reactive P is desorbed from iron oxyhydroxides under low O_2 conditions when sulfide is present, much like in the reducing sediments of temperate seagrass meadows (Jensen et al. 1995; Touchette and Burkholder 2000; Foster and Fulweiler 2019). Because of their role in changing O_2 and CO_2 gradients in coastal sediments, seagrass meadows can enhance DIP fluxes (Oshima et al. 1999; Yarbro and Carlson 2008; Eyre et al. 2011a). However, it is unclear to what degree seagrass impacts the magnitude and direction of these fluxes.

The purpose of this study was to compare how fluxes of oxygen, carbon, nitrogen, and phosphorus differed between seagrass meadows and non-vegetated sediments in two temperate coastal lagoons. To do so, we quantified *in situ* O_2, DIC, N_2, and dissolved inorganic nutrient (NO_2^-, NO_x, NH_4^+, and DIP) fluxes across the sediment-water interface in *Zostera marina* (eelgrass) meadows in the light and dark over two summers. We also measured a suite of environmental variables that could help us explain these fluxes. We hypothesized that *Z. marina* presence would enhance the magnitude of fluxes, but not change the direction of fluxes, of all constituents compared to non-vegetated sediments and that the fluxes would be positively correlated with plant morphometrics. We also hypothesized that O_2 and N_2 emission would be higher in the light compared to the dark, and conversely that emission of DIC, NH_4^+, and DIP would be higher in the dark compared to the light. Finally, we predict that temperature will be negatively correlated

with O_2 flux and positively correlated with fluxes of DIC and NH_4^+ whereas initial O_2 concentrations will be correlated with DIP and N_2 fluxes.

Methods

Site Descriptions

This study was conducted at two sites (East Harbor (42°3'24.42"N, 70°7'10.84"W) and Pleasant Bay (41°42'33.98"N, 69°57'43.96"W)) in the U.S. National Park Service Cape Cod National Seashore (Permit # CACO-2018-SCI-0001) (Figure 3.1). East Harbor is a small (1.4 km^2), shallow (1.27 m) back-barrier lagoon with a tidal range of < 0.5 m residence time of 133 days (Watts et al. 2011). In summer 2017, East Harbor contained 0.32 km^2 of submerged aquatic vegetation (SAV) comprised of both filamentous green algae and *Z. marina* (Mittermayr et al. 2020). However, there are no published estimates of *Z. marina* coverage alone.

Pleasant Bay is a larger (31.7 km^2) coastal lagoon with a tidal range of 1.4 – 1.6 m and an average depth of 2.0 m (Howes et al. 2006; Borrelli 2009). Approximately 25% (or 7.3 km^2) of Pleasant Bay is covered by *Z. marina* (Howes et al. 2006).

Sampling fluxes of O_2, DIC, N_2, and nutrients across the sediment-water interface

In situ sampling took place once in the summer of 2018 and twice in the summer of 2019 during the months of July and August. We sampled in *Z. marina* (eelgrass) dominated sediments and nearby (>2 m) non-vegetated sediments.

We used static chambers to quantify dark and light fluxes of dissolved oxygen (O_2), dissolved inorganic carbonate (DIC), and net di-nitrogen gas (N_2-N) in representative stands of vegetation (n=3) and in non-vegetated (n=3) sediments (Supplementary Information S3.1). Within each site, we deployed the chambers haphazardly and each chamber was separated by a minimum of ~2 m. Vegetated and non-vegetated sediments were sampled on consecutive days because of logistical constraints.

We conducted the dark incubation first by sealing the chamber, with no air in the headspace and no bubbles, and covered the chamber with opaque fabric. We then collected five time points of duplicate water samples over 80 – 160 minutes for O_2 and N_2-N concentration in 12 mL exetainer vials (Labco Exetainer®). We then removed the fabric and conducted the light incubation, again collecting five time points and duplicate samples over 80 – 160 minutes (Chapter 2). All samples were preserved with 25 µL of saturated zinc chloride (ZnCl) solution, capped, and stored underwater at 20 ºC until analysis (Ray et al. 2020). An additional 4 mL water sample was collected and filtered through a 0.2 µM PES syringe filter. 1 mL each of sample was then injected into duplicate pre-combusted and pre-weighed helium flushed exetainers containing 1 mL of 85% phosphoric acid for dissolved inorganic carbon (DIC) analysis. DIC vials were stored at 4 ºC until analysis (Ashford et al. 2021).

To determine dissolved nutrient (nitrite (NO_2^-), nitrite + nitrate (NO_x), ammonium (NH_4^+), and dissolved inorganic phosphorous (DIP)) fluxes across the sediment-water interface, we collected initial and final dissolved nutrient samples over 80 – 160 minutes. Water samples were filtered in the field using a GFF filter (0.7 micron pore size) and acid

washed polypropylene syringe and were stored in an acid washed, deionized water leached, polypropylene bottle at the beginning of the dark incubation, between the dark and light incubations, and at the end of the light incubation. Nutrient samples were stored on ice in the field and then at -20 ºC until analysis.

Dissolved oxygen (DO) concentration, temperature, and salinity of the chamber water were measured with a DO sensor (Hach LDO101) and a conductivity sensor (Hach CDC401) at each time point and when the opaque fabric was removed from the chamber. Light and temperature were recorded inside each chamber every minute during the light and dark incubations using HOBO pendant light and temperature loggers.

When incubations were complete, we counted *Z. marina* shoots within the collar and collected this aboveground biomass. We collected 60 cc sediment cores to determine sediment %C, %N, and C:N of the surface (top 0-1 cm) sediment. We stored sediment samples at -20 ºC until analysis.

Sample Analysis and Flux Determination

O_2, N_2, and DIC sample analysis

We determined dissolved O_2 and N_2/Argon (Ar) concentrations in each water sample using a quadrupole membrane inlet mass spectrometer (MIMS) (Kana et al. 1994). To estimate sample N_2-N concentration from N_2/Ar, we multiplied the N_2/Ar by the theoretical Ar concentration of the sample at the given temperature and salinity (Weiss 1970; Colt 1984; Fulweiler et al. 2007; Ray et al. 2020). This method provides a measurement of net N_2 fluxes (gross denitrification and annamox – gross nitrogen fixation).

We quantified the concentration of DIC as CO_2 in each sample using a GC-2014 gas chromatograph (Shimadzu, Japan) equipped with a flame ionization detector (FID) and methanizer for determination of CO_2. The instrument was equipped with HayeSep® Q and N and Shimalite® columns. N_2 gas was used as the carrier gas. 5 mL of headspace was removed from the DIC sample vials and injected into the GC to determine CO_2 concentration.

DIC concentrations as CO_2 gas were determined by comparing sample peak area to a standard curve calculated from the peak area of 7 sodium bicarbonate standards (HCO_3 concentration: 8000 uM, 6000 uM, 4000 uM, 2000 uM, 1000 uM, 600 uM, 0 uM) fixed in helium flushed exetainers with 1 mL of 85% phosphoric acid. The concentration of HCO_3 in the water sample was determined by dividing the concentration of HCO_3 by the volume of sample in the vial (Ashford et al. 2021).

Nutrient Analysis

Nitrite (NO_2^-), nitrate + nitrite (NO_x), ammonium (NH_4^+), and dissolved inorganic phosphorous (DIP) concentrations were determined with standard techniques via digital colorimetry (SEAL Auto-Analyzer 3) (Strickland and Parsons 1968). Method detection limits were 0.006 µM, 0.013 µM, 0.080 µM, and 0.010 µM, respectively.

Flux Calculations

Fluxes were determined as the linear change in concentration of O_2, DIC, and N_2-N over time accounting for chamber volume and area (Ray et al. 2020). For an O_2, DIC, or

N_2-N flux to be considered significant, $R^2 \geq 0.65$ and $p \leq 0.10$. If $R^2 < 0.65$, no flux was exhibited and a value of 0 was assigned (Ray et al. 2020). Nutrient fluxes were calculated similarly except instead of using the slope calculated from a regression, we calculated the flux using the difference in the nutrient concentration between the beginning and end of the incubation. The beginning of the dark incubation was when we put the chambers onto the collars and the end of the dark incubation and the beginning of the light incubation was when we took the opaque fabric off the chamber.

Sediment Characteristics, Plant Morphometrics, and Biogeochemistry

We dried sediment samples at 60 ºC for at least 48 hours before grinding them. % C and % N of sediments were determined on an elemental analyser (Elemental Combustion System 4010 Costech Analytical Technologies; Valencia, CA).

We determined seagrass density, leaf area index (LAI), and nutrient pollution indicator (NPI). We counted the number of ramets within each chamber to determine seagrass density and we trimmed and collected the seagrass aboveground biomass at the end of the incubation. We stored shoots at 3 ºC before processing for LAI, aboveground biomass, and NPI (Chapter 2).

Statistical Analysis

All statistical analyses were conducted in R version 4.0.3. The results of the statistical tests were considered significant when $p \leq 0.05$. We tested whether O_2, DIC, and N_2-N fluxes and nutrient fluxes across the sediment-water interface were different

between locations, seagrass vegetated and non-vegetated sediments, and between light and dark treatments using a mixed model approach. Before we began model selection, we determined the distribution of each dissolved gas and nutrient flux data set. To do this, we needed positive data, so we shifted our data by adding 0.1 plus the absolute value of the lowest flux to all fluxes of that type. We then tested whether the distributions of the shifted data best fit a normal, lognormal or gamma distribution using the 'fitdistrplus' package in R (Delignette-Muller and Dutang 2015). We found that O_2, N_2-N, NO_2^-, and NO_x data best fit a normal distribution, while NH_4^+ and DIP best fit a gamma distribution. Because DIC fluxes were zero-inflated, before the model prediction process, we modelled our zeros using a zero-adjusted gamma modification to the classic hurdle model (Zuur & Ieno, 2016, Chapter 2). We then determined the distribution of these data using the *fitdistrplus* package (Delignette-Muller and Dutang 2015). We found that DIC data best fit a normal distribution.

We determined if environmental variables were correlated using Pearson correlations between all predictor variables. We included variables in the model selection process that were not correlated ($p > 0.05$) (e.g., temperature, oxygen concentration) (Table S3.1).

We then generated multiple generalized linear models using the *lme4* package (Bates et al. 2015; Ray et al. 2019). The presence or absence of seagrass, location, and light treatment were treated as fixed effects in the models along with other non-correlated predictor variables (e.g. temperature, O_2 concentration) (Table S3.1). We included location as a fixed effect and not a random effect because we cannot calculate variance

within the model with only two categories (Clark and Linzer 2015). We constructed 31 models for each flux type (O_2, DIC, N_2-N, NO_2^-, NO_x, NH_4^+, and DIP) and we used Akaike information criterion (AIC) to select the best models (Bozdogan 1987). We compared the top two models using likelihood ratio tests through the *lrtest* function in the *lmtest* package (Hothorn et al. 2020). If the top two models were not significantly different, we used the simpler model (Table S3.2).

We determined differences between sites, vegetation treatment, and light treatment using a least square means test on seagrass, sediment, and water column characteristics. We determined if fluxes of O_2, DIC, N_2-N, NO_2^-, NO_x, NH_4^+, and DIP were correlated using Pearson correlations.

Results

Site Characteristics

Generally, water column and sediment characteristics differed significantly between sites (Table 3.1). Water column temperature and dissolved O_2 concentration were significantly higher in East Harbor than in Pleasant Bay and salinity, NO_x, NH_4^+, and DIP were significantly lower in East Harbor than in Pleasant Bay. However, there was no difference in NO_2^- concentrations between sites. Sediment characteristics in the top 0-1 cm followed a similar pattern where sediment %N was lower and C:N was higher in East Harbor compared to Pleasant Bay. Seagrass density and NPI were lower and LAI was higher in East Harbor compared to Pleasant Bay, however not statistically significantly so (Table 3.1).

O_2, DIC, and N_2 fluxes

O_2, DIC, and N_2 fluxes were highly variable within and between sites. Across both the dark and light incubation, dissolved O_2 fluxes ranged from -14.1 mmol m^{-2} h^{-1} to 11.4 mmol m^{-2} h^{-1} and did not vary by site. When combining fluxes from both sites we found that vegetated sediments had fluxes of significantly higher magnitude than non-vegetated sediments ($F_{3, 64} = 40.33$, $p < 0.001$; dark vegetated: -5.97 ± 0.18 mmol O_2 m^{-2} h^{-1}, dark non-vegetated: -3.01 ± 0.10 mmol O_2 m^{-2} h^{-1}, light vegetated: 4.34 ± 0.25 mmol O_2 m^{-2} h^{-1}, light non-vegetated: 0.92 ± 0.13 mmol O_2 m^{-2} h^{-1}). O_2 fluxes during light and dark incubations were also significantly different ($F_{3, 64} = 26.46$, $p < 0.001$). On average, -4.53 ± 0.55 mmol O_2 m^{-2} h^{-1} were taken up from the water column during dark incubations and 2.48 ± 0.57 mmol O_2 m^{-2} h^{-1} were released from sediments and eelgrass into the water column during light incubations (Figure 3.2A). Light fluxes of O_2 from non-vegetated sediments in East Harbor were significantly lower than light fluxes from vegetated sediments in East Harbor ($F_{7, 60} = 17.72$, $p < 0.001$; non-vegetated: 0.25 ± 0.77 mmol O_2 m^{-2} h^{-1}; vegetated: 4.84 ± 1.13 mmol O_2 m^{-2} h^{-1}). The best model for O_2 fluxes only contained light (Table 3.2). Light explained ~50% of the variability in the O_2 fluxes ($y = 7.01x - 4.53$, $F_{1, 66} = 78.05$, $R^2 = 0.53$, $p < 0.001$) and there was a negative relationship between O_2 flux and initial O_2 concentration across the light incubations and no relationship across the dark incubations (Figure 3.3A, B). There was no relationship between light or dark O_2 flux and temperature (Figure 3.4A, B).

DIC fluxes ranged from -27.69 to 20.39 mmol m^{-2} h^{-1}. DIC fluxes did not vary significantly between sites nor with vegetation presence or absence. However, when sites

and vegetated and non-vegetated sediment fluxes were combined, DIC fluxes from dark incubations were significantly higher than DIC fluxes from light incubations ($F_{1, 67}$ = 8.002, p = 0.006; 3.19 ± 1.33 mmol DIC m^{-2} h^{-1}, -1.56 ± 1.01 mmol DIC m^{-2} h^{-1}, respectively) (Figure 3.2B). This pattern is largely driven by the significant difference between vegetated dark and light DIC fluxes from Pleasant Bay ($F_{7, 61}$ = 2.55, p = 0.02; dark: 6.97 ± 2.89 mmol DIC m^{-2} h^{-1}, light: -4.50 ± 3.19 mmol DIC m^{-2} h^{-1}). There was no relationship between DIC flux and initial O_2 concentration (Figure 3.3C, D). The best model explaining DIC fluxes contained light and temperature (Table 3.2). Light and temperature explained ~13% of the variability in DIC fluxes ($F_{2, 66}$ = 6.30, R^2 = 0.13, p = 0.003) with a negative relationship between DIC flux and light treatment and a positive relationship between DIC flux and temperature. However, when we examined the relationship between DIC flux and temperature for each light treatment the relationships did not remain (Figure 3.4C, D).

N_2-N fluxes ranged from -5.35 to 11.79 mmol m^{-2} h^{-1}. N_2-N fluxes did not vary significantly between sites, with vegetation presence or absence, nor with light treatment and there were no significant interactions among site, vegetation presence or absence, and light treatment for N_2-N fluxes (Figure 3.2C). On average, dark incubations in both East Harbor and Pleasant Bay emitted N_2-N while light incubations in East Harbor emitted N_2-N and light incubations in Pleasant Bay took up a small amount of N_2-N. Light N_2-N fluxes in Pleasant Bay ranged from -1.78 mmol m^{-2} h^{-1} to 1.05 mmol m^{-2} h^{-1}. And 30% of the light fluxes from Pleasant Bay were negative while 30% were positive. Even though light treatment was the best predictor of N_2-N fluxes (Table 3.2), it was not a significant

predictor of N_2-N fluxes ($F_{1, 65} = 2.70$, $R^2 = 0.03$, $p = 0.11$). There were no relationships between light or dark N_2-N fluxes and initial O_2 concentration or temperature (Figure 3.3E, F; Figure 3.4E, F).

Nutrient Fluxes

In general, nutrient fluxes varied between light treatments and sites and did not vary between vegetation treatments (Figure 3.5). NO_2^- fluxes ranged from -17.57 μmol m^{-2} h^{-1} to 20.19 μmol m^{-2} h^{-1}. NO_2^- fluxes did not differ significantly between sites, with vegetation presence or absence, or with light treatments. Although average fluxes across sites and light treatments were close to zero (PB dark: 5.04 ± 1.54 μmol NO_2^- m^{-2} h^{-1}, PB light: 0.27 ± 2.11 μmol NO_2^- m^{-2} h^{-1}, EH dark: 0.07 ± 0.31 μmol NO_2^- m^{-2} h^{-1}, EH light: 0.72 ± 0.38 μmol NO_2^- m^{-2} h^{-1}) there was higher variability in fluxes from Pleasant Bay than from East Harbor (Pleasant Bay range: -17.57 – 20.19 μmol NO_2^- m^{-2} h^{-1}; East Harbor range: -2.11 – 3.94 μmol NO_2^- m^{-2} h^{-1}) (Figure 3.5A). Location was the best predictor of NO_2^- flux (Table 3.2), but it was not a significant predictor for NO_2^- fluxes ($p = 0.124$). However, there was a negative linear relationship between NO_2^- flux and temperature during the light incubations in East Harbor (Figure 3.6A). There was no relationship between NO_2^- flux and temperature in Pleasant Bay (Figure 3.6B) and no relationship between NO_2^- flux and initial O_2 concentration (Figure 3.7A, B).

NO_x fluxes were more variable in Pleasant Bay than they were in East Harbor (PB range: -17.17 – 60.45 μmol NO_x m^{-2} h^{-1}, EH range: -21.90 – 11.00 μmol NO_x m^{-2} h^{-1}) and dark fluxes in Pleasant Bay were significantly higher than dark fluxes in East Harbor ($F_{3,}$

$_{62}$ = 3.16, p = 0.03; 7.24 ± 4.31 μmol NO_x m^{-2} h^{-1}, -4.55 ± 1.51 μmol NO_x m^{-2} h^{-1}, respectively). However, light treatments did not significantly differ between sites and did not significantly differ from dark treatments (Figure 3.5B). There were no differences in NO_x flux between vegetated and non-vegetated sediments. Location explained ~8% of the variability in NO_x fluxes (y = 7.84x – 1.45, $F_{1, 64}$ = 6.94, p = 0.01), and there were no relationships between NO_x flux and temperature or initial O_2 concentration (Figure 3.6C, D; Figure 3.7C, D).

NH_4^+ fluxes were more variable in Pleasant Bay than they were in East Harbor (PB range: -93.80 – 1445.21 μmol NH_4^+ m^{-2} h^{-1}, EH range: -57.50 – 353.34 μmol NH_4^+ m^{-2} h^{-1}). NH_4^+ was released into the water column across sites and light treatments, with significantly more NH_4^+ released by the dark treatment in Pleasant Bay compared to the light treatment in Pleasant Bay and both the dark and light treatments in East Harbor ($p < 0.05$; NH_4^+ mean ± se: 459.38 ± 115.37, 139.64 ± 46.13, 28.24 ± 17.23, 29.41 ± 25.51 μmol NH_4^+ m^{-2} h^{-1}, respectively; Figure 3.5C). The best model for NH_4^+ fluxes contained location, light treatment, temperature and O_2 concentration. There was a negative linear relationship between NH_4^+ flux and temperature during the light incubation in East Harbor (Figure 3.6F) and no clear linear relationships between NH_4^+ flux and temperature in Pleasant Bay (Figure 3.6E, F) or NH_4^+ flux and O_2 concentration at either East Harbor or Pleasant Bay (Figure 3.7E, F).

Like the other nutrient fluxes, DIP fluxes were more variable in Pleasant Bay than they were in East Harbor (PB range: -26.47 – 347.63 μmol DIP m^{-2} h^{-1}, EH range: -48.45 – 41.62 μmol DIP m^{-2} h^{-1}). DIP was released into the water column across sites and light

treatments, with significantly more DIP released by the dark treatment in Pleasant Bay compared to the light treatment in Pleasant Bay and both the dark and light treatments in East Harbor ($p < 0.05$; DIP mean ± se: 63.39 ± 21.59, 39.63 ± 19.05, 1.50 ± 2.50, 5.12 ± 5.90 μmol DIP m^{-2} h^{-1}; Figure 3.5D). Location and O_2 concentration explain the variability in the DIP fluxes (Table 3.1). There was no relationship between DIP flux and temperature in either East Harbor or Pleasant Bay or for dark or light treatments (Figure 3.6G, H). While there was no linear relationship between DIP flux and initial O_2 concentration in East Harbor, there was a negative linear relationship between DIP and initial O_2 concentration during light incubations in Pleasant Bay, but not during dark incubations (Figure 3.7G, H).

Flux Correlations

There were several correlations between O_2, DIC, N_2-N, and nutrient fluxes (Table 3.3). As expected, O_2 and DIC flux were negatively correlated ($r = -0.41$, $p < 0.001$) and DIC and N_2-N flux were positively correlated ($r = 0.40$, $p < 0.001$). NO_2^- flux was negatively correlated with O_2 flux ($r = -0.28$, $p = 0.02$) and positively correlated with NH_4^+ flux ($r = 0.37$, $p = 0.002$). The strongest correlation was between NH_4^+ flux and DIP flux ($r = 0.86$, $p < 0.001$).

Discussion

Site and light had stronger influences on O_2, DIC, N_2, and dissolved inorganic nutrient fluxes than vegetation. Eelgrass increased the magnitude of O_2, DIC, and

dissolved inorganic nutrient fluxes in Pleasant Bay while there was no effect of eelgrass on N_2 fluxes at either site. Light impacted the direction of O_2 and DIC fluxes at both sites but had no significant impact on N_2 flux. Initial O_2 concentration and temperature were the environmental drivers with the strongest impacts on fluxes, with a negative relationship between initial O_2 concentration, light fluxes of O_2 and DIP, and dark fluxes of NO_2^- and a negative relationship between temperature and light fluxes of NO_2^- and NH_4^+. Over all our results show that seagrass enhance O_2, DIC, and dissolved inorganic nutrient fluxes on a site by site basis.

Drivers of dissolved oxygen and dissolved inorganic carbon fluxes

Dissolved oxygen fluxes were driven by light at both sites and for vegetated and non-vegetated sediments (Figure 3.2A). Vegetated sediments in East Harbor and Pleasant Bay released 4.84 ± 1.13 mmol O_2 m^{-2} h^{-1} and 3.90 ± 1.60 mmol O_2 m^{-2} h^{-1}, respectively in the light while non-vegetated sediments released 0.25 ± 0.77 mmol O_2 m^{-2} h^{-1} and 1.59 ± 0.75 mmol O_2 m^{-2} h^{-1}, respectively in the light. Although there was no statistical difference between vegetated and non-vegetated O_2 fluxes in the light, mean O_2 fluxes from non-vegetated sediments were ~2 to 20x lower than mean O_2 fluxes from vegetated sediments, indicating that photosynthesis was, as expected, lower in non-vegetated sediments. In addition, the O_2 fluxes observed in this study, are within the range found in the literature for *Z. marina* meadows and for temperate seagrasses in general using static core or *in situ* chamber incubation methods (Eyre and Ferguson 2002; Martin et al. 2005; Duarte et al. 2010). In non-vegetated sediments, O_2 could be produced by benthic and pelagic microalgae as well as photosynthetic bacteria and archaea (Hansen et al. 2000;

Qu et al. 2004; Gattuso et al. 2006; Cox et al. 2020). Other studies quantifying O_2 fluxes from both benthic microalgae and seagrass found similar results. For example, one study comparing *Ruppia megacarpa* vegetated sediments with non-vegetated sediments found that the non-vegetated sediments produced ~5x – 20x less O_2 (Qu et al. 2004).

During the dark treatments, although not statistically different, vegetated sediments in East Harbor and Pleasant Bay took up -4.94 ± 1.00 mmol O_2 m^{-2} h^{-1} and -7.00 ± 1.14 mmol O_2 m^{-2} h^{-1}, respectively on average while non-vegetated sediments took up lower amounts of O_2 (-2.91 ± 0.72 mmol O_2 m^{-2} h^{-1}, -3.11 ± 0.59 mmol O_2 m^{-2} h^{-1}, respectively). This indicates that more respiration was occurring in the vegetated treatments compared to the non-vegetated treatments. Generally, seagrass vegetated sediments have higher respiration rates than non-vegetated sediments due to respiration from the seagrass, respiration from the organisms living in the seagrass (e.g. crabs, bivalves, fish), and increased microbial respiration (Qu et al. 2004; Smith et al. 2004; McHenry et al. 2021). Increases in microbial respiration under seagrasses are attributed to the higher availability of labile organic matter, which is often seagrass derived (Holmer et al. 2004; Smith et al. 2004). This is likely the case in East Harbor and Pleasant Bay as well because C:N ratios are lower in eelgrass sediments indicating that more labile organic matter is available in the seagrass sediments (Table 3.2). Respiration can also increase with temperature (Marsh et al. 1986; Pietikäinen et al. 2005). However, we observed no relationship between temperature and O_2 fluxes during these incubations (Table 3.1, Figure 3.3A, B). This is likely due to the relatively small temperature range

we sampled each summer, and likely if we also collected fall or early spring rates, we would see an increase in fluxes with temperature.

As expected, DIC fluxes were driven by both light and temperature at both sites and for vegetated and non-vegetated sediments. Although light and dark treatments and vegetated and non-vegetated sediments were not statistically different (Figure 3.2B), on average light treatments in East Harbor and Pleasant Bay exhibited DIC uptake and dark treatments exhibited DIC release from vegetated sediments (light veg: -3.28 ± 2.13 mmol DIC m^{-2} h^{-1}, -4.50 ± 3.19 mmol DIC m^{-2} h^{-1}; dark veg: 4.56 ± 1.95 mmol DIC m^{-2} h^{-1}, 6.97 ± 2.89 mmol DIC m^{-2} h^{-1}, respectively) and non-vegetated sediments were small sources of DIC to the water column regardless of light treatment (light non-veg: 0.61 ± 1.46 mmol DIC m^{-2} h^{-1}, 0.21 ± 0.22 mmol DIC m^{-2} h^{-1}; dark non-veg: 0.68 ± 3.83 mmol DIC m^{-2} h^{-1}, 0.57 ± 0.60 mmol DIC m^{-2} h^{-1}, respectively). In the vegetated sediments, there is a clear signature of eelgrass photosynthesis and respiration with DIC being drawn down in the light and emitted in the dark. However, for non-vegetated sediments this pattern is unclear likely because microbial mineralization of organic matter is the main driver of DIC emission, while DIC uptake via primary production is low (Barrón et al. 2006; Delgard et al. 2016). This is a typical pattern for non-vegetated estuarine sediments as well (Ortega et al. 2005; Maher et al. 2013).

Although temperature was identified as a driver of DIC flux in our model, there was no linear relationship between DIC flux and temperature for light or dark treatments in either East Harbor or Pleasant Bay (Figure 3.4C, D). In other systems, DIC flux was correlated with water temperature (Barrón et al. 2006; Nakayama et al. 2020) and fluxes

of CO_2, one of the three inorganic carbon species making up DIC, increase with temperature (Berg et al. 2019; Burkholz et al. 2020; Van Dam et al. 2021). For example, Van Dam et al. (2021), found that 23% of the air – sea CO_2 flux in Florida Bay could be attributed to changes in temperature impacting gas solubility and Berg et al. (2019) found a two-fold increase in respiration over a temperature increase from 16 ºC to 28 ºC in *Z. marina* meadows. Like with O_2, changes in temperature impact the solubility of DIC as well as microbial metabolism, increasing respiration (Marsh et al. 1986; Pietikäinen et al. 2005). It is likely that this pattern is not clear in our data because 57% of our DIC fluxes were zero, indicating that the flux was either below our limit of detection or DIC production balanced DIC consumption in the system.

DIC fluxes were within the range of light and dark DIC fluxes from other seagrass meadows (Gacia et al. 2005; Apostolaki et al. 2010). For example, DIC fluxes from pristine and impacted *Posidonia oceanica* meadows in August were about -8 and -4 mmol m^{-2} h^{-1}, respectively, in the light and dark fluxes were about 5 and -0.5 mmol m^{-2} h^{-1}, respectively (Apostolaki et al. 2010). A mixed seagrass meadow in the Philippines released 12-15 mmol DIC m^{-2} h^{-1} in the dark and light fluxes ranged from 5.0 to -1.9 mmol DIC m^{-2} h^{-1} (Gacia et al. 2005). Like the O_2 fluxes from the vegetated sediments, the DIC fluxes show that the vegetated areas were net autotrophic during our incubations. However, the non-vegetated sediments, even though not significantly different from the vegetated sediments, emitted DIC during both the light and dark incubations, indicating that respiration dominated over photosynthesis in these areas.

Drivers of nitrogen fluxes

In general, temperate coastal sediments are net denitrifying, with some systems exhibiting nitrogen fixation (Fulweiler et al. 2007; Vieillard and Fulweiler 2012; Russell et al. 2016; Newell et al. 2016). Seagrass ecosystems generally exhibit net denitrification as well, though these systems are also known to fix N under limiting conditions (Eyre and Ferguson 2002; Eyre et al. 2013; Russell et al. 2016; Mohr et al. 2021). Here, both vegetated and non-vegetated sediments under light and dark treatments in East Harbor are net denitrifying, or N_2 emitting, with a small amount of N_2 uptake, or net nitrogen fixation, in the light treatment in Pleasant Bay and net denitrification occurring in the dark treatment (Figure 3.2B). Although there were no significant differences in light or dark treatments between sites, light treatments had lower N_2 emission than dark treatments on average with a small N_2 uptake occurring in the light treatments in Pleasant Bay (EH: 0.89 ± mmol N_2-N m^{-2} h^{-1}, 1.84 ± mmol N_2-N m^{-2} h^{-1}; PB: -0.08 ± mmol N_2-N m^{-2} h^{-1}, 1.13 ± mmol N_2-N m^{-2} h^{-1}, respectively).

While we found that light was the main driver of N_2 fluxes, other studies have shown that organic matter content and quality determine whether systems are net denitrifying or net nitrogen fixing (Fulweiler et al. 2013; Eyre et al. 2013). However, Eyre et al. (2013) also show that denitrification is lower during light incubations than during dark incubations and Russell et al. (2016) found higher rates of nitrogen fixation during light incubations for vegetated sediments than during dark incubations and non-vegetated sediments during dark and light incubations. This pattern may occur in seagrass vegetated ecosystems for three reasons. First, seagrasses and microphytobenthos compete

with nitrifiers and denitrifiers for NH_4^+ and NO_3^- in the light (Risgaard-Petersen 2003; Eyre et al. 2011b). Second, seagrasses provide habitat for nitrogen fixing cyanobacteria and endophytic bacteria (Russell et al. 2016; Mohr et al. 2021). And third, fluxes exhibiting net nitrogen fixation are an artifact due to O_2 bubbles in the chamber (Eyre et al. 2002; Inglett et al. 2015). Seagrass and microphytobenthos typically take up NH_4^+ and NO_3^- in the light (Touchette and Burkholder 2000; Risgaard-Petersen 2003). Previous studies have shown that in microphytobenthos dominated sediments, nitrifying bacteria are nitrogen limited leading to a suppression of coupled nitrification – denitrification (Risgaard-Petersen 2003). In our study, NH_4^+ fluxes are lower during light incubations than they are during dark incubations, indicating that nitrifiers may have experienced N-limitation, leading to lower coupled nitrification – denitrification, and therefore, lower N_2 emission. In seagrass ecosystems, cyanobacterial nitrogen fixers and endophytic bacteria typically fix nitrogen during the summer when water column concentrations of NO_3^- and NO_2^- are low (Russell et al. 2016; Mohr et al. 2021), as during our incubations (Table 3.1). Because we measured net N_2 fluxes with the N_2/Ar method, we can detect N fixation when the rate of nitrogen fixation exceeds the rate of denitrification or when bubbles are present in cores causing N_2 diffusion out of the water column and into the bubbles, artificially simulating N fixation (Eyre et al. 2002). In seagrass ecosystems, bubbles can come from the sediment or from the plants themselves. O_2 bubbles form in seagrass meadows when water column O_2 saturation exceeds 100% (Long et al. 2020). This is a common occurrence in some seagrass meadows during summer. In Pleasant Bay, O_2 saturation did not exceed 100% during light incubations and ranged from 48.2%

- 92.4%. Four of the five light fluxes from Pleasant Bay exhibiting net N_2 uptake were from September 2019, and three of those four fluxes were from seagrass incubations. During these incubations, O_2 % saturation ranged from 68.1 – 91.6%. Because of this, it is unlikely that N_2 fixation was artificially simulated by N_2 diffusion into O_2 bubbles.

Seagrasses typically live in low nutrient environments and use NO_3^- and NH_4^+ as nitrogen sources (Touchette and Burkholder 2000). Therefore, available dissolved inorganic nitrogen is rapidly consumed in seagrass ecosystems by seagrasses as well as by micro- and macroalgae and microbes (Touchette and Burkholder 2000). In general, NO_2^- and NO_x fluxes are close to zero in East Harbor (light: 0.72 ± 0.38 μmol NO_2^- m^{-2} h^{-1}, 1.85 ± 1.06 μmol NO_x m^{-2} h^{-1}; dark: 0.07 ± 0.31 μmol NO_2^- m^{-2} h^{-1}, -4.55 ± 1.51 μmol NO_x m^{-2} h^{-1}) and higher in magnitude in Pleasant Bay (light: 0.27 ± 2.11 μmol NO_2^- m^{-2} h^{-1}, 5.59 ± 3.35 μmol NO_x m^{-2} h^{-1}; dark: 5.04 ± 1.58 μmol NO_2^- m^{-2} h^{-1}, 7.24 ± 4.43 μmol NO_x m^{-2} h^{-1}) (Figure 3.5A, B). In East Harbor and Pleasant Bay NO_2^- and NO_x concentrations and fluxes are low, but within the range of other seagrass ecosystems (Eyre and Ferguson 2002; Apostolaki et al. 2010; Eyre et al. 2011a; b). In many seagrass ecosystems, NO_3^- uptake is regulated by light with NO_3^- uptake for most species of seagrass limited to light periods (Touchette and Burkholder 2000). In a *Thalassia testudinum* meadow, NO_x was taken up in the light and released from the sediments in the dark (Ziegler and Benner 1999) and fluxes of NO_3^- were typically lower in *Z. capricorni* vegetated sediments than in bare sediments (Eyre and Ferguson 2002).

Unlike in the studies above, in our study, location, and not light and vegetation presence, was the main driver of both NO_2^- and NOx fluxes. It is not surprising that light

is not a driver of NO_2^- and NO_x fluxes in *Z. marina* ecosystems because *Z. marina* is not limited to NO_3^- uptake in the light, unlike other seagrass species (Touchette and Burkholder 2000). However, it is surprising that there was net NO_2^- and NO_x emission from the sediments in Pleasant Bay regardless of vegetation status. NO_3^- and NO_2^- are formed during nitrification. Nitrification occurs in two processes, ammonium oxidation and nitrite oxidation. Both of these processes occur when oxygen is present (Canfield et al. 2005). Seagrass sediments are an ideal location for nitrification to occur - they are typically high in NH_4^+ and can have oxygenated rhizospheres (Pedersen et al. 1998). High NO_2^- emission from the sediments could mean that nitrification is halted at the ammonium oxidation step because O_2 is low and the ammonium oxidizers have a higher affinity for O_2 than the nitrite oxidizers, therefore, there is not enough O_2 available for the nitrite oxidation step (Canfield et al. 2005). It is likely that this the mechanism that is occurring in our systems because NO_2^- and O_2 fluxes are negatively correlated (Figure 3.6).

In coastal sediments, nitrification and denitrification are typically coupled, with nitrifiers using NH_4^+ to make NO_3^- and NO_2^- for denitrification (Jenkins and Kemp 1984). The low rates of NO_2^- and NO_x uptake and emission in East Harbor are likely the result of tight cycling of these nutrients in the system. If nitrification is occurring in East Harbor, then the resulting NO_3^- and NO_2^- are quickly taken up by denitrifiers, microalgae, or seagrass. In Pleasant Bay, however, the higher magnitude of uptake and emission may signal a decoupling of these processes, with nitrification dominating when NO_2^- and NO_x fluxes are positive and denitrification, or other dissimilatory nitrate reducing pathways,

dominating when they are negative. A previous study from a *Z. marina* meadow showed that dissimilatory nitrate reduction to ammonium (DNRA) was occurring, but that denitrification largely dominated nitrate removal (Aoki and McGlathery 2018).

Seagrass sediments, and coastal sediments in general, are often rich in NH_4^+. However, seagrasses are often N-limited because of competition for inorganic N with micro- and macroalgae and microbes, and because much of the sediment ammonium pool adsorbs to the sediment (Touchette and Burkholder 2000). In seagrass ecosystems, NH_4^+ is typically taken up in the light and released in the dark (Eyre et al. 2011a). This is the pattern NH_4^+ fluxes follow in Pleasant Bay as well, but there is no difference between dark and light NH_4^+ fluxes in East Harbor (Figure 3.5C).

In addition to being driven by light and location, NH_4^+ fluxes are also driven by temperature and initial O_2 concentration. In East Harbor, NH_4^+ flux declines as temperature increases during light incubations. This pattern could be due to increases in ammonium uptake with temperature by photosynthesizing organisms and nitrifiers or a decline in ammonium producing processes (e.g. DNRA, organic matter mineralization). However, the most likely explanation is an increase in competition for NH_4^+. One competitive process that was recently found in seagrass ecosystems is anaerobic ammonium oxidation (anammox) (Salk et al. 2017; Garcias-Bonet et al. 2018; Chen et al. 2020a). During anammox, NO_2^- is used to oxidize NH_4^+ to N_2 under anaerobic conditions (Dalsgaard and Thamdrup 2002). Salk et al. (2017) used a modified isotope pairing technique to determine that anammox accounted for 64-86% of N lost from a *Zostera muelleri* meadow. In our study, NH_4^+ fluxes are positively correlated to NO_2^-

fluxes (Table 3), indicating that annamox is potentially a N loss pathway in these systems. However, while it is impossible to tell the contribution of denitrification and anammox to the net N_2 fluxes with our method, this method would capture the anammox signal.

Drivers of DIP fluxes

Phosphorus is not a limiting nutrient in most temperate coastal ecosystems (Oviatt et al. 1995) and dissolved inorganic phosphorous (DIP) fluxes typically increase at night in temperate seagrass meadows (Touchette and Burkholder 2000; Apostolaki et al. 2010; Eyre et al. 2011b). While our sites were DIP sources on average, DIP fluxes in Pleasant Bay were ~17x higher than fluxes from East Harbor and were highest during dark incubations in Pleasant Bay and lowest in both light and dark incubations in East Harbor (Figure 3.5D). DIP fluxes in East Harbor and Pleasant Bay were within the range found for non-vegetated and vegetated locations in an eelgrass meadow in Denmark (Holmer et al. 2006) and fluxes from Pleasant Bay were higher than fluxes from *P. oceanica*, *Z. capricorni*, and *Halodule spp.* meadows (Apostolaki et al. 2010; Eyre et al. 2011a).

DIP fluxes were driven by location and O_2 concentration. In Pleasant Bay, there is a negative relationship between DIP flux and O_2 concentration in the light and there was no relationship between DIP flux and O_2 concentration in East Harbor (Figure 3.7H). DIP fluxes are commonly driven by O_2 concentrations across coastal ecosystems with more DIP released under low O_2 conditions (Jensen et al. 1995; Canfield et al. 2005). During oxic conditions, DIP is adsorbed by iron (Fe) oxyhydroxides. Under low O_2 conditions,

sulfate reduction induces the dissolution of Fe oxyhydroxides and DIP is released into the water column (Canfield et al. 2005; Boyle et al. 2014). It is likely that we do not see this pattern in East Harbor because we did not observe any hypoxic (Initial $O_2 \leq 3$ mg/L; Foster and Fulweiler 2019) events in this system, so P remained bound in the sediments.

DIP efflux also occurs because of organic matter decomposition. Coastal ecosystems are areas of high organic matter deposition and seagrasses increase the amount of labile organic matter available for decomposition (Holmer et al. 2001; Arndt et al. 2013). During organic matter mineralization, DIP and NH_4^+ are released (Krom and Berner 1981; Tezuka 1990). Here we found that DIP and NH_4^+ fluxes were highly positively correlated (Figure 3.6). We attribute this to high rates of organic matter decomposition in these environments.

The role of vegetation in coastal biogeochemistry

Overall vegetation did not have a significant impact on O_2, DIC, N_2, or nutrient fluxes. Instead, fluxes were more impacted by site and light. This indicates that the seagrass in East Harbor and Pleasant Bay do not have as much of an impact on biogeochemical cycling as in other systems. Seagrass meadows in other areas also have variable fluxes of O_2, DIC, N_2 and nutrients with some vegetated areas differing from non-vegetated areas and others exhibiting no difference (Eyre et al. 2011a; b; Russell et al. 2016; Salk et al. 2017; Garcias-Bonet et al. 2018; Hoffman et al. 2019; Chen et al. 2020b). This may be due to the sediment type (Holmer et al. 2006), nutrient enrichment (Apostolaki et al. 2010), or the age of the meadow (Barrón et al. 2004; Eyre et al. 2011a).

For example, Holmer et al. (2006) found that DIP fluxes and sediment oxygen uptake rates in *Z. marina* meadows were generally lower in sandy sediments compared to muddy sediments, and Apostolaki et al. (2010) found that a degraded *P. oceanica* meadow released DIN and DIP in the light while an unimpacted meadow took up DIN and DIP in the light. In addition, several studies have found that the biogeochemistry of seagrass meadows change as they age (Barrón et al. 2004; Greiner et al. 2013). For example, Barron et al. (2004) found that dissolved organic carbon fluxes shifted from uptake to efflux as the seagrass community aged and Greiner et al. (2013) found that carbon accumulation rates were higher in a 10 year old seagrass meadow compared to a 4 year old meadow and bare sediment. The seagrass meadow in East Harbor was only ~7 years old at the start of this study. If this meadow is maturing at the same rate as the seagrass meadow restored on the Eastern Shore of Virginia, then the meadow in East Harbor will not function as a natural meadow until 2023. Therefore, low fluxes from this area may be due to this system functioning as an immature meadow. The higher magnitude fluxes measured in Pleasant Bay, may be due to higher seagrass densities and sediment carbon content. For example, Deek et al. (2013) found that N_2 fluxes were positively correlated with organic C content and several other studies have shown that organic matter content and quality control N_2 fluxes (Fulweiler et al. 2008; Eyre et al. 2013). Our study highlights the variable nature of O_2, DIC, N_2-N and nutrient fluxes in seagrass ecosystems.

References

Aoki, L., and K. McGlathery. 2018. Restoration enhances denitrification and DNRA in subsurface sediments of Zostera marina seagrass meadows. Mar. Ecol. Prog. Ser. **602**: 87–102. doi:10.3354/meps12678

Aoki, L. R., K. J. McGlathery, and M. P. J. Oreska. 2020. Seagrass restoration reestablishes the coastal nitrogen filter through enhanced burial. Limnol. Oceanogr. **65**: 1–12. doi:10.1002/lno.11241

Apostolaki, E. T., M. Holmer, N. Marbà, and I. Karakassis. 2010. Degrading seagrass (Posidonia oceanica) ecosystems: A source of dissolved matter in the Mediterranean. Hydrobiologia **649**: 13–23. doi:10.1007/S10750-010-0255-2/FIGURES/6

Arndt, S., B. B. Jørgensen, D. E. LaRowe, J. J. Middelburg, R. D. Pancost, and P. Regnier. 2013. Quantifying the degradation of organic matter in marine sediments: A review and synthesis. Earth-Science Rev. **123**: 53–86. doi:10.1016/j.earscirev.2013.02.008

Ashford, O. S., S. Guan, D. Capone, and others. 2021. A chemosynthetic ecotone—"chemotone"—in the sediments surrounding deep-sea methane seeps. Limnol. Oceanogr. **66**: 1687–1702. doi:10.1002/LNO.11713

Barbier, E. B., S. D. Hacker, C. Kennedy, E. W. Koch, A. C. Stier, and B. R. Silliman. 2011. The value of estuarine and coastal ecosystem services. Ecol. Monogr. **81**: 169–193. doi:10.1890/10-1510.1

Barrón, C., C. M. Duarte, M. Frankignoulle, and A. V. Borges. 2006. Organic carbon

metabolism and carbonate dynamics in a Mediterranean seagrass (Posidonia oceanica), meadow. Estuaries Coasts 2006 293 **29**: 417–426. doi:10.1007/BF02784990

Barrón, C., N. Marbé, J. Terrados, H. Kennedy, and C. M. Duarte. 2004. Community metabolism and carbon budget along a gradient of seagrass (*Cymodocea nodosa*) colonization. Limnol. Oceanogr. **49**: 1642–1651. doi:10.4319/lo.2004.49.5.1642

Bates, D. ;, M. ; Mächler, B. ; Bolker, and S. Walker. 2015. Fitting Linear Mixed-Effects Models Using lme4.doi:10.3929/ethz-b-000105397

Berg, P., M. L. Delgard, P. Polsenaere, K. J. McGlathery, S. C. Doney, and A. C. Berger. 2019. Dynamics of benthic metabolism, O2, and pCO2 in a temperate seagrass meadow. Limnol. Oceanogr. **64**: 2586–2604. doi:10.1002/LNO.11236

Borrelli, M. 2009. 37 YEARS OF SHORELINE CHANGE IN PLEASANT BAY: 1868 TO 2005 A Report Prepared for the Pleasant Bay Resource Management Alliance.

Borum, J., K. Sand-Jensen, T. Binzer, O. Pedersen, and T. M. Greve. 2007. Oxygen Movement in Seagrasses. Seagrasses Biol. Ecol. Conserv. 255–270. doi:10.1007/978-1-4020-2983-7_10

Boyle, R. A., T. W. Dahl, A. W. Dale, G. A. Shields-Zhou, M. Zhu, M. D. Brasier, D. E. Canfield, and T. M. Lenton. 2014. Stabilization of the coupled oxygen and phosphorus cycles by the evolution of bioturbation. Nat. Geosci. **7**: 671–676. doi:10.1038/ngeo2213

Bozdogan, H. 1987. Model selection and Akaike's Information Criterion (AIC): The general theory and its analytical extensions. Psychometrika **52**: 345–370.

doi:10.1007/BF02294361

Burkholder, J. A. M., D. A. Tomasko, and B. W. Touchette. 2007. Seagrasses and eutrophication. J. Exp. Mar. Bio. Ecol. **350**: 46–72. doi:10.1016/j.jembe.2007.06.024

Burkholz, C., N. Garcias-Bonet, and C. M. Duarte. 2020. Warming enhances carbon dioxide and methane fluxes from Red Sea seagrass (<i>Halophila stipulacea</i>) sediments. Biogeosciences **17**: 1717–1730. doi:10.5194/bg-17-1717-2020

Canfield, D. E., E. Kristensen, and B. Thamdrup. 2005. Aquatic Geomicrobiology, 48th ed. A.J. Southward, P.A. Tyler, C.M. Young, and L.A. Fuiman [eds.]. Elsevier.

Chen, J., D. V. Erler, N. S. Wells, J. Huang, D. T. Welsh, and B. D. Eyre. 2020a. Denitrification, anammox, and dissimilatory nitrate reduction to ammonium across a mosaic of estuarine benthic habitats. Limnol. Oceanogr. lno.11681. doi:10.1002/lno.11681

Chen, J. J., D. V. Erler, N. S. Wells, J. Huang, D. T. Welsh, and B. D. Eyre. 2020b. Denitrification, anammox, and dissimilatory nitrate reduction to ammonium across a mosaic of estuarine benthic habitats. Limnol. Oceanogr. 1–17. doi:10.1002/lno.11681

Clark, T. S., and D. A. Linzer. 2015. Should I Use Fixed or Random Effects? Polit. Sci. Res. Methods **3**: 399–408. doi:10.1017/PSRM.2014.32

Colt, J. 1984. Computation of Dissolved Gas Concentrations in Water as Functions of Temperature, Salinity and Pressure. Am. Fish. Soc. Spec. Publ. 14.

Cox, T. E., J. Cebrian, M. Tabor, L. West, and J. W. Krause. 2020. Do diatoms dominate benthic production in shallow systems? A case study from a mixed seagrass bed. Limnol. Oceanogr. Lett. **5**: 425–434. doi:10.1002/LOL2.10167

Dalsgaard, T., and B. Thamdrup. 2002. Factors controlling anaerobic ammonium oxidation with nitrite in marine sediments. Appl. Environ. Microbiol. **68**: 3802–3808. doi:10.1128/AEM.68.8.3802-3808.2002/ASSET/BCAA6C9D-67E4-413C-B97A-5C6BBF428DB1/ASSETS/GRAPHIC/AM0820362003.JPEG

Van Dam, B. R., C. C. Lopes, P. Polsenaere, R. M. Price, A. Rutgersson, and J. W. Fourqurean. 2021. Water temperature control on CO2 flux and evaporation over a subtropical seagrass meadow revealed by atmospheric eddy covariance. Limnol. Oceanogr. **66**: 510–527. doi:10.1002/LNO.11620

Van Dam, B. R., C. Lopes, C. L. Osburn, and J. W. Fourqurean. 2019. Net heterotrophy and carbonate dissolution in two subtropical seagrass meadows. Biogeosciences **16**: 4411–4428. doi:10.5194/bg-2019-191

Deek, A., K. Dähnke, J. Van Beusekom, S. Meyer, M. Voss, and K. Emeis. 2013. N2 fluxes in sediments of the Elbe Estuary and adjacent coastal zones. Mar. Ecol. Prog. Ser. **493**: 9–21. doi:10.3354/meps10514

Delgard, M. L., B. Deflandre, E. Kochoni, J. Avaro, F. Cesbron, S. Bichon, D. Poirier, and P. Anschutz. 2016. Biogeochemistry of dissolved inorganic carbon and nutrients in seagrass (Zostera noltei) sediments at high and low biomass. Estuar. Coast. Shelf Sci. **179**: 12–22. doi:10.1016/j.ecss.2016.01.012

Delignette-Muller, M. L., and C. Dutang. 2015. fitdistrplus: An R package for fitting

distributions. J. Stat. Softw. **64**: 1–34. doi:10.18637/jss.v064.i04

Duarte, C. M. 2017. Reviews and syntheses: Hidden forests, the role of vegetated coastal habitats in the ocean carbon budget. Biogeosciences **14**: 301–310. doi:10.5194/bg-14-301-2017

Duarte, C. M., N. Marbà, E. Gacia, J. W. Fourqurean, J. Beggins, C. Barrón, and E. T. Apostolaki. 2010. Seagrass community metabolism: Assessing the carbon sink capacity of seagrass meadows. Global Biogeochem. Cycles **24**: 1–8. doi:10.1029/2010GB003793

Eyre, B. D., and A. J. P. Ferguson. 2002. Comparison of carbon production and decomposition, benthic nutrient fluxes and denitrification in seagrass, phytoplankton, benthic microalgae- and macroalgae-dominated warm-temperate Australian lagoons. Mar. Ecol. Prog. Ser. **229**: 43–59. doi:10.3354/meps229043

Eyre, B. D., A. J. P. Ferguson, A. Webb, D. Maher, and J. M. Oakes. 2011a. Denitrification, N-fixation and nitrogen and phosphorus fluxes in different benthic habitats and their contribution to the nitrogen and phosphorus budgets of a shallow oligotrophic sub-tropical coastal system (southern Moreton Bay, Australia). Biogeochemistry **102**: 111–133. doi:10.1007/s10533-010-9425-6

Eyre, B. D., D. Maher, J. M. Oakes, D. V. Erler, and T. M. Glasby. 2011b. Differences in benthic metabolism, nutrient fluxes, and denitrification in Caulerpa taxifolia communities compared to uninvaded bare sediment and seagrass (Zostera capricorni) habitats. Limnol. Oceanogr. **56**: 1737–1750. doi:10.4319/LO.2011.56.5.1737

Eyre, B. D., D. T. Maher, and P. Squire. 2013. Quantity and quality of organic matter (detritus) drives N2 effluxes (net denitrification) across seasons, benthic habitats, and estuaries. Global Biogeochem. Cycles **27**: 1083–1095. doi:10.1002/2013GB004631

Eyre, B. D., S. Rysgaard, T. Dalsgaard, and P. B. Christensen. 2002. Comparison of isotope pairing and N2:Ar methods for measuring sediment denitrification—Assumption, modifications, and implications. Estuaries 2002 256 **25**: 1077–1087. doi:10.1007/BF02692205

Foster, S. Q., and R. W. Fulweiler. 2019. Estuarine Sediments Exhibit Dynamic and Variable Biogeochemical Responses to Hypoxia. J. Geophys. Res. Biogeosciences **124**: 737–758. doi:10.1029/2018JG004663

Fulweiler, R. W., S. M. Brown, S. W. Nixon, and B. D. Jenkins. 2013. Evidence and a conceptual model for the co-occurrence of nitrogen fixation and denitrification in heterotrophic marine sediments. Mar. Ecol. Prog. Ser. **482**: 57–68. doi:10.3354/meps10240

Fulweiler, R. W., S. W. Nixon, B. A. Buckley, and S. L. Granger. 2007. Reversal of the net dinitrogen gas flux in coastal marine sediments. Nature **448**: 180–182. doi:10.1038/nature05963

Fulweiler, R. W., S. W. Nixon, B. A. Buckley, and S. L. Granger. 2008. Net sediment N2 fluxes in a coastal marine system-experimental manipulations and a conceptual model. Ecosystems **11**: 1168–1180. doi:10.1007/s10021-008-9187-3

Gacia, E., H. Kennedy, C. M. Duarte, J. Terrados, N. Marbà, S. Papadimitriou, and M.

Fortes. 2005. Light-dependence of the metabolic balance of a highly productive Philippine seagrass community. J. Exp. Mar. Bio. Ecol. **316**: 55–67. doi:10.1016/J.JEMBE.2004.10.008

Garcias-Bonet, N., V. M. Eguíluz, R. Díaz-Rúa, and C. M. Duarte. 2021. Host-association as major driver of microbiome structure and composition in Red Sea seagrass ecosystems. Environ. Microbiol. **23**: 2021–2034. doi:10.1111/1462-2920.15334

Garcias-Bonet, N., M. Fusi, M. Ali, D. R. Shaw, P. E. Saikaly, D. Daffonchio, and C. M. Duarte. 2018. High denitrification and anaerobic ammonium oxidation contributes to net nitrogen loss in a seagrass ecosystem in the central Red Sea. Biogeosciences **15**: 7333–7346. doi:10.5194/bg-15-7333-2018

Gattuso, J. P., B. Gentili, C. M. Duarte, J. A. Kleypas, J. J. Middelburg, and D. Antoine. 2006. Light availability in the coastal ocean: Impact on the distribution of benthic photosynthetic organisms and their contribution to primary production. Biogeosciences **3**: 489–513. doi:10.5194/BG-3-489-2006

Greiner, J. T., K. J. McGlathery, J. Gunnell, and B. A. McKee. 2013. Seagrass Restoration Enhances “Blue Carbon” Sequestration in Coastal Waters. PLoS One **8**: 1–8. doi:10.1371/journal.pone.0072469

Hansen, J. W., A. G. U. Pedersen, J. Berntsen, I. S. Rønbøg, L. S. Hansen, and B. A. Lomstein. 2000. Photosynthesis, respiration, and nitrogen uptake by different compartments of a Zostera marina community. Aquat. Bot. **66**: 281–295. doi:10.1016/S0304-3770(99)00078-9

Hoffman, D. K., M. J. McCarthy, S. E. Newell, W. S. Gardner, D. N. Niewinski, J. Gao, and T. R. Mutchler. 2019. Relative Contributions of DNRA and Denitrification to Nitrate Reduction in Thalassia testudinum Seagrass Beds in Coastal Florida (USA). Estuaries and Coasts **42**: 1001–1014. doi:10.1007/s12237-019-00540-2

Holmer, M., F. Ø. Andersen, S. L. Nielsen, and H. T. S. Boschker. 2001. The importance of mineralization based on sulfate reduction for nutrient regeneration in tropical seagrass sediments. Aquat. Bot. **71**: 1–17. doi:10.1016/S0304-3770(01)00170-X

Holmer, M., C. Carta, and F. Andersen. 2006. Biogeochemical implications for phosphorus cycling in sandy and muddy rhizosphere sediments of Zostera marina meadows (Denmark). Mar. Ecol. Prog. Ser. **320**: 141–151. doi:10.3354/MEPS320141

Holmer, M., C. M. Duarte, H. T. S. Boschker, and C. Barrón. 2004. Carbon cycling and bacterial carbon sources in pristine and impacted Mediterranean seagrass sediments. Aquat. Microb. Ecol. **36**: 227–237. doi:10.3354/AME036227

Hothorn, T., A. Zeileis, R. W. Farebrother, C. Cummins, G. Millo, and D. Mitchell. 2020. Testing Linear Regression Models.

Howes, B., S. Kelley, J. Ramsey, R. Samimy, D. Schlesinger, and E. Eichner. 2006. Massachusetts Estuaries Project Linked Watershed-Embayment Model to Determine Critical Nitrogen Loading Thresholds for the Pleasant Bay System, Towns of Orleans.

Inglett, P. W., T. M. Kana, and S. An. 2015. Denitrification Measurement Using Membrane Inlet Mass Spectrometry. Methods Biogeochem. Wetl. 503–517.

doi:10.2136/SSSABOOKSER10.C27

Invers, O., R. C. Zimmerman, R. S. Alberte, M. Pérez, and J. Romero. 2001. Inorganic carbon sources for seagrass photosynthesis: an experimental evaluation of bicarbonate use in species inhabiting temperate waters. J. Exp. Mar. Bio. Ecol. **265**: 203–217. doi:10.1016/S0022-0981(01)00332-X

Jenkins, M. C., and W. M. Kemp. 1984. The coupling of nitrification and denitrification in two estuarine sediments1,2. Limnol. Oceanogr. **29**: 609–619. doi:10.4319/LO.1984.29.3.0609

Jensen, H. S., K. J. McGlathery, R. Marino, and R. W. Howarth. 1998. Forms and availability of sediment phosphorus in carbonate sand of Bermuda seagrass beds. Limnol. Oceanogr. **43**: 799–810. doi:10.4319/LO.1998.43.5.0799

Jensen, H. S., P. B. Mortensen, F. 0. Andersen, E. Rasmussen, and A. Jensen. 1995. Phosphorus cycling in a coastal marine sediment, Aarhus Bay, Denmark. Limnol. Oceanogr. **40**: 908–917. doi:10.4319/LO.1995.40.5.0908

Kana, T. M., C. Darkangelo, M. D. Hunt, J. B. Oldham, G. E. Bennett, and J. C. Cornwell. 1994. Membrane Inlet Mass Spectrometer for Rapid High-Precision Determination of N2, O2, and Ar in Environmental Water Samples. Anal. Chem. **66**: 4166–4170. doi:10.1021/ac00095a009

Krom, M. D., and R. A. Berner. 1981. The diagenesis of phosphorus in a nearshore marine sediment. Geochim. Cosmochim. Acta **45**: 207–216. doi:10.1016/0016-7037(81)90164-2

Larkum, A. W. D., E. A. Drew, and P. J. Ralph. 2007. Photosynthesis and Metabolism in

Seagrasses at the Cellular Level, p. 323–345. *In* SEAGRASSES: BIOLOGY, ECOLOGYAND CONSERVATION. Springer Netherlands.

Lohrer, A. M., M. Townsend, S. F. Hailes, I. F. Rodil, K. Cartner, D. R. Pratt, and J. E. Hewitt. 2016. Influence of New Zealand cockles (Austrovenus stutchburyi) on primary productivity in sandflat-seagrass (Zostera muelleri) ecotones. Estuar. Coast. Shelf Sci. **181**: 238–248. doi:10.1016/J.ECSS.2016.08.045

Long, M. H., J. E. Rheuban, D. C. McCorkle, D. J. Burdige, and R. C. Zimmerman. 2019. Closing the oxygen mass balance in shallow coastal ecosystems. Limnol. Oceanogr. **64**: 2694–2708. doi:10.1002/LNO.11248

Long, M. H., K. Sutherland, S. D. Wankel, D. J. Burdige, and R. C. Zimmerman. 2020. Ebullition of oxygen from seagrasses under supersaturated conditions. Limnol. Oceanogr. **65**: 314–324. doi:10.1002/lno.11299

Maher, D. T., I. R. Santos, L. Golsby-Smith, J. Gleeson, and B. D. Eyre. 2013. Groundwater-derived dissolved inorganic and organic carbon exports from a mangrove tidal creek: The missing mangrove carbon sink? Limnol. Oceanogr. **58**: 475–488. doi:10.4319/LO.2013.58.2.0475

Marbà, N., M. Holmer, E. Gacia, and C. Barron. 2006. Seagrass beds and coastal biogeochemistry, p. 135–157. *In* Seagrasses: Biology, Ecology and Conservation. Springer Netherlands.

Marsh, J. A., W. C. Dennison, and R. S. Alberte. 1986. Effects of temperature on photosynthesis and respiration in eelgrass (Zostera marina L.). J. Exp. Mar. Bio. Ecol. **101**: 257–267. doi:10.1016/0022-0981(86)90267-4

Martin, S., J. Clavier, J.-M. Guarini, and others. 2005. Comparison of Zostera marina and maerl community metabolism. Aquat. Bot. **83**: 161–174. doi:10.1016/j.aquabot.2005.06.002

McGlathery, K. J., K. Sundbäck, and I. C. Anderson. 2007. Eutrophication in shallow coastal bays and lagoons: The role of plants in the coastal filter. Mar. Ecol. Prog. Ser. **348**: 1–18. doi:10.3354/meps07132

McHenry, J., A. Rassweiler, G. Hernan, C. K. Uejio, S. Pau, A. K. Dubel, and S. E. Lester. 2021. Modelling the biodiversity enhancement value of seagrass beds. Divers. Distrib. **27**: 2036–2049. doi:10.1111/DDI.13379

Mittermayr, A., B. Legare, and M. Borrelli. 2020. Applications of the Coastal and Marine Ecological Classification Standard (CMECS) in a Partially Restored New England Salt Marsh Lagoon. Estuaries and Coasts. doi:10.1007/s12237-020-00707-2

Mohr, W., N. Lehnen, S. Ahmerkamp, and others. 2021. Terrestrial-type nitrogen-fixing symbiosis between seagrass and a marine bacterium. Nature. doi:10.1038/s41586-021-04063-4

Moriarty, D. J. W., R. L. Iverson, and P. C. Pollard. 1986. Exudation of organic carbon by the seagrass Halodule wrightii Aschers. And its effect on bacterial growth in the sediment. J. Exp. Mar. Bio. Ecol. **96**: 115–126. doi:10.1016/0022-0981(86)90237-6

Mukai, H., I. Koike, M. Nishihira, and S. Nojima. 1989. Oxygen consumption and ammonium excretion of mega-sized benthic invertebrates in a tropical seagrass bed. J. Exp. Mar. Bio. Ecol. **134**: 101–115. doi:10.1016/0022-0981(90)90103-J

Nakagawa, T., Y. Tsuchiya, S. Ueda, M. Fukui, and R. Takahashi. 2019. Eelgrass

Sediment Microbiome as a Nitrous Oxide Sink in Brackish Lake Akkeshi, Japan. Microbes Environ. **34**: 13–22. doi:10.1264/jsme2.ME18103

Nakayama, K., K. Komai, K. Tada, H. C. Lin, H. Yajima, S. Yano, M. R. Hipsey, and J. W. Tsai. 2020. Modeling dissolved inorganic carbon considering submerged aquatic vegetation. Ecol. Modell. **431**: 109188. doi:10.1016/J.ECOLMODEL.2020.109188

Newell, S. E., M. J. McCarthy, W. S. Gardner, and R. W. Fulweiler. 2016. Sediment Nitrogen Fixation: a Call for Re-evaluating Coastal N Budgets. Estuaries and Coasts **39**: 1626–1638. doi:10.1007/s12237-016-0116-y

Oreska, M. P. J., K. J. McGlathery, L. R. Aoki, A. C. Berger, P. Berg, and L. Mullins. 2020. The greenhouse gas offset potential from seagrass restoration. Sci. Rep. **10**: 1–15. doi:10.1038/s41598-020-64094-1

Ortega, T., R. Ponce, J. Forja, and A. Gómez-Parra. 2005. Fluxes of dissolved inorganic carbon in three estuarine systems of the Cantabrian Sea (north of Spain). J. Mar. Syst. **53**: 125–142. doi:10.1016/J.JMARSYS.2004.06.006

Orth, R. J., T. J. B. Carruthers, W. C. Dennison, and others. 2006. A Global Crisis for Seagrass Ecosystems. Bioscience **56**: 987–996. doi:10.1641/0006-3568(2006)56[987:agcfse]2.0.co;2

Oshima, Y., M. J. Kishi, and T. Sugimoto. 1999. Evaluation of the nutrient budget in a seagrass bed. Ecol. Modell. **115**: 19–33. doi:10.1016/S0304-3800(98)00155-0

Oviatt, C., P. Doering, B. Nowicki, L. Reed, J. Cole, and J. Frithsen. 1995. An ecosystem level experiment on nutrient limitation in temperate coastal marine environments. Mar. Ecol. Prog. Ser. **116**: 171–179.

Pedersen, O., J. Borum, C. Duarte, and M. Fortes. 1998. Oxygen dynamics in the rhizosphere of Cymodocea rotundata. Mar. Ecol. Prog. Ser. **169**: 283–288. doi:10.3354/meps169283

Pietikäinen, J., M. Pettersson, and E. Bååth. 2005. Comparison of temperature effects on soil respiration and bacterial and fungal growth rates. FEMS Microbiol. Ecol. **52**: 49–58. doi:10.1016/J.FEMSEC.2004.10.002

Qu, W., C. Su, R. J. West, and R. J. Morrison. 2004. Photosynthetic characteristics of benthic microalgae and seagrass in Lake Illawarra, Australia. Hydrobiol. 2004 5151 **515**: 147–159. doi:10.1023/B:HYDR.0000027326.46856.0A

Rasmusson, L. M., P. Buapet, R. George, M. Gullström, P. C. B. Gunnarsson, and M. Björk. 2020. Effects of temperature and hypoxia on respiration, photorespiration, and photosynthesis of seagrass leaves from contrasting temperature regimes. ICES J. Mar. Sci. **77**: 2056–2065. doi:10.1093/ICESJMS/FSAA093

Ray, N., A. Al-Haj, and R. Fulweiler. 2020. Sediment biogeochemistry along an oyster aquaculture chronosequence. Mar. Ecol. Prog. Ser. **646**: 13–27. doi:10.3354/meps13377

Ray, N. E., T. J. Maguire, A. N. Al-Haj, M. C. Henning, and R. W. Fulweiler. 2019. Low Greenhouse Gas Emissions from Oyster Aquaculture. Environ. Sci. Technol. **53**: 9118–9127. doi:10.1021/acs.est.9b02965

Risgaard-Petersen, N. 2003. Coupled nitrification-denitrification in autotrophic and heterotrophic estuarine sediments: On the influence of benthic microalgae. Limnol. Oceanogr. **48**: 93–105. doi:10.4319/LO.2003.48.1.0093

Russell, D. G., F. Y. Warry, and P. L. M. Cook. 2016. The balance between nitrogen fixation and denitrification on vegetated and non-vegetated intertidal sediments. Limnol. Oceanogr. **61**: 2058–2075. doi:10.1002/LNO.10353

Salk, K. R., D. V. Erler, B. D. Eyre, N. Carlson-Perret, and N. E. Ostrom. 2017. Unexpectedly high degree of anammox and DNRA in seagrass sediments: Description and application of a revised isotope pairing technique. Geochim. Cosmochim. Acta **211**: 64–78. doi:10.1016/J.GCA.2017.05.012

Seymour, J. R., B. Laverock, D. A. Nielsen, S. M. Trevathan-Tackett, and P. I. Macreadie. 2018. The Microbiology of Seagrasses. Seagrasses Aust. Struct. Ecol. Conserv. 343–392. doi:10.1007/978-3-319-71354-0_12

Smith, A. C., J. E. Kostka, R. Devereux, and D. F. Yates. 2004. Seasonal composition and activity of sulfate-reducing prokaryotic communities in seagrass bed sediments. Aquat. Microb. Ecol. **37**: 183–195. doi:10.3354/AME037183

Smith, R. D., W. C. Dennison, and R. S. Alberte. 1984. Role of seagrass photosynthesis in root aerobic processes. Plant Physiol. **74**: 1055–8. doi:10.1104/pp.74.4.1055

Strickland, J., and T. Parsons. 1968. A practical handbook of seawater analysis, 2nd ed. Fisheries Research Board of Canada.

Sun, Y., Z. Song, H. Zhang, P. Liu, and X. Hu. 2020. Seagrass vegetation affect the vertical organization of microbial communities in sediment. Mar. Environ. Res. **162**: 105174. doi:10.1016/J.MARENVRES.2020.105174

Tezuka, Y. 1990. Bacterial regeneration of ammonium and phosphate as affected by the carbon:nitrogen:phosphorus ratio of organic substrates. Microb. Ecol. 1990 193 **19**:

227–238. doi:10.1007/BF02017167

Touchette, B. W., and J. A. M. Burkholder. 2000. Review of nitrogen and phosphorus metabolism in seagrasses. J. Exp. Mar. Bio. Ecol. **250**: 133–167. doi:10.1016/S0022-0981(00)00195-7

Vieillard, A. M., and R. W. Fulweiler. 2012. Impacts of long-term fertilization on salt marsh tidal creek benthic nutrient and N2 gas fluxes. Mar. Ecol. Prog. Ser. **471**: 11–22. doi:10.3354/MEPS10013

Watanabe, K., and T. Kuwae. 2015. How organic carbon derived from multiple sources contributes to carbon sequestration processes in a shallow coastal system? Glob. Chang. Biol. **21**: 2612–2623. doi:10.1111/GCB.12924

Watts, I. M., J. Dean Rosati, and M. Borrelli. 2011. Re-Establishing a Historical Inlet At East Harbor, Cape Cod, Masssachusetts. Proc. Coast. Sediments 419–429. doi:10.1142/9789814355537_0032

Weiss, R. F. 1970. The solubility of nitrogen, oxygen and argon in water and seawater. Deep Sea Res. Oceanogr. Abstr. **17**: 721–735. doi:10.1016/0011-7471(70)90037-9

Yarbro, L. A., and P. R. Carlson. 2008. Community oxygen and nutrient fluxes in seagrass beds of Florida Bay, USA. Estuaries and Coasts **31**: 877–897. doi:10.1007/S12237-008-9071-6/TABLES/9

Ziegler, S., and R. Benner. 1999. Nutrient cycling in the water column of a subtropical seagrass meadow. Mar. Ecol. Prog. Ser. **188**: 51–62. doi:10.3354/MEPS188051

Zuur, A. F., and E. N. Ieno. 2016. Beginner's guide to zero-inflated models with R, Highland Statistics Ltd.

Acknowledgements

The Cape Cod National Seashore Nickerson Fellowship, Sigma Xi, Boston University Biogeoscience, the Limnology & Oceanography Research Exchange (LOREX), the Boston University Martin Luther King, Jr. Fellowship, and the Boston University Department of Earth & Environment provided funding for this research to ANA. Rhode Island Sea Grant and Woods Hole Sea Grant provided funding to support RWF. We would like to acknowledge Dr. Alyssa Novak for help identifying research sites. We would like to thank Mr. Norval Reece and Mrs. Anne Reece for generous use of their parking spot and beach access at one of the sites. Thank you to Brendan Kelly, Nick Ray, Claudia Mazur, Nia Bartolucci, Melissa Hagy, Cristian Triana, Gretchen McCarthy, Anniina Haka, and Ena Miculinic for field help and to Tyler Chidsey, John Rezza, Kwetz Mexika, Joel Sparks, and Nilotpal Ghosh for help in the lab. Thank you to Cedric Fichot for the use of their elemental analyzer.

Tables

Table 3.1. Site characteristics for water column, sediment, and seagrass in East Harbor and Pleasant Bay, MA (USA). Mean (± standard error) water column temperature, dissolved oxygen (O_2) concentration, salinity, and surface water nutrient concentrations (ammonium: NH_4^+, nitrite: NO_2^-, nitrite + nitrate: NO_x, and dissolved inorganic phosphorus: DIP), sediment surface (top 0-1 cm depth) % nitrogen (N), % carbon (C), and carbon to nitrogen molar ratio (C:N), seagrass density, leaf area index (LAI), and nutrient pollution indicator (NPI) for sampling dates during summer 2018 (n=1) and summer 2019 (n=2). Superscripts with different letters indicate statistically different values (least square means, $p < 0.05$) between sites.

		East Harbor	Pleasant Bay
Water column	Temperature (ºC)	25.5 ± 0.4^{a}	23.3 ± 0.4^{b}
	Dissolved O_2 (mg L^{-1})	6.46 ± 0.22^{a}	5.58 ± 0.22^{b}
	Salinity (ppt)	25.8 ± 0.30^{a}	32.5 ± 0.08^{b}
	NO_2^- (µM)	0.04 ± 0.00^{a}	0.05 ± 0.00^{a}
	NO_x (µM)	0.12 ± 0.02^{a}	0.22 ± 0.02^{b}
	NH_4^+ (µM)	0.86 ± 0.11^{a}	2.79 ± 0.39^{b}
	DIP (µM)	0.41 ± 0.02^{a}	0.92 ± 0.07^{b}
Sediment	N (%)	0.04 ± 0.01^{a}	0.06 ± 0.01^{b}
	C (%)	0.60 ± 0.07^{a}	0.64 ± 0.07^{a}
	C:N	16.99 ± 1.14^{b}	12.26 ± 1.18^{b}
Seagrass	Density (shoots m^{-2})	$305.9 (\pm 34.9)^{a}$	$410.3 (\pm 48.2)^{a}$
	LAI ($m^2 m^{-2}$)	$0.0084 (\pm 0.0013)^{a}$	$0.0072 (\pm 0.0014)^{a}$
	NPI (%N leaf $mass^{-1}$)	$0.65 (\pm 0.23)^{a}$	$1.15 (\pm 0.27)^{a}$

Table 3.2. Best generalized linear models describing fluxes of oxygen (O_2), dissolved inorganic carbon (DIC), di-nitrogen gas (N_2-N), and nutrient fluxes (i.e., ammonium (NH_4^+), nitrite (NO_2^-), nitrite + nitrate (NO_x), dissolved inorganic phosphorus (DIP)) based on Aikaike's Information Criterion (AIC) and Likelihood Ratio Tests. All variables were fixed effects. See Supplemental Table S3.2 for model comparisons.

Flux	Distribution	Best Model
O_2	Normal	Light
DIC	Normal (post ZAG)	Light + Temperature
N_2-N	Normal	Light
NO_2^-	Normal	Location
NO_x	Normal	Location
NH_4^+	Gamma	Location + Light + Temperature + [O_2]
DIP	Gamma	Location + [O_2]

Table 3.3. Pearson correlation coefficients between sediment-water interface fluxes of oxygen (O_2), dissolved inorganic carbon (DIC), di-nitrogen gas (N_2-N), and nutrients (nitrite (NO_2^-), nitrite + nitrate (NO_x), ammonium (NH_4^+), and dissolved inorganic phosphorus (DIP). Bold correlation coefficients signify a significant ($p < 0.05$) correlation between fluxes

	O_2 Flux	DIC Flux	N_2-N Flux	NO_2^- Flux	NO_x Flux	NH_4^+ Flux	DIP Flux
O_2 Flux							
DIC Flux	**-0.41**						
N_2-N Flux	0.05	**0.40**					
NO_2^- Flux	**-0.28**	0.18	0.12				
NO_x Flux	0.11	-0.14	-0.06	0.28			
NH_4^+ Flux	-0.16	0.16	0.02	**0.37**	0.10		
DIP Flux	-0.17	0.08	-0.04	0.22	0.10	**0.86**	

Figures

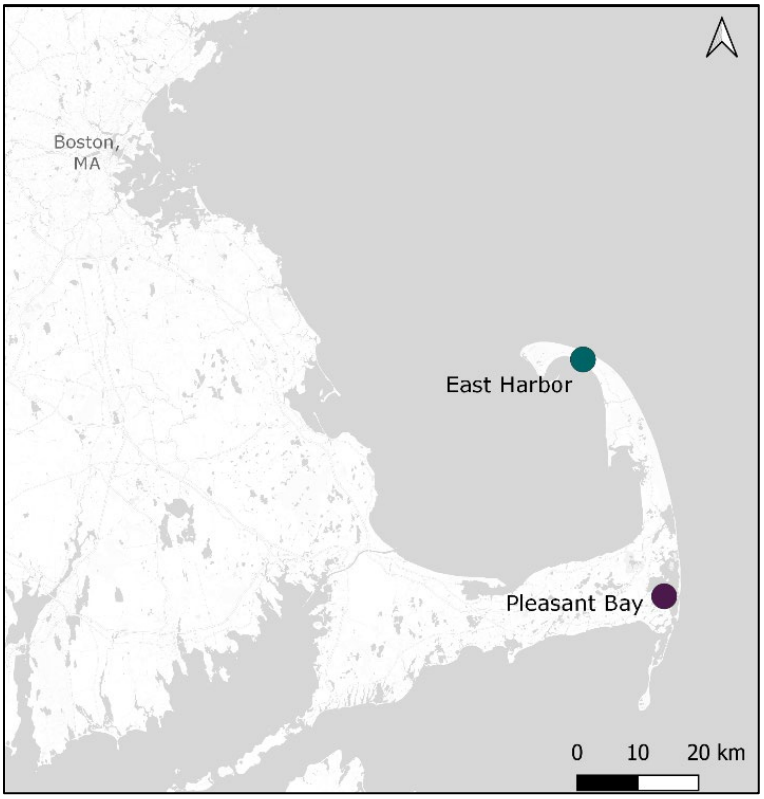

Figure 3.1. Map of sampling locations on Cape Cod, Massachusetts, USA: East Harbor (green circle) and Pleasant Bay (purple circle).

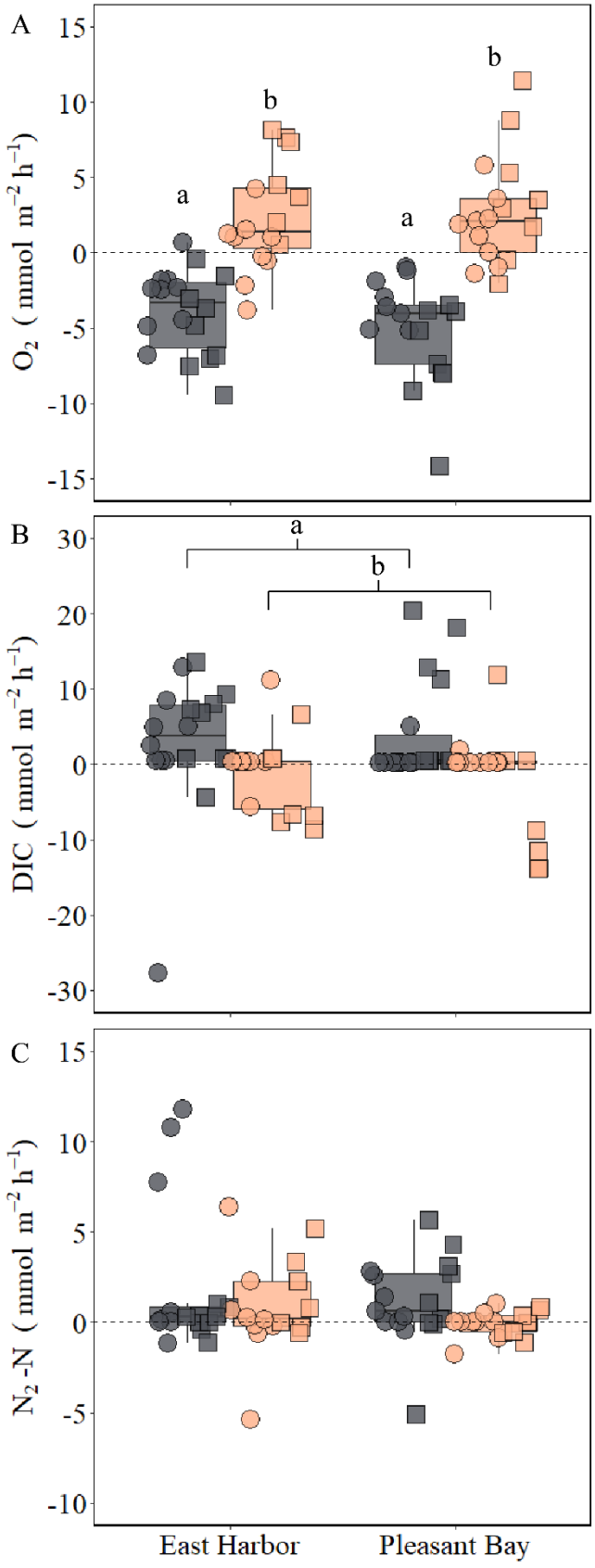
A
B
C
O_2 (mmol m^{-2} h^{-1})
DIC (mmol m^{-2} h^{-1})
N_2 -N (mmol m^{-2} h^{-1})
15
10
5
0
-5
-10
-15
30
20
10
0
-10
-20
-30
a
b
a
b
a
b
East Harbor
Pleasant Bay

Figure 3.2. Fluxes of (A) dissolved oxygen (O_2), (B) dissolved inorganic carbon (DIC), and (C) di-nitrogen (N_2-N) gas in East Harbor and Pleasant Bay from non-vegetated (circles) and vegetated (squares) sediments in the light (peach symbol) and dark (grey symbol). Positive values indicate flux into the water column while negative values indicate uptake by the sediment. Letters indicate significant differences between light and dark fluxes (O_2 flux: $F_{3, 64} = 26.46$, $p < 0.001$; DIC flux: $F_{1, 67} = 8.00$, $p = 0.006$). There were no significant differences between light and dark fluxes for N_2-N. There were no significant differences between vegetated and non-vegetated areas or sites for O_2, DIC, and N_2-N fluxes.

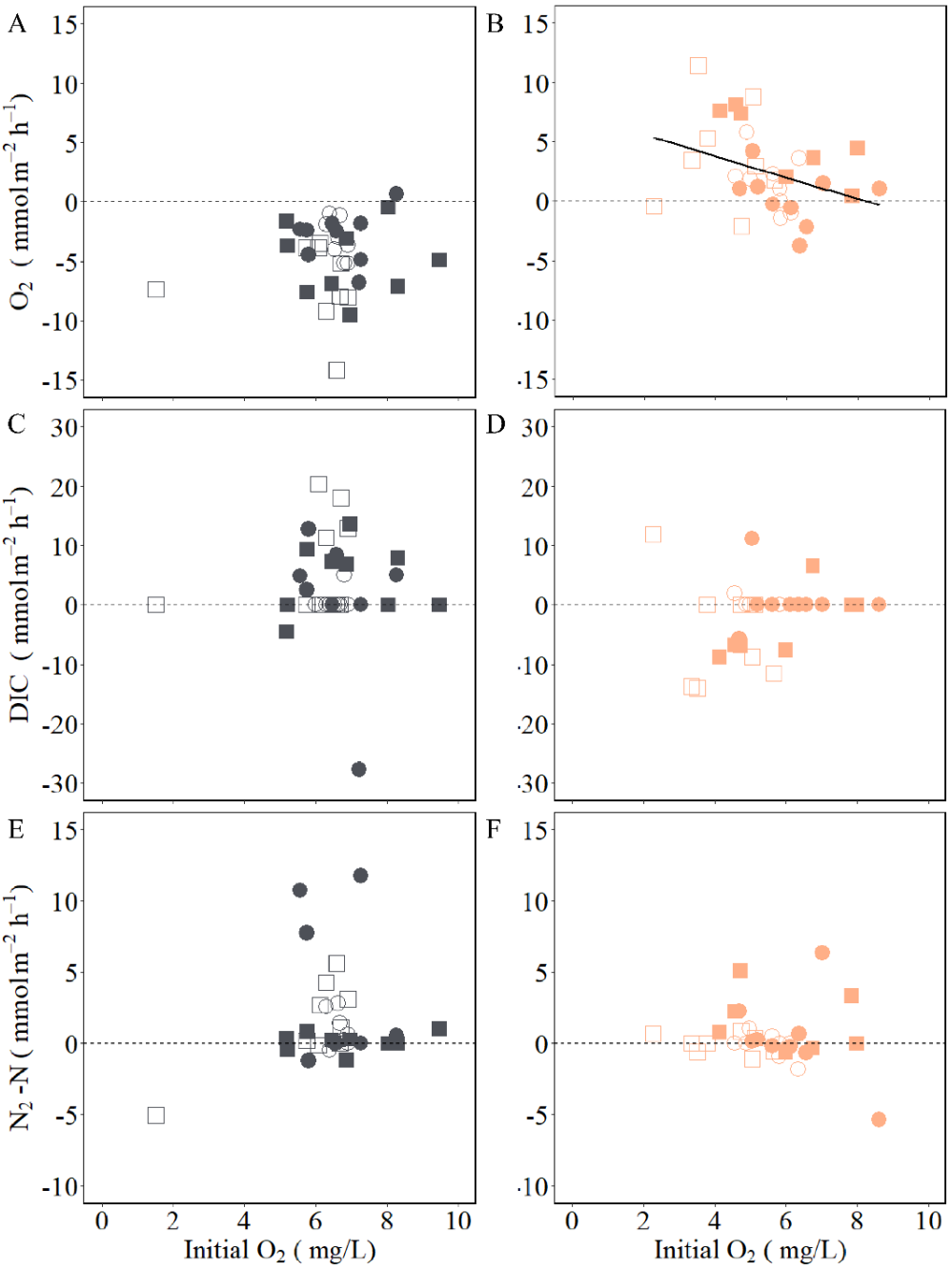

Figure 3.3. Dissolved oxygen (O_2; A-B), dissolved inorganic carbon (DIC; C-D), and di-nitrogen (N_2-N; E-F) fluxes as a function of initial O_2 concentration for dark (grey; A,C,E) and light (peach; B,D,F) incubations from vegetated (square) and non-vegetated (circle) sediments in East Harbor (filled) and Pleasant Bay (open). Positive fluxes indicate emission into the water column while negative fluxes indicate uptake by the sediment. There was a weak negative relationship between O_2 flux and initial O_2 concentration across all light fluxes (A, solid line: y = -0.91x +

7.45, $F_{31} = 4.34$, $R^2 = 0.09$, $p = 0.05$). There are no other relationships ($p > 0.05$) between dissolved gas fluxes and initial O_2 concentration during dark or light incubations at either site. Initial O_2 concentration during the light incubation is the O_2 concentration when opaque jackets were removed from the chambers after the dark incubation.

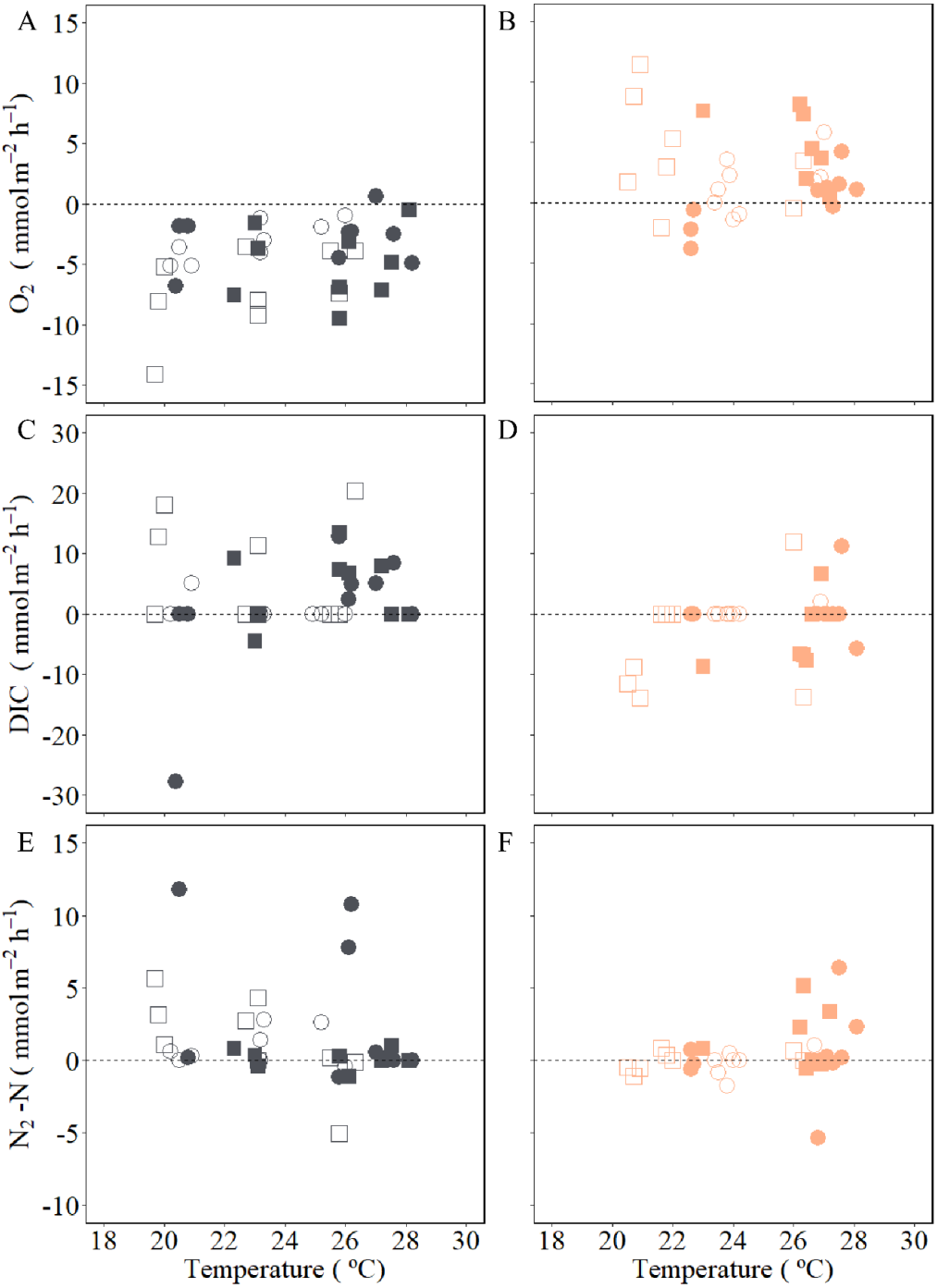

Figure 3.4. Dissolved oxygen (O_2; A-B), dissolved inorganic carbon (DIC; C-D), and di-nitrogen (N_2-N; E-F) fluxes as a function of temperature for dark (grey; A,C,E) and light (peach; B,D,F) incubations from vegetated (square) and non-vegetated (circle) sediments in East Harbor (filled) and Pleasant Bay (open). Positive fluxes indicate emission into the water column while negative

fluxes indicate uptake by the sediment. There were no significant relationships ($p > 0.05$) between dissolved gas fluxes and temperature during dark or light incubations at either site.

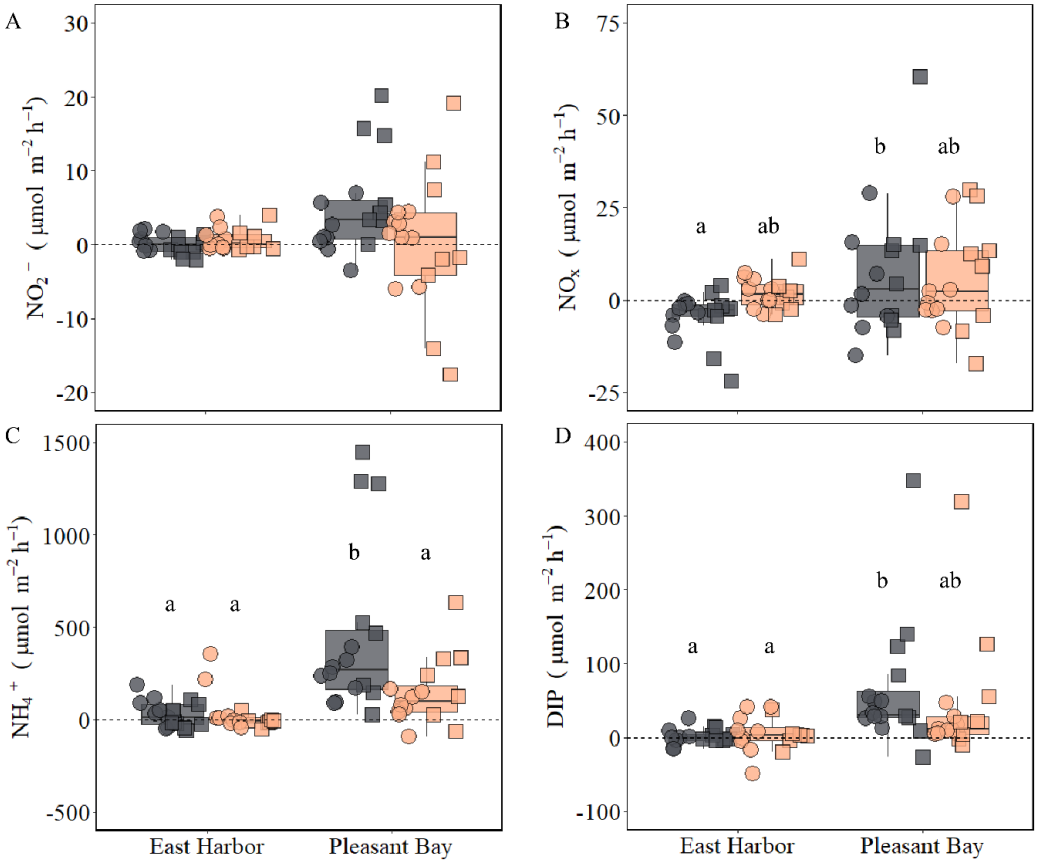

Figure 3.5. Fluxes of (A) nitrite (NO_2^-), (B) nitrite + nitrate (NO_x), (C) Ammonium (NH_4^+), and (D) dissolved inorganic phosphorous (DIP) for dark (grey) and light incubations (peach) in non-vegetated (circle) and vegetated (square) sediments in East Harbor and Pleasant Bay. Positive fluxes indicate emission into the water column while negative fluxes indicate uptake by the sediment. Letters indicate significant differences between light and dark incubations and sites (NH_4^+ (gamma): $p < 0.05$; NO_x (normal): $F_{62} = 3.16$, $p = 0.03$; DIP (gamma): $p < 0.05$). There were no significant differences between light incubations and site for NO_2^- fluxes and there were no significant differences between vegetated and non-vegetated areas for any of the nutrient fluxes.

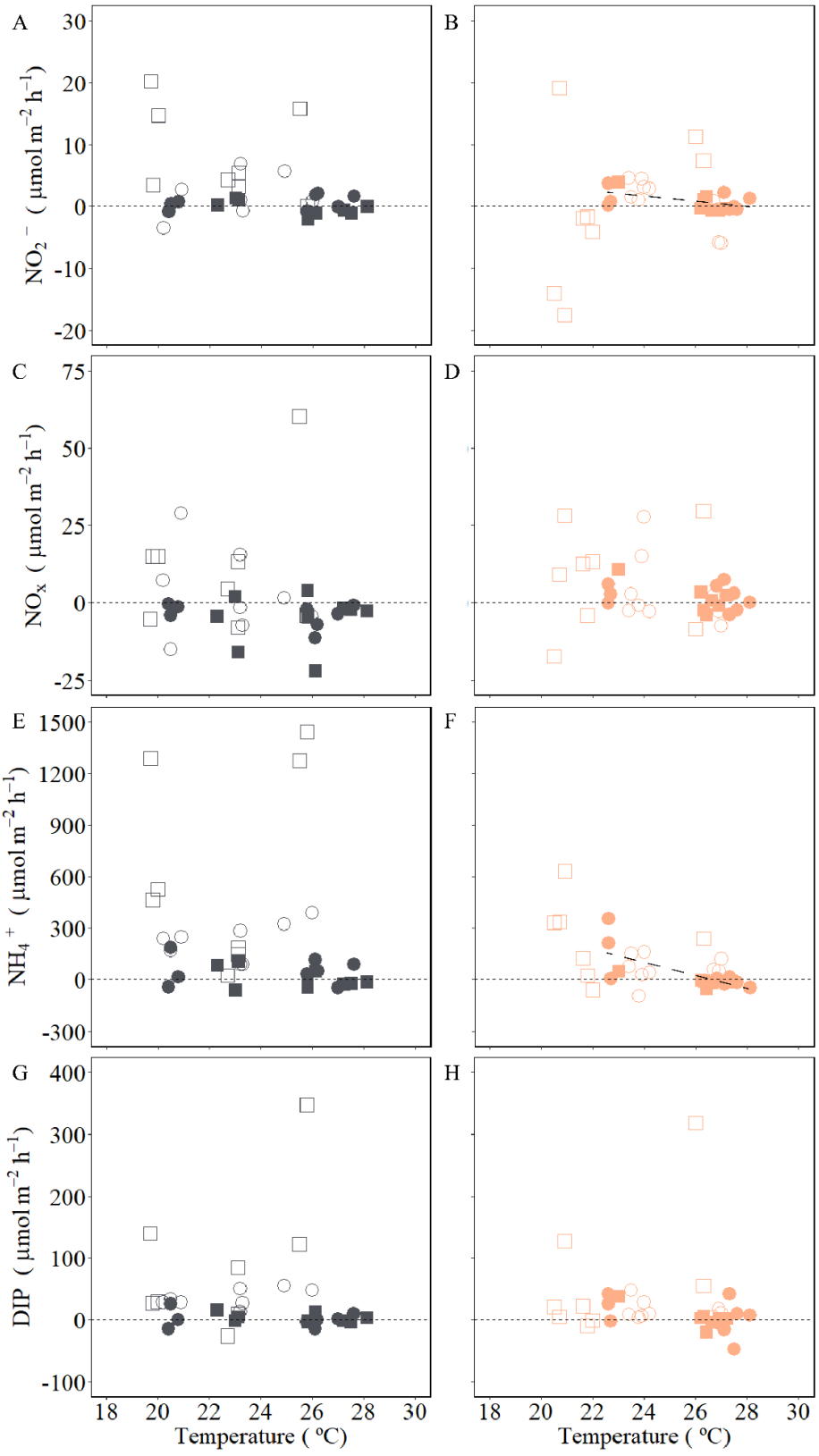
A
B
C
D
E
F
G
H
NO_2^- (μmol m^{-2} h^{-1})
NO_x (μmol m^{-2} h^{-1})
NH_4^+ (μmol m^{-2} h^{-1})
DIP (μmol m^{-2} h^{-1})
30
20
10
0
-10
-20
75
50
25
0
-25
1500
1200
900
600
300
0
-300
400
300
200
100
0
-100
18
20
22
24
26
28
30
Temperature (℃)

Figure 3.6. Nitrite (NO_2^-; A,B), nitrite + nitrate (NO_x; C,D), Ammonium (NH_4^+; E,F), and dissolved inorganic phosphorus (DIP; G,H) fluxes as a function of temperature in East Harbor (filled points) and Pleasant Bay (open points) for dark (grey; A,C,E,G) and light (peach; B,D,F,H) fluxes in vegetated (square) and non-vegetated (circle) sediments. Positive fluxes indicate emission into the water column while negative fluxes indicate uptake by the sediment. There was a negative relationship between NO_2^- flux and temperature during light incubations in East Harbor (B, dashed line; $y = -0.40x + 11.11$, $F = 5.38$, $R^2 = 0.23$, $p = 0.04$) and there was a negative relationship between NH_4^+ flux and temperature during light incubations in East Harbor (F, dashed line; $y = -38.39x + 1024.77$, $F = 15.18$, $R^2 = 0.49$, $p < 0.005$). There were no other relationships ($p > 0.05$) between nutrient fluxes and temperature during light or dark incubations at either site.

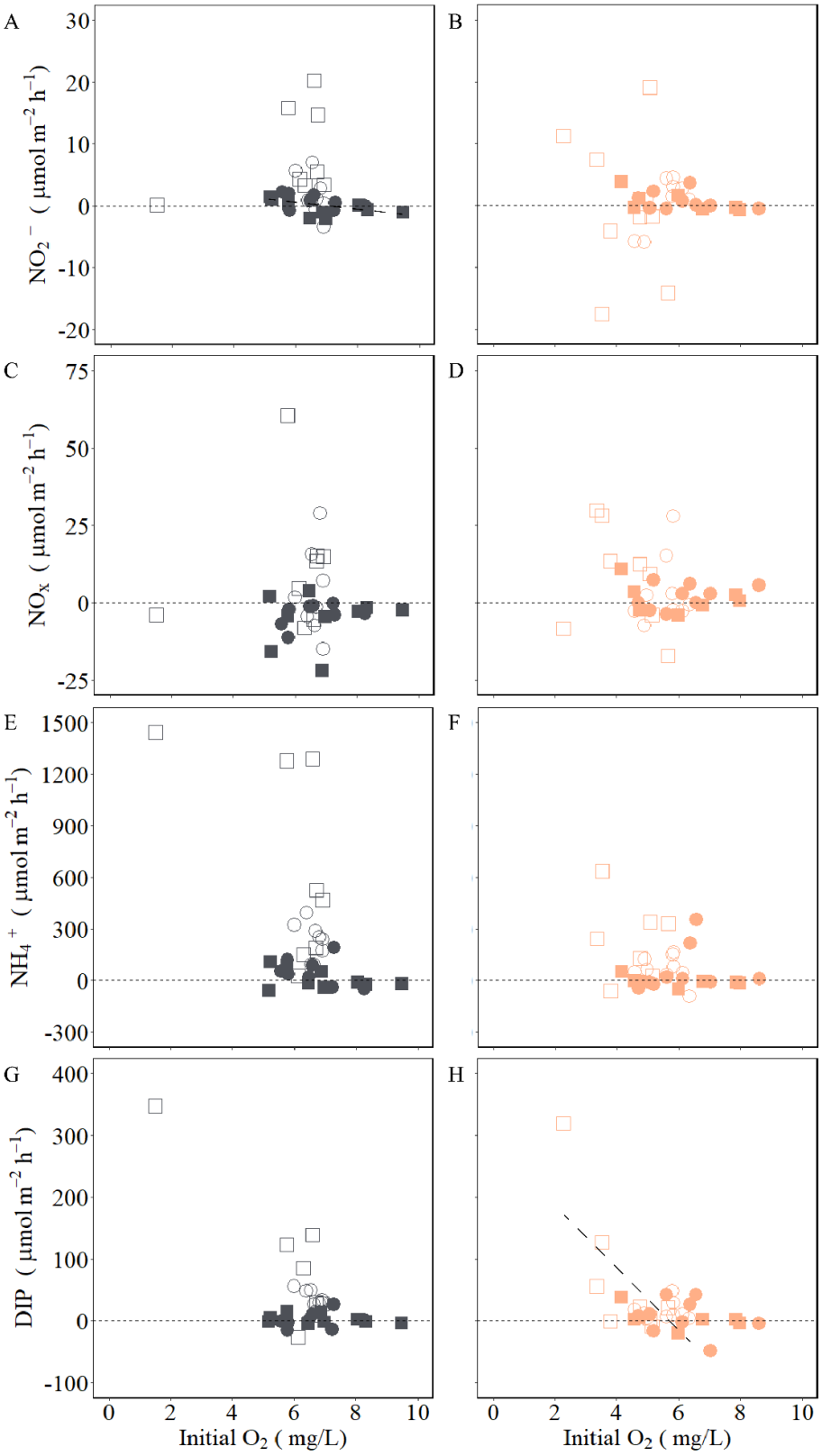
A
B
C
D
E
F
G
H
NO_2^- (μmol m^{-2} h^{-1})
NO_x (μmol m^{-2} h^{-1})
NH_4^+ (μmol m^{-2} h^{-1})
DIP (μmol m^{-2} h^{-1})
30
20
10
0
-10
-20
75
50
25
0
-25
1500
1200
900
600
300
0
-300
400
300
200
100
0
-100
0
2
4
6
8
10
Initial O_2 (mg/L)
Initial O_2 (mg/L)

Figure 3.7. Nitrite (NO_2^-; A,B), nitrite + nitrate (NO_x; C,D), ammonium (NH_4^+; E,F), and dissolved inorganic phosphorus (DIP; G,H) fluxes as a function of initial dissolved oxygen concentration in East Harbor (filled points) and Pleasant Bay (open points) for dark (grey; A,C,E,G) and light (peach; B,D,F,H) fluxes in vegetated (square) and non-vegetated (circle) sediments. Positive fluxes indicate emission into the water column while negative fluxes indicate uptake by the sediment. There was a negative relationship between dark NO_2^- flux and initial O_2 concentration in East Harbor (A; $y = -0.52x + 3.57$, $F_{1, 15} = 4.57$, $R^2 = 0.18$, $p = 0.05$). There was a negative relationship between DIP flux and initial O_2 concentration in Pleasant Bay for light incubations (H; $y = -50.41x + 287.34$, $F_{15} = 15.68$, $R^2 = 0.48$, $p = 0.001$). There were no other relationships ($p > 0.05$) between nutrient fluxes and O_2 concentration during light or dark incubations at either site.

APPENDIX

Appendix 1: Supporting Information for:

A Synthesis of Methane Emissions from Shallow Vegetated Coastal Ecosystems

Alia N. Al-Haj[1*], Robinson W. Fulweiler[1,2]

[1]Boston University, Department of Earth and Environment, 675 Commonwealth Avenue, Boston, MA 02215

[2]Boston University, Department of Biology, 5 Cummington Mall, Boston, MA 02215

Corresponding author: Alia N. Al-Haj (email: aalhaj@bu.edu)

This file includes:

Supporting Information Text

Supporting Text 1.1:

To find the literature used in this analysis, we used the "Advanced Search" feature on Google Scholar using the search terms "Seagrass + methane", "Mangrove + methane" and "Salt marsh + methane" with the exact phrase "methane flux." These searches returned 209, 891, and 1,560 results, respectively. To further downselect the mangrove and salt marsh results, articles with at least one of the following words were selected "g CH_4", "mol CH_4", "mg CH_4", "ug CH_4", "umol CH_4", "nmol CH_4" returning 98 and 209 results, respectively. We further screened these papers to ensure a flux from the described ecosystem was included and did not include data from mesocosm/manipulation studies. We also include other literature cited within these papers that was not returned in the Google Scholar search results for a final total of 97 papers reviewed here. We completed the literature search on 12/3/2018.

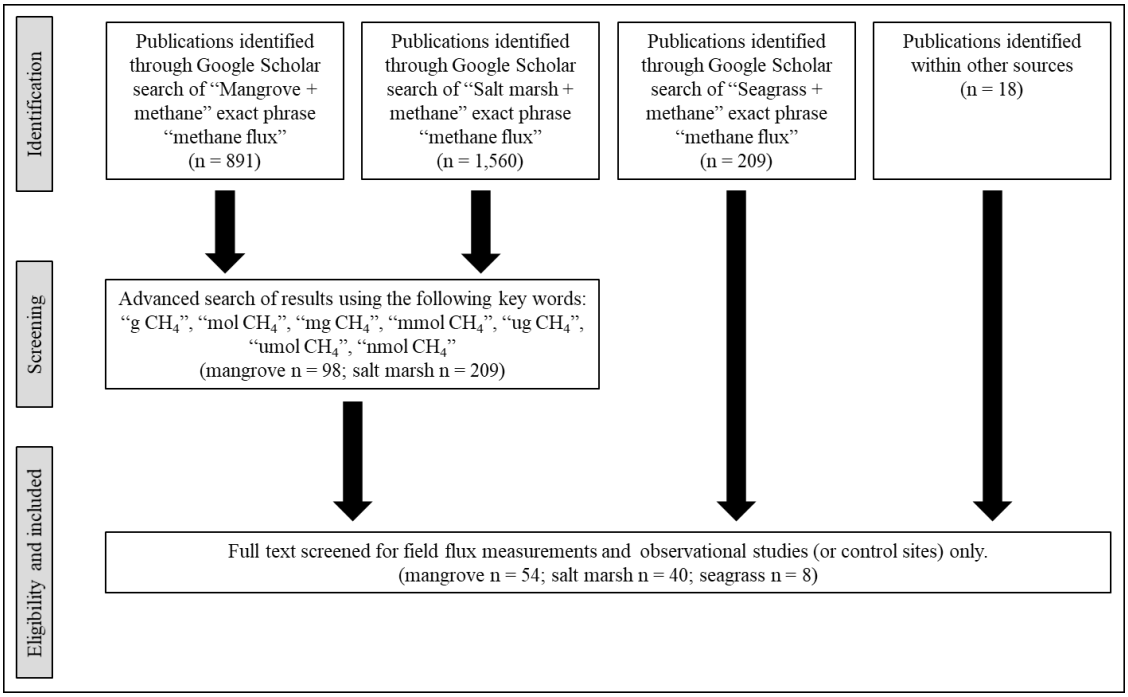

Supporting Figure S1.1 Flow chart describing the down-selection method used in this analysis.

Supporting Text 1.2:

We report the median and range of the data for each VCE because our data are not normally distributed. In this case the median and range show where most of the data falls. However, they do not account for the high variability in our methane fluxes. Because of the limited data from VCEs and lack of continuous measurements from these systems, the mean and standard error give us a better idea of the impact these several high emitting sites may have on the global methane budget.

Supporting Table S1.1 Methane emissions (in μmol CH_4 m^{-2} d^{-1} ± standard error) from vegetated coastal ecosystems separated by salinity category (oligohaline: 0.5-5 ppt, mesohaline: 5-18 ppt, polyhaline: 18-30 ppt, euhaline: > 30 ppt, NR = not reported). Values with the same lower case letter are not significantly different.

	Oligohaline	**Mesohaline**	**Polyhaline**	**Euhaline**	**NR**
median	3902.24[bc]	347.33[bd]	614.40[b]	93.96[a]	80.31[a]
range	5.61 - 94129.68	-14.96 - 47529.93	8.88 - 55830.17	-5.12 - 2684.71	-92.6 - 164588.53
mean ± SE	10876.18 ± 4923.96	3495.67 ± 1164.53	4775.28 ± 2060.23	2684.71 ± 2423.98	3879.61 ± 2088.74
n	19	61	29	30	84

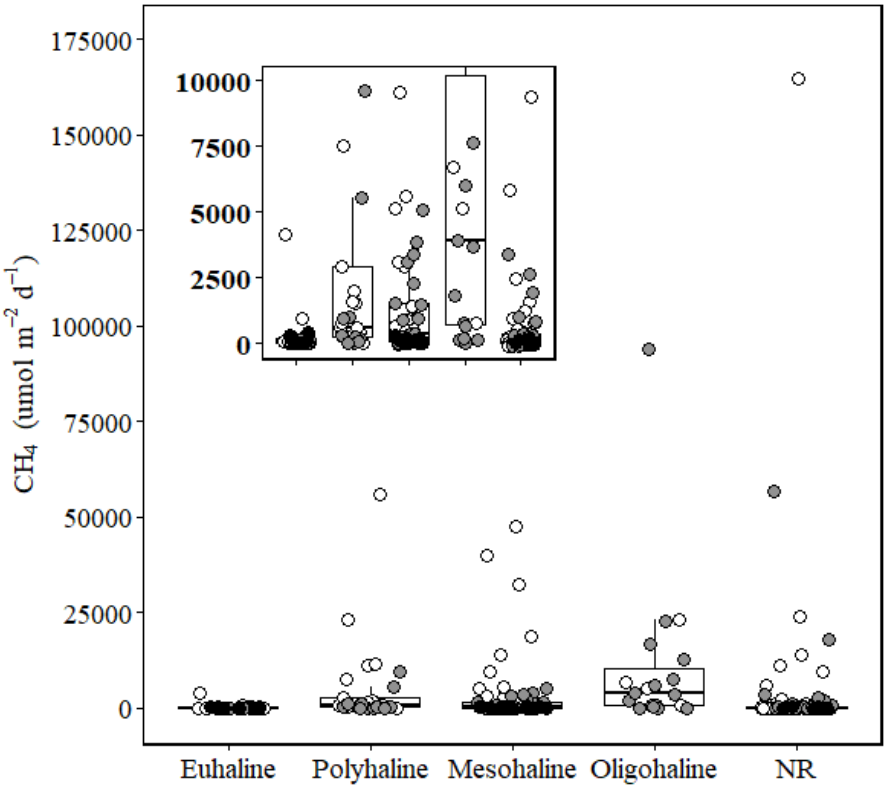

Supporting Figure S1.2 Average CH_4 fluxes from each reviewed study separated by salinity category: euhaline (≥ 30 ppt, n = 30), polyhaline (18 – 30 ppt, n = 29), mesohaline (5 – 18 ppt, n = 61), oligohaline (0.5 – 5 ppt, n = 19), and NR (not reported in the study, n = 84). Colors represent vegetation type (mangrove = white circle, salt marsh = grey circle, seagrass = black circle). Data are available via https://figshare.com/articles/Coastal_CH4_Review_Data/9202097.

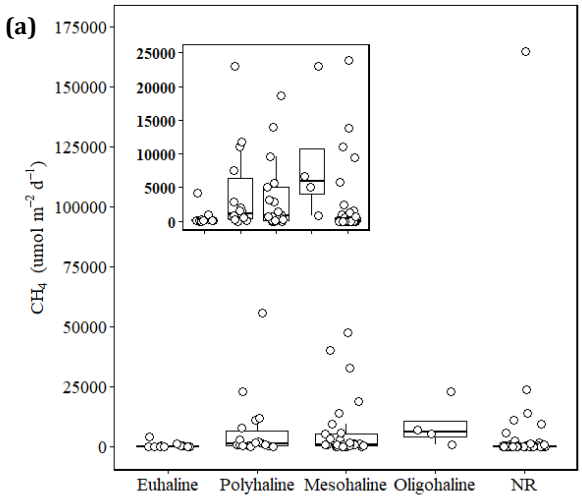
(a)
175000
150000
125000
100000
75000
50000
25000
0
25000
20000
15000
10000
5000
0
CH4 (umol m-2 d-1)
Euhaline
Polyhaline
Mesohaline
Oligohaline
NR

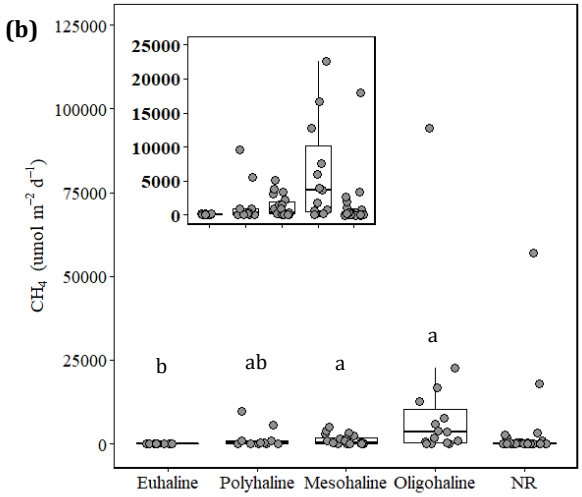
(b)
125000
100000
75000
50000
25000
0
25000
20000
15000
10000
5000
0
CH4 (umol m-2 d-1)
b
ab
a
a
Euhaline
Polyhaline
Mesohaline
Oligohaline
NR

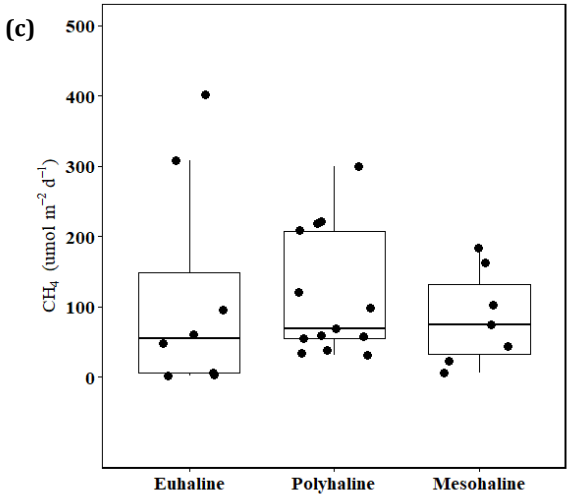
(c)
500
400
300
200
100
0
CH4 (umol m-2 d-1)
Euhaline
Polyhaline
Mesohaline

Figure S1.3 Methane fluxes separated by salinity type from (a) mangrove, (b) salt marsh, and (c) seagrass studies. Note the different scale on the y-axis on each graph. There were no oligohaline sites in the seagrass data. Letters on the salt marsh figure (b) indicate significant differences ($p < 0.05$).

Supporting Text 1.3:

Global methane flux rate from each vegetation type:

$$Global\ CH_4\ flux\ rate\ (Tmol\ CH_4\ yr^{-1}) = \left(\frac{Mean\ CH_4\ Flux\ \left(\frac{umol\ CH_4}{m^2 d}\right) * \frac{1 mol\ C}{1 mol\ CH_4} * \frac{365\ days}{yr}}{1.0E^{18}\ \frac{umol}{Tmol}} \right) * Global\ area_{\min\ or\ max}\ (m^2)$$

$$Standard\ Error = (Standard\ Deviation\ mean\ CH_4\ Flux)/\sqrt{n}$$

where n = number of observations, where an observation is the mean CH_4 flux from one site within one study.

Supporting Text 1.4:

Increase in global marine methane budget:

$$\%\ Increase = \frac{Vegetation\ Global\ CH_4\ flux\ rate\ (Tmol\ C\ yr^{-1})_{\min\ or\ max}}{0.57\ (Tmol\ C\ yr^{-1})}\ \text{x}\ 100\%$$

where 0.57 Tmol C yr^{-1} is the global marine methane emission rate.

Supporting Text 1.5:

Global Warming Potential 100 year (GWP)

$$GWP = Global\ CH_4\ flux\ rate\ (Tmol\ CH_4\ yr^{-1}) * \frac{32\ Tmol\ CO_{2eq}}{1\ Tmol\ CH_4}$$

Supporting Text 1.6:

Sustained Flux Global Warming Potential 100 year (SFGWP)

$$SFGWP = Global\ CH_4\ flux\ rate\ (Tmol\ CH_4\ yr^{-1}) * \frac{45\ Tmol\ CO_{2eq}}{1\ Tmol\ CH_4}$$

Supporting Table S1.2 Mangrove median CH_4 flux rate, global CH_4 flux rate, increase in global marine CH_4 budget, global warming potential, and sustained flux global warming potential including and not including the Yang et al. (2018) Zhangjiang River Estuary observation.

		Not Including Yang et al. (2018) observation	**Including Yang et al. (2018) observation**
CH_4 flux rate (μmol CH_4 m^{-2} d^{-1})	median	279.17[a]	284.91[a]
	range	-67.33 - 72867.83	-67.33 - 164588.50
Aerial Extent (km^2)		137760 - 152361	137760 - 152361
Global CH_4 flux rate (Tmol CH_4-C yr^{-1})	mean ± SE	0.23 ± 0.01 0.25 ± 0.06	0.30 ± 0.09 0.33 ± 0.10
Increase in global marine CH_4 budget (%)		40.2 - 44.5	53.0 - 58.6
Global C burial (Tmol C yr^{-1})	mean ± SE	2.59 ± 0.45 2.86 ± 0.49	2.59 ± 0.45 2.86 ± 0.49
Global Warming Potential (Tmol $CO_{2\ eq}$ y^{-1})		7.33 - 8.11	9.67 - 10.70
Sustained Flux Global Warming Potential (Tmol CO_{2eq} y^{-1})		10.31 - 11.40	13.60 - 15.05
Global Area Source		McLeod et al. 2011	McLeod et al. 2011

Supporting Table S1.3 Median methane flux from each VCE by sampling technique. Letters represent significant differences amongst sampling types. Italicized sampling types were removed from the analysis due to observation number (n), where observations are the mean CH_4 flux from each site within each study.

	Mangrove		Salt marsh		Seagrass	
	median	**n**	**median**	**n**	**median**	**n**
air samples	*2.48*	1	-	-	-	-
CRDS	21.16[a]	14	*1.21*	1	54.55	8
floating chamber	*2024.17*	3	-	-	-	-
flux tower	*32597.75*	2	-	-	-	-
Infra-red gas analyzer	*1471.41*	3	-	-	-	-
NDIR	*164588.50*	1	-	-	-	-
sediment cores	*106.30*	2	280.55	3	-	-
static chamber	290.65[b]	75	227.24	66	74.81	7
water samples	2933.60[b]	8	-	-	68.50	13
eddy covariance	-	-	*5063.04*	1	-	-
flow through chamber	-	-	159.91	12	-	-

Appendix 2 Supplementary Information for: Temperate seagrass meadow carbon sequestration can be enhanced by methane and nitrous oxide uptake

Alia N. Al-Haj[1] (https://ocid.org/0000-0003-1899-5117), Tyler Chidsey[2], & Robinson W. Fulweiler[1,2] (https://orcid.org/0000-0003-0871-4246)

[1]Department of Earth & Environment, Boston University, Boston, MA, U.S.A

[2]Deparment of Biology, Boston University, Boston, MA, U.S.A

Supplementary Information

S2.1. In situ benthic chamber description

24 hours before making flux measurements, we pushed stainless steel collars (20 cm in diameter, 5 cm deep) topped with a rubber gasket into the sediment until the gasket was flush with the sediment surface. Before sampling, we fastened a plexiglass cylinder (20 cm in diameter, 31.1 cm in height) outfitted with an opaque jacket to the collar. We closed the cylinders at the other end by fastening a flat plexiglass top to the cylinder. We used reflective "blackout" fabric jackets for our dark measurements to keep the light out without increasing the temperature. Seals between components were made water/gas tight with marine lubricant (Aqua Shield Grease). The water overlying the sediment was gently mixed with an aquarium pump. We attached a bag filled with site water to a port on the chamber to replace water removed during sampling.

S2.2. Description of headspace equilibration and greenhouse gas analysis

Headspace equilibration was performed by injecting 5 mL of high purity helium (UHP He) into each exetainer vial while simultaneously removing 5 mL of sample. Vials were shaken for 20 seconds and allowed to equilibrate for at least 1 h. After equilibration, 4 mL of headspace were removed from the exetainer and injected into a GC-2014 gas chromatograph (Shimadzu, Japan) equipped with a flame ionization detector (FID) and methanizer for determination CH_4 and CO_2 and an electron capture detector (ECD) with a ^{63}Nickel (Ni) source for determination of N_2O. The instrument is equipped with HayeSep® Q and N and Shimalite® columns. N_2 gas was used as the carrier gas and the make-up gas was a P5 mixture (5% methane, argon balance) for the ECD.

S2.3. Description of greenhouse gas externally mixed standards and gas chromatograph detection limits

The externally mixed standard contained 4.977 ppm CH_4, 495 ppb N_2O, and 4991 ppm CO_2 in N_2. The standard curve was calculated by mixing the following ratios of standard to UHP He: 5:0, 4:1, 3:2, 2:3, 1:4, and 0:5. CH_4 and N_2O standard curves had an $R^2 > 0.995$. Minimum detection limits for CH_4 and N_2O, were 83.2 ppb and 16.8 ppb, respectively.

S2.4. Calculation for comparing system-wide air-sea CH_4 and N_2O fluxes to C sequestration (C_{seq}) rates

$$\boldsymbol{C_{seq}\ (g\ C\ m^{-2}\ y^{-1}) = \left[C_{seq\ non-veg} * \left(\frac{area_{non-veg}}{area_{total}}\right)\right] + \left[C_{seq\ veg} * \left(\frac{area_{veg}}{area_{total}}\right)\right]}$$

S2.5. Calculation for CO_{2eq}-C uptake rates

CO_{2eq}-C uptake rate = (CO_{2eq}-C_{seq}) – (CO_{2eq}-CH_4 air-sea flux) – (CO_{2eq}-N_2O air sea flux)

Supplementary Tables

Table S2.1. Area and organic carbon (C_{org}) accumulation rates in vegetated and non-vegetated sediments of East Harbor and Pleasant Bay.

	East Harbor		Pleasant Bay	
	vegetated	**non-vegetated**	**vegetated**	**non-vegetated**
Area (km^2)	0.15[a]	2.75	7.3[b]	24.4
C_{org} accumulation rate ($g\ m^{-2}\ y^{-1}$)	20 (8 - 230)[c]	15.3 (4.3 - 45.3)[d]	8 ± 2	15.3 (4.3 - 45.3)[d]

[a] estimated 5% of total area from Portnoy et al. (2006)

[b] eelgrass area from Howes et al. (2006)

[c] median (range) from Novak et al. (2020)

[d] median (range) from Prentice et al. (2020)

Table S2.2. Correlation coefficients (r) from Pearson correlation tests for each predictor variable (salinity, temperature (Temp), initial ammonium concentration (NH3_T1), initial nitrite concentration (NO2_T1), initial nitrate + nitrite concentration (NOx_T1), initial dissolved inorganic phosphorous concentration (oP_T1), initial nitrate concentration (NO3_T1), initial dissolved inorganic nitrogen concentration (DIN_T1), seagrass density (Density), leaf area index (LAI), % N in the top 0-1 cm of sediment (pN_0.1), % N in the top 1-2 cm of sediment (pN_1.2), % N in the top 2-3 cm of sediment (pN_2.3), % N in the top 3-4 cm of sediment (pN_3.4), % C in the top 0-1 cm of sediment (pC_0.1), % C in the top 1-2 cm of sediment (pC_1.2), % C in the top 2-3 cm of sediment (pC_2.3), % C in the top 3-4 cm of sediment (pC_3.4), C:N in the top 0-1 cm of sediment (CN_0.1), C:N in the top 1-2 cm of sediment (CN_1.2), C:N in the top 2-3 cm of sediment (CN_2.3), C:N in the top 3-4 cm of sediment (CN_3.4), oxygen flux across the sediment-water interface (FO2), nutrient pollution indicator (NPI)) measured. Bold correlation coefficients have a p-value < 0.05 indicating a significant correlation.

	Salinity	Temp	NH3_T1	NO2_T1	NOx_T1	oP_T1	NO3_T1	DIN_T1	Density	LAI	pN_0.1	pN_1.2	pN_2.3	pN_3.4	pC_0.1	pC_1.2	pC_2.3	pC_3.4	CN_0.1	CN_1.2	CN_2.3	CN_3.4	FO2	NPI
Salinity	*1.00*	**-0.38**	**0.41**	0.09	**0.38**	**0.60**	**0.38**	**0.40**	0.18	0.14	**0.36**	**0.54**	**0.49**	**0.49**	0.11	**0.42**	0.19	**0.39**	-0.26	-0.20	**-0.58**	**-0.38**	0.01	0.03
Temp	**-0.38**	*1.00*	-0.09	-0.02	-0.19	-0.07	-0.19	-0.15	-0.20	-0.22	**-0.43**	**-0.44**	**-0.41**	**-0.43**	-0.11	-0.23	**-0.28**	**-0.28**	**0.41**	**0.36**	0.21	**0.37**	0.17	-0.28
NH3_T1	**0.41**	-0.09	*1.00*	**0.64**	**0.58**	**0.88**	**0.47**	**1.00**	**0.37**	-0.04	**0.52**	**0.39**	0.28	0.20	**0.46**	0.19	0.15	0.07	-0.13	-0.22	-0.19	-0.21	0.15	0.43
NO2_T1	0.09	-0.02	**0.64**	*1.00*	**0.62**	**0.55**	**0.43**	**0.66**	0.01	**-0.39**	-0.23	**-0.33**	-0.18	-0.23	**-0.37**	**-0.52**	0.05	**-0.40**	**-0.32**	-0.27	**0.37**	-0.13	0.15	0.13
NOx_T1	**0.38**	-0.19	**0.58**	**0.62**	*1.00*	**0.44**	**0.97**	**0.62**	0.04	-0.17	0.02	-0.02	0.07	-0.03	-0.14	-0.14	0.10	-0.22	-0.23	-0.27	-0.02	-0.28	-0.02	-0.09
oP_T1	**0.60**	-0.07	**0.88**	**0.55**	**0.44**	*1.00*	**0.32**	**0.87**	**0.38**	0.02	**0.46**	**0.55**	**0.43**	**0.45**	0.24	0.28	0.19	**0.35**	-0.28	**-0.30**	**-0.43**	**-0.31**	0.16	0.25
NO3_T1	**0.38**	-0.19	**0.47**	**0.43**	**0.97**	**0.32**	*1.00*	**0.51**	0.04	-0.08	0.06	0.02	0.08	-0.01	-0.07	-0.02	0.07	-0.16	-0.17	-0.20	-0.10	-0.25	-0.06	-0.13
DIN_T1	**0.40**	-0.15	**1.00**	**0.66**	**0.62**	**0.87**	**0.51**	*1.00*	**0.39**	0.01	**0.49**	**0.40**	**0.29**	0.22	**0.39**	0.21	0.18	0.07	-0.20	-0.22	-0.17	-0.24	0.12	0.42
Density	0.18	-0.20	**0.37**	0.01	0.04	**0.38**	0.04	**0.39**	*1.00*	**0.77**	**0.44**	**0.56**	**0.49**	**0.49**	0.16	**0.41**	0.24	**0.48**	**-0.36**	-0.27	**-0.29**	-0.23	0.03	-0.39
LAI	0.14	-0.22	-0.04	**-0.39**	-0.17	0.02	-0.08	0.01	**0.77**	*1.00*	**0.35**	**0.55**	**0.47**	**0.59**	0.09	**0.47**	**0.37**	**0.50**	**-0.32**	-0.22	**-0.31**	-0.29	-0.02	**-0.71**
pN_0.1	**0.36**	**-0.43**	**0.52**	-0.23	0.02	**0.46**	0.06	**0.49**	**0.44**	**0.35**	*1.00*	**0.75**	**0.65**	**0.62**	**0.77**	**0.73**	**0.48**	**0.68**	-0.23	-0.01	-0.12	0.00	-0.01	0.34
pN_1.2	**0.54**	**-0.44**	**0.39**	**-0.33**	-0.02	**0.55**	0.02	**0.40**	**0.56**	**0.55**	**0.75**	*1.00*	**0.82**	**0.76**	**0.44**	**0.80**	**0.52**	**0.65**	**-0.38**	**-0.34**	**-0.52**	**-0.46**	0.01	**0.46**
pN_2.3	**0.49**	**-0.41**	0.28	-0.18	0.07	**0.43**	0.08	**0.29**	**0.49**	**0.47**	**0.65**	**0.82**	*1.00*	**0.75**	0.26	**0.68**	**0.84**	**0.66**	**-0.43**	-0.27	**-0.45**	**-0.40**	-0.04	0.10
pN_3.4	**0.49**	**-0.43**	0.20	-0.23	-0.03	**0.45**	-0.01	0.22	**0.49**	**0.59**	**0.62**	**0.76**	**0.75**	*1.00*	0.21	**0.65**	**0.48**	**0.89**	**-0.45**	-0.24	**-0.46**	**-0.55**	-0.05	-0.03
pC_0.1	0.11	-0.11	**0.46**	**-0.37**	-0.14	0.24	-0.07	**0.39**	0.16	0.09	**0.77**	**0.44**	0.26	0.21	*1.00*	**0.59**	0.22	**0.36**	**0.40**	**0.29**	0.16	**0.31**	0.01	**0.48**
pC_1.2	**0.42**	-0.23	0.19	**-0.52**	-0.14	0.28	-0.02	0.21	**0.41**	**0.47**	**0.73**	**0.80**	**0.68**	**0.65**	**0.59**	*1.00*	**0.47**	**0.71**	-0.07	0.23	-0.25	-0.08	0.00	0.24
pC_2.3	0.19	**-0.28**	0.15	0.05	0.10	0.19	0.07	0.18	0.24	**0.37**	**0.48**	**0.52**	**0.84**	**0.48**	0.22	**0.47**	*1.00*	**0.43**	-0.27	-0.05	-0.01	-0.11	-0.03	0.08
pC_3.4	**0.39**	**-0.28**	0.07	**-0.40**	-0.22	**0.35**	-0.16	0.07	**0.48**	**0.50**	**0.68**	**0.65**	**0.66**	**0.89**	**0.36**	**0.71**	**0.43**	*1.00*	-0.27	0.02	**-0.29**	-0.20	-0.04	-0.05
CN_0.1	-0.26	**0.41**	-0.13	**-0.32**	-0.23	-0.28	-0.17	-0.20	**-0.36**	**-0.32**	-0.23	**-0.38**	**-0.43**	**-0.45**	**0.40**	-0.07	-0.27	-0.27	*1.00*	**0.45**	**0.35**	**0.42**	0.03	0.20
CN_1.2	-0.20	**0.36**	-0.22	-0.27	-0.27	**-0.30**	-0.20	-0.22	-0.27	-0.22	-0.01	**-0.34**	-0.27	-0.24	**0.29**	0.23	-0.05	0.02	**0.45**	*1.00*	**0.59**	**0.75**	-0.02	-0.29
CN_2.3	**-0.58**	0.21	-0.19	**0.37**	-0.02	**-0.43**	-0.10	-0.17	**-0.29**	**-0.31**	-0.12	**-0.52**	**-0.45**	**-0.46**	0.16	-0.25	-0.01	**-0.29**	**0.35**	**0.59**	*1.00*	**0.69**	0.03	-0.11
CN_3.4	**-0.38**	**0.37**	-0.21	-0.13	-0.28	**-0.31**	-0.25	-0.24	-0.23	-0.29	0.00	**-0.46**	**-0.40**	**-0.55**	**0.31**	-0.08	-0.11	-0.20	**0.42**	**0.75**	**0.69**	*1.00*	0.01	-0.13
FO2	0.01	0.00	0.03	-0.15	-0.04	-0.02	-0.01	-0.04	0.02	-0.01	-0.04	-0.05	-0.10	-0.11	0.07	0.01	-0.20	-0.04	0.16	0.06	-0.09	0.02	*1.00*	0.08
NPI	0.03	-0.28	0.43	0.13	-0.09	0.25	-0.13	0.42	-0.39	**-0.71**	0.34	**0.46**	0.10	-0.03	**0.48**	0.24	0.08	-0.05	0.20	-0.29	-0.11	-0.13	0.00	*1.00*

Table S2.3. Best models describing sediment-water interface fluxes of methane (CH_4) and nitrous oxide (N_2O), p-value, and R^2. No models included random effects.

Flux	Distribution	Fixed Effects	p-value	R^2
CH_4	Normal (after zero-adjusted model)	Vegetation Presence + %C in top 0-1 cm sediment	< 0.0001	0.46
		Vegetation Presence + %C in top 0-1 cm sediment + O_2 Flux	<0.0001	0.47
N_2O	Normal (after zero-adjusted model)	Vegetation Presence	0.13	0.03
		LAI	0.23	0.01

Table S2.4. AIC scores for generalized linear models generated for CH_4 and N_2O fluxes across the sediment-water interface. All variables were treated as fixed effects. An "N" below the variable name means it was not used in the model, while a "Y" indicates it was. The bold AIC value indicates the best model for each flux type following model selection.

Model Variables							Model AIC Score	
Location	Vegetation presence	Light Treatment	Salinity	O_2 Flux	LAI	%C (0-1 cm)	CH_4	N_2O
Y	N	N	N	N	N	N	201.76	346.02
N	Y	N	N	N	N	N	191.05	**344.21**
N	N	Y	N	N	N	N	202.92	346.56
N	N	N	Y	N	N	N	201.78	346.21
N	N	N	N	Y	N	N	201.72	346.53
N	N	N	N	N	Y	N	196.60	345.06
N	N	N	N	N	N	Y	184.22	345.63
Y	Y	N	N	N	N	N	192.67	345.94
Y	N	Y	N	N	N	N	203.74	347.99
Y	N	N	Y	N	N	N	203.72	347.97
Y	N	N	N	Y	N	N	202.68	347.92
Y	N	N	N	N	Y	N	197.71	346.62
Y	N	N	N	N	N	Y	185.07	347.12
N	Y	Y	N	N	N	N	193.05	346.16
N	Y	N	Y	N	N	N	192.71	346.07
N	Y	N	N	Y	N	N	191.67	346.12
N	Y	N	N	N	Y	N	192.94	346.21
N	Y	N	N	N	N	Y	**175.00**	345.67
N	N	Y	Y	N	N	N	203.76	348.19
N	N	Y	N	Y	N	N	202.99	348.53
N	N	Y	N	N	Y	N	198.60	347.02
N	N	Y	N	N	N	Y	186.17	347.60
N	N	N	Y	Y	N	N	202.71	348.12
N	N	N	Y	N	Y	N	198.05	346.87
N	N	N	Y	N	N	Y	185.66	347.37
N	N	N	N	Y	Y	N	197.12	347.00
N	N	N	N	Y	N	Y	184.48	347.56
N	N	N	N	N	Y	Y	179.07	346.27
Y	Y	Y	N	N	N	N	194.67	347.89
Y	Y	N	Y	N	N	N	194.67	347.85
Y	Y	N	N	Y	N	N	193.37	347.83
Y	Y	N	N	N	Y	N	194.59	347.93
Y	Y	N	N	N	N	Y	176.59	347.42
Y	N	Y	Y	N	N	N	205.70	349.94
Y	N	Y	N	Y	N	N	204.09	349.92
Y	N	Y	N	N	Y	N	199.71	348.58
Y	N	Y	N	N	N	Y	187.01	349.10
Y	N	N	Y	Y	N	N	204.65	349.88
Y	N	N	Y	N	Y	N	199.58	348.38

Table S4. Continued

Model Variables							Model AIC Score	
Location	Vegetation presence	Light Treatment	Salinity	O_2 Flux	LAI	%C (0-1 cm)	CH_4	N_2O
Y	N	N	Y	N	N	Y	186.65	348.96
Y	N	N	N	Y	Y	N	198.36	348.53
Y	N	N	N	Y	N	Y	185.48	349.02
Y	N	N	N	N	Y	Y	180.19	347.87
N	Y	Y	Y	N	N	N	195.70	348.03
N	Y	Y	N	Y	N	N	192.59	348.12
N	Y	Y	N	N	Y	N	194.93	348.16
N	Y	Y	N	N	N	Y	176.98	347.63
N	Y	N	Y	Y	N	N	193.41	347.97
N	Y	N	Y	N	Y	N	194.58	348.07
N	Y	N	Y	N	N	Y	176.92	347.58
N	Y	N	N	Y	Y	N	193.59	348.12
N	Y	N	N	Y	N	Y	174.98	347.58
N	Y	N	N	N	Y	Y	177.00	347.67
N	N	Y	Y	Y	N	N	204.14	350.12
N	N	Y	Y	N	Y	N	200.04	348.83
N	N	Y	Y	N	N	Y	187.60	349.35
N	N	Y	N	Y	Y	N	198.03	349.00
N	N	Y	N	Y	N	Y	185.65	349.56
N	N	Y	N	N	Y	Y	181.05	348.23
N	N	N	Y	Y	Y	N	198.68	348.80
N	N	N	Y	Y	N	Y	186.04	349.27
N	N	N	Y	N	Y	Y	180.91	348.15
N	N	N	N	Y	Y	Y	178.90	348.21
Y	Y	Y	Y	N	N	N	196.67	349.80
Y	Y	Y	N	Y	N	N	194.39	349.82
Y	Y	Y	N	N	Y	N	196.59	349.89
Y	Y	Y	N	N	N	Y	178.57	349.38
Y	Y	N	Y	Y	N	N	195.37	348.74
Y	Y	N	Y	N	Y	N	196.57	349.83
Y	Y	N	Y	N	N	Y	177.97	349.23
Y	Y	N	N	Y	Y	N	195.32	349.82
Y	Y	N	N	Y	N	Y	176.67	349.30
Y	Y	N	N	N	Y	Y	178.58	349.40
Y	N	Y	Y	Y	N	N	206.08	351.88
Y	N	Y	Y	N	Y	N	201.59	350.33
Y	N	Y	Y	N	N	Y	188.61	350.93
Y	N	Y	N	Y	Y	N	199.42	350.53

Table S4. Continued

Model Variables							Model AIC Score	
Location	Vegetation presence	Light Treatment	Salinity	O_2 Flux	LAI	%C (0-1 cm)	CH_4	N_2O
Y	N	Y	N	Y	N	Y	186.79	351.01
Y	N	Y	N	N	Y	Y	182.15	349.84
Y	N	N	Y	Y	Y	N	200.21	350.30
Y	N	N	Y	Y	N	Y	187.00	350.86
Y	N	N	Y	N	Y	Y	180.54	349.45
Y	N	N	N	Y	Y	Y	180.16	349.78
N	Y	Y	Y	Y	N	N	194.44	349.97
N	Y	Y	Y	N	Y	N	196.58	350.03
N	Y	Y	Y	N	N	Y	178.89	349.54
N	Y	Y	N	Y	Y	N	194.54	350.12
N	Y	Y	N	Y	N	Y	175.74	349.58
N	Y	Y	N	N	Y	Y	178.98	349.62
N	Y	N	Y	Y	Y	N	195.32	349.97
N	Y	N	Y	Y	N	Y	176.94	349.48
N	Y	N	Y	N	Y	Y	178.91	349.58
N	Y	N	N	Y	Y	Y	176.96	349.58
N	N	Y	Y	Y	Y	N	199.73	350.80
N	N	Y	Y	Y	N	Y	187.33	351.27
N	N	Y	Y	N	Y	Y	182.88	350.12
N	N	Y	N	Y	Y	Y	179.62	350.20
N	N	N	Y	Y	Y	Y	180.81	350.07
Y	Y	Y	Y	Y	N	N	196.39	351.74
Y	Y	Y	Y	N	Y	N	198.57	351.78
Y	Y	Y	Y	N	N	Y	179.96	351.18
Y	Y	Y	N	Y	Y	N	196.35	351.82
Y	Y	Y	N	Y	N	Y	177.53	351.30
Y	Y	N	Y	Y	Y	N	197.31	351.73
Y	Y	N	Y	Y	N	Y	177.96	351.12
Y	Y	N	Y	N	Y	Y	197.82	351.16
Y	Y	N	N	Y	Y	Y	178.63	351.29
Y	N	Y	Y	Y	Y	N	201.19	352.30
Y	N	Y	Y	Y	N	Y	188.22	352.86
Y	N	Y	Y	N	Y	Y	182.53	351.40
Y	N	Y	N	Y	Y	Y	181.03	351.78
N	Y	Y	Y	Y	Y	N	196.38	351.97
N	Y	Y	Y	Y	N	Y	177.73	351.48
N	Y	Y	Y	N	Y	Y	180.89	351.54
N	Y	Y	N	Y	Y	Y	177.70	351.58
N	Y	N	Y	Y	Y	Y	178.92	351.47

Table S2.4. Continued

Model Variables							Model AIC Score	
Location	Vegetation presence	Light Treatment	Salinity	O_2 Flux	LAI	%C (0-1 cm)	CH_4	N_2O
N	N	Y	Y	Y	Y	Y	181.59	352.07
Y	Y	Y	Y	Y	Y	N	198.35	353.73
Y	Y	Y	Y	Y	N	Y	178.66	353.12
Y	Y	Y	Y	N	Y	Y	181.81	353.11
Y	Y	Y	N	Y	Y	Y	179.47	353.29
Y	Y	N	Y	Y	Y	Y	179.73	353.06
Y	N	Y	Y	Y	Y	Y	180.86	353.37
N	Y	Y	Y	Y	Y	Y	179.69	353.47
Y	Y	Y	Y	Y	Y	Y	180.33	355.06

Table S2.5. P-value estimates of pairwise comparisons of sediment-water interface CH_4 and N_2O fluxes derived from the least-square means tests of models of vegetation presence.

Vegetation Presence	CH_4	N_2O
Vegetated - Non-vegetated	**<0.001**	0.752

Table S2.6. P-value estimates of pairwise comparisons of sediment-water interface CH_4 and N_2O fluxes derived from the least-square means tests of models of light treatment.

Light Treatment	CH_4	N_2O
Light-Dark	0.648	0.712

Table S2.7. P-value estimates of pairwise comparisons of sediment-water interface CH_4 and N_2O fluxes derived from the least-square means tests of models of sampling locations.

Location	CH_4	N_2O
East Harbor - Pleasant Bay	0.110	0.617

Table S2.8. Mean, standard error (SE), degrees of freedom, t ratio, and p-value of comparisons of sediment-water interface CH_4 fluxes from the least-square means tests of models of vegetation presence by location.

contrast	**mean**	**SE**	**df**	**t ratio**	**p-value**
Ctrl EH - Seagrass EH	-0.0217	0.551	64	-0.039	1
Ctrl EH - Ctrl PB	0.8338	0.525	64	1.587	0.393
Ctrl EH - Seagrass PB	-2.4948	0.533	64	-4.682	0.0001
Seagrass EH - Ctrl PB	0.8555	0.551	64	1.553	0.4126
Seagrass EH - Seagrass PB	-2.4731	0.558	64	-4.431	0.0002
Ctrl PB - Seagrass PB	-3.3286	0.533	64	-6.246	<.0001

Supplementary Figures

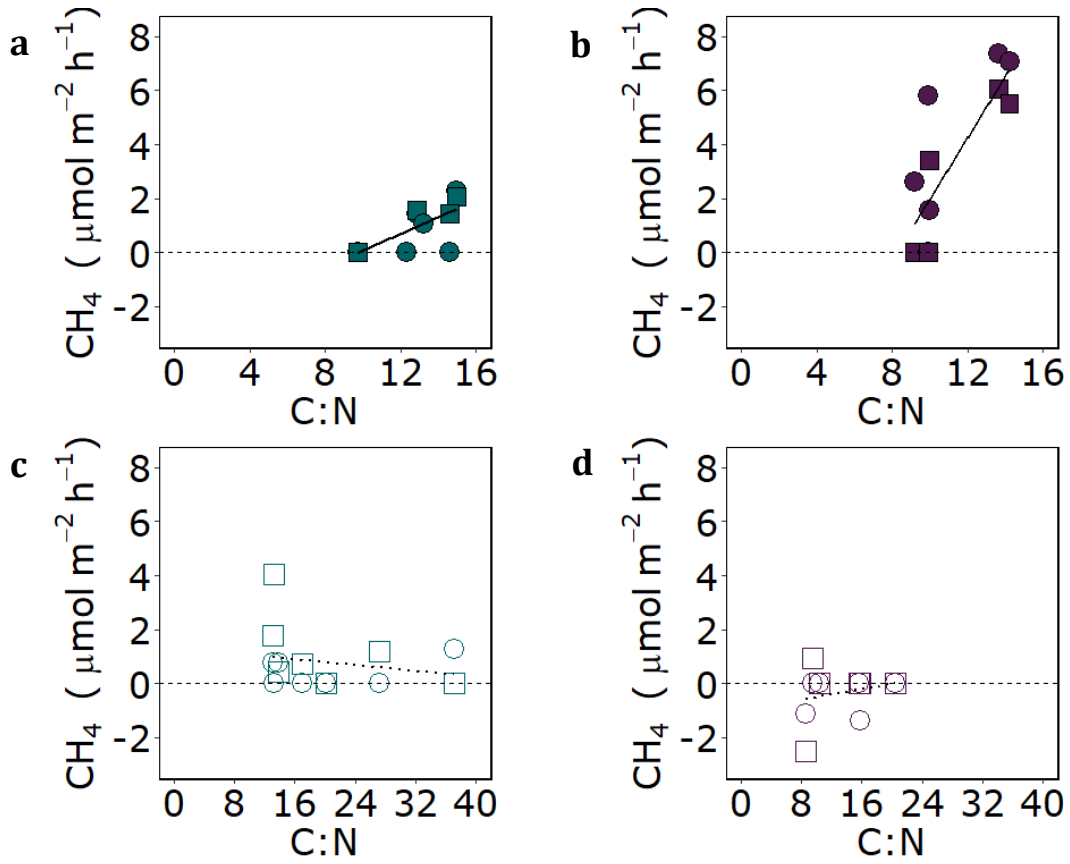

Figure S2.1 Sediment-water column methane (CH_4) flux as a function of C:N in the surface (top 0-1 cm) sediments from eelgrass vegetated sediments (a,b) and non-vegetated sediments (b,c) in East Harbor (a,c) and Pleasant Bay (b,d) over light (square) and dark (circle) incubations. Positive fluxes indicate emission into the water column while negative fluxes indicate uptake by the sediment. There is a positive relationship between CH_4 flux and C:N in vegetated sediments of Pleasant Bay (solid line, $y = 1.14x - 9.39$, $R^2 = 0.60$, $p = 0.002$) and East Harbor (solid line, $y = 0.34x - 3.43$, $R^2 = 0.50$, $p = 0.009$). There is no relation between CH_4 flux and C:N in non-vegetated sediments of Pleasant Bay and East Harbor (dotted line, $R^2 = -0.04$, $p = 0.45$; $R^2 = -0.03$, $p = 0.47$, respectively).

Appendix 3: Supplementary Information for Chapter 3: Fluxes of dissolved inorganic carbon, nitrogen, and phosphorus are highly variable in *Z. marina* meadows

S3.1. *In situ* benthic chamber description

Stainless steel collars (20 cm in diameter, 5 cm deep) were placed into vegetated and non-vegetated sediments approximately 24 hours before making flux measurements (See Chapter 2). A plexiglass chamber (20 cm in diameter, 31.1 cm in height) was fastened to the rubber gasket on top of the collar before sampling. Each chamber was outfitted with an opaque jacket. Then the cylinders were closed at the other end flat plexiglass cap. The cap was also outfitted with opaque "blackout" fabric for dark measurements to keep the light out. We used Aqua Shield marine lubricant to ensure seals were gas- and water-tight. Water was mixed with an aquarium pump inside of the chamber and water was replaced during sampling by an attached bag that we filled with site water at the beginning of the dark incubation. To begin the light incubation following the dark incubation, we removed the opaque jacket. Over the course of the entire dark then light incubation period approximately 1100 mL was removed, or ~10% of the overlying water volume.

Table S3.1. Correlation table of environmental variables. Correlation coefficients (r) for Pearson correlations between salinity, temperature (Temp), oxygen concentration ($[O_2]$), ammonium concentration ($[NH_4^+]$), nitrite concentration ($[NO_2^-]$), nitrite + nitrate concentration ($[NO_x]$), dissolved inorganic phosphorus concentration ([DIP]), nitrate concentration ($[NO_3^-]$), dissolved inorganic nitrogen concentration ([DIN]), seagrass density (density), leaf area index (LAI), sediment percent nitrogen (%N) from 0-1, 1-2, 2-3, and 3-4 cm depth, sediment percent carbon (%C) from 0-1, 1-2, 2-3, and 3-4 cm depth, molar carbon to nitrogen ratio (C:N) 0-1, 1-2, 2-3, and 3-4 cm depth, and nutrient pollution index (see Chapter 2 methods for description of how this was calculated). Bold correlation coefficients have a p-value < 0.05.

	Salinity	Temp	[O2]	[NH4+]	[NO2-]	[NOx]	[DIP]	Density	LAI	%N (0-1)	%N (1-2)	%N (2-3)	%N (3-4)	%C (0-1)	%C (1-2)	%C (2-3)	%C (3-4)	C:N (0-1)	C:N (1-2)	C:N (2-3)	C:N (3-4)	NPI
Salinity		**-0.42**	**-0.40**	**0.41**	0.08	**0.37**	**0.60**	0.18	0.13	**0.36**	**0.53**	**0.49**	**0.49**	0.10	**0.41**	0.19	**0.38**	-0.27	-0.20	**-0.58**	**-0.39**	0.06
Temp	**-0.42**		0.07	-0.10	-0.02	-0.23	-0.09	-0.20	-0.21	**-0.45**	**-0.47**	**-0.44**	**-0.45**	-0.14	-0.27	**-0.30**	**-0.32**	**0.40**	**0.35**	0.20	**0.34**	-0.31
[O2]	**-0.40**	0.07		**-0.59**	**-0.33**	**-0.30**	**-0.62**	**-0.47**	-0.18	-0.22	-0.09	-0.10	-0.05	**-0.31**	-0.12	-0.13	-0.07	-0.17	-0.11	-0.11	-0.15	0.19
[NH4+]	**0.41**	-0.10	**-0.59**		**0.64**	**0.58**	**0.88**	**0.36**	-0.04	**0.53**	**0.42**	**0.30**	0.21	**0.48**	0.22	0.17	0.09	-0.12	-0.21	-0.18	-0.19	**0.45**
[NO2-]	0.08	-0.02	**-0.33**	**0.64**		**0.63**	**0.55**	0.02	**-0.38**	-0.22	**-0.30**	-0.16	-0.22	**-0.35**	**-0.49**	0.06	**-0.39**	**-0.32**	-0.27	**0.37**	-0.12	0.12
[NOx]	**0.37**	-0.23	**-0.30**	**0.58**	**0.63**		**0.44**	0.01	-0.20	0.04	0.01	0.10	-0.03	-0.11	-0.10	0.14	-0.21	-0.22	-0.26	0.00	-0.27	-0.03
[DIP]	**0.60**	-0.09	**-0.62**	**0.88**	**0.55**	**0.44**		**0.37**	0.02	**0.46**	**0.55**	**0.44**	**0.45**	0.24	**0.29**	0.20	**0.36**	-0.28	**-0.30**	**-0.42**	**-0.31**	0.27
Density	0.18	-0.20	**-0.47**	**0.36**	0.02	0.01	**0.37**		**0.77**	**0.42**	**0.52**	**0.46**	**0.48**	0.13	**0.38**	0.22	**0.46**	**-0.37**	-0.28	**-0.29**	-0.25	-0.39
LAI	0.13	-0.21	-0.18	-0.04	**-0.38**	-0.20	0.02	**0.77**		**0.32**	**0.50**	**0.44**	**0.57**	0.06	**0.42**	**0.34**	**0.47**	**-0.33**	-0.23	**-0.32**	**-0.31**	**-0.71**
%N (0-1 cm)	**0.36**	**-0.45**	-0.22	**0.53**	-0.22	0.04	**0.46**	**0.42**	**0.32**		**0.75**	**0.66**	**0.62**	**0.77**	**0.73**	**0.49**	**0.68**	-0.23	-0.01	-0.11	0.00	0.37
%N (1-2 cm)	**0.53**	**-0.47**	-0.09	**0.42**	**-0.30**	0.01	**0.55**	**0.52**	**0.50**	**0.75**		**0.83**	**0.76**	**0.45**	**0.80**	**0.54**	**0.65**	**-0.37**	**-0.34**	**-0.51**	**-0.45**	**0.48**
%N (2-3 cm)	**0.49**	**-0.44**	-0.10	**0.30**	-0.16	0.10	**0.44**	**0.46**	**0.44**	**0.66**	**0.83**		**0.75**	0.27	**0.68**	**0.85**	**0.66**	**-0.43**	-0.26	**-0.44**	**-0.39**	0.16
%N (3-4 cm)	**0.49**	**-0.45**	-0.05	0.21	-0.22	-0.03	**0.45**	**0.48**	**0.57**	**0.62**	**0.76**	**0.75**		0.21	**0.65**	**0.48**	**0.89**	**-0.45**	-0.24	**-0.45**	**-0.55**	0.00
%C (0-1 cm)	0.10	-0.14	**-0.31**	**0.48**	**-0.35**	-0.11	0.24	0.13	0.06	**0.77**	**0.45**	0.27	0.21		**0.59**	0.24	**0.36**	**0.40**	**0.29**	0.16	**0.31**	**0.50**
%C (1-2 cm)	**0.41**	-0.27	-0.12	0.22	**-0.49**	-0.10	**0.29**	**0.38**	**0.42**	**0.73**	**0.80**	**0.68**	**0.65**	**0.59**		**0.48**	**0.71**	-0.07	0.23	-0.23	-0.07	0.28
%C (2-3 cm)	0.19	**-0.30**	-0.13	0.17	0.06	0.14	0.20	0.22	**0.34**	**0.49**	**0.54**	**0.85**	**0.48**	0.24	**0.48**		**0.44**	-0.26	-0.05	0.00	-0.10	0.12
%C (3-4 cm)	**0.38**	**-0.32**	-0.07	0.09	**-0.39**	-0.21	**0.36**	**0.46**	**0.47**	**0.68**	**0.65**	**0.66**	**0.89**	**0.36**	**0.71**	**0.44**		-0.28	0.02	**-0.29**	-0.20	-0.01
C:N (0-1 cm)	-0.27	**0.40**	-0.17	-0.12	**-0.32**	-0.22	-0.28	**-0.37**	**-0.33**	-0.23	**-0.37**	**-0.43**	**-0.45**	**0.40**	-0.07	-0.26	-0.28		**0.45**	**0.35**	**0.42**	0.16
C:N (1-2 cm)	-0.20	**0.35**	-0.11	-0.21	-0.27	-0.26	**-0.30**	-0.28	-0.23	-0.01	**-0.34**	-0.26	-0.24	**0.29**	0.23	-0.05	0.02	**0.45**		**0.59**	**0.75**	-0.31
C:N (2-3 cm)	**-0.58**	0.20	-0.11	-0.18	**0.37**	0.00	**-0.42**	**-0.29**	**-0.32**	-0.11	**-0.51**	**-0.44**	**-0.45**	0.16	-0.23	0.00	**-0.29**	**0.35**	**0.59**		**0.69**	-0.12
C:N (3-4 cm)	**-0.39**	**0.34**	-0.15	-0.19	-0.12	-0.27	**-0.31**	-0.25	**-0.31**	0.00	**-0.45**	**-0.39**	**-0.55**	**0.31**	-0.07	-0.10	-0.20	**0.42**	**0.75**	**0.69**		-0.12
NPI	0.06	-0.31	0.19	**0.45**	0.12	-0.03	0.27	-0.39	**-0.71**	0.37	**0.48**	0.16	0.00	**0.50**	0.28	0.12	-0.01	0.16	-0.31	-0.12	-0.12	

Table S3.2. AIC scores for generalized linear models generated for fluxes across the sediment-water interface of O_2 fluxes, di-nitrogen gas (N_2-N), dissolved inorganic carbon (DIC), and nutrient fluxes (i.e., ammonium (NH_4^+), nitrite (NO_2^-), nitrite + nitrate (NO_x), dissolved inorganic phosphorus (DIP)). All variables were fixed effects. Bold AICs indicate the best model for the flux type.

	Model AIC Values						
Model	**O_2**	**N_2-N**	**DIC**	**NH_4^+**	**NO_2^-**	**NO_x**	**DIP**
Location	1350.502	1254.826	475.844	829.259	**421.611**	**520.281**	676.891
Vegetation	1350.477	1256.059	475.590	851.279	423.408	526.470	688.206
Light	**1297.469**	**1253.761**	468.061	849.328	422.066	526.359	692.428
Temperature	1347.739	1255.974	473.587	846.920	423.029	525.555	692.402
$[O_2]$	1340.640	1255.584	473.318	848.795	424.074	525.988	668.230
Location + Vegetation	1352.439	1256.417	477.589	825.604	422.919	521.607	673.619
Location + Light	1299.151	1254.100	470.054	823.347	421.378	521.622	678.209
Location + Temperature	1349.403	1254.546	475.021	829.868	423.464	522.262	677.647
Location + $[O_2]$	1340.801	1256.491	474.976	828.667	423.332	522.219	**662.002**
Vegetation + Light	1299.443	1255.132	469.898	847.286	423.514	527.658	689.907
Vegetation + Temperature	1349.725	1257.430	475.167	845.357	424.472	527.071	689.925
Vegetation + $[O_2]$	1341.902	1257.328	474.668	848.161	425.393	527.600	669.606
Light + Temperature	1298.310	1255.505	**465.795**	844.854	423.474	526.285	694.110
Light + $[O_2]$	1298.099	1255.623	469.663	841.548	423.729	527.738	667.802
Temperature + $[O_2]$	1338.758	1256.963	473.206	839.198	425.029	526.509	667.835
Location + Vegetation + Light	1301.120	1255.490	471.892	820.480	422.808	522.855	675.070
Location + Vegetation + Temperature	1351.390	1255.848	476.572	827.394	424.819	523.603	672.919
Location + Vegetation + $[O_2]$	1341.971	1258.186	476.280	826.773	424.451	523.595	663.123
Location + Light + Temperature	1300.300	1254.454	466.579	824.984	423.377	523.510	678.364
Location + Light + $[O_2]$	1299.036	1256.097	471.562	820.343	423.377	523.618	661.224
Location + Temperature + $[O_2]$	1340.437	1256.342	473.331	827.339	425.232	524.190	663.788
Vegetation + Light + Temperature	1300.250	1256.782	467.447	842.938	424.988	527.714	691.696
Vegetation + Light + $[O_2]$	1300.090	1257.087	471.363	841.895	425.318	529.253	669.354
Vegetation + Temperature + $[O_2]$	1340.225	1258.613	474.322	840.626	426.452	528.215	669.679
Light + Temperature + $[O_2]$	1298.571	1257.309	467.626	829.325	425.222	527.869	667.388
Location + Vegetation + Light + Temperature	1302.240	1255.579	468.195	822.412	424.808	524.780	673.899
Location + Vegetation + Light + $[O_2]$	1301.017	1257.436	473.240	819.836	424.793	524.789	662.567
Location + Vegetation + Temperature + $[O_2]$	1341.839	1257.753	474.169	827.704	426.404	525.588	665.105
Location + Light + Temperature + $[O_2]$	1300.258	1256.444	467.903	**817.623**	425.375	525.508	663.065
Vegetation + Light + Temperature + $[O_2]$	1300.570	1258.702	469.155	830.883	426.848	529.454	669.277
Location + Vegetation + Light + Temperature + $[O_2]$	1302.253	1257.481	469.228	818.797	426.793	526.722	664.530

BIBLIOGRAPHY

List of Abbreviated Journal Titles

Aquat. Bot.	Aquatic Botany
Biogeochem.	Biogeochemistry
Biol. Bull.	The Biological Bulletin
Biol. Fertil. Soils	Biology and Fertility of Soils
Biol. Lett.	Biology Letters
Commun. Earth Environ.	Communications Earth & Environment
Curr. Biol.	Current Biology
Ecol. Eng.	Ecological Engineering
Environ. Microbiol.	Environmental Microbiology
Environ. Sci. Technol.	Environmental Science and Technology
Estuar. Coast. Shelf Sci.	Estuarine, Coastal and Shelf Science
Front. Ecol. Environ.	Frontiers in Ecology and the Environment
Front. Mar. Sci.	Frontiers in Marine Science
Front. Microbiol.	Frontiers in Microbiology
Geochim. Cosmochim. Acta	Geochimica et Cosmochimica Acta
Global Biogeochem. Cycles	Global Biogeochemical Cycles
Glob. Chang. Biol	Global Change Biology
J. Chem. Eng. Data	Journal of Chemical & Engineering Data
J. Ecol.	Journal of Ecology
J. Geophys. Res.	Journal of Geophysical Research
J. Geophys. Res. Atmos.	Journal of Geophysical Research: Atmospheres
J. Geophys. Res. Biogeosciences	Journal of Geophysical Research: Biogeosciences
J. Geophys. Res. Ocean.	Journal of Geophysical Research: Oceans
J. Stat. Softw.	Journal of Statistical Software
Limnol. Oceanogr.	Limnology and Oceanography
Limnol. Oceanogr. Methods	Limnology and Oceanography: Methods
Mar. Chem.	Marine Chemistry
Mar Ecol Prog Ser	Marine Ecology Progress Series
Nat. Commun.	Nature Communications
Nat. Geosci.	Nature Geoscience
New Phytol.	New Phytologist
Northeast. Nat.	Northeastern Naturalist
Proc. Coast. Sediments	The Proceedings of the Coastal Sediments
Proc. Natl. Acad. Sci.	Proceedings of the National Academy of Sciences of the United States of America
Sci. Total Environ.	Science of the Total Environment
Sci. Rep.	Scientific Reports

Adams, C. A., Andrews, J. E., & Jickells, T. (2012). Nitrous oxide and methane fluxes vs. carbon, nitrogen and phosphorous burial in new intertidal and saltmarsh sediments. *Science of the Total Environment*, *434*, 240–251. https://doi.org/10.1016/j.scitotenv.2011.11.058

Al-Haj, A. N., and R. W. Fulweiler. 2020. A synthesis of methane emissions from shallow vegetated coastal ecosystems. Glob. Chang. Biol. **26**: 2988–3005. doi:10.1111/gcb.15046

Allen, D., Dalal, R. C., Rennenberg, H., & Schmidt, S. (2011). Seasonal variation in nitrous oxide and methane emissions from subtropical estuary and coastal mangrove sediments, Australia. *Plant Biology*, *13*(1), 126–133. https://doi.org/10.1111/j.1438-8677.2010.00331.x

Almazroui, M., Nazrul Islam, M., Athar, H., Jones, P. D., & Rahman, M. A. (2012). Recent climate change in the Arabian Peninsula: annual rainfall and temperature analysis of Saudi Arabia for 1978-2009. *International Journal of Climatology*, *32*(6), 953–966. https://doi.org/10.1002/joc.3446

Alongi, D. M. (2002). Present state and future of the world's mangrove forests. *Environmental Conservation*, *29*(3), 331–349. https://doi.org/10.1017/S0376892902000231

Alongi, D. M. (2008). *Carbon Cycling and Storage in Mangrove Forests*. https://doi.org/10.1146/annurev-marine-010213-135020

Alongi, D. M., Trott, L. A., Rachmansyah, Tirendi, F., McKinnon, A. D., & Undu, M. C. (2008). Growth and development of mangrove forests overlying smothered coral reefs, Sulawesi and Sumatra, Indonesia. *Marine Ecology Progress Series*, *370*, 97–109. https://doi.org/10.3354/meps07661

Amorocho, J., and J. J. DeVries. 1980. A new evaluation of the wind stress coefficient over water surfaces. J. Geophys. Res. Ocean. **85**: 433–442. doi:10.1029/JC085IC01P00433

Aoki, L., and K. McGlathery. 2018. Restoration enhances denitrification and DNRA in subsurface sediments of Zostera marina seagrass meadows. Mar. Ecol. Prog. Ser. **602**: 87–102. doi:10.3354/meps12678

Aoki, L. R., K. J. McGlathery, and M. P. J. Oreska. 2020. Seagrass restoration reestablishes the coastal nitrogen filter through enhanced burial. Limnol. Oceanogr. **65**: 1–12. doi:10.1002/lno.11241

Apostolaki, E. T., M. Holmer, N. Marbà, and I. Karakassis. 2010. Degrading seagrass (Posidonia oceanica) ecosystems: A source of dissolved matter in the Mediterranean. Hydrobiologia **649**: 13–23. doi:10.1007/S10750-010-0255-2/FIGURES/6

Arndt, S., B. B. Jørgensen, D. E. LaRowe, J. J. Middelburg, R. D. Pancost, and P. Regnier. 2013. Quantifying the degradation of organic matter in marine sediments: A review and synthesis. Earth-Science Rev. **123**: 53–86. doi:10.1016/j.earscirev.2013.02.008

Ashford, O. S., S. Guan, D. Capone, and others. 2021. A chemosynthetic ecotone—"chemotone"—in the sediments surrounding deep-sea methane seeps. Limnol. Oceanogr. **66**: 1687–1702. doi:10.1002/LNO.11713

Atkinson, L. P., & Hall, J. R. (1976). Methane Distribution and Production in Georgia Salt-Marsh. *Estuarine and Coastal Marine Science*, *4*(6), 677–686. https://doi.org/10.1016/0302-3524(76)90074-8

Aubinet, M., Vesala, T., & Papale, D. (2012). *Eddy Covariance: A Practical Guide to Measurement and Data Analysis*. Springer.

Bahlmann, E., Weinberg, I., Lavrič, J. V., Eckhardt, T., Michaelis, W., Santos, R., & Seifert, R. (2015). Tidal controls on trace gas dynamics in a seagrass meadow of the Ria Formosa lagoon (southern Portugal). *Biogeosciences*, *12*(6), 1683–1696. https://doi.org/10.5194/bg-12-1683-2015

Banerjee, K., Paneerselvam, A., Ramachandran, P., Ganguly, D., Singh, G., & Ramesh, R. (2018). Seagrass and macrophyte mediated CO2 and CH4 dynamics in shallow coastal waters. *PLoS ONE*, *13*(10), 1–22. https://doi.org/10.1371/journal.pone.0203922

Bange, H. W., Bergmann, K., Hansen, H. P., Kock, A., Koppe, R., Malien, F., & Ostrau, C. (2010). Dissolved methane during hypoxic events at the Boknis Eck time series station (Eckernförde Bay, SW Baltic Sea). *Biogeosciences*, *7*(4), 1279–1284. https://doi.org/10.5194/bg-7-1279-2010

Banta, G. T., Giblin, A. E., Hobbie, J. E., & Tucker, J. (1995). Benthic respiration and nitrogen release in Buzzards Bay, Massachusetts. *Journal of Marine Research*, *53*, 107–135. https://doi.org/10.1357/0022240953213287

Barbier, E. B., Hacker, S. D., Kennedy, C., Koch, E. W., Stier, A. C., & Silliman, B. R. (2011). The value of estuarine and coastal ecosystem services. *Ecological Monographs*, *81*(2), 169–193. https://doi.org/10.1890/10-1510.1

Barrón, C., C. M. Duarte, M. Frankignoulle, and A. V. Borges. 2006. Organic carbon metabolism and carbonate dynamics in a Mediterranean seagrass (Posidonia oceanica), meadow. Estuaries Coasts 2006 293 **29**: 417–426. doi:10.1007/BF02784990

Barrón, C., N. Marbé, J. Terrados, H. Kennedy, and C. M. Duarte. 2004. Community metabolism and carbon budget along a gradient of seagrass (*Cymodocea nodosa*) colonization. Limnol. Oceanogr. **49**: 1642–1651. doi:10.4319/lo.2004.49.5.1642

Bartlett, K. B., Bartlett, D. S., Harriss, R. C., & Sebacher, D. I. (1987). Methane Emissions along a Salt Marsh Salinity Gradient. *Biogeochemistry*, Vol. 4, pp. 183–202. https://doi.org/10.2307/1468663

Bartlett, K. B., & Harriss, R. C. (1993). Review and assessment of methane emissions from wetlands. *Chemosphere*, *26*(1–4), 261–320. https://doi.org/10.1016/0045-6535(93)90427-7

Bartlett, K. B., R. C. Harriss, and D. I. Sebacher. 1985. Methane flux form coastal salt marshes. J. Geophys. Res. **90**: 5710–5720. doi:10.1029/JD090iD03p05710

Bastviken, D., J. Cole, M. Pace, and L. Tranvik. 2004. Methane emissions from lakes: Dependence of lake characteristics, two regional assessments, and a global estimate. Global Biogeochem. Cycles **18**: 1–12. doi:10.1029/2004GB002238

Bates, D. ;, M. ; Mächler, B. ; Bolker, and S. Walker. 2015. Fitting Linear Mixed-Effects Models Using lme4.doi:10.3929/ethz-b-000105397

Benway, H. M., Alin, S. R., Boyer, E., Cai, W.-J., Coble, P. G., Cross, J. N., … Smith, R. A. (2016). *A science plan for carbon cycle research in North American coastal waters. Report of the Coastal CARbon Synthesis (CCARS) community workshop, August 19-21, 2014*. https://doi.org/10.1575/1912/7777

Berg, P., M. L. Delgard, P. Polsenaere, K. J. McGlathery, S. C. Doney, and A. C. Berger. 2019. Dynamics of benthic metabolism, O2, and pCO2 in a temperate seagrass meadow. Limnol. Oceanogr. **64**: 2586–2604. doi:10.1002/LNO.11236

Biswas, H., Mukhopadhyay, S. K., Sen, S., & Jana, T. K. (2007). Spatial and temporal patterns of methane dynamics in the tropical mangrove dominated estuary, NE coast of Bay of Bengal, India. *Journal of Marine Systems*, *68*(1–2), 55–64. https://doi.org/10.1016/j.jmarsys.2006.11.001

Bižić-Ionescu, M., D. Ionescu, M. Günthel, K. W. Tang, and H.-P. Grossart. 2018. Oxic Methane Cycling: New Evidence for Methane Formation in Oxic Lake Water.doi:10.1007/978-3-319-53114-4_10-1

Blaabjerg, V., & Finster, K. (1998). Sulphate reduction associated with roots and rhizomes of the marine macrophyte Zostera marina. *Aquatic Microbial Ecology*, *15*(3), 311–314. https://doi.org/10.3354/ame015311

Borges, A. V., J. P. Vanderborght, L. S. Schiettecatte, F. Gazeau, S. Ferrón-Smith, B. Delille, and M. Frankignoulle. 2004. Variability of the gas transfer velocity of CO2 in a macrotidal estuary (the Scheldt). Estuaries **27**: 593–603. doi:10.1007/BF02907647

Borrelli, M. 2009. 37 YEARS OF SHORELINE CHANGE IN PLEASANT BAY: 1868 TO 2005 A Report Prepared for the Pleasant Bay Resource Management Alliance.

Borrelli, M., B. A. Oakley, J. B. Hubeny, H. Love, T. L. Smith, B. J. Legare, and T. Lucas. 2020. The Use of Multimodal Data to Augment Shallow-Water Benthic Habitat Maps for Pleasant Bay, Cape Cod, Massachusetts: Stratigraphic Data and Seafloor Maps. Northeast. Nat. **27**: 48–75. doi:10.1656/045.027.S1003

Borum, J., K. Sand-Jensen, T. Binzer, O. Pedersen, and T. M. Greve. 2007. Oxygen Movement in Seagrasses. Seagrasses Biol. Ecol. Conserv. 255–270. doi:10.1007/978-1-4020-2983-7_10

Boyle, R. A., T. W. Dahl, A. W. Dale, G. A. Shields-Zhou, M. Zhu, M. D. Brasier, D. E. Canfield, and T. M. Lenton. 2014. Stabilization of the coupled oxygen and phosphorus cycles by the evolution of bioturbation. Nat. Geosci. **7**: 671–676. doi:10.1038/ngeo2213

Bozdogan, H. 1987. Model selection and Akaike's Information Criterion (AIC): The general theory and its analytical extensions. Psychometrika **52**: 345–370. doi:10.1007/BF02294361

Breitburg, D., Levin, L. A., Oschlies, A., Grégoire, M., Chavez, F. P., Conley, D. J., … Zhang, J. (2018). Declining oxygen in the global ocean and coastal waters. *Science (New York, N.Y.)*, *359*(6371), eaam7240. https://doi.org/10.1126/science.aam7240

Bridgham, S. D., Cadillo-Quiroz, H., Keller, J. K., & Zhuang, Q. (2013). Methane emissions from wetlands: biogeochemical, microbial, and modeling perspectives from local to global scales. *Global Change Biology*, *19*(5), 1325–1346. https://doi.org/10.1111/gcb.12131

Burkholder, J. M., Tomasko, D. A., & Touchette, B. W. (2007). Seagrasses and eutrophication. *Journal of Experimental Marine Biology and Ecology*, *350*(1–2), 46–72. https://doi.org/10.1016/J.JEMBE.2007.06.024

Burkholz, C., N. Garcias-Bonet, and C. M. Duarte. 2020. Warming enhances carbon dioxide and methane fluxes from Red Sea seagrass (<i>Halophila

stipulacea</i>) sediments. Biogeosciences **17**: 1717–1730. doi:10.5194/bg-17-1717-2020

Caballero-Alfonso, A. M., Carstensen, J., & Conley, D. J. (2015). Biogeochemical and environmental drivers of coastal hypoxia. *Journal of Marine Systems*, *141*, 190–199. https://doi.org/10.1016/J.JMARSYS.2014.04.008

Cabezas, A., W. J. Mitsch, C. MacDonnell, L. Zhang, F. Bydałek, and A. Lasso. 2018. Methane emissions from mangrove soils in hydrologically disturbed and reference mangrove tidal creeks in southwest Florida. Ecol. Eng. **114**: 57–65. doi:10.1016/j.ecoleng.2017.08.041

Cable, J. E., Bugna, G. C., Burnett, W. C., & Chanton, J. P. (1996). Application of ^{222} Rn and CH_4 for assessment of groundwater discharge to the coastal ocean. *Limnology and Oceanography*, *41*(6), 1347–1353. https://doi.org/10.4319/lo.1996.41.6.1347

Caffrey, J. M., & Kemp, W. M. (1991). Seasonal and spatial patterns of oxygen production, respiration and root-rhizome release in Potamogeton perfoliatus L. and Zostera marina L. *Aquatic Botany*, *40*(2), 109–128. https://doi.org/10.1016/0304-3770(91)90090-R

Cahoon, D. R., Hensel, P., Rybczyk, J., McKee, K. L., Proffitt, C. E., & Perez, B. C. (2003). Mass tree mortality leads to mangrove peat collapse at Bay Islands, Honduras after Hurricane Mitch. *Journal of Ecology*, *91*(6), 1093–1105. https://doi.org/10.1046/j.1365-2745.2003.00841.x

Camillini, N. 2020. Carbon and Nitrogen Cycling in Soil. Ph.D. Thesis, Southern Cross Univ.

Canfield, D. E., E. Kristensen, and B. Thamdrup. 2005. Aquatic Geomicrobiology, 48th ed. A.J. Southward, P.A. Tyler, C.M. Young, and L.A. Fuiman [eds.]. Elsevier.

Carini, S., N. Weston, C. Hopkinson, J. Tucker, A. Giblin, and J. Vallino. 1996. Gas exchange rates in the Parker River estuary, Massachusetts. Biol. Bull. **191**: 333–335.

Carlton, J. M. (1974). Land-building and Stabilization by Mangroves. *Environmental Conservation*, *1*(4), 285–294. https://doi.org/10.1017/S0376892900004926

Cattrijsse, A., & Hampel, H. (2006). European intertidal marshes: a review of their habitat functioning and value for aquatic organisms. *Marine Ecology Progress Series*, *324*, 293–307. https://doi.org/10.3354/meps324293

Cavanaugh, K. C., Dangremond, E. M., Doughty, C. L., Park Williams, A., Parker, J. D., Hayes, M. A., … Feller, I. C. (2019). Climate-driven regime shifts in a mangrove–salt marsh ecotone over the past 250 years. *Proceedings of the National Academy of*

Sciences of the United States of America, *116*(43), 21602–21608. https://doi.org/10.1073/pnas.1902181116

Chauhan, R., Ramanathan, A. L., & Adhya, T. K. (2008). Assessment of methane and nitrous oxide flux from mangroves along Eastern coast of India. *Geofluids*, *8*(4), 321–332. https://doi.org/10.1111/j.1468-8123.2008.00227.x

Chauhan, Rita, Datta, A., Ramanathan, A. L., & Adhya, T. K. (2015). Factors influencing spatio-temporal variation of methane and nitrous oxide emission from a tropical mangrove of eastern coast of India. *Atmospheric Environment*, *107*, 95–106. https://doi.org/10.1016/j.atmosenv.2015.02.006

Chen, G. C., Tam, N. F. Y., Wong, Y. S., & Ye, Y. (2011). Effect of wastewater discharge on greenhouse gas fluxes from mangrove soils. *Atmospheric Environment*, *45*(5), 1110–1115. https://doi.org/10.1016/j.atmosenv.2010.11.034

Chen, Guang C., Ulumuddin, Y. I., Pramudji, S., Chen, S. Y., Chen, B., Ye, Y., … Wang, J. K. (2014). Rich soil carbon and nitrogen but low atmospheric greenhouse gas fluxes from North Sulawesi mangrove swamps in Indonesia. *Science of the Total Environment*, *487*(1), 91–96. https://doi.org/10.1016/j.scitotenv.2014.03.140

Chen, J. J., D. V. Erler, N. S. Wells, J. Huang, D. T. Welsh, and B. D. Eyre. 2020. Denitrification, anammox, and dissimilatory nitrate reduction to ammonium across a mosaic of estuarine benthic habitats. Limnol. Oceanogr. 1–17. doi:10.1002/lno.11681

Cheng, X., Peng, R., Chen, J., Luo, Y., Zhang, Q., An, S., … Li, B. (2007). CH4 and N2O emissions from Spartina alterniflora and Phragmites australis in experimental mesocosms. *Chemosphere*, *68*(3), 420–427. https://doi.org/10.1016/J.CHEMOSPHERE.2007.01.004

Chmura, G. L., Kellman, L., & Guntenspergen, G. R. (2011). The greenhouse gas flux and potential global warming feedbacks of a northern macrotidal and microtidal salt marsh. *Environmental Research Letters*, *6*(4). https://doi.org/10.1088/1748-9326/6/4/044016

Christianen, M. J. A., van Belzen, J., Herman, P. M. J., van Katwijk, M. M., Lamers, L. P. M., van Leent, P. J. M., & Bouma, T. J. (2013). Low-Canopy Seagrass Beds Still Provide Important Coastal Protection Services. *PLoS ONE*, *8*(5), e62413. https://doi.org/10.1371/journal.pone.0062413

Chu, H., Chen, J., Gottgens, J. F., Ouyang, Z., John, R., Czajkowski, K., & Becker, R. (2014). Net ecosystem methane and carbon dioxide exchanges in a Lake Erie coastal marsh and a nearby cropland. *Journal of Geophysical Research: Biogeosciences*, *119*, 722–740. https://doi.org/10.1002/2013JG002520

Chuang, P. C., Young, M. B., Dale, A. W., Miller, L. G., Herrera-Silveira, J. A., & Paytan, A. (2017). Methane fluxes from tropical coastal lagoons surrounded by mangroves, Yucatán, Mexico. *Journal of Geophysical Research: Biogeosciences*, *122*(5), 1156–1174. https://doi.org/10.1002/2017JG003761

Clark, J. F., P. Schlosser, H. J. Simpson, M. Stute, R. Wanninkhof, and D. T. Ho. 1995. Relationship between Gas Transfer Velocities and Wind Speeds in The Tidal Hudson River Determined by the Dual Tracer Technique. *Air-Water Gas Transfer: Selected papers from the third international symposium on air-water gas transfer*. 785–800.

Clark, T. S., and D. A. Linzer. 2015. Should I Use Fixed or Random Effects? Polit. Sci. Res. Methods **3**: 399–408. doi:10.1017/PSRM.2014.32

Cloern, J. E., Abreu, P. C., Carstensen, J., Chauvaud, L., Elmgren, R., Grall, J., … Yin, K. (2016). Human activities and climate variability drive fast-paced change across the world's estuarine-coastal ecosystems. *Global Change Biology*, *22*(2), 513–529. https://doi.org/10.1111/gcb.13059

Coates, C. J., and M. Wyman. 2017. A denitrifying community associated with a major, marine nitrogen fixer. Environ. Microbiol. **19**: 4978–4992. doi:10.1111/1462-2920.14007

Colt, J. 1984. Computation of Dissolved Gas Concentrations in Water as Functions of Temperature, Salinity and Pressure. Am. Fish. Soc. Spec. Publ. 14.

Costa, K. C., & Leigh, J. A. (2014). Metabolic versatility in methanogens. *Current Opinion in Biotechnology*, *29*, 70–75. https://doi.org/10.1016/J.COPBIO.2014.02.012

Cotovicz, L. C., Knoppers, B. A., Brandini, N., Poirier, D., Costa Santos, S. J., & Abril, G. (2016). Spatio-temporal variability of methane (CH4) concentrations and diffusive fluxes from a tropical coastal embayment surrounded by a large urban area (Guanabara Bay, Rio de Janeiro, Brazil). *Limnology and Oceanography*, *61*, S238–S252. https://doi.org/10.1002/lno.10298

Cox, T. E., J. Cebrian, M. Tabor, L. West, and J. W. Krause. 2020. Do diatoms dominate benthic production in shallow systems? A case study from a mixed seagrass bed. Limnol. Oceanogr. Lett. **5**: 425–434. doi:10.1002/LOL2.10167

Cowan, T., Purich, A., Perkins, S., Pezza, A., Boschat, G., Sadler, K., … Sadler, K. (2014). More Frequent, Longer, and Hotter Heat Waves for Australia in the Twenty-First Century. *Journal of Climate*, *27*(15), 5851–5871. https://doi.org/10.1175/JCLI-D-14-00092.1

Cowardin, L. M., Carter, V., Golet, F. C., & LaRoe, E. T. (1979). *Classification of Wetlands and Deepwater Habitats of the United States*. Washington, DC.

Dalsgaard, T., and B. Thamdrup. 2002. Factors controlling anaerobic ammonium oxidation with nitrite in marine sediments. Appl. Environ. Microbiol. **68**: 3802–3808. doi:10.1128/AEM.68.8.3802-3808.2002/ASSET/BCAA6C9D-67E4-413C-B97A-5C6BBF428DB1/ASSETS/GRAPHIC/AM0820362003.JPEG

Davidson, E. A., Ishida, F. Y., & Nepstad, D. C. (2004). Effects of an experimental drought on soil emissions of carbon dioxide, methane, nitrous oxide, and nitric oxide in a moist tropical forest. *Global Change Biology*, *10*(5), 718–730. https://doi.org/10.1111/j.1365-2486.2004.00762.x

Davidson, N. C., & Finlayson, C. M. (2019). Updating global coastal wetland areas presented in Davidson and Finlayson (2018). *Marine and Freshwater Research*. https://doi.org/10.1071/MF19010

Davis, T. R., Harasti, D., Smith, S. D. A., & Kelaher, B. P. (2016). Using modelling to predict impacts of sea level rise and increased turbidity on seagrass distributions in estuarine embayments. *Estuarine, Coastal and Shelf Science*, *181*, 294–301. https://doi.org/10.1016/J.ECSS.2016.09.005

Deborde, J., P. Anschutz, F. Guérin, and others. 2010. Methane sources, sinks and fluxes in a temperate tidal Lagoon: The Arcachon lagoon (SW France). Estuar. Coast. Shelf Sci. **89**: 256–266. doi:10.1016/j.ecss.2010.07.013

Deek, A., K. Dähnke, J. Van Beusekom, S. Meyer, M. Voss, and K. Emeis. 2013. N2 fluxes in sediments of the Elbe Estuary and adjacent coastal zones. Mar. Ecol. Prog. Ser. **493**: 9–21. doi:10.3354/meps10514

Deemer, B. R., and M. A. Holgerson. 2021. Drivers of Methane Flux Differ Between Lakes and Reservoirs, Complicating Global Upscaling Efforts. J. Geophys. Res. Biogeosciences **126**: e2019JG005600. doi:10.1029/2019JG005600

DeLaune, R. D., C. J. Smith, and W. H. Patrick. 1983. Methane release from Gulf coast wetlands. Tellus B **35 B**: 8–15. doi:10.1111/j.1600-0889.1983.tb00002.x

Delgard, M. L., B. Deflandre, E. Kochoni, J. Avaro, F. Cesbron, S. Bichon, D. Poirier, and P. Anschutz. 2016. Biogeochemistry of dissolved inorganic carbon and nutrients in seagrass (Zostera noltei) sediments at high and low biomass. Estuar. Coast. Shelf Sci. **179**: 12–22. doi:10.1016/j.ecss.2016.01.012

Delignette-Muller, M. L., and C. Dutang. 2015. fitdistrplus: An R package for fitting distributions. J. Stat. Softw. **64**: 1–34. doi:10.18637/jss.v064.i04

Descloux, S., V. Chanudet, D. Serça, and F. Guérin. 2017. Methane and nitrous oxide annual emissions from an old eutrophic temperate reservoir. Sci. Total Environ. **598**: 959–972. doi:10.1016/J.SCITOTENV.2017.04.066

Diaz-Valbuena, L. R., H. L. Leverenz, C. D. Cappa, G. Tchobanoglous, W. R. Horwath, and J. L. Darby. 2011. Methane, Carbon Dioxide, and Nitrous Oxide Emissions from Septic Tank Systems. Environ. Sci. Technol. **45**: 2741–2747. doi:10.1021/ES1036095

Diefenderfer, H. L., Cullinan, V. I., Borde, A. B., Gunn, C. M., & Thom, R. M. (2018). High-frequency greenhouse gas flux measurement system detects winter storm surge effects on salt marsh. *Global Change Biology*, *24*(12), 5961–5971. https://doi.org/10.1111/gcb.14430

Dlugokencky, E. J., Nisbet, E. G., Fisher, R., & Lowry, D. (2011). Global atmospheric methane: budget, changes and dangers. *Philosophical Transactions of the Royal Society A: Mathematical, Physical and Engineering Sciences*, *369*(1943), 2058–2072. https://doi.org/10.1098/rsta.2010.0341

Dole, R., Hoerling, M., Kumar, A., Eischeid, J., Perlwitz, J., Quan, X.-W., … Zhang, T. (2014). The Making of an Extreme Event: Putting the Pieces Together. *Bulletin of the American Meteorological Society*, *95*(3), 427–440. https://doi.org/10.1175/BAMS-D-12-00069.1

Doughty, C. L., Langley, J. A., Walker, W. S., Feller, I. C., Schaub, R., & Chapman, S. K. (2016). Mangrove Range Expansion Rapidly Increases Coastal Wetland Carbon Storage. *Estuaries and Coasts*, *39*(2), 385–396. https://doi.org/10.1007/s12237-015-9993-8

Dowrick, D. J., Freeman, C., Lock, M. A., & Reynolds, B. (2006). Sulphate reduction and the suppression of peatland methane emissions following summer drought. *Geoderma*. https://doi.org/10.1016/j.geoderma.2005.06.003

Duarte, C M, Middelburg, J. J., & Caraco, N. (2005). Major role of marine vegetation on the oceanic carbon cycle. In *Biogeosciences* (Vol. 2).

Duarte, C. M., N. Marbà, E. Gacia, J. W. Fourqurean, J. Beggins, C. Barrón, and E. T. Apostolaki. 2010. Seagrass community metabolism: Assessing the carbon sink capacity of seagrass meadows. Global Biogeochem. Cycles **24**: 1–8. doi:10.1029/2010GB003793

Duarte, Carlos M. (2017). Reviews and syntheses: Hidden forests, the role of vegetated coastal habitats in the ocean carbon budget. *Biogeosciences*, *14*(2), 301–310. https://doi.org/10.5194/bg-14-301-2017

Dubey, S. K. (2005). Microbial ecology of methane emission in rice agroecosystem: a review. *Applied Ecology and Environmental Research*, *3*(2), 1–27.

Dutta, M. K., Bianchi, T. S., & Mukhopadhyay, S. K. (2017). Mangrove Methane Biogeochemistry in the Indian Sundarbans: A Proposed Budget. *Frontiers in Marine Science*, *4*(June), 1–15. https://doi.org/10.3389/fmars.2017.00187

Egger, M., W. Lenstra, D. Jong, and others. 2016. Rapid sediment accumulation results in high methane effluxes from coastal sediments. PLoS One **11**: e0161609. doi:10.1371/journal.pone.0161609

Emery, H. E., and R. W. Fulweiler. 2014. Spartina alterniflora and invasive Phragmites australis stands have similar greenhouse gas emissions in a New England marsh. Aquat. Bot. **116**: 83–92. doi:10.1016/j.aquabot.2014.01.010

Emery, H. E., and R. W. Fulweiler. 2017. Incomplete tidal restoration may lead to persistent high CH4 emission. Ecosphere **8**: e01968. doi:10.1002/ecs2.1968

Emery, H. E., Angell, J. H., & Fulweiler, R. W. (2019). Salt Marsh Greenhouse Gas Fluxes and Microbial Communities Are Not Sensitive to the First Year of Precipitation Change. *Journal of Geophysical Research: Biogeosciences*, 2018JG004788. https://doi.org/10.1029/2018JG004788

Engle, D., & Melack, J. M. (2000). Methane emissions from an Amazon floodplain lake: Enhanced release during episodic mixing and during falling water. *Biogeochemistry*, *51*(1), 71–90. https://doi.org/10.1023/A:1006389124823

Eong, O. J. (1993). Mangroves - a carbon source and sink. *Chemosphere*, *27*(6), 1097–1107. https://doi.org/10.1016/0045-6535(93)90070-L

Etheridge, D. M., Steele, L. P., Francey, R. J., & Langenfelds, R. L. (1998). Atmospheric methane between 1000 A.D. and present: Evidence of anthropogenic emissions and climatic variability. *Journal of Geophysical Research: Atmospheres*, *103*(D13), 15979–15993. https://doi.org/10.1029/98JD00923

Eyre, B. D., and A. J. P. Ferguson. 2002. Comparison of carbon production and decomposition, benthic nutrient fluxes and denitrification in seagrass, phytoplankton, benthic microalgae- and macroalgae-dominated warm-temperate Australian lagoons. Mar. Ecol. Prog. Ser. **229**: 43–59. doi:10.3354/meps229043

Eyre, B. D., A. J. P. Ferguson, A. Webb, D. Maher, and J. M. Oakes. 2011a. Denitrification, N-fixation and nitrogen and phosphorus fluxes in different benthic habitats and their contribution to the nitrogen and phosphorus budgets of a shallow

oligotrophic sub-tropical coastal system (southern Moreton Bay, Australia). Biogeochemistry **102**: 111–133. doi:10.1007/s10533-010-9425-6

Eyre, B. D., D. Maher, J. M. Oakes, D. V. Erler, and T. M. Glasby. 2011b. Differences in benthic metabolism, nutrient fluxes, and denitrification in Caulerpa taxifolia communities compared to uninvaded bare sediment and seagrass (Zostera capricorni) habitats. Limnol. Oceanogr. **56**: 1737–1750. doi:10.4319/LO.2011.56.5.1737

Eyre, B. D., D. T. Maher, and P. Squire. 2013. Quantity and quality of organic matter (detritus) drives N2 effluxes (net denitrification) across seasons, benthic habitats, and estuaries. Global Biogeochem. Cycles **27**: 1083–1095. doi:10.1002/2013GB004631

Eyre, B. D., S. Rysgaard, T. Dalsgaard, and P. B. Christensen. 2002. Comparison of isotope pairing and N2:Ar methods for measuring sediment denitrification—Assumption, modifications, and implications. Estuaries 2002 256 **25**: 1077–1087. doi:10.1007/BF02692205

Fennel, K., Alin, S., Barbero, L., Evans, W., Bourgeois, T., Cooley, S., … Wang, Z. A. (2019). Carbon cycling in the North American coastal ocean: a synthesis. *Biogeosciences*, *16*(6), 1281–1304. https://doi.org/10.5194/bg-16-1281-2019

Forbrich, I., Giblin, A. E., & Hopkinson, C. S. (2018). Constraining Marsh Carbon Budgets Using Long-Term C Burial and Contemporary Atmospheric CO $_2$ Fluxes. *Journal of Geophysical Research: Biogeosciences*, *123*(3), 867–878. https://doi.org/10.1002/2017JG004336

Ford, H., Garbutt, A., Jones, L., & Jones, D. L. (2012). Methane, carbon dioxide and nitrous oxide fluxes from a temperate salt marsh: Grazing management does not alter Global Warming Potential. *Estuarine, Coastal and Shelf Science*, *113*, 182–191. https://doi.org/10.1016/j.ecss.2012.08.002

Foster, S. Q., & Fulweiler, R. W. (2019). Estuarine Sediments Exhibit Dynamic and Variable Biogeochemical Responses to Hypoxia. *Journal of Geophysical Research: Biogeosciences*, *124*(4), 737–758. https://doi.org/10.1029/2018JG004663

Foster, Sarah Q., & Fulweiler, R. W. (2016). Sediment Nitrous Oxide Fluxes Are Dominated by Uptake in a Temperate Estuary. *Frontiers in Marine Science*, *3*(March), 1–13. https://doi.org/10.3389/fmars.2016.00040

Fourqurean, J. W., C. M. Duarte, H. Kennedy, and others. 2012. Seagrass ecosystems as a globally significant carbon stock. Nat. Geosci. **5**: 505–509. doi:10.1038/ngeo1477

Freeman, C., Nevison, G. B., Kang, H., Hughes, S., Reynolds, B., & Hudson, J. A. (2002). Contrasted effects of simulated drought on the production and oxidation of

methane in a mid-Wales wetland. *Soil Biology and Biochemistry*. https://doi.org/10.1016/S0038-0717(01)00154-7

Friedrichs, C. T., & Perry, J. E. (2001). Tidal Salt Marsh Morphodynamics: A Synthesis. In *Journal of Coastal Research*.

Fulweiler, R. W., S. M. Brown, S. W. Nixon, and B. D. Jenkins. 2013. Evidence and a conceptual model for the co-occurrence of nitrogen fixation and denitrification in heterotrophic marine sediments. Mar. Ecol. Prog. Ser. **482**: 57–68. doi:10.3354/meps10240

Fulweiler, R. W., S. W. Nixon, B. A. Buckley, and S. L. Granger. 2007. Reversal of the net dinitrogen gas flux in coastal marine sediments. Nature **448**: 180–182. doi:10.1038/nature05963

Fulweiler, R. W., S. W. Nixon, B. A. Buckley, and S. L. Granger. 2008. Net sediment N2 fluxes in a coastal marine system-experimental manipulations and a conceptual model. Ecosystems **11**: 1168–1180. doi:10.1007/s10021-008-9187-3

Gacia, E., & Duarte, C. M. (2001). Sediment Retention by a Mediterranean Posidonia oceanica Meadow: The Balance between Deposition and Resuspension. *Estuarine, Coastal and Shelf Science*, *52*, 505–514. https://doi.org/10.1006

Gacia, E., Granata, T. C., & Duarte, C. M. (1999). An approach to measurement of particle flux and sediment retention within seagrass (Posidonia oceanica) meadows. *Aquatic Botany*, *65*, 255–268.

Gacia, E., H. Kennedy, C. M. Duarte, J. Terrados, N. Marbà, S. Papadimitriou, and M. Fortes. 2005. Light-dependence of the metabolic balance of a highly productive Philippine seagrass community. J. Exp. Mar. Bio. Ecol. **316**: 55–67. doi:10.1016/J.JEMBE.2004.10.008

Gammal, J., Norkko, J., Pilditch, C. A., & Norkko, A. (2017). Coastal Hypoxia and the Importance of Benthic Macrofauna Communities for Ecosystem Functioning. *Estuaries and Coasts*, *40*(2), 457–468. https://doi.org/10.1007/s12237-016-0152-7

Ganguly, D., Dey, M., Mandal, S. K., De, T. K., & Jana, T. K. (2008). Energy dynamics and its implication to biosphere-atmosphere exchange of CO2, H2O and CH4in a tropical mangrove forest canopy. *Atmospheric Environment*, *42*(18), 4172–4184. https://doi.org/10.1016/j.atmosenv.2008.01.022

Gao, G. F., Li, P. F., Shen, Z. J., Qin, Y. Y., Zhang, X. M., Ghoto, K., … Zheng, H. L. (2018). Exotic Spartina alterniflora invasion increases CH4 while reduces CO2

emissions from mangrove wetland soils in southeastern China. *Scientific Reports*, *8*(1), 9243. https://doi.org/10.1038/s41598-018-27625-5

Gao, G. F., P. F. Li, J. X. Zhong, and others. 2019. Spartina alterniflora invasion alters soil bacterial communities and enhances soil N2O emissions by stimulating soil denitrification in mangrove wetland. Sci. Total Environ. **653**: 231–240. doi:10.1016/J.SCITOTENV.2018.10.277

Gao, Y., X. Liu, N. Yi, Y. Wang, J. Guo, Z. Zhang, and S. Yan. 2013. Estimation of N2 and N2O ebullition from eutrophic water using an improved bubble trap device. Ecol. Eng. **57**: 403–412. doi:10.1016/j.ecoleng.2013.04.020

Garcias-Bonet, N., and C. M. Duarte. 2017. Methane Production by Seagrass Ecosystems in the Red Sea. Front. Mar. Sci. **4**. doi:10.3389/fmars.2017.00340

Garcias-Bonet, N., V. M. Eguíluz, R. Díaz-Rúa, and C. M. Duarte. 2021. Host-association as major driver of microbiome structure and composition in Red Sea seagrass ecosystems. Environ. Microbiol. **23**: 2021–2034. doi:10.1111/1462-2920.15334

Garcias-Bonet, N., M. Fusi, M. Ali, D. R. Shaw, P. E. Saikaly, D. Daffonchio, and C. M. Duarte. 2018. High denitrification and anaerobic ammonium oxidation contributes to net nitrogen loss in a seagrass ecosystem in the central Red Sea. Biogeosciences **15**: 7333–7346. doi:10.5194/bg-15-7333-2018

Gattuso, J. P., B. Gentili, C. M. Duarte, J. A. Kleypas, J. J. Middelburg, and D. Antoine. 2006. Light availability in the coastal ocean: Impact on the distribution of benthic photosynthetic organisms and their contribution to primary production. Biogeosciences **3**: 489–513. doi:10.5194/BG-3-489-2006

Gelesh, L., Marshall, K., Boicourt, W., & Lapham, L. (2016). Methane concentrations increase in bottom waters during summertime anoxia in the highly eutrophic estuary, Chesapeake Bay, U.S.A. *Limnology and Oceanography*, *61*, S253–S266. https://doi.org/10.1002/lno.10272

Gerard, G., and J. Chanton. 1993. Quantification of methane oxidation in the rhizosphere of emergent aquatic macrophytes: defining upper limits. Biogeochem. 1993 232 **23**: 79–97. doi:10.1007/BF00000444

Giani, L., Bashan, Y., Holguin, G., & Strangmann, A. (1996). Characteristics and methanogenesis of the Balandra lagoon mangrove soils, Baja California sur, Mexico. *Geoderma*, *72*(1–2), 149–160. https://doi.org/10.1016/0016-7061(96)00023-7

Gillooly, J. F., Brown, J. H., West, G. B., Savage, V. M., & Charnov, E. L. (2001). Effects of Size and Temperature on Metabolic Rate. *Science*, *293*(5538), 2248–2248.

Giri, C., Ochieng, E., Tieszen, L. L., Zhu, Z., Singh, A., Loveland, T., … Duke, N. (2011). Status and distribution of mangrove forests of the world using earth observation satellite data. *Global Ecology and Biogeography*, *20*(1), 154–159. https://doi.org/10.1111/j.1466-8238.2010.00584.x

Gonsalves, M.-J., Fernandes, C. E. G., Fernandes, S. O., Kirchman, D. L., & Bharathi, P. A. L. (2011). Effects of composition of labile organic matter on biogenic production of methane in the coastal sediments of the Arabian Sea. *Environmental Monitoring and Assessment*, *182*(1–4), 385–395. https://doi.org/10.1007/s10661-011-1883-3

Grasset, C., S. Moras, A. Isidorova, R.-M. Couture, A. Linkhorst, and S. Sobek. 2021. An empirical model to predict methane production in inland water sediment from particular organic matter supply and reactivity. Limnol. Oceanogr. **9999**: lno.11905. doi:10.1002/LNO.11905

Greiner, J. T., K. J. McGlathery, J. Gunnell, and B. A. McKee. 2013. Seagrass Restoration Enhances "Blue Carbon" Sequestration in Coastal Waters. PLoS One **8**: 1–8. doi:10.1371/journal.pone.0072469

Grosso, S. J. Del, W. J. Parton, A. R. Mosier, and others. 2000. General CH4 oxidation model and comparisons of CH4 Oxidation in natural and managed systems. Global Biogeochem. Cycles **14**: 999–1019. doi:10.1029/1999GB001226

Guirguis, K., Gershunov, A., Schwartz, R., & Bennett, S. (2011). Recent warm and cold daily winter temperature extremes in the Northern Hemisphere. *Geophysical Research Letters*, *38*(17), n/a-n/a. https://doi.org/10.1029/2011GL048762

Hamilton, S. E., & Casey, D. (2016). Creation of a high spatio-temporal resolution global database of continuous mangrove forest cover for the 21st century (CGMFC-21). *Global Ecology and Biogeography*, *25*(6), 729–738. https://doi.org/10.1111/geb.12449

Hansen, J. W., A. G. U. Pedersen, J. Berntsen, I. S. Rønbøg, L. S. Hansen, and B. A. Lomstein. 2000. Photosynthesis, respiration, and nitrogen uptake by different compartments of a Zostera marina community. Aquat. Bot. **66**: 281–295. doi:10.1016/S0304-3770(99)00078-9

Harttung, S. A., K. R. Radabaugh, R. P. Moyer, J. M. Smoak, and L. G. Chambers. 2021. Coastal riverine wetland biogeochemistry follows soil organic matter distribution along a marsh-to-mangrove gradient (Florida, USA). Sci. Total Environ. **797**: 149056. doi:10.1016/J.SCITOTENV.2021.149056

Heiss, E. M., Fields, L., & Fulweiler, R. W. (2012). Directly measured net denitrification rates in offshore New England sediments. *Continental Shelf Research*, *45*, 78–86. https://doi.org/10.1016/j.csr.2012.06.002

Hendriks, I. E., Sintes, T., Bouma, T. J., & Duarte, C. M. (2008). Experimental assessment and modeling evaluation of the effects of the seagrass Posidonia oceanica on flow and particle trapping. *Marine Ecology Progress Series*, *356*, 163–173. https://doi.org/10.3354/meps07316

Hirota, M., Senga, Y., Seike, Y., Nohara, S., & Kunii, H. (2007). Fluxes of carbon dioxide, methane and nitrous oxide in two contrastive fringing zones of coastal lagoon, Lake Nakaumi, Japan. *Chemosphere*, *68*(3), 597–603. https://doi.org/10.1016/j.chemosphere.2007.01.002

Hoffman, D. K., M. J. McCarthy, S. E. Newell, W. S. Gardner, D. N. Niewinski, J. Gao, and T. R. Mutchler. 2019. Relative Contributions of DNRA and Denitrification to Nitrate Reduction in Thalassia testudinum Seagrass Beds in Coastal Florida (USA). Estuaries and Coasts **42**: 1001–1014. doi:10.1007/s12237-019-00540-2

Holm, G. O., Perez, B. C., McWhorter, D. E., Krauss, K. W., Johnson, D. J., Raynie, R. C., & Killebrew, C. J. (2016). Ecosystem Level Methane Fluxes from Tidal Freshwater and Brackish Marshes of the Mississippi River Delta: Implications for Coastal Wetland Carbon Projects. *Wetlands*, *36*(3), 401–413. https://doi.org/10.1007/s13157-016-0746-7

Holmer, M., Andersen, F. Ø., Nielsen, S. L., & Boschker, H. T. S. (2001). The importance of mineralization based on sulfate reduction for nutrient regeneration in tropical seagrass sediments. *Aquatic Botany*, *71*(1), 1–17. https://doi.org/10.1016/S0304-3770(01)00170-X

Holmer, M., C. Carta, and F. Andersen. 2006. Biogeochemical implications for phosphorus cycling in sandy and muddy rhizosphere sediments of Zostera marina meadows (Denmark). Mar. Ecol. Prog. Ser. **320**: 141–151. doi:10.3354/MEPS320141

Holmer, M., C. M. Duarte, H. T. S. Boschker, and C. Barrón. 2004. Carbon cycling and bacterial carbon sources in pristine and impacted Mediterranean seagrass sediments. Aquat. Microb. Ecol. **36**: 227–237. doi:10.3354/AME036227

Holmer, M., Gribsholt, B., & Kistensen, E. (2002). Effects of sea level rise on growth of Spartina anglica and oxygen dynamics in rhizosphere and salt marsh sediments. *Mar Ecol Prog Ser*, *225*, 197–204.

Hothorn, T., A. Zeileis, R. W. Farebrother, C. Cummins, G. Millo, and D. Mitchell. 2020. Testing Linear Regression Models.

Howes, B., S. Kelley, J. Ramsey, R. Samimy, D. Schlesinger, and E. Eichner. 2006. Massachusetts Estuaries Project Linked Watershed-Embayment Model to Determine Critical Nitrogen Loading Thresholds for the Pleasant Bay System, Towns of Orleans.

Howes, B. L., & Teal, J. M. (1994). Oxygen loss from Spartina alterniflora and its relationship to salt marsh oxygen balance. *Oecologia*, *97*(4), 431–438. https://doi.org/10.1007/BF00325879

Hyndes, G. A., Heck, K. L., Vergés, A., Harvey, E. S., Kendrick, G. A., Lavery, P. S., … Wilson, S. (2016). Accelerating Tropicalization and the Transformation of Temperate Seagrass Meadows. *BioScience*, *66*(11), 938–948. https://doi.org/10.1093/biosci/biw111

Inglett, P. W., T. M. Kana, and S. An. 2015. Denitrification Measurement Using Membrane Inlet Mass Spectrometry. Methods Biogeochem. Wetl. 503–517. doi:10.2136/SSSABOOKSER10.C27

Invers, O., R. C. Zimmerman, R. S. Alberte, M. Pérez, and J. Romero. 2001. Inorganic carbon sources for seagrass photosynthesis: an experimental evaluation of bicarbonate use in species inhabiting temperate waters. J. Exp. Mar. Bio. Ecol. **265**: 203–217. doi:10.1016/S0022-0981(01)00332-X

IPCC, Pachauri, R. K., & Meyer, L. A. (2014). Climate Change 2014: Synthesis Report. Contribution of Working Groups I, II, and III to the Fifth Assessment Report of the Intergovernmental Panel on Climate Change. In *IPCC AR5 Synthesis Report Website*. Geneva, Switzerland.

Irvine, I. C., Vivanco, L., Bentley, P. N., & Martiny, J. B. H. (2012). The effect of nitrogen enrichment on C1-cycling microorganisms and methane flux in salt marsh sediments. *Frontiers in Microbiology*, *3*(MAR), 1–10. https://doi.org/10.3389/fmicb.2012.00090

Jayathilake, D. R. M., & Costello, M. J. (2018). A modelled global distribution of the seagrass biome. *Biological Conservation*, *226*, 120–126. https://doi.org/10.1016/J.BIOCON.2018.07.009

Jeffrey, L. C., G. Reithmaier, J. Z. Sippo, S. G. Johnston, D. R. Tait, Y. Harada, and D. T. Maher. 2019. Are methane emissions from mangrove stems a cryptic carbon loss pathway? Insights from a catastrophic forest mortality. New Phytol. doi:10.1111/nph.15995

Jenkins, M. C., and W. M. Kemp. 1984. The coupling of nitrification and denitrification in two estuarine sediments1,2. Limnol. Oceanogr. **29**: 609–619. doi:10.4319/LO.1984.29.3.0609

Jensen, H. S., K. J. McGlathery, R. Marino, and R. W. Howarth. 1998. Forms and availability of sediment phosphorus in carbonate sand of Bermuda seagrass beds. Limnol. Oceanogr. **43**: 799–810. doi:10.4319/LO.1998.43.5.0799

Jensen, H. S., P. B. Mortensen, F. 0. Andersen, E. Rasmussen, and A. Jensen. 1995. Phosphorus cycling in a coastal marine sediment, Aarhus Bay, Denmark. Limnol. Oceanogr. **40**: 908–917. doi:10.4319/LO.1995.40.5.0908

Jha, C. S., Rodda, S. R., Thumaty, K. C., Raha, A. K., & Dadhwal, V. K. (2014). Eddy covariance based methane flux in Sundarbans mangroves, India. *Journal of Earth System Science*, *123*(5), 1089–1096. https://doi.org/10.1007/s12040-014-0451-y

Jiang, L.-Q., W.-J. Cai, and Y. Wang. 2008. A comparative study of carbon dioxide degassing in river- and marine-dominated estuaries. Limnol. Oceanogr. **53**: 2603–2615. doi:10.4319/LO.2008.53.6.2603

Jørgensen, C. J., S. Struwe, and B. Elberling. 2012. Temporal trends in N2O flux dynamics in a Danish wetland – effects of plant-mediated gas transport of N2O and O2 following changes in water level and soil mineral-N availability. Glob. Chang. Biol. **18**: 210–222. doi:10.1111/J.1365-2486.2011.02485.X

Jung, C., & Schindler, D. (2019). Changing wind speed distributions under future global climate. *Energy Conversion and Management*, *198*. https://doi.org/10.1016/j.enconman.2019.111841

Kana, T. M., C. Darkangelo, M. D. Hunt, J. B. Oldham, G. E. Bennett, and J. C. Cornwell. 1994. Membrane Inlet Mass Spectrometer for Rapid High-Precision Determination of N2, O2, and Ar in Environmental Water Samples. Anal. Chem. **66**: 4166–4170. doi:10.1021/ac00095a009

Kelleway, J. J., Saintilan, N., Macreadie, P. I., Skilbeck, C. G., Zawadzki, A., & Ralph, P. J. (2016). Seventy years of continuous encroachment substantially increases "blue carbon" capacity as mangroves replace intertidal salt marshes. *Global Change Biology*, *22*(3), 1097–1109. https://doi.org/10.1111/gcb.13158

Kim, G., & Hwang, D.-W. (2002). Tidal pumping of groundwater into the coastal ocean revealed from submarine ^{222}Rn and CH_4 monitoring. *Geophysical Research Letters*, *29*(14), 23-1-23–24. https://doi.org/10.1029/2002GL015093

Kim, J., S. B. Verma, and D. P. Billesbach. 1999. Seasonal variation in methane emission from a temperate Phragmites-dominated marsh: effect of growth stage and plant-mediated transport. Glob. Chang. Biol. **5**: 433–440. doi:10.1046/j.1365-2486.1999.00237.x

King, G M, & Wiebe, W. J. (1978). Methane release from soils of a South Carolina salt marsh. *Geochimica et Cosmochimica Acta*, *42*, 343–348.

King, Gary M. (1984). Utilization of hydrogen, acetate, and "noncompetitive"; substrates by methanogenic bacteria in marine sediments. *Geomicrobiology Journal*, *3*(4), 275–306. https://doi.org/10.1080/01490458409377807

Konnerup, D., J. M. Betancourt-Portela, C. Villamil, and J. P. Parra. 2014. Nitrous oxide and methane emissions from the restored mangrove ecosystem of the Ciénaga Grande de Santa Marta, Colombia. Estuar. Coast. Shelf Sci. **140**: 43–51. doi:10.1016/j.ecss.2014.01.006

Krauss, K. W., Holm, G. O., Perez, B. C., McWhorter, D. E., Cormier, N., Moss, R. F., … Raynie, R. C. (2016). Component greenhouse gas fluxes and radiative balance from two deltaic marshes in Louisiana: Pairing chamber techniques and eddy covariance. *Journal of Geophysical Research: Biogeosciences*, *121*(6), 1503–1521. https://doi.org/10.1002/2015JG003224

Kristensen, E., Flindt, M. R., Ulomi, S., Borges, A. V., Abril, G., & Bouillon, S. (2008). Emission of CO2 and CH4 to the atmosphere by sediments and open waters in two Tanzanian mangrove forests. *Marine Ecology Progress Series*, *370*, 53–67. https://doi.org/10.3354/meps07642

Krithika, K., Purvaja, R., & Ramesh, R. (2008). Fluxes of methane and nitrous oxide from an Indian mangrove. *Current Science*, *94*(2), 218–224.

Krom, M. D., and R. A. Berner. 1981. The diagenesis of phosphorus in a nearshore marine sediment. Geochim. Cosmochim. Acta **45**: 207–216. doi:10.1016/0016-7037(81)90164-2

Kvenvolden, K. A., & Rogers, B. W. (2005). Gaia's breath—global methane exhalations. *Marine and Petroleum Geology*, *22*(4), 579–590. https://doi.org/10.1016/J.MARPETGEO.2004.08.004

Laanbroek, H. J. (2010). Methane emission from natural wetlands: interplay between emergent macrophytes and soil microbial processes. A mini-review. *Annals of Botany*, *105*(1), 141–153. https://doi.org/10.1093/aob/mcp201

Larkum, A. W. D., E. A. Drew, and P. J. Ralph. 2007. Photosynthesis and Metabolism in Seagrasses at the Cellular Level, p. 323–345. *In* SEAGRASSES: BIOLOGY, ECOLOGYAND CONSERVATION. Springer Netherlands.

Lavery, P. S., Mateo, M. Á., Serrano, O., & Rozaimi, M. (2013). Variability in the Carbon Storage of Seagrass Habitats and Its Implications for Global Estimates of Blue Carbon Ecosystem Service. *PLoS ONE*, *8*(9). https://doi.org/10.1371/journal.pone.0073748

Lee, K. S., F. T. Short, and D. M. Burdick. 2004. Development of a nutrient pollution indicator using the seagrass, Zostera marina, along nutrient gradients in three New England estuaries. Aquat. Bot. **78**: 197–216. doi:10.1016/j.aquabot.2003.09.010

Lee, S. Y., Primavera, J. H., Dahdouh-Guebas, F., McKee, K., Bosire, J. O., Cannicci, S., … Record, S. (2014). Ecological role and services of tropical mangrove ecosystems: a reassessment. *Global Ecology and Biogeography*, *23*(7), 726–743. https://doi.org/10.1111/geb.12155

Legare, B. J., O. C. Nichols, A. Mittermayr, and M. Borrelli. 2020. Relationships between Species Communities as Determined by Analysis of Data from Multiple Surveys of Pleasant Bay, Cape Cod, MA. Northeast. Nat. **27**: 114–131. doi:10.1656/045.027.s1005

Leifer, I., & Patro, R. K. (2002). The bubble mechanism for methane transport from the shallow sea bed to the surface: A review and sensitivity study. *Continental Shelf Research*, *22*(16), 2409–2428. https://doi.org/10.1016/S0278-4343(02)00065-1

Le Mer, J., & Roger, P. (2001). Production, oxidation, emission and consumption of methane by soils: A review. *European Journal of Soil Biology*, *37*(1), 25–50. https://doi.org/10.1016/S1164-5563(01)01067-6

Li, H., Dai, S., Ouyang, Z., Xie, X., Guo, H., Gu, C., … Zhao, B. (2018). Multi-scale temporal variation of methane flux and its controls in a subtropical tidal salt marsh in eastern China. *Biogeochemistry*, *137*(1–2), 163–179. https://doi.org/10.1007/s10533-017-0413-y

Li, Y., Wang, D., Chen, Z., Jin, H., Hu, H., Chen, J., … Yang, Z. (2018). Role of Scirpus mariqueter on Methane Emission from an Intertidal Saltmarsh of Yangtze Estuary. *Sustainability*, *10*(4), 1139. https://doi.org/10.3390/su10041139

Livesley, S. J., & Andrusiak, S. M. (2012). Temperate mangrove and salt marsh sediments are a small methane and nitrous oxide source but important carbon store. *Estuarine, Coastal and Shelf Science*, *97*, 19–27. https://doi.org/10.1016/j.ecss.2011.11.002

Livingston, G. P., & Hutchinson, G. L. (1995). Enclosure-based measurement of trace gas exchange; applications and sources of error. In P. A. Matson, R. C. Harriss, & P. A. Matson (Eds.), *Biogenic Trace Gases : Measuring Emissions From Soil And Water.* (pp. 14–51). John Wiley & Sons.

Lohrer, A. M., M. Townsend, S. F. Hailes, I. F. Rodil, K. Cartner, D. R. Pratt, and J. E. Hewitt. 2016. Influence of New Zealand cockles (Austrovenus stutchburyi) on primary productivity in sandflat-seagrass (Zostera muelleri) ecotones. Estuar. Coast. Shelf Sci. **181**: 238–248. doi:10.1016/J.ECSS.2016.08.045

Long, M. H., J. E. Rheuban, D. C. McCorkle, D. J. Burdige, and R. C. Zimmerman. 2019. Closing the oxygen mass balance in shallow coastal ecosystems. Limnol. Oceanogr. **64**: 2694–2708. doi:10.1002/LNO.11248

Long, M. H., K. Sutherland, S. D. Wankel, D. J. Burdige, and R. C. Zimmerman. 2020. Ebullition of oxygen from seagrasses under supersaturated conditions. Limnol. Oceanogr. **65**: 314–324. doi:10.1002/lno.11299

Lovelock, C. E., and C. M. Duarte. 2019. Dimensions of Blue Carbon and emerging perspectives. Biol. Lett. **15**: 23955–6900. doi:10.1098/RSBL.2018.0781

Lu, C. Y., Wong, Y. S., Tam, N. F. Y., Ye, Y., & Lin, P. (1999). Methane flux and production from sediments of a mangrove wetland on Hainan Island, China. *Mangroves and Salt Marshes*, *3*(1), 41–49. https://doi.org/10.1023/A:1009989026801

Lyimo, L. D., Gullström, M., Lyimo, T. J., Deyanova, D., Dahl, M., Hamisi, M. I., & Björk, M. (2018). Shading and simulated grazing increase the sulphide pool and methane emission in a tropical seagrass meadow. *Marine Pollution Bulletin*, *134*, 89–93. https://doi.org/10.1016/J.MARPOLBUL.2017.09.005

Lyimo, T. J., Pol, A., & Camp, H. J. M. O. (2002). Methane emission, sulphide concentration and redox potential profiles in Mtoni mangrove sediment, Tanzania. *Western Indian Ocean Journal of Marine Science*, *1*, 71–80.

Macreadie, P. I., A. Anton, J. A. Raven, and others. 2019. The future of Blue Carbon science. Nat. Commun. **10**. doi:10.1038/s41467-019-11693-w

Macreadie, P. I., Ollivier, Q. R., Kelleway, J. J., Serrano, O., Carnell, P. E., Ewers Lewis, C. J., … Lovelock, C. E. (2017). Carbon sequestration by Australian tidal marshes. *Scientific Reports*, *7*(1), 44071. https://doi.org/10.1038/srep44071

Magenheimer, J. F., Moore, T. R., Chmura, G. L., & Daoust, R. J. (1996). Methane and Carbon Dioxide Flux from a Macrotidal Salt Marsh, Bay of Fundy, New Brunswick. *Estuaries*, *19*(1), 139. https://doi.org/10.2307/1352658

Maher, D. T., Drexl, M., Tait, D. R., Johnston, S. G., & Jeffrey, L. C. (2019). iAMES: An i nexpensive, A utomated M ethane E bullition S ensor. *Environmental Science & Technology*, *53*(11), 6420–6426. https://doi.org/10.1021/acs.est.9b01881

Maher, D. T., I. R. Santos, L. Golsby-Smith, J. Gleeson, and B. D. Eyre. 2013. Groundwater-derived dissolved inorganic and organic carbon exports from a mangrove tidal creek: The missing mangrove carbon sink? Limnol. Oceanogr. **58**: 475–488. doi:10.4319/LO.2013.58.2.0475

Marbà, N., M. Holmer, E. Gacia, and C. Barron. 2006. Seagrass beds and coastal biogeochemistry, p. 135–157. *In* Seagrasses: Biology, Ecology and Conservation. Springer Netherlands.

Marinho, C., Campos, E., Guimarães, J., & Esteves, F. (2012). Effect of sediment composition on methane concentration and production in the transition zone of a mangrove (Sepetiba Bay, Rio de Janeiro, Brazil). *Brazilian Journal of Biology*, *72*(3), 429–436. https://doi.org/10.1590/S1519-69842012000300003

Marsh, J. A., W. C. Dennison, and R. S. Alberte. 1986. Effects of temperature on photosynthesis and respiration in eelgrass (Zostera marina L.). J. Exp. Mar. Bio. Ecol. **101**: 257–267. doi:10.1016/0022-0981(86)90267-4

Martens, C. S., & Berner, R. A. (1974). Methane production in the interstitial waters of sulfate-depleted marine sediments. *Science*, *185*(4157), 1167–1169. https://doi.org/10.1126/science.185.4157.1167

Martin, R. M., & Moseman-Valtierra, S. (2017). Different short-term responses of greenhouse gas fluxes from salt marsh mesocosms to simulated global change drivers. *Hydrobiologia*, *802*(1), 71–83. https://doi.org/10.1007/s10750-017-3240-1

Martin, S., J. Clavier, J.-M. Guarini, and others. 2005. Comparison of Zostera marina and maerl community metabolism. Aquat. Bot. **83**: 161–174. doi:10.1016/j.aquabot.2005.06.002

McGlathery, K. J. (2001). MACROALGAL BLOOMS CONTRIBUTE TO THE DECLINE OF SEAGRASS IN NUTRIENT-ENRICHED COASTAL WATERS. *Journal of Phycology*, *37*(4), 453–456. https://doi.org/10.1046/j.1529-8817.2001.037004453.x

McGlathery, K. J., K. Sundbäck, and I. C. Anderson. 2007. Eutrophication in shallow coastal bays and lagoons: The role of plants in the coastal filter. Mar. Ecol. Prog. Ser. **348**: 1–18. doi:10.3354/meps07132

McHenry, J., A. Rassweiler, G. Hernan, C. K. Uejio, S. Pau, A. K. Dubel, and S. E. Lester. 2021. Modelling the biodiversity enhancement value of seagrass beds. Divers. Distrib. **27**: 2036–2049. doi:10.1111/DDI.13379

McKain, K., A. Down, S. M. Raciti, and others. 2015. Methane emissions from natural gas infrastructure and use in the urban region of Boston, Massachusetts. Proc. Natl. Acad. Sci. **112**: 1941–1946. doi:10.1073/PNAS.1416261112

McKEE, K. L., & ROOTH, J. E. (2008). Where temperate meets tropical: multi-factorial effects of elevated CO 2 , nitrogen enrichment, and competition on a mangrove-salt marsh community. *Global Change Biology*, *14*(5), 971–984. https://doi.org/10.1111/j.1365-2486.2008.01547.x

McLeod, E., G. L. Chmura, S. Bouillon, and others. 2011. A blueprint for blue carbon: Toward an improved understanding of the role of vegetated coastal habitats in sequestering CO2. Front. Ecol. Environ. **9**: 552–560. doi:10.1890/110004

Mcowen, C. J., Weatherdon, L. V, Bochove, J.-W. Van, Sullivan, E., Blyth, S., Zockler, C., … Fletcher, S. (2017). A global map of saltmarshes. *Biodiversity Data Journal*, (5), e11764. https://doi.org/10.3897/BDJ.5.e11764

Middelburg, J. J., Klaver, G., Nieuwenhuize, J., Wielemaker, A., De Haas, W., Vlug, T., & Van Der Nat, J. F. W. A. (1996). Organic matter mineralization in intertidal sediments along an estuarine gradient. *Marine Ecology Progress Series*, *132*, 157–168.

Mittermayr, A., B. Legare, and M. Borrelli. 2020. Applications of the Coastal and Marine Ecological Classification Standard (CMECS) in a Partially Restored New England Salt Marsh Lagoon. Estuaries and Coasts. doi:10.1007/s12237-020-00707-2

Mohr, W., N. Lehnen, S. Ahmerkamp, and others. 2021. Terrestrial-type nitrogen-fixing symbiosis between seagrass and a marine bacterium. Nature. doi:10.1038/s41586-021-04063-4

Möller, I., Kudella, M., Rupprecht, F., Spencer, T., Paul, M., van Wesenbeeck, B. K., … Schimmels, S. (2014). Wave attenuation over coastal salt marshes under storm surge conditions. *Nature Geoscience*, *7*(10), 727–731. https://doi.org/10.1038/ngeo2251

Moriarty, D. J. W., R. L. Iverson, and P. C. Pollard. 1986. Exudation of organic carbon by the seagrass Halodule wrightii Aschers. And its effect on bacterial growth in the sediment. J. Exp. Mar. Bio. Ecol. **96**: 115–126. doi:10.1016/0022-0981(86)90237-6

Mukai, H., I. Koike, M. Nishihira, and S. Nojima. 1989. Oxygen consumption and ammonium excretion of mega-sized benthic invertebrates in a tropical seagrass bed. J. Exp. Mar. Bio. Ecol. **134**: 101–115. doi:10.1016/0022-0981(90)90103-J

Mukhopadhyay, S. K., Biswas, H., De, T. K., Sen, B. K., Sen, S., & Jana, T. K. (2002). Impact of Sundarban mangrove biosphere on the carbon dioxide and methane mixing ratios at the NE Coast of Bay of Bengal, India. *Atmospheric Environment*, *36*(4), 629–638. https://doi.org/10.1016/S1352-2310(01)00521-0

Murray, R., D. Erler, J. Rosentreter, D. Maher, and B. Eyre. 2018. A seasonal source and sink of nitrous oxide in mangroves: Insights from concentration, isotope, and isotopomer measurements. Geochim. Cosmochim. Acta **238**: 169–192. doi:10.1016/j.gca.2018.07.003

Murray, R. H., D. V. Erler, and B. D. Eyre. 2015. Nitrous oxide fluxes in estuarine environments: response to global change. Glob. Chang. Biol. **21**: 3219–3245. doi:10.1111/gcb.12923

Nagelkerken, I., Blaber, S. J. M., Bouillon, S., Green, P., Haywood, M., Kirton, L. G., … Somerfield, P. J. (2008). The habitat function of mangroves for terrestrial and marine fauna: A review. *Aquatic Botany*, *89*(2), 155–185. https://doi.org/10.1016/J.AQUABOT.2007.12.007

Nakagawa, T., Y. Tsuchiya, S. Ueda, M. Fukui, and R. Takahashi. 2019. Eelgrass Sediment Microbiome as a Nitrous Oxide Sink in Brackish Lake Akkeshi, Japan. Microbes Environ. **34**: 13–22. doi:10.1264/jsme2.ME18103

Nakayama, K., K. Komai, K. Tada, H. C. Lin, H. Yajima, S. Yano, M. R. Hipsey, and J. W. Tsai. 2020. Modeling dissolved inorganic carbon considering submerged aquatic vegetation. Ecol. Modell. **431**: 109188. doi:10.1016/J.ECOLMODEL.2020.109188

Needelman, B. A., I. M. Emmer, S. Emmett-Mattox, S. Crooks, J. P. Megonigal, D. Myers, M. P. J. Oreska, and K. McGlathery. 2018. The Science and Policy of the Verified Carbon Standard Methodology for Tidal Wetland and Seagrass Restoration. Estuaries and Coasts **41**: 2159–2171. doi:10.1007/s12237-018-0429-0

Negandhi, K., Edwards, G., Kelleway, J. J., Howard, D., Safari, D., & Saintilan, N. (2019). Blue carbon potential of coastal wetland restoration varies with inundation and rainfall. *Scientific Reports*, *9*(1), 4368. https://doi.org/10.1038/s41598-019-40763-8

Nellemann, C., & Corcoran, E. (2009). *Blue Carbon: The Role of Healthy Oceans in Binding Carbon : a Rapid Response Assessment*. UNEP/Earthprint.

Neubauer, S. C., and J. P. Megonigal. 2015. Moving Beyond Global Warming Potentials to Quantify the Climatic Role of Ecosystems. Ecosystems **18**: 1000–1013. doi:10.1007/s10021-015-9879-4

Newell, S. E., M. J. McCarthy, W. S. Gardner, and R. W. Fulweiler. 2016. Sediment Nitrogen Fixation: a Call for Re-evaluating Coastal N Budgets. Estuaries and Coasts **39**: 1626–1638. doi:10.1007/s12237-016-0116-y

Nisbet, E. G., Manning, M. R., Dlugokencky, E. J., Fisher, R. E., Lowry, D., Michel, S. E., … White, J. W. C. (2019). Very Strong Atmospheric Methane Growth in the 4 Years 2014–2017: Implications for the Paris Agreement. *Global Biogeochemical Cycles*, *33*(3), 318–342. https://doi.org/10.1029/2018GB006009

Nixon, S. W. (1995). Coastal marine eutrophication: A definition, social causes, and future concerns. *Ophelia*, Vol. 41, pp. 199–219. https://doi.org/10.1080/00785236.1995.10422044

Nixon, S. W., Fulweiler, R. W., Buckley, B. A., Granger, S. L., Nowicki, B. L., & Henry, K. M. (2009). The impact of changing climate on phenology, productivity, and benthic–pelagic coupling in Narragansett Bay. *Estuarine, Coastal and Shelf Science*, *82*(1), 1–18. https://doi.org/10.1016/J.ECSS.2008.12.016

Nóbrega, G. N., Ferreira, T. O., Siqueira Neto, M., Queiroz, H. M., Artur, A. G., Mendonça, E. D. S., … Otero, X. L. (2016). Edaphic factors controlling summer (rainy season) greenhouse gas emissions (CO2and CH4) from semiarid mangrove soils (NE-Brazil). *Science of the Total Environment*, *542*, 685–693. https://doi.org/10.1016/j.scitotenv.2015.10.108

Nordlund, L. M., Koch, E. W., Barbier, E. B., & Creed, J. C. (2016). Seagrass Ecosystem Services and Their Variability across Genera and Geographical Regions. *PLOS ONE*, *11*(10), e0163091. https://doi.org/10.1371/journal.pone.0163091

Novak, A. B., M. C. Pelletier, P. Colarusso, and others. 2020. Factors Influencing Carbon Stocks and Accumulation Rates in Eelgrass Meadows Across New England, USA. Estuaries and Coasts **43**: 2076–2091. doi:10.1007/s12237-020-00754-9

Nowicki, T. P. 1994. The Prospects for Coastal Residential Development Under the Cape Cod Commission Stewardship. Massachusetts Institute of Technology.

Ondiviela, B., Losada, I. J., Lara, J. L., Maza, M., Galván, C., Bouma, T. J., & van Belzen, J. (2014). The role of seagrasses in coastal protection in a changing climate. *Coastal Engineering*, *87*, 158–168. https://doi.org/10.1016/J.COASTALENG.2013.11.005

Oremland, R. S., Marsh, L. M., & Polcin, S. (1982). Methane production and simultaneous sulphate reduction in anoxic, salt marsh sediments. *Nature*, *296*(5853), 143–145. https://doi.org/10.1038/296143a0

Oremland, R. S., & Taylor, B. F. (1978). Sulfate reduction and methanogenesis in marine sediments. *Geochimica et Cosmochimica Acta*, *42*(2), 209–214. https://doi.org/10.1016/0016-7037(78)90133-3

Oreska, M. P. J., K. J. McGlathery, L. R. Aoki, A. C. Berger, P. Berg, and L. Mullins. 2020. The greenhouse gas offset potential from seagrass restoration. Sci. Rep. **10**: 1–15. doi:10.1038/s41598-020-64094-1

Ortega, T., R. Ponce, J. Forja, and A. Gómez-Parra. 2005. Fluxes of dissolved inorganic carbon in three estuarine systems of the Cantabrian Sea (north of Spain). J. Mar. Syst. **53**: 125–142. doi:10.1016/J.JMARSYS.2004.06.006

Orth, R. J., T. J. B. Carruthers, W. C. Dennison, and others. 2006. A Global Crisis for Seagrass Ecosystems. Bioscience **56**: 987–996. doi:10.1641/0006-3568(2006)56[987:agcfse]2.0.co;2

Oshima, Y., M. J. Kishi, and T. Sugimoto. 1999. Evaluation of the nutrient budget in a seagrass bed. Ecol. Modell. **115**: 19–33. doi:10.1016/S0304-3800(98)00155-0

Othman, M. A. (1994). Value of mangroves in coastal protection. *Hydrobiologia*, *285*(1–3), 277–282. https://doi.org/10.1007/BF00005674

Oviatt, C., P. Doering, B. Nowicki, L. Reed, J. Cole, and J. Frithsen. 1995. An ecosystem level experiment on nutrient limitation in temperate coastal marine environments. Mar. Ecol. Prog. Ser. **116**: 171–179.

Parashar, D. C., Gupta, P. K., Rai, J., Sharma, R. C., & Singh, N. (1993). Effect of soil temperature on methane emission from paddy fields. *Chemosphere*, *26*(1–4), 247–250. https://doi.org/10.1016/0045-6535(93)90425-5

Pedersen, O., Borum, J., Duarte, C., & Fortes, M. (1998). Oxygen dynamics in the rhizosphere of Cymodocea rotundata. *Marine Ecology Progress Series*, *169*, 283–288. https://doi.org/10.3354/meps169283

Pendleton, L., Donato, D. C., Murray, B. C., Crooks, S., Jenkins, W. A., Sifleet, S., … Baldera, A. (2012). Estimating Global "Blue Carbon" Emissions from Conversion and Degradation of Vegetated Coastal Ecosystems. *PLoS ONE*, *7*(9), e43542. https://doi.org/10.1371/journal.pone.0043542

Pi, N., Tam, N. F. Y., Wu, Y., & Wong, M. H. (2009). Root anatomy and spatial pattern of radial oxygen loss of eight true mangrove species. *Aquatic Botany*, *90*(3), 222–230. https://doi.org/10.1016/J.AQUABOT.2008.10.002

Pietikäinen, J., M. Pettersson, and E. Bååth. 2005. Comparison of temperature effects on soil respiration and bacterial and fungal growth rates. FEMS Microbiol. Ecol. **52**: 49–58. doi:10.1016/J.FEMSEC.2004.10.002

Poffenbarger, H. J., B. A. Needelman, and J. P. Megonigal. 2011. Salinity influence on methane emissions from tidal marshes. Wetlands **31**: 831–842. doi:10.1007/s13157-011-0197-0

Portnoy, J., S. Smith, E. Gwilliam, and K. Chapman. 2006. Annual Report on Estuarine Restoration at East Harbor (Truro, MA), Cape Cod National Seashore, September 2006.

Prentice, C., K. L. Poppe, M. Lutz, and others. 2020. A Synthesis of Blue Carbon Stocks, Sources, and Accumulation Rates in Eelgrass (Zostera marina) Meadows in the Northeast Pacific . Global Biogeochem. Cycles **34**. doi:10.1029/2019gb006345

Purvaja, R., & Ramesh, R. (2000). Human impacts on methane emission from mangrove ecosystems in India. *Regional Environmental Change*, *1*(2), 86–97. https://doi.org/10.1007/PL00011537

Purvaja, R., & Ramesh, R. (2001). Natural and and anthropogenic methane emission from coastal wetlands of South India. *Environmental Management*, *27*(4), 547–557. https://doi.org/10.1007/s002670010169

Purvaja, Ramachandran, Ramesh, R., & Frenzel, P. (2004). Plant-mediated methane emission from an Indian mangrove. *Global Change Biology*, *10*(11), 1825–1834. https://doi.org/10.1111/j.1365-2486.2004.00834.x

Qu, W., C. Su, R. J. West, and R. J. Morrison. 2004. Photosynthetic characteristics of benthic microalgae and seagrass in Lake Illawarra, Australia. Hydrobiol. 2004 5151 **515**: 147–159. doi:10.1023/B:HYDR.0000027326.46856.0A

Raposa, K. B., Weber, R. L. J., Ekberg, M. C., & Ferguson, W. (2017). Vegetation Dynamics in Rhode Island Salt Marshes During a Period of Accelerating Sea Level Rise and Extreme Sea Level Events. *Estuaries and Coasts*, *40*(3), 640–650. https://doi.org/10.1007/s12237-015-0018-4

Rasmusson, L. M., P. Buapet, R. George, M. Gullström, P. C. B. Gunnarsson, and M. Björk. 2020. Effects of temperature and hypoxia on respiration, photorespiration, and

photosynthesis of seagrass leaves from contrasting temperature regimes. ICES J. Mar. Sci. **77**: 2056–2065. doi:10.1093/ICESJMS/FSAA093

Ray, N., A. Al-Haj, and R. Fulweiler. 2020. Sediment biogeochemistry along an oyster aquaculture chronosequence. Mar. Ecol. Prog. Ser. **646**: 13–27. doi:10.3354/meps13377

Ray, N. E., T. J. Maguire, A. N. Al-Haj, M. C. Henning, and R. W. Fulweiler. 2019. Low Greenhouse Gas Emissions from Oyster Aquaculture. Environ. Sci. Technol. **53**: 9118–9127. doi:10.1021/acs.est.9b02965

Raymond, P. A., & Cole, J. J. (2001). Gas Exchange in Rivers and Estuaries: Choosing a Gas Transfer Velocity. *Estuaries*, *24*(2), 312. https://doi.org/10.2307/1352954

Reading, M. J., I. R. Santos, D. T. Maher, L. C. Jeffrey, and D. R. Tait. 2017. Shifting nitrous oxide source/sink behaviour in a subtropical estuary revealed by automated time series observations. Estuar. Coast. Shelf Sci. **194**: 66–76. doi:10.1016/j.ecss.2017.05.017

Reeburgh, W. S. 2007. Oceanic Methane Biogeochemistry.doi:10.1021/CR050362V

Rees, A. P., I. J. Brown, A. Jayakumar, G. Lessin, P. J. Somerfield, and B. B. Ward. 2021. Biological nitrous oxide consumption in oxygenated waters of the high latitude Atlantic Ocean. Commun. Earth Environ. 2021 21 **2**: 1–8. doi:10.1038/s43247-021-00104-y

Rhee, T. S., A. J. Kettle, and M. O. Andreae. 2009. Methane and nitrous oxide emissions from the ocean: A reassessment using basin-wide observations in the Atlantic. J. Geophys. Res. Atmos. **114**. doi:10.1029/2008JD011662

Risgaard-Petersen, N. 2003. Coupled nitrification-denitrification in autotrophic and heterotrophic estuarine sediments: On the influence of benthic microalgae. Limnol. Oceanogr. **48**: 93–105. doi:10.4319/LO.2003.48.1.0093

Rosentreter, J. A., A. N. Al-Haj, R. W. Fulweiler, and P. Williamson. 2021a. Methane and Nitrous Oxide Emissions Complicate Coastal Blue Carbon Assessments. Global Biogeochem. Cycles **35**: e2020GB006858. doi:10.1029/2020GB006858

Rosentreter, J. A., A. V. Borges, B. R. Deemer, and others. 2021b. Half of global methane emissions come from highly variable aquatic ecosystem sources. Nat. Geosci. **14**: 225–230. doi:10.1038/s41561-021-00715-2

Rosentreter, J. A., D. T. Maher, D. V Erler, R. H. Murray, and B. D. Eyre. 2018. Methane emissions partially offset “blue carbon” burial in mangroves. Sci. Adv. **4**: eaao4985. doi:10.1126/sciadv.aao4985

Rosentreter, J. A., D. T. Maher, D. T. Ho, M. Call, J. G. Barr, and B. D. Eyre. 2017. Spatial and temporal variability of CO_2 and CH_4 gas transfer velocities and quantification of the CH_4 microbubble flux in mangrove dominated estuaries. Limnol. Oceanogr. **62**: 561–578. doi:10.1002/lno.10444

Roslev, P., & King, G. M. (1996). Regulation of methane oxidation in a freshwater wetland by water table changes and anoxia. *FEMS Microbiology Ecology*, *19*(2), 105–115. https://doi.org/10.1111/j.1574-6941.1996.tb00203.x

Rozema, J., Dorel, F., Janissen, R., Lenssen, G., Broekman, R., Arp, W., & Drake, B. G. (1991). Effect of elevated atmospheric CO2 on growth, photosynthesis and water relations of salt marsh grass species. *Aquatic Botany*, *39*(1–2), 45–55. https://doi.org/10.1016/0304-3770(91)90021-V

Russell, D. G., F. Y. Warry, and P. L. M. Cook. 2016. The balance between nitrogen fixation and denitrification on vegetated and non-vegetated intertidal sediments. Limnol. Oceanogr. **61**: 2058–2075. doi:10.1002/LNO.10353

Saintilan, N., Wilson, N. C., Rogers, K., Rajkaran, A., & Krauss, K. W. (2014). Mangrove expansion and salt marsh decline at mangrove poleward limits. *Global Change Biology*, *20*(1), 147–157. https://doi.org/10.1111/gcb.12341

Salk, K. R., D. V. Erler, B. D. Eyre, N. Carlson-Perret, and N. E. Ostrom. 2017. Unexpectedly high degree of anammox and DNRA in seagrass sediments: Description and application of a revised isotope pairing technique. Geochim. Cosmochim. Acta **211**: 64–78. doi:10.1016/J.GCA.2017.05.012

Santos, I. R., Dimova, N., Peterson, R. N., Mwashote, B., Chanton, J., & Burnett, W. C. (2009). Extended time series measurements of submarine groundwater discharge tracers (222Rn and CH4) at a coastal site in Florida. *Marine Chemistry*, *113*(1–2), 137–147. https://doi.org/10.1016/J.MARCHEM.2009.01.009

Saunois, M., Jackson, R. B., Bousquet, P., Boulter, B., & Canadell, J. G. (2016). The growing role of methane in anthropogenic climate change. *Environmental Research Letters*, *11*. https://doi.org/10.1088/1748-9326/11/12/120207

Scholander, P. F., van Dam, L., & Scholander, S. I. (1955). Gas Exchange in the Roots of Mangroves. *American Journal of Botany*, *42*(1), 92. https://doi.org/10.2307/2438597

Seymour, J. R., B. Laverock, D. A. Nielsen, S. M. Trevathan-Tackett, and P. I. Macreadie. 2018. The Microbiology of Seagrasses. Seagrasses Aust. Struct. Ecol. Conserv. 343–392. doi:10.1007/978-3-319-71354-0_12

Shakhova, N., Semiletov, I., Leifer, I., Sergienko, V., Salyuk, A., Kosmach, D., … Gustafsson, Ö. (2014). Ebullition and storm-induced methane release from the East Siberian Arctic Shelf. *Nature Geoscience*, *7*(1), 64–70. https://doi.org/10.1038/ngeo2007

Shepard, C. C., Crain, C. M., & Beck, M. W. (2011). The Protective Role of Coastal Marshes: A Systematic Review and Meta-analysis. *PLoS ONE*, *6*(11), e27374. https://doi.org/10.1371/journal.pone.0027374

Short, F., Carruthers, T., Dennison, W., & Waycott, M. (2007). Global seagrass distribution and diversity: A bioregional model. *Journal of Experimental Marine Biology and Ecology*, *350*(1–2), 3–20. https://doi.org/10.1016/J.JEMBE.2007.06.012

Slomp, C. P., & Van Cappellen, P. (2004). Nutrient inputs to the coastal ocean through submarine groundwater discharge: controls and potential impact. *Journal of Hydrology*, *295*(1–4), 64–86. https://doi.org/10.1016/J.JHYDROL.2004.02.018

Smith, A. C., J. E. Kostka, R. Devereux, and D. F. Yates. 2004. Seasonal composition and activity of sulfate-reducing prokaryotic communities in seagrass bed sediments. Aquat. Microb. Ecol. **37**: 183–195. doi:10.3354/AME037183

Smith, R. D., W. C. Dennison, and R. S. Alberte. 1984. Role of seagrass photosynthesis in root aerobic processes. Plant Physiol. **74**: 1055–8. doi:10.1104/pp.74.4.1055

Sorrell, B. K., & Downes, M. T. (2004). Water velocity and irradiance effects on internal transport and metabolism of methane in submerged Isoetes alpinus and Potamogeton crispus. *Aquatic Botany*, *79*(2), 189–202. https://doi.org/10.1016/J.AQUABOT.2004.02.004

Spalding, M. (2010). *World Atlas of Mangroves*. https://doi.org/10.4324/9781849776608

Steinle, L., J. Maltby, T. Treude, and others. 2017. Effects of low oxygen concentrations on aerobic methane oxidation in seasonally hypoxic coastal waters. Biogeosciences **14**: 1631–1645. doi:10.5194/bg-14-1631-2017

Strickland, J., and T. Parsons. 1968. A practical handbook of seawater analysis, 2nd ed. Fisheries Research Board of Canada.

Sturm, K., Z. Yuan, B. Gibbes, U. Werner, and A. Grinham. 2014. Methane and nitrous oxide sources and emissions in a subtropical freshwater reservoir, South East Queensland, Australia. Biogeosciences **11**: 5245–5258. doi:10.5194/BG-11-5245-2014

Sun, Y., Z. Song, H. Zhang, P. Liu, and X. Hu. 2020. Seagrass vegetation affect the vertical organization of microbial communities in sediment. Mar. Environ. Res. **162**: 105174. doi:10.1016/J.MARENVRES.2020.105174

Sun, Z., L. Wang, H. Tian, H. Jiang, X. Mou, and W. Sun. 2013. Fluxes of nitrous oxide and methane in different coastal Suaeda salsa marshes of the Yellow River estuary, China. Chemosphere **90**: 856–865. doi:10.1016/J.CHEMOSPHERE.2012.10.004

Takahashi, M., Noonan, S. H. C., Fabricius, K. E., & Collier, C. J. (2016). The effects of long-term *in situ* CO 2 enrichment on tropical seagrass communities at volcanic vents. *ICES Journal of Marine Science: Journal Du Conseil*, *73*(3), 876–886. https://doi.org/10.1093/icesjms/fsv157

Tezuka, Y. 1990. Bacterial regeneration of ammonium and phosphate as affected by the carbon:nitrogen:phosphorus ratio of organic substrates. Microb. Ecol. 1990 193 **19**: 227–238. doi:10.1007/BF02017167

Thayer, G. W., & Stuart, H. H. (1974). The Bay Scallop Makes Its Bed of Seagrass. *Marine Fisheries Review*, *36*(7), 27–30.

Tian, H., R. Xu, J. G. Canadell, and others. 2020. A comprehensive quantification of global nitrous oxide sources and sinks. Nature **586**: 248–256. doi:10.1038/s41586-020-2780-0

Timmers, P. H. A., Welte, C. U., Koehorst, J. J., Plugge, C. M., Jetten, M. S. M., & Stams, A. J. M. (2017). Reverse Methanogenesis and Respiration in Methanotrophic Archaea. *Archaea*, *2017*, 1–22. https://doi.org/10.1155/2017/1654237

Tokoro, T., S. Hosokawa, E. Miyoshi, K. Tada, K. Watanabe, S. Montani, H. Kayanne, and T. Kuwae. 2014. Net uptake of atmospheric CO 2 by coastal submerged aquatic vegetation. Glob. Chang. Biol. **20**: 1873–1884. doi:10.1111/gcb.12543

Touchette, B. W., and J. A. M. Burkholder. 2000. Review of nitrogen and phosphorus metabolism in seagrasses. J. Exp. Mar. Bio. Ecol. **250**: 133–167. doi:10.1016/S0022-0981(00)00195-7

Trevathan-Tackett, S. M., A. C. G. Thomson, P. J. Ralph, and P. I. Macreadie. 2018. Fresh carbon inputs to seagrass sediments induce variable microbial priming responses. Sci. Total Environ. **621**: 663–669. doi:10.1016/j.scitotenv.2017.11.193

Turner, A. J., Frankenberg, C., & Kort, E. A. (2019). Interpreting contemporary trends in atmospheric methane. *Proceedings of the National Academy of Sciences of the United States of America*, *116*(8), 2805–2813. https://doi.org/10.1073/pnas.1814297116

Ueyama, M., Takeuchi, R., Takahashi, Y., Ide, R., Ataka, M., Kosugi, Y., … Saigusa, N. (2015). Methane uptake in a temperate forest soil using continuous closed-chamber measurements. *Agricultural and Forest Meteorology*, *213*, 1–9. https://doi.org/10.1016/J.AGRFORMET.2015.05.004

Van Dam, B. R., C. C. Lopes, P. Polsenaere, R. M. Price, A. Rutgersson, and J. W. Fourqurean. 2021. Water temperature control on CO2 flux and evaporation over a subtropical seagrass meadow revealed by atmospheric eddy covariance. Limnol. Oceanogr. **66**: 510–527. doi:10.1002/LNO.11620

Van Dam, B. R., C. Lopes, C. L. Osburn, and J. W. Fourqurean. 2019. Net heterotrophy and carbonate dissolution in two subtropical seagrass meadows. Biogeosciences **16**: 4411–4428. doi:10.5194/bg-2019-191

Vieillard, A. M., and R. W. Fulweiler. 2012. Impacts of long-term fertilization on salt marsh tidal creek benthic nutrient and N2 gas fluxes. Mar. Ecol. Prog. Ser. **471**: 11–22. doi:10.3354/MEPS10013

Wang, F., Chen, N., Yan, J., Lin, J., Guo, W., Cheng, P., … Tian, Y. (2019). Major Processes Shaping Mangroves as Inorganic Nitrogen Sources or Sinks: Insights From a Multidisciplinary Study. *Journal of Geophysical Research: Biogeosciences*, 2018JG004875. https://doi.org/10.1029/2018JG004875

Wang, H., Liao, G., D'Souza, M., Yu, X., Yang, J., Yang, X., & Zheng, T. (2016). Temporal and spatial variations of greenhouse gas fluxes from a tidal mangrove wetland in Southeast China. *Environmental Science and Pollution Research*, *23*(2), 1873–1885. https://doi.org/10.1007/s11356-015-5440-4

Wanninkhof, R. 2014. Relationship between wind speed and gas exchange over the ocean revisited. Limnol. Oceanogr. Methods **12**: 351–362. doi:10.4319/lom.2014.12.351

Wanninkhof, R. (1992). Relationship between wind speed and gas exchange over the ocean. *Journal of Geophysical Research*, *97*(C5), 7373. https://doi.org/10.1029/92JC00188

Watanabe, K., and T. Kuwae. 2015. How organic carbon derived from multiple sources contributes to carbon sequestration processes in a shallow coastal system? Glob. Chang. Biol. **21**: 2612–2623. doi:10.1111/GCB.12924

Watts, I. M., J. Dean Rosati, and M. Borrelli. 2011. Re-Establishing a Historical Inlet At East Harbor, Cape Cod, Masssachusetts. Proc. Coast. Sediments 419–429. doi:10.1142/9789814355537_0032

Waycott, M., Duarte, C. M., Carruthers, T. J. B., Orth, R. J., Dennison, W. C., Olyarnik, S., … Williams, S. L. (2009). Accelerating loss of seagrasses across the globe threatens coastal ecosystems. *Proceedings of the National Academy of Sciences*, *106*(30), 12377–12381. https://doi.org/10.1073/pnas.0905620106

Weber, T., N. A. Wiseman, and A. Kock. 2019. Global ocean methane emissions dominated by shallow coastal waters. Nat. Commun. **10**: 4584. doi:10.1038/s41467-019-12541-7

Weiss, R. F. 1970. The solubility of nitrogen, oxygen and argon in water and seawater. Deep Sea Res. Oceanogr. Abstr. **17**: 721–735. doi:10.1016/0011-7471(70)90037-9

Weiss, R. F. (1981). Determinations of Carbon Dioxide and Methane by Dual Catalyst Flame Ionization Chromatography and Nitrous Oxide by Electron Capture Chromatography. *Journal of Chromatographic Science*, *19*(12), 611–616. https://doi.org/10.1093/chromsci/19.12.611

Weiss, R. F., and B. A. Price. 1980. Nitrous oxide solubility in water and seawater. Mar. Chem. **8**: 347–359. doi:10.1016/0304-4203(80)90024-9

Welti, N., Hayes, M., & Lockington, D. (2017). Seasonal nitrous oxide and methane emissions across a subtropical estuarine salinity gradient. *Biogeochemistry*, *132*(1–2), 55–69. https://doi.org/10.1007/s10533-016-0287-4

Wiesenburg, D. A., and N. L. J. Guinasso. 1979. Equilibrium solubilities of methane, carbon monoxide, and hydrogen in water and sea water. J. Chem. Eng. Data **24**: 356–360. doi:10.1021/JE60083A006

Wilson, B. J., Mortazavi, B., & Kiene, R. P. (2015). Spatial and temporal variability in carbon dioxide and methane exchange at three coastal marshes along a salinity gradient in a northern Gulf of Mexico estuary. *Biogeochemistry*, *123*(3), 329–347. https://doi.org/10.1007/s10533-015-0085-4

Winfrey, M. R., & Ward, D. M. (1983). Substrates for sulfate reduction and methane production in intertidal sediments. *Applied and Environmental Microbiology*, *45*(1), 193–199.

Woodroffe, C. D., Rogers, K., McKee, K. L., Lovelock, C. E., Mendelssohn, I. A., & Saintilan, N. (2016). Mangrove Sedimentation and Response to Relative Sea-Level Rise. *Annual Review of Marine Science*, *8*(1), 243–266. https://doi.org/10.1146/annurev-marine-122414-034025

Xiang, J., Liu, D., Ding, W., Yuan, J., & Lin, Y. (2015). Invasion chronosequence of Spartina Alterniflora on methane emission and organic carbon sequestration in a

coastal marsh. *Atmospheric Environment*, *112*, 72–80. https://doi.org/10.1016/j.atmosenv.2015.04.035

Xu, L., Lin, X., Amen, J., Welding, K., & McDermitt, D. (2014). Impact of changes in barometric pressure on landfill methane emission. *Global Biogeochemical Cycles*, *28*(7), 679–695. https://doi.org/10.1002/2013GB004571

Yang, B., X. Li, S. Lin, Z. Xie, Y. Yuan, M. Espenberg, J. Pärn, and Ü. Mander. 2020. Invasive Spartina alterniflora can mitigate N2O emission in coastal salt marshes. Ecol. Eng. **147**: 105758. doi:10.1016/J.ECOLENG.2020.105758

Yang, W.-B., Yuan, C.-S., Huang, B.-Q., Tong, C., & Yang, L. (2018). Emission Characteristics of Greenhouse Gases and Their Correlation with Water Quality at an Estuarine Mangrove Ecosystem – the Application of an In-situ On-site NDIR Monitoring Technique. *Wetlands*, *38*, 723–738. https://doi.org/10.1007/s13157-018-1015-8

Yarbro, L. A., and P. R. Carlson. 2008. Community oxygen and nutrient fluxes in seagrass beds of Florida Bay, USA. Estuaries and Coasts **31**: 877–897. doi:10.1007/S12237-008-9071-6/TABLES/9

Ye, W., Zhang, G., Zhu, Z., Han, Y., Wang, L., & Sun, M. (2016). Methane distribution and sea-to-air flux in the East China Sea during the summer of 2013: Impact of hypoxia. *Deep Sea Research Part II: Topical Studies in Oceanography*, *124*, 74–83. https://doi.org/10.1016/J.DSR2.2015.01.008

Yu, K. W., Z. P. Wang, and G. X. Chen. 1997. Nitrous oxide and methane transport through rice plants. Biol. Fertil. Soils 1997 243 **24**: 341–343. doi:10.1007/S003740050254

Yuan, J., D. Liu, Y. Ji, J. Xiang, Y. Lin, M. Wu, and W. Ding. 2019. Spartina alterniflora invasion drastically increases methane production potential by shifting methanogenesis from hydrogenotrophic to methylotrophic pathway in a coastal marsh. J. Ecol. **107**: 2436–2450. doi:10.1111/1365-2745.13164

Yuan, J., Ding, W., Liu, D., Kang, H., Freeman, C., Xiang, J., & Lin, Y. (2015). Exotic Spartina alterniflora invasion alters ecosystem-atmosphere exchange of CH4and N2O and carbon sequestration in a coastal salt marsh in China. *Global Change Biology*, *21*(4), 1567–1580. https://doi.org/10.1111/gcb.12797

Yvon-Durocher, G., Allen, A. P., Bastviken, D., Conrad, R., Gudasz, C., St-Pierre, A., … del Giorgio, P. A. (2014). Methane fluxes show consistent temperature dependence across microbial to ecosystem scales. *Nature*, *507*(7493), 488–491. https://doi.org/10.1038/nature13164

Zeng, Y., D. A. Friess, T. V. Sarira, K. Siman, and L. P. Koh. 2021. Global potential and limits of mangrove blue carbon for climate change mitigation. Curr. Biol. doi:10.1016/j.cub.2021.01.070

Zhang, G.-L., Zhang, J., Liu, S.-M., Ren, J.-L., & Zhao, Y.-C. (2010). Nitrous oxide in the Changjiang (Yangtze River) Estuary and its adjacent marine area: Riverine input, sediment release and atmospheric fluxes. *Biogeosciences*, *7*, 3505–3516. https://doi.org/10.5194/bg-7-3505-2010

Zhang, J., Gilbert, D., Gooday, A. J., Levin, L., Naqvi, S. W. A., Middelburg, J. J., … Van der Plas, A. K. (2010). Natural and human-induced hypoxia and consequences for coastal areas: synthesis and future development. *Biogeosciences*, *7*(5), 1443–1467. https://doi.org/10.5194/bg-7-1443-2010

Zhang, Y., Ding, W., Cai, Z., Valerie, P., & Han, F. (2010). Response of methane emission to invasion of Spartina alterniflora and exogenous N deposition in the coastal salt marsh. *Atmospheric Environment*, *44*(36), 4588–4594. https://doi.org/10.1016/j.atmosenv.2010.08.012

Zheng, S., B. Wang, G. Xu, and F. Liu. 2020. Effects of Organic Phosphorus on Methylotrophic Methanogenesis in Coastal Lagoon Sediments With Seagrass (Zostera marina) Colonization. Front. Microbiol. **0**: 1770. doi:10.3389/FMICB.2020.01770

Zheng, X., Guo, J., Song, W., Feng, J., Lin, G., Zheng, X., … Lin, G. (2018). Methane Emission from Mangrove Wetland Soils Is Marginal but Can Be Stimulated Significantly by Anthropogenic Activities. *Forests*, *9*(12), 738. https://doi.org/10.3390/f9120738

Zhuang, G.-C., Elling, F. J., Nigro, L. M., Samarkin, V., Joye, S. B., Teske, A., & Hinrichs, K.-U. (2016). Multiple evidence for methylotrophic methanogenesis as the dominant methanogenic pathway in hypersaline sediments from the Orca Basin, Gulf of Mexico. *Geochimica et Cosmochimica Acta*, *187*, 1–20. https://doi.org/10.1016/J.GCA.2016.05.005

Zhuang, G.-C., V. B. Heuer, C. S. Lazar, and others. 2018. Relative importance of methylotrophic methanogenesis in sediments of the Western Mediterranean Sea. Geochim. Cosmochim. Acta **224**: 171–186. doi:10.1016/J.GCA.2017.12.024

Ziegler, S., and R. Benner. 1999. Nutrient cycling in the water column of a subtropical seagrass meadow. Mar. Ecol. Prog. Ser. **188**: 51–62. doi:10.3354/MEPS188051

Zuur, A. F., and E. N. Ieno. 2016. Beginner's guide to zero-inflated models with R, Highland Statistics Ltd.

CURRICULUM VITAE